4-5-2019

Investigating the Proteinaceous Regulome of the *Acinetobacter baumannii*

Leila G. Casella
University of South Florida, leilacasella@me.com

Investigating the Proteinaceous Regulome of the *Acinetobacter baumannii*

by

Leila G. Casella

A dissertation submitted in partial fulfillment
of the requirements for the degree of
Doctor of Philosophy
Department of Cell Biology, Microbiology, and Molecular Biology
College of Arts and Sciences
University of South Florida

Major Professor: Lindsey N. Shaw, PhD
Prahathees Eswara, PhD
James Riordan, PhD
Burt Anderson PhD

Date of Approval
April 29, 2019

Keywords: Gene Regulation, Energy, Metabolism, Iron

ACKNOWLEDGEMENTS

First and foremost, to my mentor Dr. Lindsey Shaw, I want to thank you for having me in your lab and support me not only academically but in times that I was in much need of a hand. I wanted to thank you for those times that you have pushed me to develop my scientific thinking and become a better scientist.

Dr Prahathees Eswara,Dr. Burt Anderson, and Dr. James Riordan thank you for your support and the insights provided that raised ideas and guided my projects. I would like to thank everyone in the Shaw lab including former members that have left to continue their journeys for your support and for those times of laughs that made easier the long days in the lab.

To my mom, thank you for understanding and let me be away from you to pursue my goals without making me feel guilty, you know it was not an easy decision.

TABLE OF CONTENTS

List of Tables....iv

List of Figures....v

Abstract....vii

Chapter I: Introduction....1
The Genus Acinetobacter....1
Acinetobacter baumannii History and Identifying Features....2
The infections of *A. baumannii*....4
The Drug Resistance of *A. baumannii*....7
The Mechanisms of Drug Resistance in *A. baumannii*....8
A. baumannii as a Public Health Treat....10
The Virulence Factors of *A. baumannii*....11
Genome Plasticity of *A. baumannii*....15
Regulation in *A. baumannii*....16
A. baumannii Metabolism....19
Metal Acquisition in *A. baumannii*....22
Project aim....24

Chapter II: Towards The Complete Proteinaceous Regulome of *Acinetobacter baumannii*....26
Note to Reader....26

Chapter III: Identification of a Novel Two Component System Governing Membrane Energetics in *Acinetobacter baumannii*....27
Abstract....27
Introduction....28
Materials and Methods....31
Bioinformatic analysis....31
Strains and growth conditions....32
Construction of an *arcAB-lacZ* transcriptional fusion strain....33
Construction of *arcA* and *arcB* complementation strains....33
Transcriptional profiling assays using β-galactosidase....34
Intracellular pH measurement....35
Membrane Depolarization Assay....35
RNA Sequencing and Bioinformatic Analysis....36
Quantitative real time PCR....37
Intracellular metabolite quantification assays....38

Antimicrobial susceptibility assays....39
Assaying ATP levels within cells....39
Determination of cytochrome oxidase activity....40
Results. 40
Identification of ArcAB homologs in the genome of *Acinetobacter baumannii.* 40
Expression of the ArcAB TCS is induced upon disruption of the proton gradient in *A. baumannii* 45
Disruption of ArcAB impairs the PMF in *A. baumannii.* 47
Transcriptomic profiling reveals a shift in expression of genes required for glucose utilization upon *arcA* disruption. 49
Increased glycolytic influx in the *arcA* mutant favors activation of the Pta-AckA pathway generating acetate from pyruvate. 53
arcA mutants of *A. baumannii* use an incomplete TCA Cycle, instead favoring the glyoxylate shunt. 54
NADH levels are increased in the *arcA* mutant as a result of its hyperactive glyoxylate shunt....57
The altered metabolic state of *arcAB* mutants favors ATP production via substrate phosphorylation....58
Cytochrome oxidase activity is reduced as a result of *arcAB* disruption...60
The accumulation of oxaloacetate in *arcA* mutant cells leads to aminoglycoside hyper-susceptibility. 62
Discussion. 63

Chapter IV: Characterization of a novel *fec*-operon responsive to hemin in *Acinetobacter baumannii* 69
Abstract 69
Introduction. 70
Materials and Methods....73
Bioinformatic analysis....73
Strains and growth conditions....74
Construction of a *fecA-lacZ* transcriptional fusion strain. 74
Construction of *fecR* and *hemO* complementation strains....75
Growth assays. 76
Transcriptional profiling assays using β-galactosidase. 76
RNA-seq analsyis. 77
qRT-PCR....78
Hemin measurements. 79
Human serum survival assay....80
Results 80
The FecI operon of *A. baumannii* has a distinct set of genes compared to homologs in other organisms....80
The presence of hemin or hemoglobin as a sole iron source impacts growth of the *fecI* and *fecR* mutant strains. 83
Transcriptional analysis reveals that *A. baumannii fecA* is induced in ..... response to hemin and hemoglobin....85

Global transcriptomic analysis reveals altered expression of iron metabolic pathways upon disruption of *fecI*. 86
Disruption of the heme oxygenase *hemO* leads to hemin and hemoglobin.. dependent growth impairment. 90
....
Disruption of *hemO* results in a higher intracellular heme concentration compared to the wild-type....91
Discussion 94

Chapter V: Final Discussion....99
Final Discussion 99
Future Directions....110

References 114

Appendix 1 132

Appendix 2. Supplemental Figures 145
Figure S1. Protein alignments of ABUW_2427 from *A. baumannii* alongside ArcB proteins from a variety of organisms....145
Figure S2. Protein alignments of ABUW_2426 from *A. baumannii* alongside ArcA proteins from a variety of organisms....146
Figure S3. The *arcAB* promoter is induced upon exposure to CCCP....147
Figure S4. qPCR validation of RNA-seq data....147
Figure S5. Disruption of ArcAB does not affect susceptibility to non-aminoglycoside antibiotics....148

Appendix 3 Supplemental tables 149
Table 1S Genes differentially expressed in the *arcA* mutant strain……149
Table 2S. Genes differentially expressed in the *fecI* mutant strain……..173

LIST OF TABLES

Table1: Bacteria strains, plasmids and cloning primers.....32

Table 2: List of qPCR primers used in this study. 37

Table 3: Blast analysis of ABUW_2427 and ABUW_2426 from *A. baumannii* identifies them as ArcAB homologs. 41

Table 4: Bacteria strains, plasmids and cloning primers.....75

Table 5: List of qPCR primers used in this study 78

Table 6: BLAST analysis of ABUW_2987, ABUW_2986 and ABUW_2985 from *A.baumannii* identifies them as homologs of FecI, FecR and FecA, respectively.....81

LIST OF FIGURES

Figure 1: Predicted topology of ArcB from *A. baumannii*.....42

Figure 2: Syntenic comparison of the *arcAB* module from *A. baumannii* 45

Figure 3: *arcAB* transcription is induced upon exposure to the protonophore CCCP.....46

Figure 4: *A. baumannii arcAB* mutants have a reduced intracellular pH and depolarized membrane. 49

Figure 5: Transcriptomic profiling of the *arcA* mutant. 50

Figure 6: Metabolic map for *A. baumannii* indicating nodes of change in the *arcA* mutant.....52

Figure 7: Disruption of ArcAB leads to increased glucose concentrations within the cell 53

Figure 8: Increased pyruvate levels in *arcA* and *arcB* mutant strains leads to a glyoxalate shunt that favors acetate production. 54

Figure 9: Disruption of ArcAB leads to the accumulation of oxaloacetate and succinate as a result of an impaired TCA cycle. 56

Figure 10: Disruption of ArcAB results in elevated intracellular NADH levels.....58

Figure 11: *arcAB* mutants produce ATP via substrate phosphorylation more efficiently than through oxidative phosphorylation 60

Figure 12: The altered metabolic state of *arcAB* mutants results in impaired aerobic respiration. 61

Figure 13: ArcAB mutants demonstrate increased susceptibility to aminoglycoside antibiotics.....62

Figure 14: Genomic organization of the *fecI*-like operon from *A. baumannii* and related Gram-negative organisms. 82

Figure 15: Predicted topology plots of outermembrane receptor proteins within the

homologous *fec* operons.....83

Figure 16: The presence of hemin or hemoglobin as a sole iron source affects growth of the *fecI* and *fecR* mutant strains.....84

Figure 17 Complementation of *ΔfecR in trans* restores growth to wild-type levels in the presence of hemoglobin or hemin as sole iron source.....85

Figure 18: The *fecA* promoter of *A. baumannii* is specifically responsive to either hemin or hemoglobin in a FecI-FecR dependent manner.....86

Figure 19: Transcriptomic Profiling of the *fecI* mutant. 87

Figure 20: qRT-PCR analysis validates RNA-seq data for genes with altered expression upon *ΔfecI* disruption.....88

Figure 21: Disruption of *hemO* leads to growth impairment in the presence of hemin or human hemoglobin.....91

Figure 22: Disruption of *hemO* leads to increased levels of hemin within the *A. baumannii* cell. 92

Figure 23: Disruption of *hemO* leads to reduce survival in human serum. 93

Figure 24: Model for perceiving hemin in the environment via the *fec*-operon of *A. baumannii.* 98

Figure 25. Model for activation of ArcAB in *A. baumannii.* 113

Figure 26 Predictive model of putative promoters of the *fec*-operon in *A*. *baumannii.* 113

ABSTRACT

Acinetobacter baumannii is an opportunistic pathogen that overtime has evolved into one of the most problematic pathogens due to its ability to overcome antibiotic pressures and harshly environments in the host and hospital environments. In this context, its genomic evolution due to its capacity to acquire genes that contribute to its pathogenic and antibiotic resistance nature has been the subject of research in the last decades providing with the identification of several proteins aiding in the process of pathogenicity. Although these findings have contributed to our understanding of *A. baumannii* pathogenic traits, the regulatory network that control their expression are less understood. As such, our first efforts to study gene regulation in this organism were focused on defining the complete set of regulatory proteins in *A. baumannii*. As such, we examined the genome of a highly pathogenic multidrug resistance (MDR) *A. baumannii* strain AB5075 and comparative analyses to understand evolution of regulatory networks were performed using *A. baumannii* strains with different MDR profiles. This work generated a complete set of regulatory proteins identified in AB5075. This tool serves us as a foundation to investigate the function of uncharacterized regulatory proteins in this organism. As a result of this, we characterized the role of a two-component system in controlling metabolic pathways and found that its disruption is detrimental for energy generation processes. In addition, we defined the role of an extracytoplasmic sigma factor that is required for efficient growth in the presence of hemin as a sole iron source. Overall, the work of this dissertation

presents findings describing regulatory roles of a novel TCS and a sigma factor that will extend the knowledge of gene regulation in *A. baumannii*.

CHAPTER I: INTRODUCTION

The Genus Acinetobacter

Acinetobacter species were first isolated from soil samples in the earlier 1900's by the microbiologist Martinus Weillem Beijerinck [1]. At the time, these species were known as *Micrococcus- calco-aceticus,* a name that was given based on their cell morphology (small coccobacilli) and ability to grow in minimal mineral media containing calcium acetate as a sole carbon source [1]. In the years following, bacteria were identified as sharing common phenotypic characteristics with *Micrococcus- calco-aceticus,* including a lack of pigmentation and motility, cocci-rod cell shape, and an inability to use glucose as an lone carbon source, under different names, including *Herrellea vaginicola*, *Mima polyphorma*, *Moraxella lowffi*, *Moraxella glucidolytica*, *Acinetobacter spp*., and *Neisseria spp*. [2,3]. As a result, it was difficult to classify these organisms into a single genus due to the diversity of existing genus names, and epithets containing these species that were phenotypically indistinguishable.

The first comprehensive taxonomic study published by Baumann, *et. al*. in 1967 tested hundreds of bacterial species sharing phenotypes previously reported under different names, for their oxidase activity and ability to use a myriad of carbon sources. This led to the classification of all these species into three main groups *Moraxella osloenesis*, *Moraxella lacunata,* and *Nesseria catarrhalis* [4]. Following this publication, in 1968,

Baumann, *et. al.*, based on an extensive biochemical examination of 106 bacteria strains belonging to species from the *Mima-Herrellea, Acinetobacter spp.,* and*, Moraxella spp.,* were able to distinguish and classify a group of bacteria within the genus of *Acinetobacter* [5]. These studies for the first time provided a detail description of the characteristics observed in species that were grouped within the *Acinetobacter* genus. Thus, *Acinetobacter* species were described as Gram-negative bacteria cells that switch from rods to cocci cell shape while transitioning from exponential to stationary growth, lack motility, are strictly aerobic, catalase positive and oxidase negative, incapable of fermenting glucose, and have a prodigious ability to use acetate, ammonia, nitrogen, and a significant number of organic compounds as a sole carbon source [5,6]. These distinct features reported in *Acinetobacter* species resulted in their recognition as single species known as *Acinetobacter calcoaceticus* within the *Acinetobacter* genus in 1971 at the International Committee Meeting on Nomenclature of Bacteria by the Sub-committee on the Taxonomy of *Moraxella* and Allied Bacteria [7].

A. baumannii **History and Identifying Features**

Historically, bacteria belonging to the *Acinetobacter* genus are commonly found in water and soil, yet pathogenic strains causing a variety of infections such as osteomyelitis, pneumonia, urinary tract infections, vaginal infections in adults with weakened immune systems and fatal meningitis in infants started to be reported as earlier as the 1950's [8,9]. With the appearance of opportunistic pathogenic strains of *Acinetobacter*, the nutritional requirements and distinct lack of oxidase activity could not further differentiate among pathogenic and non-pathogenic species contained in the genus [10-12]. It wasn't until the

emergence of new technologies such as DNA hybridization that made it possible to define precisely *Acinetobacter* species at the genomic level. The first such study in 1986 examined 266 *Acinetobacter* strains using a combination of DNA hybridization and phenotypic assays resulting in the identification of 12 *Acinetobacter* species that included genomic species 1, 2, 4, 5, 7, and 8, named *Acinetobacter calcoaceticus*, *Acinetobacter baumannii*, *Acinetobacter haemolyticus, Acinetobacter junii, Acinetobacter johnsonii,* and *Acinetobacter lwoffii*, respectively[13]. Despite progress made in the identification of *Acinetobacter* species, a major drawback of differentiation among *Acinetobacter baumannii* and *Acinetobacter calcoaceticus* was highlighted by findings of their shared DNA relatedness, which is as high as 97% according to Nishimura *et. al* [14].

Subsequent phenotypic and molecular studies on members of the *Acinetobacter* spp. denoted 26 species and 9 genomic species [15,16]. Of note, the genomic species group includes 4 closely related species associated with nosocomial infections known as the *Acinetobacter calcoaceticus-baumannii* complex, which is comprised of: i) *Acinetobacter* genomic species 3, ii) *Acinetobacter* genomic species 13TU, iii) *A. calcoaceticus* and iv) *A. baumannii* [17]. Among members of this complex, *A. calcoaceticus* is the only environmental bacterium that has not been recovered from clinical samples, however the complex is still known as *Acinetobacter calcoaceticus-baumannii* due to the indistinguishable phenotypes among these two organisms. However, further studies exploiting the heterogeneity of genes such as 16SrRNA, *recA*, *rpoB*, and *gyrB* among the *A. calcoaceticus-baumannii* complex have been used to single out these clinical isolates[15].

As discussed above, differentiation of *Acinetobacter* species at the genus and epithet level has been the subject of research for over a century. Along this journey, the transition from basic biochemical assays to genomic driven technologies have served to differentiate among *Acinetobacter* species. Overall, this section summarizes findings derived from more than 100 years of research in the *Acinetobacter* field that has led to a more accurate identification and definition of the pathogenic bacterium *A. baumannii,* which is the best characterized organism within the *Acinetobacter* genus over the last four decades because of its multidrug resistance (MDR) nature and pathogenesis.

The Infections of *A. baumannii*

During the first quarter of the 20th century, *A. baumannii,* (previously reported under different names), were infrequently associated with nosocomial infections compared to other causative agents, including *Streptococcus pyogenes* and *Staphylococcus aureus* [18]. Nevertheless, during this period *A. baumannii* infections were documented in patients with weakened immune system as a result of clinical conditions, including burns and trauma or chronic disease, e.g. kidney and pulmonary diseases [8,9,11,19]. Soon after the recognition of the *Acinetobacter* genus in 1971, epidemiological studies focusing on *Acinetobacter* infections were the starting point for clinicians to recognize the role of this bacterium as a causative agent for a wide spectrum of diseases, including pulmonary infections, septicemia, urinary tract infections, wound infections, and cellulitis [20-22].

In this context, the high occurrence of *A. baumannii* infections in patients that require devices such as respirators, catheters, or surgical implants, as well as the mortality rates, which can be as high as 44% among patients that developed pulmonary infections, were

common findings of epidemiology studies during the period of 1970 -1977 [10,12,20]. A surveillance study in the United states during 1978 reported an increase of 14% in *A. baumannii* infections compared to those documented within 1974-1977 [23]. Perhaps this increase in *A. baumannii* infections can be attributed to the extraordinary ability of this bacterium to survive on surfaces for long periods of time in, for example, hospital settings. Alongside this, there has been an uptick in invasive medical procedures and implants during this time, providing favorable conditions for this pathogen to persist and cause diseases in comprised hosts. Despite this fact, therapeutic options such as sulfonamides and aminoglycosides remained effective for controlling these infections[10].

A major complication that has emerged in the control of *A. baumannii* infections, however, is the appearance of *A. baumannii* drug resistant strains, with the earliest reports dating back to the 1990's, initially in Asia and European countries [24-30]. Among these reports, one of the first was published by Siau *et. Al,* and describes the strong association of antibiotic resistance in *A. baumannii* strains isolated from patients treated for wounds and urinary infections, and from ICU patients that required the use of mechanical ventilators [22]. In this regard, pneumonia has become one of the most prevalent diseases caused by *A. baumannii* strains worldwide, and it has been proposed that the ability of this pathogen to adhere and form biofilms on surfaces such as endotracheal tubes used for mechanical ventilation provides a vehicle to establish ventilator associated pneumonia infections (VAP) [31,32].

In 2001, cases of MDR *A. baumannii* strains isolated from critically ill wounded US soldiers gave exposure to this pathogen in the mainstream as well as medical literature. In this example, US hospitals and bases in Iraq and Afghanistan reported that 97% of *A. baumannii* infections developed into bacteremia between 2002 and 2004 among soldiers with trauma injuries [33]. Consequently, military health care facilities encountered increased mortality, longer periods of recovery, and the need for surgical removal of extremities due to MDR *A. baumannii* infections [34-36]. Indeed, the ability of this organism to disseminate from primary sites of infections to the bloodstream increases the risk of developing bacteremia in patients, ultimately leading to untreatable infections due to the prevalence of MDR *A. baumannii* strains [36].

Multiple retrospective studies in US hospitals have reported death rates of between 49.6% to 76% among patients with sepsis linked to *A. baumannii* infections [37]. Furthermore, several US epidemiological studies have documented the increasing trend of MDR in *A. baumannii* strains and the challenges this adds to the control of *A. baumannii* infections among patients. A study focused on health care associated infections during 2011-2014 found that 64% of *A. baumannii* VAP infections were caused by MDR strains. More alarming, this pathogen has already moved into communities causing pneumonia in individuals with chronic diseases such as diabetes, kidney disease or alcoholism [38,39]. Community associated *A. baumannii* infections are found increasingly in countries with tropical climates, or during the summer season in places such as Alabama and Northern cities in the USA that perhaps reflect conditions that favors survival of *A. baumannii* [40].

Regarding a timeline for *A. baumannii* infections, a notably recent trend is the evolution of this bacterium that, although once considered avirulent, today is known for its ability to cause a broad spectrum of diseases. These are largely a result of its presence in nosocomial environments, and its ability to overcome host barriers by means of using medical devices as shuttles to gain entry to the host. Ultimately, the whole situation is complicated by the rapid and continued emergence of strains resistance to antibiotic therapeutics treatments commonly used in the clinic.

The Drug Resistance of *A. baumannii*

The steadily rising rates of MDR *A. baumannii* strains in the last 30 years have complicated the management of the *Acinetobacter* diseases as we mentioned in the previous section. In this regard, the common therapeutic options to treat *Acinetobacter* infections in the 1970s included single or combination administration of aminoglycosides and carbenicillin [10]. However, the high prevalence of genes encoding aminoglycoside modifying enzymes, β-lactamases, and the presence of porins reducing outer membrane permeability renders many clinical strains resistant to these antibiotics[41,42]. These was the first drug resistant phenotypes in this bacterium that led clinicians to move toward the use of β-lactam antibiotics such as cephalosporin [43-45]. The effectiveness of cephalosporins was short lived, however, and within a period of five years (1998-2001), the *ampC* gene encoding a Cephalosporinase was found to be prevalent among clinical strains, with carriage reportedly as high as 60% in hospitals around the world [39,46,47]. At this point, other antibiotics including fluoroquinoles, tetracyclines, and the carbapenems, imipenem and meropenem, were proven to be effective therapies to control MDR *A.*

baumannii infections [48]. Unfortunately, a rapid development of resistance displayed by this pathogen to all these existing antibiotics has resulted in the rise of mortality rates among patients infected with this organism [49].

Thus, what is next alternative to treat *Acinetobacter* infections unresponsive to standard therapies? The usage of polymyxin, a drug that was discontinued due to toxicity in the 1960's, has been the answer to control this problematic pathogen in recent years. Indeed, polymyxin inhaling therapies are now used for the treatment of *A. baumannii* VAP infections, whilst its toxic effects remain a complication [50,51]. In addition to this, increasing trends of *A. baumannii* polymyxin resistance in several countries, including the Unites States, is now a concern, highlighting the critical need for research and the development of new effective antibiotic agents [52-55].

The Mechanisms of Drug Resistance in *A. baumannii*

With the emergence of MDR *A. baumannii* strains, research has uncovered intrinsic and acquired mechanisms that has provided us with a better understanding of the drug resistance evolution in *A. baumannii*. Such mechanisms are illustrated by the constitutive expression of multiple efflux pumps systems, including AdeABC and AdeIJK, and the reduced expression of porins that together limit the passage of antibiotics such as aminoglycosides, cephalosporin, carbapenems, and tetracycline [56]. Beyond this, the natural ability of *A. baumannii* to acquire and transfer genes facilitates a rapid adaptation to antibiotics pressures. Indeed, analysis of the genomes for MDR *A. baumannii* strains

has resulted in the identification of plasmids, transposons, and insertion elements such as the 86kb pathogenicity island, AbaR, that harbors genes important for metal and antibiotic resistance, the class integron 1 containing beta-lactamase genes, also found in *Klebsiella pneumoniae*, and the insertion sequences *ISAba1*, *ISAba125* required for the expression of cephalosporinases, and carbapenemases [16,57].

In addition to genetic elements and intrinsic determinants, modification of cellular targets e.g. DNA gyrase, topoisomerase IV and 16S rRNA present an additional strategy that provides resistance to quinolones and aminoglycosides respectively [58,59]. Apart from these mechanisms, the structural modification of lipopolysaccharides (LPS), resulting in loss of LPS, or the addition of the amino-sugars phosphoethanolamine or galactosamine to the lipid A, lead to reduction in the overall negative charge in the outermembrane that hinders the entrance of polymyxin to the cell [60,61].

In this section a summary of findings that have identified drug resistance mechanisms in *A. baumannii* have advance our knowledge of the strategies used by this pathogen to rapidly adapt to and overcome antibiotic pressures. It does this via its ability to acquire antibiotic resistant genes in combination with intrinsic mechanisms that exposes the threat of this pathogen in times of scarce novel antibiotics, which places us in the position today that is considered the beginning of the post-antibiotic era".

Acinetobacter baumannii as a Public Health Threat

As early as the 1980s, surveillance reports documented cases of *A. baumannii* outbreaks worldwide [62-64]. In the USA, the National Healthcare Safety Network (NHSN) reported an estimated range of (41,400 – 83,000) *A. baumannii* infections annually in the USA and 1,000,000 worldwide [65]. Recently, the Centers for Disease Control and Prevention (CDC) reported that approximately 60% of all *A. baumannii* infections are associated with multidrug resistant strains [66]. In addition, the combined effects of $389 million in healthcare cost and 4,590 deaths associated with *A. baumannii* multidrug resistant infections presents a worrisome problem for the US health system [65]. In light of this, in 2017 the World Health Organization (WHO) published a list of top priority pathogens, which includes *A. baumannii,* largely as a result of its prevalent multidrug resistant nature and negative impacts on the outcomes of patients treated with standard antibiotic therapies. A major reason for the WHO list was to advocate for substantially more research to develop effective therapeutic alternatives to treat MDR infections, such as those caused by *A. baumannii* [15].

A major distinction for pathogens within the *Acinetobacter calcoaceticus* - *Acientobacter baumannii* complex is its natural reservoir. Unlike other *Acinetobacter* species, which have been recovered from diverse sources, including: soil, water, food and poultry, *A. baumannii* has been exclusively isolated from clinical samples [67]. Strikingly, as a result of its ability to use a myriad of carbon sources, adapt to temperature shifts, and survive harsh conditions, this bacterium has turned hospitals and health care assisting facilities into its reservoirs[68]. Indeed, its persistence in countless hospital environments has been

described in numerous reports, demonstrating the resilient nature of *A. baumannii* [69-71]. Perhaps one of the most striking cases described an MDR *A. baumannii* isolate that caused a two year long outbreak in a Netherlands hospital. In this situation it was demonstrated that, despite being on an empty bottle devoid of nutrients for nearly a year, the bacterium remained viable; a pattern of survival that mimics methicillin-resistant *S. aureus* (MRSA) strains in hospitals [72]. Similarly, positive *A. baumannii* air cultures from Intensive Care Units (ICU) rooms in US hospitals have also been reported[73].

The ubiquity of *A. baumannii* strains in health care facilities, alongside its ability to remain viable on dry surfaces and its extreme resistance to desiccation and chemical disinfectants, further complicate its eradication from hospitals[15]. From the infection control perspective, failure to eliminate this pathogen from hospital environments is of great concern, as mechanical ventilators, urinary catheters, and surgical instruments are just a few examples of devices that provide a shuttle for *A. baumannii* to enter the host and establish infection. As a result, disinfection and the development of sterilization techniques to eradicate and minimize the risk of *Acinetobacter* infections in clinical settings, has been an area of active research in recent years.

The Virulence Factors of *A. baumannii*

Another aspect that is equally important as the evolution of MDR phenotypes is the emergence of contemporary clinical isolates that display more virulent phenotypes when compared to their historic counterparts, such as the drug susceptible *A. baumannii* strains

ATCC 19606 and ATCC 17978 isolated in the 1950s. The increase in virulence observed in this pathogen stems from the variable size of its genome, defined by the presence of plasmids, transposons, and insertion elements; highlighting the role of gain and loss of genes during the process of adaptation in the host and to the hospital setting [74]. Despite considering this organism an "opportunistic pathogen" that can colonize healthy individuals without causing diseases, *A. baumannii* is without debate a major threat for unhealthy individuals.

In the course of infection, biofilm formation facilitates cell adherence, providing a protective shield that is able to thwart external stressors, including host cationic peptides and antibiotic treatments. In this regard, *A. baumannii* is well known for its ability to form biofilms on medical devices used for invasive procedures [75]. Research has identified several genes involved in adherence and biofilm formation, including the csu/A/BABCDE operon, the biofilm-associated protein (BaP) and capsule formation [76,77]. First discovered as a virulence factor required for cell adhesion and biofilms is the outer-membrane protein A (OmpA). Studies have revealed its interaction with host factors such as fibronectin and host-immune cells, highlighting its role in establishing infection. Sugawara *et al*. identified this protein as a porin protein and Ramkumar *et. al* in a more recent paper shed light onto the permeability properties of this porin, explaining its direct role in antibiotic resistance[78,79]. Other factors recently associated with adherence includes a partner secretion system AbFhaB/AbFhaC that is required for attachment to epithelial cells, fibronectin, and virulence in murine and worm models of infection; and the Type 1

secretion system (T1SS) that is proposed to secrete the biofilm-associated proteins (BAP) [80,81].

Evasion or modulation of the innate immune system is also required for infection. In line with this notion, the presence of the K1 locus is required for capsule synthesis, a virulence factor that is important for survival in serum, human ascites fluids, and, murine models [82]. In addition, several groups have studied the role of LPS for *A. baumannii* serum survival, demonstrating that LPS-deficient strains exhibit decreased survival in serum and are less virulent in animal models [61,83].

The characteristic role of lipid A as a potent immune toxic molecule in other Gram-negative pathogens, such as *Escherichia coli* or *Pseudomonas aeruginosa,* has also been observed in *A. baumannii.* Studies has found that lipid A from *A. baumannii* induces the signaling of TLR2/TLR4 receptors found in host immune cells [84]. This pathogen-host interaction initiates a storm of cytokine production and pro inflammatory molecules leading to clinical symptoms such as fever, increased heart rate, and damage to blood vessels during *A. baumannii* bacteremia. It has also been shown that *A. baumannii* add galactosamine or phosphoethanolamine groups to its lipid A, conferring resistance to the cationic host peptides LL-37 and the antibiotic colistin [60]. Other virulence factors important for serum resistance and colonization are the phospholipases C and D; as disruption of genes encoding these proteins decreases the ability of *A. baumannii* to invade epithelial cells and survive in blood compared to other tissues 24 hours after initial inoculation [85].

Perhaps these results could reflect their important role for survival in blood, allowing the development of septicemia, which is one of the most prevalent *A. baumannii* infections.

As nutrients are depleted, bacteria disseminate to proximal sites of infections. To achieve this, bacteria rely on several mechanisms, including interaction with host cells, proteolysis, and, motility. Although first characterized as a non-motile bacterium, the motility patterns among *A. baumannii* clinical isolates are diverse. It has been shown that *A. baumannii* displays surface associated and twitching motility [86]. A connection between motility and several factors, including iron chelated media, blue light, and autoinducer molecules has been established [87,88]. In addition, the capsule genes *epsA*, *ptK*, the *lpsB* gene involved in LPS synthesis, as well as type IV pili and the fimbriae protein A (PilA), have been shown to affect motility in *A. baumannii* [88].

Finally, the role of proteases in other pathogenic bacteria, including deregulation of complement and coagulation cascades, and dispersal of biofilms to facilitate detachment of cells and proliferation, has been demonstrated. The *A. baumannii* genome has several hypothetical proteases, although thus far only the serine protease PFK and the coagulation targeting metallo-endopeptidase of *A. baumannii* (CpaA) have been characterized [89,90]. The PFK protease has been implicated in biofilm dispersion and protection from complement killing, whilst the CpaA protease allows *A. baumannii* to survive in blood and serum as a result of its ability to cleave the purified factor (FV), and fibrinogen, resulting in conditions that promotes dissemination and survival [90].

Genome Plasticity of *A. baumannii*

Amplified fragment length polymorphism (AFLP) analysis of hypervirulent MDR *A. baumannii* outbreak strains recovered from different geographic sites worldwide has led to the classification of three primary international clonal lineages: CC1, CC2 and CC3 [57]. Although other methods such as MLST (multi-locus sequenced typing) are used to classify strains based on mutations present in elements such as housekeeping genes, this section will focus on the use of whole genome sequencing (WGS) as a tool that has revealed unique findings that suggest the concept of genome plasticity in *A. baumannii*.

With the development of sequencing technologies and the availability of more than 2000 genomes of *A. baumannii* strains, unique signatures within isolates belonging to lineages CC1, CC2, and CC3 have been reported [91-93]. These findings have added an additional criterion to define these lineages based on the presence of genetic elements responsible for their multidrug resistance phenotypes that are otherwise absent in the genome of the drug susceptible ATCC 17978, and the environmental microbe *A. baylyi*. [57,94]. Specifically, strains belonging to CC1 possess a signature pathogenic island known as AbaR1 [57,93]. This pathogenic island has been suggested to originate from insertions and transposition events that led to the incorporation of antibiotic genes present in *Pseudomonas*, *Salmonella* and *Escherichia* species into the AbaR1 cluster of *A. baumannii*. Similarly, strains belonging to CC2 lineages are characterized by the presence of eight unique islands that bear several genes required for antibiotic resistance and virulence, including phage proteins, antitoxins, and hemolysins [95]. Of particular note, CC2 strains also contain a pathogenic island named AbaR2 that lacks an extensive region from an integration site

in AbaR1 to 116 nucleotides upstream of the *aphA1* gene, suggesting a deletion event and perhaps divergence from a common ancestor [95]. Strains grouped in the CC3 lineage have the signature genes *aphA6* and *aadB,* which are associated with a class 1 integron conferring resistance to aminoglycosides [96]. In addition, the presence of efflux genes of type *tetA and* ribosomal protection genes of type *tet (M)* are found in this lineage, which allows for resistance to tetracycline and minocycline antibiotics, respectively [97].

In one study, two *A. baumannii* clinical isolates recovered from the same patient named AB210 and AB211 were collected before and after tigecycline treatment respectively. Sequencing analysis revealed a disruption of the *mutS* (DNA repair gene) in AB211 that perhaps could explain the presence of single nucleotide polymorphisms (SNP) in this strain, including one in the *adeS* sensor histidine kinase, which has been linked to increased activity of the AdeABC efflux system in response to tigecycline exposure [98]. Similarly, other studies have found genetic variation as a result of deletions and SNPs in strains from the same clonal lineages collected from the same patients. These findings have provided evidence of the plasticity of the *A. baumannii* genome that enable this bacterium to quickly adapt to antibiotic pressures and stress conditions encountered within the host.

Regulation in *A. baumannii*

The adaptability of *A. baumannii* to unique niches within a host requires a regulatory network able to respond to intrinsic signals, facilitating survival. Given the attention that

this bacterium has gained due to the recurrent recovery of MDR strains from patients, the increase in research within the *Acinetobacter* field has led to the identification of genes with roles in drug and disinfectants resistance, biofilm formation, metal acquisition, motility, and the secretion of virulence factors. However, more recently, this research has extended towards the characterization of regulatory proteins, including two component systems (TCS) and transcription factors (TF).

In this context, genes with putative regulatory functions associated with antibiotic resistance guided much of the initial research in this field, resulting in the identification of the two component systems (TCSs) AdeRS and BaeSR, which have overlapping regulatory roles in controlling expression of the AdeABC efflux pump system [56,99]. The AdeRS regulon is comprised of 579 genes, and deletion of AdeRS leads to a decrease in virulence and biofilm formation [100]. The TCS BaeSR is found to controls expression of the AdeIJK and MacAB TolC efflux pumps systems and is required to resist osmotic stress conditions [99,101].

Further research has characterized three other TCSs: BfmRS, GacSA, and PmrAB [74,102]. BfmRS has been shown to control expression of the *cusA/BABCDE* genes required for biofilm formation[103]. A more recent study identified 1827 genes differentially expressed upon disruption of *bfmRS*, and defined a direct role for BmfRS in regulating cell morphology associated with different growth phases [104]. Work by Peleg *et. al.*, screening of an *A. baumannii* mutant library in a *C. elegans* model of infection identified a gene encoding the GacS sensor as being essential for survival in this model [105]. A subsequent

study identified GacA as the response regulator of GacS, which directly regulates metabolic genes, including the phenylacetate operon which has been found to be important in evasion of the immune system [102,106]. Finally, the PmrAB system have been implicated in controlling genes required for LPS modification resulting in the development of colistin resistance [74,94].

In addition to TCSs, the role of transcriptional regulators in the adaptation and pathogenesis of *A. baumannii* has become the topic of much investigation. The examination of changes in levels of siderophore production, for example, led to the identification of the iron uptake regulator Fur [107]. Work by Hood *et.al* focused on the effects of zinc host sequestration and identified the zinc uptake regulator Zur. Further studies have established the requirement for this latter factor in survival during the course of infection in a murine model of pneumonia [108,109]. Recently, screening of an AB5075 transposon mutant library in a worm model uncovered the requirement of 31 putative transcriptional regulators for survival[110]. From this work, two independent studies following these findings characterized two important regulators: The first, ABUW_1645, was found to induce a phenotypic switch correlated with capsule production and increased virulence [111]. The second, named GigA, was characterized as an orphan response regulator linked to the anti-sigma -sigma factor GigB [112]. In this study, it was proposed that GigA dephosphorylates GigB, resulting in sequestration of the anti-sigma factor NPr, allowing RpoE (σ^E) to function during stressful conditions [112]. Finally, the TF BlsA was found to regulate motility and biofilm formation in response to light, highlighting

the potential role of this regulator to use light as a clue to adapt to external environments; although the significance of this regulator in the context of infection is still unknown [87].

Although these studies have provided some understanding of the regulatory framework within this bacterium, it is important to consider that there are a vast number of uncharacterized regulatory proteins in *A. baumannii*; which forms the focus of the next chapter of this dissertation. Collectively, research is required to elucidate the role of these regulatory proteins, which could aid in explaining the extraordinary capacity of *A. baumannii* to adapt and evolve so rapidly, bestowing it with a great ability to cause disease and persist in the most harsh of environments.

A baumannii Metabolism

A combination of nutrient uptake and nutrient utilization pathways to meet energy requirements for growth and cellular maintenance is of great importance for bacteria to survive and adapt to ever changing environments. In this vein, *A. baumannii* is considered to have a metabolic adaptability that allows for growth when supplemented with nutrients including amino acids (L-phenylalanine, L-histidine, L-leucine, L-arginine, D- malate and L-ornithine), saccharides (glucarate, glucose, xylose, and arabinose) mucin, acetate and ethanol as a carbon sources. [13]. In support of this, a global proteomic analysis examined the cytoplasmic and membrane proteinaceous composition of *A. baumannii* strain ATCC17978, revealing the presence of 37 membrane and 155 cytoplasmic proteins as having putative metabolic functions. These included a glucose sensitive porin that is

homologous to OprB in *P. aeruginosa,* which enables the diffusion of glucose, mannitol, glycerol, and fructose into the cell [113]. In the cytoplasmic fraction, around 36% of proteins were associated with metabolism of amino acids including glutamine, serine, aspartate, methionine, cysteine, tryptophan, lysine, glutamine, proline, histidine, leucine, isoleucine, and valine, suggesting that *A. baumannii* has sturdy amino acid metabolism. Further worked by Farrugia *et.al*. examined the ability of 4 representative clinical isolates to use a panel of 190 individual carbon and nitrogen substrates to support growth. Of this set, 80 carbon and nitrogen sources tested positive for utilization, including amino acids, nitrate, nitrite, ammonia, carboxylic acids, and sugars. These phenotypes were correlated to genes present in the genomes of these strains, supporting the existence of systems dedicated for catabolism and energy generation from these substrates [114,115].

Despite the identification of genes with putative functions in metabolism via proteomic and genomic technologies, a functional characterization of factors, and their involvement in metabolic pathways used for assimilation and utilization of different carbon sources in *A. baumannii* has only just begun. One such example comes from the characterization of genes encoding the Histidine (His) utilization system and a Zinc metalloprotease chaperon *(zigA),* which showed that both are required to allow for histidine degradation to ammonia and glutamate as a nitrogen source and carbon source respectively. [116]. The genes contained in the *paa* operon encode the phenylacetate pathway in *A. baumannii,* which allows for growth on L-phenylalanine as a sole carbon. This operon is required for degradation of this amino acid, and results in the generation of intermediates acetyl-coA and succinyl-coA that are incorporated into the tricarboxylic acid (TCA) cycle. Further to

this, the presence of the porin CarO has been found to be required for L-ornithine uptake and its disruption affects the ability of *A. baumannii* to grow in minimal media supplemented with this amino acid [117]. Additionally, screening of a Tn mutant library of *A. baumannii* uncovered genes required for cysteine/sulfur assimilation, which were also shown to be essential for survival in a worm model of infection [110]. All these studies have collectively provided a further understanding of the function of genes in *A. baumannii* that support amino acid metabolism. Given the presence of putative genes and the ability of *A. baumannii* to grow on the presence of a vast number of amino acids, however, characterization of other pathways required for their assimilation has still yet to be performed [118].

A. baumannii has notably been found to grow in the presence of ethanol as a sole carbon source [119]. Ethanol can be degraded to acetate via acetaldehyde, which is further used to generate acety-coA feeding the TCA cycle [120]. A transcriptional study examined genes differentially expressed in the presence of ethanol and found that several encoding alcohol dehydrogenases, phosphotransacetylase, and acetate kinase were upregulated; supporting the ability of this organism to convert ethanol to acetate that can be further assimilated via the TCA cycle. [121]. In addition, *A. baumannii* can grow on glucose despite the absence of genes encoding hexokinase or glucosekinase, which are required for glucose phosphorylation in the first step of glycolysis. However, the presence glucose dehydrogenases and the pyrroquinoline (PQQ), used to convert glucose to gluconate that then enters Entner-Doudoroff pathway, provides a route in this organism to use glucose as a substrate for growth. Overall these studies have suggested the presence of genes

in *A. baumannii* that allow the use of different metabolic pathways, favoring those for utilization of amino acids that provide a metabolic plasticity for rapid adaptation in response to nutrient availability.

Metal Acquisition in *A. baumannii*

Another important factor in bacterial metabolism is the ability to acquire and utilize metals that are essential for growth and cellular process [122]. The most extensively studied metal acquisition systems in *A. baumannii* is that of iron. In humans, extracellular iron concentrations are maintained between 10-30μM in which ferric iron (Fe^{+3}) is predominantly found to be associated with the host proteins lactoferrin and transferrin. In such conditions, *A. baumannii* is known to express iron sequestering molecules known as siderophores to obtain iron from these host iron proteins [122,123]. The first such siderophore system identified was in strain *A. baumannii* 8399. This system secretes the iron chelator 2,3 -dihydroxybenzoic acid (DHBA), which allows for binding of Fe^{+3} bound to transferrin [124]. Following this, Antunes *et. al.* analyzed the genome of 50 clinical isolates (and identified conservation among 49 of them) of an operon having genes for the production of the siderophore hydroxamate, which was found to be upregulated in iron limited conditions [86,125]. Among the siderophore systems present in this bacterium, the most studied iron acquisition system is the catechol-hydroxymate siderophore acinetobactin that was first identified in work published by Mihara *et. al* who reported a cluster of 18 genes with putative iron acquisition functions [126]. Further phenotypic assays performed in strains with disruption of each gene in this cluster revealed the role of genes *basABCDEFGHIJ* in production of acinetobactin and *barAB* for iron transport [126]. In

addition to the acinetobactin system, a parallel ferric acinetobactin system in *A. baumannii* exists which is comprised of an ABC tripartite system (BauD and BauC putative inner membrane proteins and the putative ferric-siderophore transport ATPase BauE), a putative lipoprotein BauB, and the outer-membrane receptor BauA Disruption of genes encoding these proteins have resulted in reduced growth during limited iron limited conditions supporting their role in iron acquisition in *A. baumannii* [124].

The essential role of genes involved in iron acquisition within the infection process has been demonstrated in *ex vivo* and *in vivo* models. For example, the disruption of genes with functions in production or secretion of acinetobactin siderophores have led to decreased survival in A549 epithelial cells and in the Galleria *mellonella* and mouse sepsis models [127]. Another source of iron is the reduced form of iron Ferrous iron (Fe^{+2}). Several gram-negative bacteria possess genes dedicated to transport ferrous iron into the cell [122]. One transporter conserved among some Gram- negative pathogenic bacteria is the FeoAB system. In *A. baumannii* the FeoAB system has been identified and its disruption resulted in decreased survival in blood, growth defects in limited iron media and increased susceptibility to polymyxin [128].

In addition to iron, zinc is an essential cofactor for numerous enzymes, including metalloproteases. A zinc acquisition system homologous to those in other pathogenic bacteria, including *Pseudomonas aeruginosa, Streptococcus pneumoniae and Listeria monocytogenes*, was discovered in *A. baumannii* [129]. The study published by the Skaar group identified the genes encoding key zinc transporters in *A. baumannii*. This system

was found to be important for competition in zinc acquisition against the host zinc chelator Calprotectin, a protein found in neutrophils, in a mouse pneumonia model [116,129]. Finally, manganese has been shown to be important for bacterial infection as it is used as a cofactor for bacterial proteins with diverse biological functions. In vitro studies have shown that calprotectin also acts as a manganese chelator, with antimicrobial activity against many different pathogenic bacteria, including *A. baumannii* [116]. In a recent studied L. Juttukonda *et. al.* identified a manganese transport system required for growth and virulence in the presence of calprotectin [130].

All this work together shows the importance of *A. baumannii* metal acquisition systems in the course of infection, which allow it to overcome host nutritional limitation strategies. Although these studies have started to reveal these mechanisms in the context of *A. baumannii* infections, more studies are required to provide a better understanding of their role in metal homeostasis and infection, which could aid in the development of new antimicrobials.

Project Aim.

The emergence of virulent and MDR *A. baumannii* strains have directed most of the *Acinetobacter* field towards the identification of virulence determinants and understanding their contribution to pathogenicity and drug resistance. However, the regulatory framework and controlling mechanisms that account for the successful adaptability of this organism are poorly defined. With this in mind, this dissertation sought to further investigate the regulatory framework of this organism. As such, the first part of this work

will present the repertoire of regulatory proteins in *A. baumannii* with an emphasis on their conservation among strains with different virulence and MDR profiles. The primary rationale for this was to use this information to perhaps explain their role in pathogenicity and the evolution of this bacterium. The second aim seeks to explore the function of *A. baumannii* two-components systems, focusing on a homolog of ArcAB and its role in controlling metabolic process for energy generation. Ultimately, the third aim will identify and discuss the role of an uncharacterized operon containing homologs genes to the *fecI* operon found in other Gram-negative bacteria, and its function in the context of iron acquisition. Collectively, the work presented in this dissertation will provide further insights and a deeper understanding of the regulatory framework that exists within *A. baumannii*, and how this contributes to growth survival, adaptation and virulence.

CHAPTER II

TOWARD THE COMPLETE PROTEINACEOUS REGULOME OF ACINETOBACTER BAUMANNII

Note to the reader. This chapter was previously published as a manuscript, and has been included with permission form the publisher. (Appendix 1).

CHAPTER III

IDENTIFICATION OF A NOVEL TWO COMPONENT SYSTEM GOVERNING MEMBRANE ENERGETICS IN ACINETOBACTER BAUMANNII

ABSTRACT. The emergence of hypervirulet multidrug resistant *Acinetobacter baumannii* strains has increased public health awareness worldwide. Whilst genes have been linked to virulence and antimicrobial resistance, the characterization of genes with potential regulatory roles towards these behaviors are still ill-defined. Previously, we reported the identification of regulatory elements in *A. baumannii*, which includes 14 two-component systems (TCSs). Of these, only six have been well characterized to date. A bioinformatic analysis performed on the remaining 8 systems identified the (RR) ABUW_2426, and its corresponding sensor kinase (ABUW_2427) as a homolog of the ArcAB from *E. coli*. Transcriptional analysis using a reporter gene fusion showed that the ABUW_2426/ABUW_2427 operon was induced by the protonophore carbonyl cyanide m-chlorophenylhydrazone (CCCP). Additionally, decreases in intracellular pH and reduced response to dissipation of the electrochemical gradient and increased depolarization of the cytoplasmic membrane were observed in both mutant strains. RNA seq analysis revealed an altered expression of genes involved in energy generation and measurement of metabolites generated via aerobic energy generation pathways further support an altered energy state in our mutants. In summary, we demonstrate that disruption of ABUW_2426/ABUW_2427 alters the metabolic state of *A. baumannii*,

concomitantly affecting energy generating pathways dependent processes resulting in an increased susceptibility to aminoglycosides.

INTRODUCTION

Acinetobacter baumannii is a Gram-negative bacterial pathogen commonly associated with life threating and deadly diseases, including skin and soft-tissue infections, urinary-tract infections, ventilator associated pneumonia, meningitis, endocarditis and septicemia. Such infections are commonly in patients from healthcare facilities, and primarily those in intensive care units [34,131-133]. The first line therapeutics used to treat *A. baumannii* infections are broad spectrum antibiotics, including cephalosporins, fluoroquinolones and carbapenems[17,48,134]. Resistance among clinical isolates to these agents is, however, becoming increasingly common, leading physicians to explore alternatives, such as aminoglycosides, to treat multidrug-resistant (MDR) infections [135,136]. Unfortunately, the recurrent isolation of pan-resistant *A. baumannii* strains on a global scale has complicated such therapeutic intervention[47,137-140]. As a result, the Worldwide Health Organization (WHO) has categorized *A. baumannii* in the highest priority group of pathogens, who are defined as being the most critical organisms for new antimicrobial drug development[141].

During infection, bacterial pathogens encounter myriad of unfavorable environmental conditions, including osmotic stress, heat stress, acid stress, oxidative stress, nutrient limitation and host cationic antimicrobial peptides[142,143]. Under these harsh conditions,

survival is dependent on an adaptive response controlled by regulatory elements, such as transcriptional regulators (TF), σ factors and two-component systems (TCSs)[144-146]. Of these regulatory elements, TCSs are widely employed by bacteria to sense and response to environmental stimuli[147]. TCSs normally consist of a membrane sensor histidine kinase (HK) that, upon perceiving external insult, autophosphorylates at a conserved histidine residue[148,149]. This phosphate group is then transferred to a conserved aspartate residue on its cytoplasmic response regulator (RR) partner that is typically a DNA binding protein[150,151]. This signal transduction cascade leads to the coordinated activation or repression of genes required for a wealth of responses, including biofilm formation, motility, and the expression of adherence proteins, exotoxins, efflux pumps and outer membrane porins [152].

Recently, we performed a study to identify the entire proteinaceous regulome of *A. baumannii* strains. As part of this work we identified 14 TCSs conserved within the genome of a variety of representative clinical isolates,[153] with only six having been characterized to date, including BfmSR, PmrAB, AdeRS, BaeRS, Ompr-EnvZ and GacSA [56,99,112,154-156]. These systems have been shown to influence the expression of genes required for various functions, including motility, biofilm formation, metabolism and the expulsion of antimicrobials via efflux pumps. *[100,101,157]*

Herein, we present the characterization of one of the uncharacterized TCS, demonstrating that it is an *A. baumannii* homolog of the ArcAB system (Aerobic Respiratory Control) found in *E. coli* and other organisms [158,159]. Early work on this

system, using an *arcA* mutant of *E. coli*, revealed alterations in the enzymatic activity of proteins belonging to the TCA (tricarboxylic acid cycle), glyoxylate shunt, and other energy generation pathways, alongside the repression of genes involved in anaerobic respiration in the presence of oxygen.[158]. Later work identified ArcB as the sensor partner of the ArcA response regulator[159,160], demonstrating that, in the absence of oxygen, autophosphorylation of ArcB leads to the phosphotransfer to ArcA and activation/repression of genes associated with energy generation, glycolysis, fermentation, and cellular respiration[161-163]. Although oxygen levels were initially proposed as the activation signal for ArcAB, the kinase activity of ArcB is in fact dependent on changes in the redox state of the cell as a result of variation in ubiquinone and menaquinone concentrations [164-166]. In the presence of oxygen the transfer of electrons from quinones to cysteine residues located in the N-terminal domain of ArcB has the effect of silencing ArcB kinase activity and suppressing the activation of ArcA [167].

ArcAB homologs with similar functions have also been reported in other organisms, including *Salmonella enterica, Shewanella oneidensis, and Haemophilus influenzae*[168-172]. Independent studies on ArcAB in these organisms has identified genes functioning in motility, metabolism, and cell division as belonging to the ArcA regulome[173-175]. Other studies in *H. influenzae* and *S. enterica* have also shown the important regulatory role of ArcAB in responding to oxidative stress induced by H_2O_2 [174] [173]. Similar results to this latter point have also been reported in *E. coli* [176]. Further work has demonstrated a role for ArcA in facilitating *E. coli* colonization of the intestinal epithelium in a mouse model, a niche that is devoid of oxygen [177]. In *S. enterica*, *arcA* and *arcB* have been shown to be

required for dissemination in a murine model of infection, and for survival in macrophages[178].

Using a bioinformatic approach, we identified the ABUW_2426 RR and its cognate HK ABUW_2427 as homolog of ArcAB from *E. coli*. Transcriptional analysis revealed that the proton ionophore carbonyl cyanide m-chlorophenylhydrazone (CCCP), which collapses the PMF, induces the *arcAB* promoter. Further to this, we determined that disruption of *arcA* and *arcB* in *A. baumannii* leads to decreased membrane polarity and acidification of the cytoplasm. Transcriptomic profiling of an *arcA* mutant revealed altered expression of genes involved in metabolism and energy generation, leading to an abundance of metabolites produced from an overactive glyoxylate shunt, and increased activity of energy generation pathways typically used by bacteria growing in the absence of oxygen. Collectively, our data identifies the ABUW_2426/2427 TCS as an ArcAB homolog that controls the expression of a variety of genes necessary for modulating membrane energetics and metabolic pathways in *A. baumannii*.

MATERIAL AND METHODS

Bioinformatic analyses. A search for homologues of ABUW_2426 and ABUW_2427 in the genome of *Escherichia coli* K-12 MG1655 (GenBank accession no. NC_000913), was performed using blastp searches (with an *E* value ≤10^{-20} and coverage of ≥60%). Protein sequences of ArcA and ArcB from *Eschericha coli*, *Salmonella enterica, Vibrio cholerae, Haemophilus influenzae, and Shewanella oneidensis* were downloaded from the NCBI

ftp server (www.ncbi.nlm.nih.gov/genome) and alignments were generated using CLC Genomics Workbench (version 7.6.1; CLC bio). Topology maps of ArcA and ArcB proteins were generated using the protter tool (http://wlab.ethz.ch/protter/start/).

Strains and growth conditions. The strains and cloning primers used in this study are listed in **Table 1**. All strains were cultured in lysogenic broth (LB), unless otherwise indicated, with shaking at 37°C. When appropriate, antibiotics were added for selection: tetracycline at a final concentration of 5 μg/mL and hygromycin at a final concentration of 140 μg/mL. Mutants of ABUW_2426 (*arcA*) and ABUW_2427 (*arcB*) were acquired from the AB5075 transposon mutant library[179]. Strains were confirmed using primers OL4155/OL4156 (*arcA*) or OL4157/OL4158 (*arcB*). Unless stated otherwise, synchronous cultures were prepared as follows: *A. baumannii* strains were grown in LB overnight at 37°C with shaking. These cultures were then diluted 1:100 into 100mL of fresh LB, grown to exponential phase, before being used to seed new 100mL cultures at an OD_{600} of 0.05.

Table 1. Bacteria strains, plasmids and cloning primers

Strain	Description	Source
E. coli		
DH5α	Cloning strain	[1]
A. baumannii		
AB5075	Wild-type strain	[2]
AB5075 178::T26	AB5075 with transposon insertion in ABUW_2426	[2]
AB5075 156::T26	AB5075 with transposon insertion in ABUW_2427	[2]
LGC2591	AB5075 178::T26 complemented with pMQ557::*arcA*	This study
LGC2592	AB5075 156::T26 complemented with pMQ557::*arcB*	This study
LGC2463	AB5075 containing pSLG2 (P_{arcB}–*lacZ* fusion)	This study
Plasmids		
pMQ557	Cloning vector for complementation	Gift, Dr. R. Shanks, University of Pittsburgh
pAZ106	Promotorless *lacZ* insertion vector	[3]

Table 1 (Continued)

pSLG1	pAZ106::P_{arcB}–*lacZ*	This study
pSLG2	pMQ557::P_{arcB}–*lacZ*	This study
pSLG3	pMQ557::*arcA*	This study
pSLG4	pMQ557::*arcB*	This study
Primers		
OL4155	ATGCCCGGGGGTAATCAAGTCAAGGTCGA	This study
OL4156	ATGCCCGGGTTAGTGGTGGTGGTGGTGGTGTTGCTTATCCTGAATCAATC	This study
OL4158	ATGCCCGGGTTAGTGGTGGTGGTGGTGGTGGTGAAACTCTTGCACCAAGC	This study
OL4169	ATGGGATCCATAACCGCTGCCCACCATGCT	This study
OL4170	ATGGAATTCTACGACAATTGCTGCCCATA	This study
OL4230	ATGCTCGAGATAACCGCTGCCCACCATGCT	This study
OL4232	ATGGCGGCCGCGACCCAACGCTGCCCGAGAAA	This study

*Underscore indicates restriction enzyme site

Construction of an *arcAB-lacZ* transcriptional fusion strain. A PCR fragment was generated that begins 500 nt 5' of *arcB* and ends 1309 nt 3' of it, using primers OL4169/OL4170. This fragment was cloned into the vector pAZ106, which contains a promoter-less *lacZ* cassette, creating plasmid pSLG1. This plasmid was then used to amplify the P_{arcB}-*lacZ* fusion fragment using primers OL4230/OL4232, which was subsequently cloned into the *A. baumannii* shuttle vector pMQ557, resulting in plasmid pSLG2. AB5075 was then transformed with pSLG2, and colonies were selected using LB plates supplemented with hygromycin (plasmid encoded). All strains were confirmed by PCR.

Construction of *arcA* and *arcB* complementation strains. A 3,979 bp fragment including 500 bp upstream and downstream of the *arcB* gene, and a 4,945 bp fragment that is identical to the first, but also includes the complete *arcA* gene as well, were amplified using primers OL4155/OL4158 and OL4155/OL4156, respectively. These PCR products were cloned into pMQ557, creating plasmids pSLG4 and pSLG3, respectively. Clones were confirmed by PCR and Sanger sequencing (MWG Operon), before being transformed into the relevant *A. baumannii arcA* and *arcB* mutants. *A. baumannii* strains were again confirmed by PCR and Sanger sequencing (MWG Operon).

Transcriptional profiling assays using β-galactosidase. A plate-based screening assay was performed as previously described [180]. Briefly, LB plates were overlaid with 5mL of LB top agar (0.7% w/v) supplemented with X-Gal at a final concentration of 40μg/mL and the *A. baumannii* P_{arcA}-*lacZ* fusion strain. Sterile disks were placed on plates and each disk was inoculated with 10μL of a given chemical stressor. Plates were incubated overnight at 37°C and induction of expression was recorded as a blue halo around the filter discs. For expression over time, synchronize cultures at an OD_{600} of 0.05 were prepared in LB as detailed above, before the following compounds were added at subinhibitory concentrations: Chloramphenicol = 12.5 μg/mL, Ampicillin = 100 μg/mL, Gentamicin = 100 μg/mL, Sulfanilamide = 100 μg/mL, CCCP = 6.25 μg/mL N'N' dicyclohexylcarbodiimide (DCCD) 100 μg/mL, Valinomycin 25 μg/mL, and 2-4 dinitrophenol 75 μg/mL. Cultures were incubated with shaking at 37°C, with 0.1mL samples collected every hour. Levels of β-galactosidase were measured as described previously[181]. Results are presented from three independent experiments.

Intracellular pH measurement. Synchronous cultures were prepared in Mueller Hinton Broth (MHB) before being centrifuged and washed with a potassium phosphate buffer, pH 7.0, supplemented with 5mM EDTA. Cell were then pelleted again and resuspended in the same buffer, followed by the addition of the BCECF-AM dye at a final concentration of 20μM. Samples were then incubated for 30 minutes at room temperature. After this time, cells were pelleted, washed and resuspended in the same buffer, followed by the addition of glucose to a final concentration of 10mM. Samples were incubated for 5 minutes at 37 °C, before 200μL aliquots were withdrawn and added to the wells of a 96-well plate. Fluorescence signals were read for 5 minutes at an excitation of 490nm and emission of 530nm using a BioTek Synergy II plate reader. As a control, CCCP at a sub-inhibitory concentration of 6.25 μg/mL was added to decrease the intracellular pH. To create a calibration curve, cells were resuspended in high potassium buffers with a pH range from 6.5 to 8.0. Results are presented from three independent experiments.

Membrane Depolarization Assay. Membrane depolarization was measured using the membrane potential sensitive fluorescent DISC3 dye (3,3'-Dipropylthiadicarbocyanine Iodide). Synchronous cultures of the wild-type and its *arcA* and *arcB* mutants were prepared as detailed above before being harvested by centrifugation and washed 3 times with 5 mM HEPES buffer, pH 7.2, containing 5mM glucose. Samples were then resuspended to an OD_{600} of 0.05 in the same buffer. Cell suspensions were incubated with 100mM KCl and 2 μM of DISC3 for 15 min at room temperature. Mixtures were added to the wells of 96 well plates, and lysozyme was added at decreasing concentrations. Fluorescence was monitored at an excitation wavelength of 662nm and an emission

wavelength of 670nm. Reads were taken for a period of 30 minutes at 2 minutes intervals. Results are presented from three independent experiments.

RNA Sequencing and Bioinformatic Analysis. RNAseq experiments were performed as described previously [182]. Briefly, synchronous cultures of the *A. baumannii* wild-type and *arcA* mutant strain were prepared in biological triplicate. After growth for 1 hours, CCCP was added to a final sub-inhibitory concentration of 6.25 µg /mL. Cultures were allowed to grow for 2 additional hours, before 5 mL was harvested from each flask. This was added to 5 mL of ice-cold PBS, pelleted by centrifugation at 4°C, and the supernatant removed. Total RNA was isolated using a RNeasy Kit (Qiagen) and DNA was removed using a TURBO DNA-free kit (Ambion). Sample quality was assessed using an Agilent 2100 Bioanalyzer system with an RNA 6000 Nano kit (Agilent). AN RNA integrity value of >9.7 was used as a cutoff. Prior to mRNA enrichment, biological triplicate RNA samples were pooled at equal concentrations followed by rRNA removal using a Ribo-Zero Kit for Gram Negative Bacteria (Illumina) and a MICROBExpress Bacterial mRNA enrichment kit (Agilent). Removal efficiency of rRNA was confirmed using an Agilent 2100 Bioanalyzer system and an RNA 6000 Nano kit (Agilent). Library preparation was performed using the TruSeq Stranded mRNA Kit (Illumina) omitting mRNA enrichment steps. Quality, concentration, and the average fragment size of each sample was assessed with an Agilent TapeStation and High Sensitivity DNA ScreenTape kit. Library concentration for the pooling of barcoded samples was assessed by qPCR using a KAPA Library Quantification kit (KAPA Biosystems). Samples were run on an Illumina MiSeq with a corresponding 150-cycle MiSeq Reagent kit. Upon completion, data was exported

from BaseSpace (Illumina) in fastq format and uploaded to Qiagen Bioinformatics for analysis. Data was aligned to the AB5075 reference genome (NZ_CP008706.1), and experimental comparisons were carried out after quantile normalization using the Qiagen Bioinformatics experimental fold change feature. https://www.ncbi.nlm.nih.gov/geo/. Raw data from this study can be found at GEO Accession number GSE123635, Token oxczecoehvyxfah.

Quantitative real time PCR. Quantitative real time PCR (qPCR) analyses were conducted as described previously using primers detailed in **Table 2**. [181] Bacteria cultures were grown and RNA extracted as described for the RNA-seq experiment in this study. Data is derived from three independent replicates.

Table 2. List of qPCR primers used in this study.

Strain		qPCRGene
OL4498	CCTAGAGATAGTGGACGTTACTCG	*16S* ***F***
OL4499	CCAGTATCGAATGCAATTCCCAAG	*16S* ***R***
OL4694	TTCACGAGATTAATACTGACTGGAG	*pqqA* ***F***
OL4695	ACCAATACGTAAATCAGTGAAAGC	*pqqA* ***R***
OL4696	AGGCAATGTCGGTGATATTC	*gcdH* ***F***
OL4697	TGTAATCGAGGCACGTAAAC	*gcdH* ***R***
OL4698	CTTGCGCCTGGTTCTAAA	*acnA* ***F***
OL4699	AAAGGACCTGAGTTACCAATAC	*acnA* ***R***

Table 2. (Continued)

OL4700	AGTTCATACAACCGCCAATAC	*Pta* **F**
OL4701	CACAGTCACCGTAGACATAGA	*Pta* **R**
OL4702	CTATGGTTTCCACGGTACAAG	*ackA* **F**
OL4703	CACAAGTCGAGCTACCATTAC	*ackA* **R**
OL4704	CTTCATTCGCTGAAGCATTAC	*eno* **F**
OL4705	AAACCACCTTCATCACCTAC	*eno* **R**
OL4706	GTCAGGTGTTAGCGGTAAAT	*sdhC* **F**
OL4707	CAAATCCTTCTGGTGAAGATAATG	*sdhC* **R**
OL4708	GCAAACATTCGTGGAAGATTAC	*Pil* **F**
OL4709	GATGGCTAATACACAGCACTT	*Pil* **R**
OL4710	CACGTTTAATCGCTCCTCTT	*atpB* **F**
OL4711	GTGAGGGTCCATACCAAATAC	*atpB* **R**
OL4712	GGTTCTTGGAATATCCGTTGTA	*csuB* **F**
OL4713	AACCATTCTTCATACGTCTTGT	*csuB* **R**

Letters in bold indicate F= Forward ; R= Reverse

Intracellular metabolite quantification assays. To measure intracellular metabolite concentrations, the wild-type and its *arcA* and *arcB* mutants, alongside complemented strains, were synchronized and grown for 3 hours in LB media. For glucose quantification, cultures were supplemented with glucose to a final concentration of 0.2% w/v. After 3 hours, cells were collected by centrifugation and lysed using a Mini BeadBeater -16 (Biospec). For acetate, pyruvate and succinate quantification, cells were resuspended in

100µL of their dedicated assay buffer (Biovision) before lysis. For pyruvate quantification, cells were not lysed, but instead were pelleted by centrifugation and pyruvate was extracted with 4 volumes of pyruvate assay buffer (Biovision). For NADH, cells were also not lysed, but instead were pelleted by centrifugation and total NADH (NADH and NAD) extracted with 400 µL extraction buffer (Biovision). NAD was decomposed by incubating samples for 30min at 60 °C. Intracellular metabolite quantification was then performed using a: glucose colorimetric assay kit (Biovision), acetate colorimetric assay kit (Biovision), pyruvate colorimetric assay kit (Biovision) oxaloacetate colorimetric assay kit (Biovision), succinate colorimetric assay kit (Biovision), or NADH colorimetric assay kit (Biovision), all as per the manufacturer's protocol. All data is derived from three independent replicates

Antimicrobial susceptibility assays. Overnight cultures from the wild-type and its *arcA* and *arcB* mutants were diluted 1:1000 in fresh MHB and 180µL was transferred to the wells of a 96-well plate. Antibiotics were added to wells in decreasing concentrations to a final volume of 200µL. Plates were incubated at 37°C and the OD_{600} was determined following overnight incubation to quantify growth or lack thereof. All assays were performed in biological triplicate.

Assaying ATP levels within cells. The wild-type and its *arcA* and *arcB* mutants, alongside complemented strains, were synchronized and grown for 3 hours in LB media. Following 1 hour of growth, CCCP was added to a final sub-inhibitory concentration of 6.25 µg /mL and cultures were allowed to grow for 2 additional hours. Cells were then

washed and pelleted by centrifugation, resuspended in HEPES buffer and allowed to incubate on ice for 30 minutes. These samples were then incubated in the presence of pyruvate (10mM) at 30 °C for 30 minutes. After incubation cells were collected and resuspended in ATP buffer (Biovision), before being lysed using a Mini BeadBeater -16 (Biospec). ATP quantification was performed using an ATP colorimetric assay kit (Biovision) following the manufacturer's protocol. Data is derived from three independent replicates.

Determination of cytochrome oxidase activity. The wild-type and its *arcA* and *arcB* mutants, alongside complemented strains, were synchronized and grown for 3 hours in LB media. Cells were collected and resuspended in 1X assay buffer (10mM Tris-HCl, 120mM KCl pH 7.0) before being lysed using a Mini BeadBeater -16 (Biospec). Cytochrome activity was quantified using a cytochrome c oxidase assay kit (Sigma-Aldrich) following the manufacturer's protocol. Data is derived from three independent replicates.

RESULTS

Identification of ArcAB homologs in the genome of *Acinetobacter baumannii*. Previously, our group performed a global analysis of the *A. baumannii* genome, identifying its complete set of regulatory factors.[153] To extend this work herein, we focused our attention on the 14 two component systems identified in strain AB5075. While six of these have been studied, the remaining TCSs have yet to be characterized. As such, we

performed a smart BLASTP analysis to identify homologs that could provide insight into possible functions of the uncharacterized TCSs. In so doing, we identified a response regulator and histidine kinase (ABUW_2426 and ABUW_2427, hereafter referred to as Anoxic Respiration Control (ArcAB)), with strong similarities to other previously characterized ArcAB modules found in *Escherichia coli, Salmonella enterica, Vibrio cholerae, Haemophilus influenzae, and Shewanella oneidensis.* (**Supplemental Figures S1 and S2, Table 3**).

Table 3. Blast analysis of ABUW_2427 and ABUW_2426 from *A. baumannii* identifies them as ArcAB homologs.

Organism	Protein	Identity[1]	Similarity[2]	Reference
Escherichia coli	ArcB	31%	54%	[4]
	ArcA	24%	46%	
Salmonella enterica	ArcB	31%	54%	[5]
	ArcA	24%	46%	
Haemophilus influenzae	ArcB	29%	49%	[6]
	ArcA	27%	48%	
Shewanella oneidensis	ArcB	30%	50%	[7]
	ArcA	27%	44%	
Vibrio cholera	ArcB	30%	52%	[8]
	ArcA	26%	47%	

[1]Shown is the percent identity from a BLASTP analysis using ABUW_2426 (ArcA) and ABUW_2427 (ArcB).
[2]Shown is the percent similarity from a BLASTP analysis using ABUW_2426 (ArcA) and ABUW_2427 (ArcB).

Looking at the topology of the *A. baumannii* sensor ArcB revealed a membrane bound HK with 14 transmembrane (TM) domains and very limited exposure to the periplasm; with both the N- and C-terminus orienting to the cytoplasm (**Figure 1**). The *A. baumannii* HK seemingly lacks an obvious input sensory domain, which is perhaps explained by the observation that HKs with large numbers of TM domains typically sense membrane

associated stress[150,151]. Interestingly the ArcB of *H. influenzae* also lacks a sensory domain, but is able to complement an *arcB* mutant of *E. coli*, suggesting that this domain maybe not be required for ArcB function[171]. Beyond this, the *A. baumannii* HK has a classic transmitter domain (aa683-749) that harbors a conserved histidine residue (H693), a HTApase domain (aa796-909) and a receiver domain (aa930-1042) with a conserved aspartic residue (D980). The presence of both, transmitter and receiver domains in the same HK (including other ArcB homologs) has previously been described (known as HK hybrids) and is believed to enhance the signal transmission via a phosphorelay mechanism.

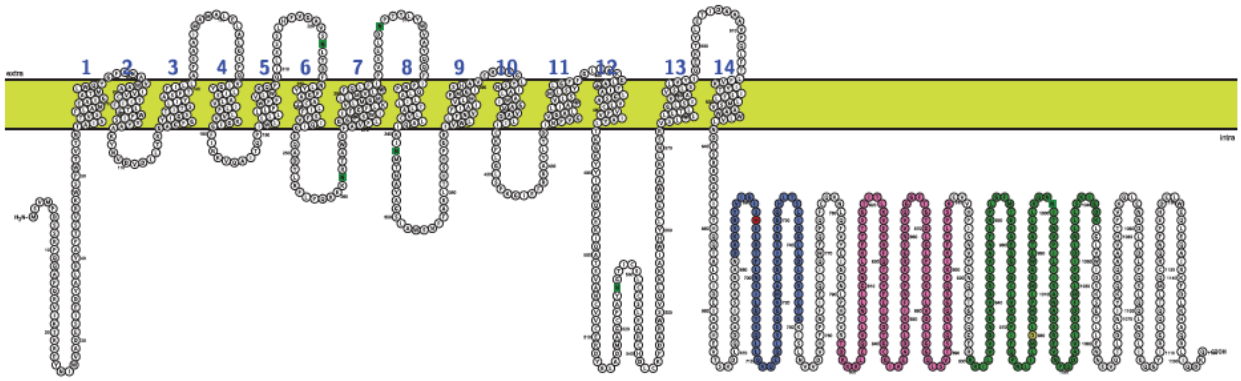

Figure 1. Predicted topology of ArcB from *A. baumannii*. Shown is the predicted topology of ArcB from *A. baumannii* generated using the Protter bioinformatic website. Depicted are 14 predicted transmembrane domains. Blue shading indicates amino acids located in the transmitter domain. Red shading indicates the conserved histidine reside (H693). Pink shading indicates amino acids located in the HTApase domain. Green shading indicates residues located in the receiver domain. Yellow shading indicates the conserved aspartic acid residue (D980).

Of note, although present in other ArcB proteins, the *A. baumannii* homolog seemingly lacks a phosphotransferase (Hpt) domain, which participates in the phosphorelay mechanism of hybrid HKs. In this scenario, activation of ArcA is achieved by the transfer of a phosphate within ArcB from a histidine residue in the transmitter domain, to an

aspartic acid residue in its receiver domain, and finally to a second histidine residue in the phosphotransferase (Hpt) domain. From here, ArcB transfers the phosphate to an aspartic residue of ArcA located in its receiver domain.[183-185]. The lack of a Hpt domain in the ArcB of *A. baumannii* could suggest the participation of an additional protein harboring a Hpt domain. In such a situation, the Hpt containing protein could accept the phosphate group from the aspartic acid residue located in the receiver domain of ArcB and transfer it to ArcA. Indeed, this type of signaling pathway has been described for the RcsCB TCS of *E. coli* [186].

We also found differences in sequence homology in areas that facilitate regulation of phosphotransfer in ArcB. Specifically, the *E. coli* ArcB has two cysteine residues (aa180, aa241) within its sensor domain that are oxidized by quinones during aerobic growth to facilitate dephosphorylation of ArcA. Conversely, during anaerobic growth reduction of these cysteine residues occurs as a result of decreased ubiquinone pools, which induces ArcB kinase activity, leading to phosphorylation of ArcA. This dual-cysteine arrangement is only conserved in *S. enterica*, whilst *V. cholera* and *A. baumannii* only have Cys 180, whilst *H. influenzae* and *S. oneidensis* appear to lack both residues. The lack of conservation of both cysteine residues does not appear to affect the function of ArcB in these organisms, suggesting that regulation of ArcB kinase is potentially quite variable across different organisms[171,187].

We also generated alignments for ArcA proteins, and found that all organisms have a conserved aspartic acid within the N-terminus that is known to be phosphorylated by ArcB

to activate ArcA in *E. coli*. Beyond this, we found a strong conservation of amino acid residues in the regulatory domain located at the interface α4-β-5-α5 from ArcA in *E. coli*, including those residues present at the interface of this region that facilitate dimer formation[188]. Lastly, the ArcA proteins from each of the organisms used in our comparison analysis have been classified as OmpR family members based on conservation of the C-terminal winged- helix turn helix (HTH) binding motif that distinguishes RR regulators grouped in this family[189]. Interestingly, we observed low conservation of this region in the ArcA protein of *A. baumannii*. Indeed, in a previous bioinformatic study by our group on the proteinaceous regulome of *A. baumannii*, we classified ABUW_2426 as a LuxR-type response regulator based on homology of its tetrahelical HTH motif [153,189]. As such, this would perhaps suggest a divergent origin and/or function of the ArcA protein within *A. baumannii*.

We next compared the *arcAB* genomic organization in *A. baumannii* with previously characterized *arcAB* clusters from the same five different bacteria (**Figure 2**). In *E. coli* and *S. enterica* the genetic organization is very similar, with *arcB* located 4 genes upstream of its RR *arcA*. Conversely, in *S. oneidensis arcA* is located 7 genes upstream of *arcB*. *V. cholera* has a more traditional arrangement, with the RR located adjacent to the sensor but in the opposite transcriptional direction. Finally, *A. baumannii* is the only organism from this collection that bears a classic TCS arrangement, with *arcB* and *arcA* clustering immediately adjacent to each other, in the same transcriptional direction. Interestingly, with the exception of *E. coli* and *S. enterica*, none of the organisms maintain any type of similarity for surrounding genes, with each encoded in entirely unrelated areas

of the genome. This unique arrangement could perhaps reflect horizontal acquisition of these genes across different species.

Expression of the ArcAB TCS is induced upon disruption of the proton gradient in *A. baumannii*. To explore a potential function for the putative ArcAB cluster in *A.*

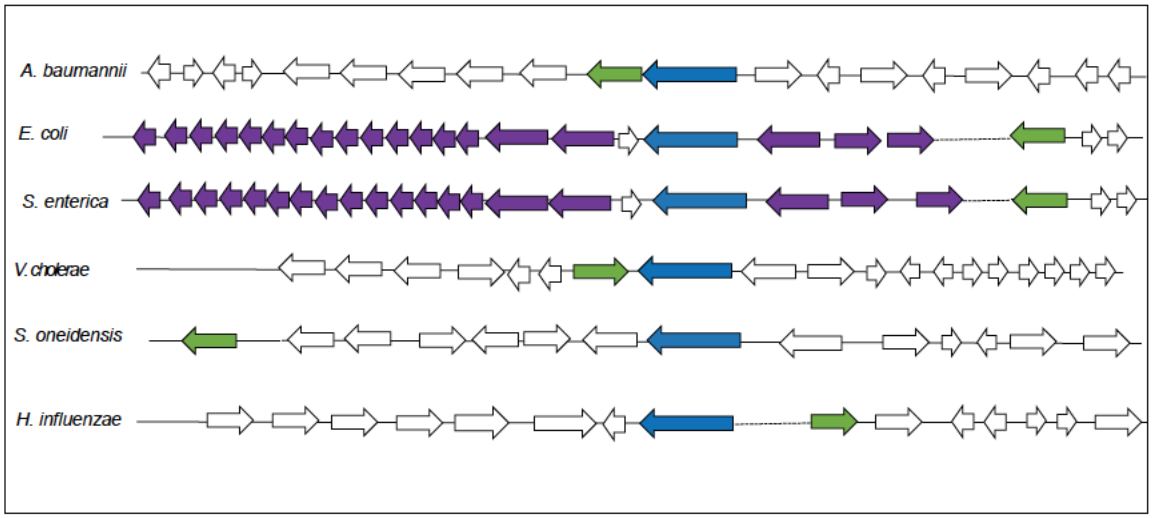

Figure 2. **Syntenic comparison of the *arcAB* module from *A. baumannii.*** Genes are shown as arrows indicating the direction of transcription. Green arrows indicate *arcA* genes, whilst blue arrows indicate *arcB* genes. White arrows correspond to genes with no similarity to any surrounding gene across the various organisms. Purple arrows indicate genes of shared homology between *E. coli* and *S. enterica*, encoding proteins with the same known or predicted function.

baumannii we first set out to examine how its transcription is induced in the cell by external stress. As such, a *lacZ*-reporter gene fusion was created for the *arcAB* promoter in the wild-type strain and used in a plate-based disk diffusion-based assay detailed by us previously [190]. Of the 23 different compounds used, which elicited myriad cellular stresses (including, DNA stress, oxidative stress, osmotic stress, detergent stress, alkali stress, acid stress, nitric oxide stress, alcohol stress, and membrane stress), we observed that only the protonophore CCCP resulted in enhanced expression of the *arcAB* promoter (**Supplemental Figure S3**).

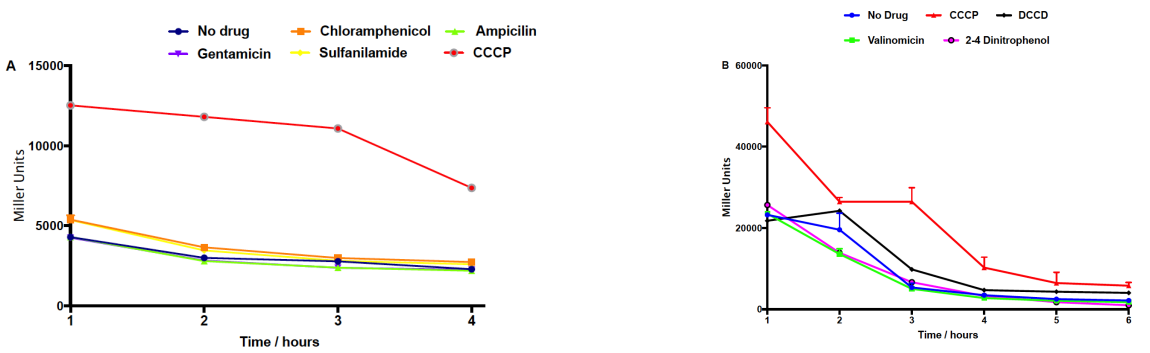

Figure 3. *arcAB* transcription is induced upon exposure to the protonophore CCCP. ß-galactosidase activity of an *arcAB-lacZ* fusion strain was measured hourly during exposure to sub-inhibitory concentrations of the agents shown. Transcriptional activity is expressed as Miller Units. Data is derived from three independent experiments, with error bars shown as +/- SEM.

To validate this observation, β-Galactosidase activity in the fusion strain was measured over time in the presence or absence of sub-inhibitory levels of several compounds used in the plate-based screen. Again, we observed that transcription from this promoter was very low in all conditions other than those containing CCCP (**Figure 3A**). This finding is of interest because CCCP has the effect of collapsing the PMF by shuttling protons against the electrochemical gradient across the cell membrane, into the cytoplasm. This results in a decline in proton-coupled ATP production, and thus changes in the energy state of the cell; resulting from decreased movement of electrons along the respiratory chain, and a concomitant reduction in ubiquinone pools [191,192]. To explore this phenotype more broadly, we next measured the activity of this promoter in the presence of uncouplers with different mechanism of actions. These included N'N' dicyclohexylcarbodiimide (DCCD), an inhibitor of the ATPase subunit F_o/F_1 that impedes translocation of H^+ resulting in the arrest of ATP production; valinomycin, an uncoupler that increases the efflux of potassium (K^+) ions and disrupts membrane potential; and 2-4 dinitrophenol, a protonophore that translocate H^+ ions against the electrochemical

gradient. Interestingly, we again observed that *arcAB* promoter activity was only higher in the presence of CCCP as compared to the other uncouplers, supporting a specific response of the *arcAB* promoter to this agent (**Figure 3B**). This corroborates that seen for other ArcAB systems, which sense a reduction in the concentration of quinones during electron flow, and the subsequent decline in ATP production, as the respiratory chain ceases; which effectively mirrors a diminished PMF caused by CCCP. [168,172,187,193,194]

Disruption of ArcAB impairs the PMF in *A. baumannii*. Given that our transcriptional studies demonstrate that *A. baumannii* induces expression of *arcAB* in response to a decreased PMF and limited cellular ATP (induced by CCCP), we next wanted to determine if deletion of *arcA* or *arcB* resulted in an altered PMF within the cell. Collectively, the PMF consists of a transmembrane proton gradient (△pH) and a transmembrane potential (ΔΨ), both of which are important for maintenance of an electrochemical gradient across the cell membrane [195,196]

Accordingly, we first used the pH sensitive dye BCECF-AM to measure the transmembrane proton gradient. This dye crosses the bacterial membrane and is hydrolyzed by bacterial esterases to give a fluorescence signal used as a measure of intracellular pH. Upon treatment of the wild-type, *arcA* and *arcB* mutants and complemented strains with this dye, alongside an addition of glucose to energize the cells, a steady increase in the intracellular pH was observed for the parent and complemented strains. This indicates active pumping of (H^+) protons across the membrane as a result of active glycolysis. (**Figure 4A**). In contrast, the *arcA* and *arcB* mutants showed no significant changes in intracellular pH during this same analysis, indicating a lack of

proton exchange across their membranes. In addition, we also observed an overall lower intracellular pH for both mutant strains, indicating a higher proton (H^+) concentration within the cell. This would again suggest the mutants lack the ability to pump H^+ ions out of the cell, confirming an ablated transmembrane proton gradient in these strains.

As an additional step in these analyses, we also added the protonophore CCCP midway through incubation as a control. This would have the effect of bringing protons (H^+) across the membrane to decrease the intracellular pH. As expected, a rapid decrease in the intracellular pH of the wild-type and complemented strains was observed, followed by recovery from cytoplasmic acidification, indicating the ability of these strains to respond to intracellular pH shifts. In contrast, we did not observe any changes in the intracellular pH for either mutant upon addition of CCCP. The lack of response to CCCP from our mutant strains is logical given that this molecule requires an energized membrane to produce its H^+ transport effect; whilst our mutant strains appear to have defects in their membrane energetics.

We next sought to measure transmembrane potential using the voltage sensitive dye DiSC3 (5), which accumulates and quenches itself in negatively charged cytoplasmic membranes. Thus, when membranes are depolarized the DiSC3 (5) dye is released because the cytoplasmic membrane is less negatively charged, resulting in increased fluorescence. As shown in **figure 4B**, DiSC3 (5) fluorescence increased 2-fold in intensity in the *arcA and arcB* mutants, compared to the parental and complemented strains. Thus, it would appear that our mutant strains have a destabilized cellular membrane, indicating that the second component of the PMF, transmembrane potential, is also disrupted.

Taken together, these results suggest that disruption of *arcAB* hinders energy generation pathways (a hallmark of *arcAB* mutants in other organisms [164,197]), resulting in imbalances of PMF components.

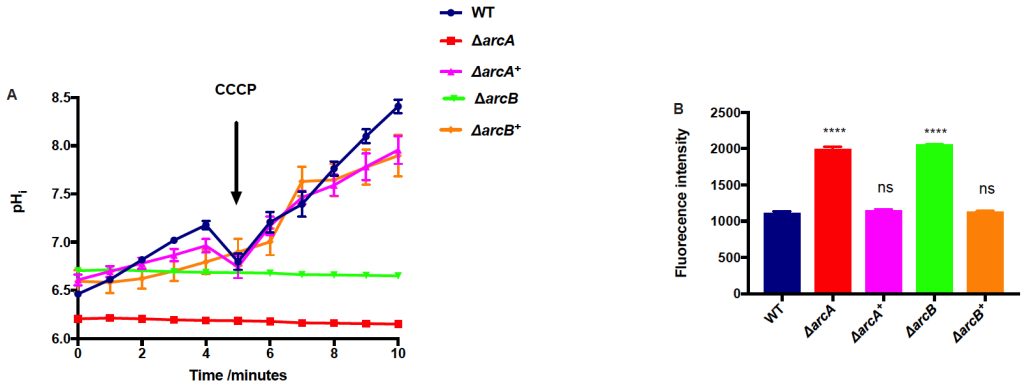

Figure 4. *A. baumannii arcAB* mutants have a reduced intracellular pH and depolarized membrane. (A) Intracellular pH was measured using the pH sensitive dye BCECF_AM. Exponentially growing cells were treated with the dye alongside the addition of glucose to a final concentration of 10mM. A black arrow indicates the time at which CCCP was added to cultures to a final concentration of 6.25 µg/mL, which is sub-inhibitory. Data is derived from 3 independent experiments, with error bars shown as +/- SEM. **(B)** Depolarization of the cytoplasmic membrane was monitored by measuring release of the fluorescence dye DiSC3 (5). Data is derived from three independent experiments, with error bars shown as +/- SEM. Student's t-test was used to assess statistical significance, **** = $p<0.0001$. ns = not significant relative to the wild-type.

Transcriptomic profiling reveals a shift in expression of genes required for glucose utilization upon *arcA* disruption. To determine if the ArcAB system in *A. baumannii* has functional similarity to that of other organisms, and to specifically hone in on its mechanistic role, we next set out to explore its regulon using RNA-seq technologies. Given that transcription from the *arcAB* promoter is minimal under standard conditions (above and in [198]), and that CCCP dramatically induces the expression of this system, we performed these experiments using the wild-type and *arcA* mutant grown in the presence of a sub inhibitory concentration of this compound for 2h. Upon analysis, we identified 725 genes that were significantly differentially expressed between the two

strains at a level ≥ 2-fold. (**Figure 5A, Supplemental Table S1**). This included 379 that were upregulated in the mutant strain, and 346 that were downregulated. These findings were confirmed via qRT-PCR for a collection of unrelated genes, demonstrating similar fold changes in all cases (**Supplemental Figure S4**). When these alterations were parsed into their ontological groups (**Figure 5B**) we found that the majority of transcriptional changes were for genes associated with regulatory-, transport-, energy- or metabolic-functions.

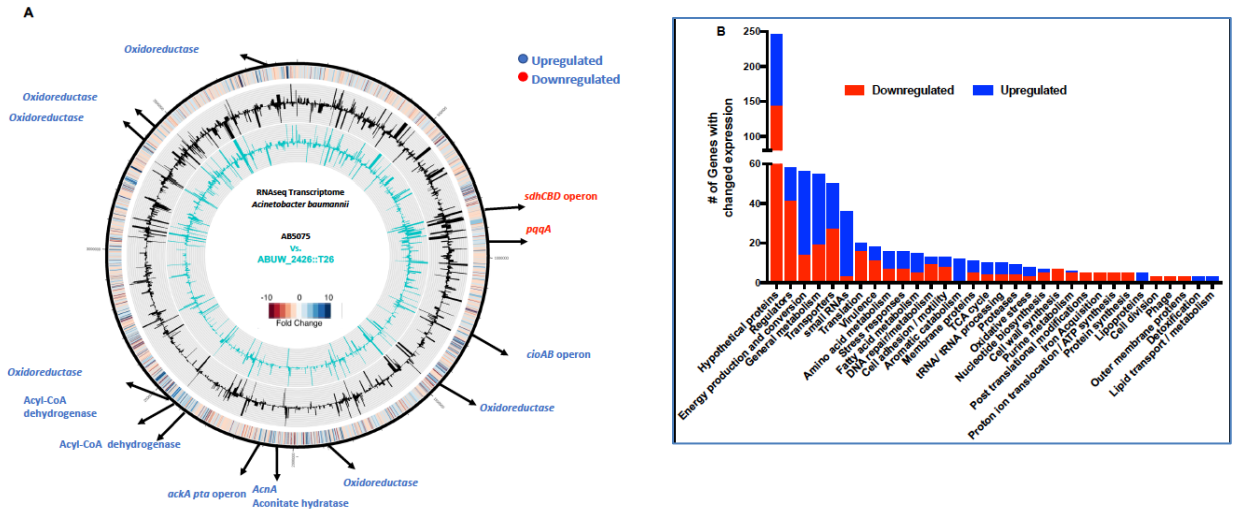

Figure 5. Transcriptomic profiling of the *arcA* mutant. (**A**) Genomic map showing major transcriptional changes in *ΔarcA* compared to the parental strain after 2h of exposure to a sub-inhibitory concentration (6.25 µg /mL) of the protonophore CCCP. The outermost circle represents a heat map of changes in *ΔarcA* compared to AB5075. The middle circle (black) depicts RPKM values for AB5075. The inner circle (turquoise) depicts RPKM values for *ΔarcA.* Black arrows at specific locations within the map highlight genes that function in energy conversion and production. Genes in blue are upregulated and in red are downregulated in *ΔarcA*. (B) Categorization of genes differentially expressed in *ΔarcA* compared to AB5075 based on predicted functions.

One of the most striking findings from this collection was a 30-fold decrease in expression of the Coenzyme PQQ synthesis protein A (*pqqA*). This enzyme is involved in Pyrroquinolone quinone (PQQ) synthesis, which is a required cofactor for the conversion of glucose to gluconate in *Acinetobacter calcoaceticus* [199,200]. This is important because *A. baumannii* is unable to undergo the initial steps of the glycolytic pathway as it lacks the

early components of the Embden-Meyerhof-Parnas (EMP)[114]. Instead it metabolizes gluconate to gluconate-6-P initially via the Entner Doudoroff pathway (ED), before processing this further via the remaining ED pathway, or the Pentose Phosphate pathway (PP) (**Figure 6**). From here, this can be fed into the later stages of glycolysis via those EMP pathway genes that are present in *A. baumannii*. Given the magnitude of this change in *pqqA* expression, one might reasonably expect that glucose would potentially accumulate in our mutant strain, given its potentially impaired ability to process this carbon source metabolically. As such, we determined the intracellular concentration of glucose within our various strains (**Figure 7**). In so doing we noted that our mutants have an increased concentration of intracellular glucose compared to the wild-type and complemented strains. This suggests an accumulation of glucose in the mutants, which may serve as a response to its slower processing within their cells.

Interestingly, genes encoding enzymes from the EMP and PP pathways that would process the generated gluconate-6-P are also downregulated in our mutant strain. These include glyceraldehyde-3-phosphate dehydrogenase (gap = -2.34) and phosphopyruvate hydratase enolase (*eno* = -2.55) from the EMP pathway, and ribulose-phosphate 3-epimerase (*rpe* =-2.06) from the PP pathways. This would tend to suggest that our mutant strain might bypass these metabolic avenues, and instead choose to create pyruvate, which could be fed in the TCA cycle (**Figure 6**). To test this, we measured the intracellular concentration of pyruvate for our wildtype, mutants and complemented strains (**Figure 8A**). In so doing, we noted that our *arcA* and *arcB* mutants had much higher levels of pyruvate (*arcA* = 1.92mM and *arcB* = 3.21 mM) compared to the wildtype (0.5mM) and

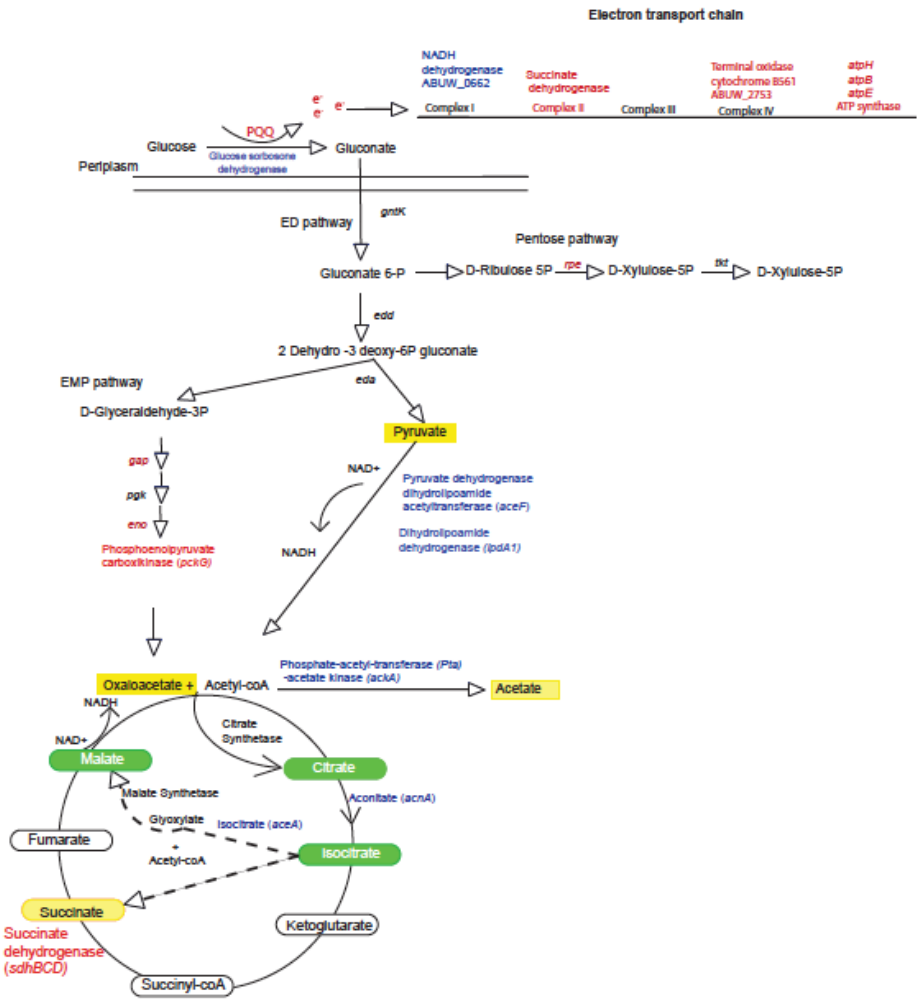

Figure 6. Metabolic map for *A. baumannii* indicating nodes of change in the *arcA* mutant. Shown is a metabolic map for *A. baumannii* depicting genes with altered expression from the transcriptomic analysis of *⊿arcA*. Blue font indicates genes upregulated in the mutant, whilst red indicates genes that are downregulated. Green boxes indicate metabolites of the glyoxylate pathway. Dashed arrows indicate the two products formed (glyoxylate and succinate) from isocitrate conversion through the glyoxylate shunt. Yellow boxes indicate accumulated metabolites in the *⊿arcA* strain.

complemented strains (*arcA*$^{+}$ = 1.2 mM and *arcB*$^{+}$ = 0.67 mM). Interestingly, elevated levels of pyruvate have been previously reported in *arcA* mutants of *E. coli* as a result of a higher influx of glucose via the ED pathway[197].

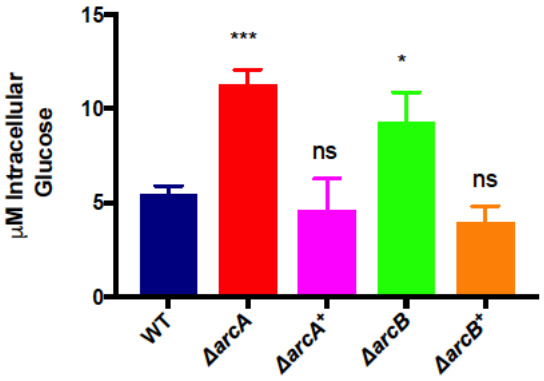

Figure 7. Disruption of ArcAB leads to increased glucose concentrations within the cell . Cultures from exponentially growing strains were lysed and glucose concentrations measured using a glucose colorimetric assay kit (Biovision). Data is derived from three independent experiments. Error bars are shown in +/- SEM. Significance was determined using a Student's t-test, * = $p<0.05$, *** =$p<0.0001$, ns = not significant relative to the wild-type.

Increased glycolytic influx in the *arcA* mutant favors activation of the Pta-AckA pathway generating acetate from pyruvate. Interestingly, our RNA-seq dataset reveals increased expression of the pyruvate dehydrogenase dihydrolipoamide acetyltransferase (*aceF*) and dihydrolipoamide dehydrogenase (*lpdA1*), which form the pyruvate dehydrogenase complex that converts pyruvate to acetyl CoA (**Figure 6**). This would make sense given that our mutant accumulates pyruvate, and that the generated acetyl-coA could then be fed into the TCA cycle to generate energy. Additionally, when bacterial cells grow rapidly in the presence of excessive amounts of glucose, the phosphotransacetylase-acetate kinase (Pta-AckA) pathway is known to be induced, favoring the conversion of acetyl-coA to acetate [120,201] to prevent what is known as carbon overflow, which can have toxic effects. Interestingly, we found the *ackA-pta* operon was upregulated in the *arcA* mutant (*ackA* = 3.37 and *pta* = 3.54 fold), thus it seems reasonable to hypothesize that our *arcA* mutant might be preventing carbon overflow, caused by excessive glucose accumulation and consumption, by generating higher

amounts of acetate. To explore this, the wild-type, mutants, and complemented strains were cultured in LB media, and cells were collected to measure intracellular acetate levels. As shown in **figure 8B**, we observed that the *arcA* and *arcB* mutants had significantly higher concentrations of intracellular acetate (*arcA* = 25.4 nmol/mL and *arcB* = 32.60 nmol/mL) than the wild-type (10.27 nmol/mL) and complemented strains ($arcA^+$ = 9.57nmol/mL and $arcB^+$ = 14.64 nmol/mL). Accordingly, it appears that upon disruption of *arcA* cells do indeed produce significantly more pyruvate, which is redirected towards acetate production so as to prevent the potentially negative effects of excessive carbon flow through the TCA cycle.

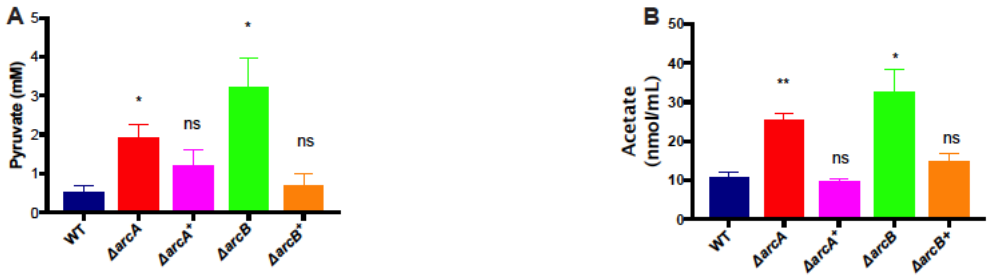

Figure 8. Increased pyruvate levels in *arcA* and *arcB* mutant strains leads to a glyoxalate shunt that favors acetate production. The levels of pyruvate (**A**) or acetate (**B**) was measured in exponentially growing cells using either a pyruvate colorimetric assay kit (Biovision) or an acetate colorimetric assay kit (Biovision). Data is derived from three independent experiments, with error bars shown as +/- SEM. Student's t-test was used to assess statistical significance * = $p<0.05$, ** =$p<0.001$, ns = not significant relative to the wild-type

***arcA* mutants of *A. baumannii* use an incomplete TCA Cycle, instead favoring the glyoxylate shunt:** When examining the expression of genes for the TCA cycle in *A. baumannii*, we noted that aconitate hydratase-1 (*acnA*) and isocitrate lyase (*aceA*) were both upregulated in our mutant strain. This latter gene is of particular interest as it is used to circumvent the complete TCA cycle, instead facilitating the glyoxylate shunt (**Figure**

6). This finding would appear to make sense as we also observed diminished expression of succinate dehydrogenase, which allows for the conversion of succinate within the TCA cycle into fumarate. As such, one would predict that our *arcA* mutant is unable to complete the full TCA cycle, and is thus forced into using the glyoxylate shunt to generate energy. As a consequence, the malate produced would be converted to oxaloacetate, which in turn would then have two fates: Firstly, oxaloacetate can be converted into phosphoenolpyruvate that can be funneled into gluconeogenesis. Importantly, in our mutant, the enzyme phosphoenolpyruvate carboxykinase, which catalyzes the conversion of oxaloacetate to phosphoenolpyruvate is downregulated. Secondly, citrate synthetase catalyzes the 1:1 condensation of oxaloacetate and Acetyl-coA to generate citrate, thus continuing the glyoxylate shunt. Because the glyoxylate cycle produces increased oxaloacetate that is used for gluconeogenesis, and that the enzyme required for this step is downregulated in our mutant, it could be possible that oxaloacetate accumulates in mutant cells. To test this, we grew our wild-type, mutants and complemented strains in LB media, and measured oxaloacetate concentrations within cells. Upon analysis, we observed that both *arcA* and *arcB* mutants had higher amounts of oxaloacetate (*arcA* = 27.87µmol/µL and *arcB* = 22. 65 µmol/µL) than the wildtype (8.51 µmol/µL) and complemented strains ($arcA^+$ = 9.69 µmol/µL and $arcB^+$ = 5.46 µmol/µL) (**Figure 9A**). These results confirm that our mutants accumulate oxaloacetate as a result of an impaired conversion of oxaloacetate to phosphoenolpyruvate.

Of note, the glyoxylate pathway has the interesting side effect of generating succinate as a byproduct. As suggested earlier, the *arcA* mutant has diminished expression of the

enzyme that converts succinate into fumurate, succinate dehydrogenase. As such, one might reasonably predict that the limited activity of this enzyme would lead to accumulation of succinate within our *arcA* mutant cells as a result of a stalled TCA cycle. Accordingly, the wild-type, mutant and complemented strains were grown in LB media, before extracts were generated and the level of succinate within cells determined (**Figure 9B**). In so doing, we noted that the *arcA* and *arcB* mutants had much higher levels of succinate within their cells (*arcA* = 41.47 and *arcB* = 43.20 ng/mL). Conversely, succinate levels were lower in the parental (11.71ng/ml) and complemented strains (*arcA*$^+$ = 15.87ng/mL and *arcB*$^+$ 13.24ng/mL). As such, this confirms our hypothesis and RNAseq data, that a stalled TCA cycle created by decreased succinate dehydrogenase expression has the result of succinate accumulation in mutant cells.

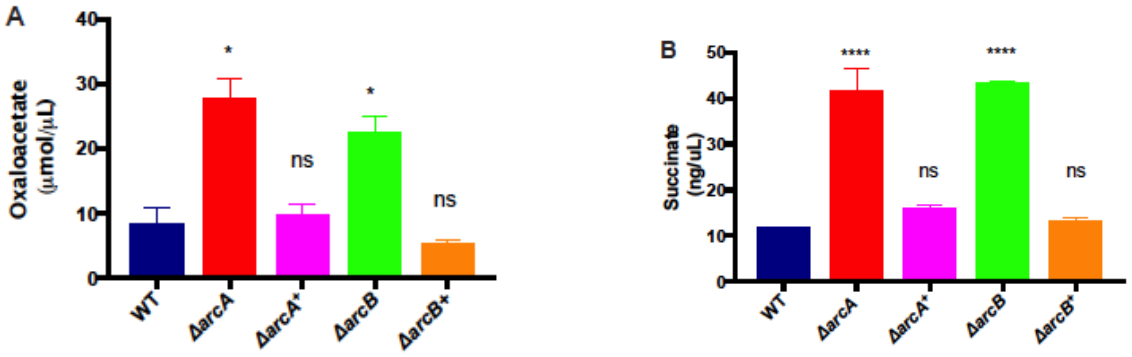

Figure 9. Disruption of ArcAB leads to the accumulation of oxaloacetate and succinate as a result of an impaired TCA cycle. The concentration of oxaloacetate (**A**) or succinate (**B**) was measured in exponentially growing cells using either an oxaloacetate colorimetric assay kit (Biovision) a succinate colorimetric assay kit (Biovision). Data is derived from three independent experiments, with error bars shown as +/- SEM. Student's t-test was used to assess statistical significance * = $p<0.05$, **** = $p<0.0001$, ns = not significant relative to the wild-type.

NADH levels are increased in the *arcA* mutant as a result of its hyperactive glyoxylate shunt: During the glyoxylate shunt, malate is converted to oxaloacetate by the enzyme malate dehydrogenase. This has the side effect of generating NADH as a byproduct (**Figure 6**). As such, one might reasonably hypothesize that our *arcA* mutant, engaging in a hyperactive glyoxylate shunt, would have increased cellular levels of NADH as a consequence. Accordingly, we next set out to measure the NADH levels in our collection of strains (**Figure 10**). In so doing, we observed that the *arcA* and *arcB* mutants had significantly higher levels of NADH (*arcA* = 4.9pmol/mg and *arcB* = 5.2 pmol/mg, respectively) compared to the wildtype and complemented strains (WT = 3.1pmol/mg, $\triangle arcA^{+}$ = 3.3 pmol/mg and $\triangle arcB^{+}$ = 3.2 pmol/mg). This implies that the increased levels of NADH in our mutants may be the result of a hyperactive activity of TCA enzymes generating NADH. Additionally, the excess NADH produced is perhaps unable to be oxidized via the ETC due to a reduction in its activity[202]. This is supported by our transcriptome analysis, which showed decreased expression of genes encoding the succinate dehydrogenase complex (*sdhC* -3.72*, sdhD* -2.4tyrt3 and *sdhB* -2.05), also known as complex II, which has distinct roles in both the TCA cycle and ETC; a gene encoding part of the cytochromes b_{c1} complex III, (*cyoE* -2.64 fold) which has a high affinity for oxygen; a putative complex IV terminal oxidase cytochrome B561 (ABUW_2753, -4.14 fold); and genes within the ATP generation machinery: *atpH, atpB* and *atpE* (-2.65, -2.28 and -2.02 fold)[203] [204]. All this together supports a disruption of the respiratory chain that likely result in a decreased electron flow and explains the lack of proton gradient in our mutants in the presence of glucose.

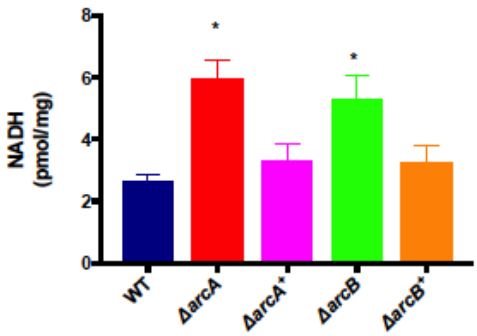

Figure 10. Disruption of ArcAB results in elevated intracellular NADH levels. Intracellular levels of NADH were measured in exponentially growing cells for the wild-type, △*arcA*, △*arcA*$^{+}$, △*arcB* and △*arcB*$^{+}$ strains using a colorimetric assay kit (Biovision). Data is derived from three independent experiments, with error bars shown as +/- SEM. Student's t-test was used to assess statistical significance, * = $p<0.05$.

The altered metabolic state of *arcAB* mutants favors ATP production via substrate phosphorylation: The generation of ATP in bacteria occurs via two major processes: oxidative phosphorylation, which is dependent on a functional PMF; and substrate phosphorylation, which is dependent on the partial oxidation of metabolites [205-207] .Given that we observed an imbalance in the PMF of our mutant strains, as well as a seemingly impaired ETC, one might hypothesize that the first of these two processes would be diminished upon *arcAB* disruption. As such, to test our hypothesis the wild-type, and its *arcA* and *arcB* mutants, alongside their complemented strains, were grown for 3 hours before being processed to determine their ATP levels (**Figure 11A)**. These assays were performed in the presence of pyruvate, which, during aerobic growth, is converted to acetyl-CoA before being oxidized via the TCA cycle, resulting in the donation of electrons to the ETC; thus feeding both pathways for bacterial ATP generation. Upon comparing this data to that generated in the absence of pyruvate, we observed a slight increase in ATP levels in our mutants (*arcA*= 28.7 pmol/ µL, *arcB* = 47.9 pmol/µL) as compared to the wildtype and complemented strains (wild-type = 17.2 pmol/µL, △*arcA*$^{+}$= 16.0 pmol/µL

and △*arcB*$^{+}$ =14.6.pmol/μL) (**Figure 11A)**. These findings may be the result of the hyperactive glyoxylate shunt observed in our mutants strains, which would result in the enhanced generation of ATP via substrate phosphorylation. Conversely, when ATP levels were measured after incubation with pyruvate, we observed reduced ATP levels (*arcA*= 85.0 pmol/ μL, *arcB* = 30.7.pmol/μL) in both mutants when compared to the WT and complemented strains (wild-type 106.6 pmol/μL, △*arcA*$^{+}$= 121.1 pmol/μL and △*arcB*$^{+}$ =83.6.pmol/μL) (**Figure 11B)**. These results are perhaps explained by a stimulation of the TCA cycle in our wild-type and complemented strains, resulting in excess ATP generation. The fact that our mutants demonstrate diminished ATP production in these assays compared to the parent are perhaps a result of an impaired ability to generate ATP via oxidative phosphorylation.

We next hypothesized that ATP levels amongst the various strains might be equalized by inhibition of the ETC in the wild-type and complemented strains, impairing their capacity to engage in oxidative phosphorylation. As such, we repeated these studies in the presence of sub-inhibitory concentrations of CCCP, which disrupts the electrochemical gradient. When these assays were performed (**Figure 11C)**, the basal ATP levels across all strains was found to be essentially the same. After treatment with CCCP and pyruvate, however, we found that the *ΔarcA* and*ΔarcB* mutants (220.4 pmol/μL and 151.7 pmol/μL, respectively) demonstrated significantly higher levels of ATP when compared to the wildtype and complemented strains (wild-type = 108.3 pmol/μL, △*arcA*$^{+}$= 95.5 pmol/μL and △*arcB*$^{+}$ = 105.1 pmol/μL) **(Figure 11D).** As such, it would appear that when ATP generation via oxidative phosphorylation is abolished by the addition CCCP our mutants

actually generate higher levels of ATP than the wild-type and complemented strains. Collectively, these data suggest that our mutant strains are impaired in their capacity to produce ATP via oxidative phosphorylation, but compensate for this defect by their capacity for ATP generation via substrate phosphorylation.

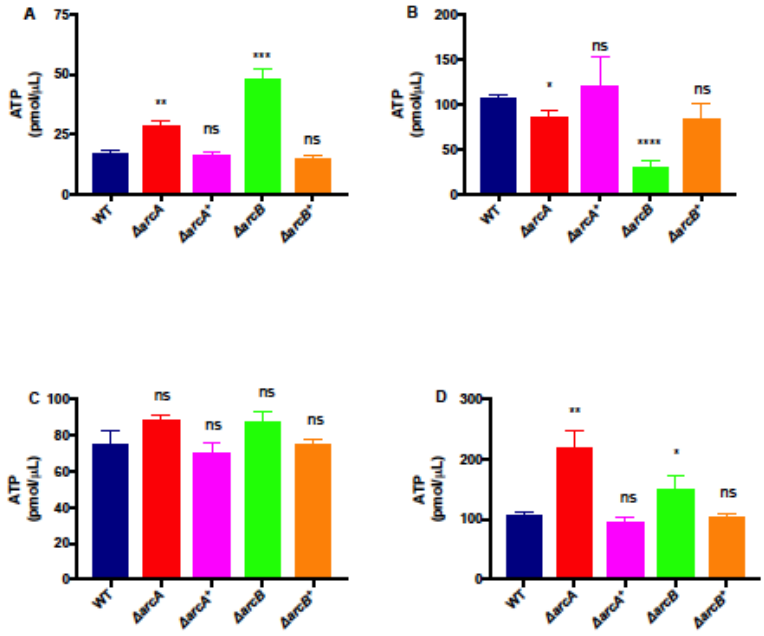

Figure 11. *arcAB* mutants produce ATP via substrate phosphorylation more efficiently than through oxidative phosphorylation. Intracellular ATP levels were measured using a colorimetric assay kit (Biovision) in exponentially growing cells from the wild-type, Δ*arcA*, Δ*arcA*$^{+}$, Δ*arcB* and Δ*arcB*$^{+}$ strains. Strains were grown in LB alone (A), or LB containing: pyruvate (10mM), a sub-inhibitory concentration of CCCP (6.25 µg mL^{-1}) (C), both CCCP (6.25 µg mL^{-1}) and pyruvate (10mM). Data is derived from three independent experiments, with error bars shown +/- SEM. Student's t-test was used to assess statistical significance, * = $p<0.05$, ** =$p<0.01$, *** =$p<0.001$, **** = $p<0.0001$, ns = not significant relative to the wild-type.

Cytochrome oxidase activity is reduced as a result of *arcAB* disruption: Our findings above suggest that our mutants have increased production of ATP via substrate

phosphorylation, whilst generating lower ATP levels via oxidative phosphorylation. This effect seems to be mediated via an altered ETC in our mutants, which hinders ATP production as a result of an impaired PMF. To test this hypothesis, we used an assay that measures activity of the cytochrome oxidase C to gauge activity of the ETC (**Figure 12**). In so doing, we observed lower activity of cytochrome oxidase in our mutants (△*arcA* = 0.02 U/mL and △*arcB* = 0.04 U/mL) compared to our wildtype (0.11 U/mL) and complemented strains (△*arcA*$^{+}$= 0.08 and △*arcB*$^{+}$ = 0.07). Collectively, these findings suggest that disruption of *arcAB* affects the function of the aerobic respiratory chain, impacting the energy status of the cell, which in turns upregulates alternative metabolic and energy generation pathways in our mutants.

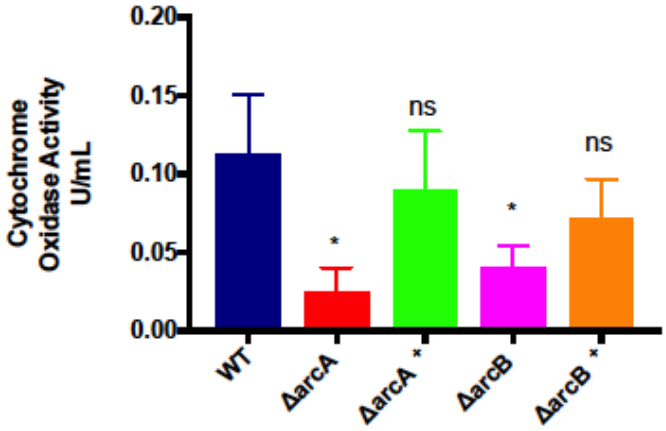

Figure 12. The altered metabolic state of *arcAB* mutants results in impaired aerobic respiration. Cytochrome activity was measured in exponentially growing cells of the wild-type, △*arcA*, △*arcA*$^{+}$, △*arcB* and △*arcB*$^{+}$ strains using a colorimetric assay kit (Sigma-Aldrich). Activity of the cytochrome oxidase is expressed in U/mL, where U is defined as one unit needed to oxidize 1.0 μmol of ferricytochrome in one minute at pH 7.0 at 25 °C. Data is derived from three independent experiments, with error bars shown as +/- SEM. Student's t-test was used to assess statistical significance, * = $p<0.05$, ns = not significant relative to the wild-type.

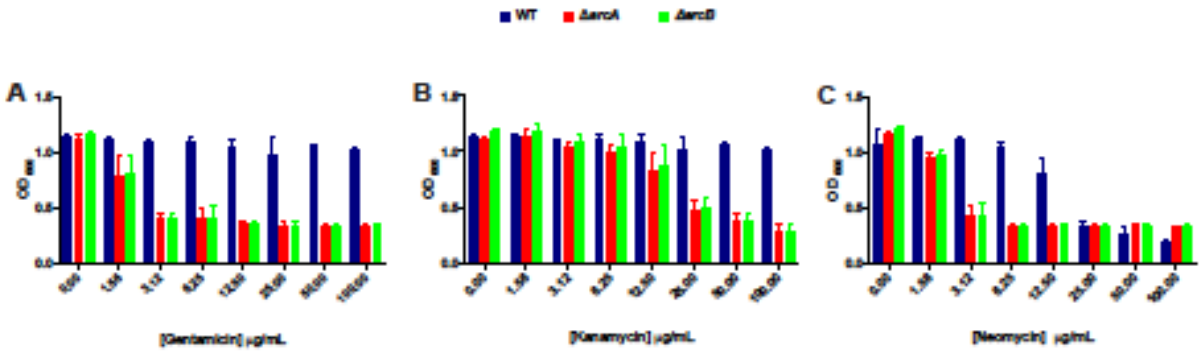

Figure 13. ArcAB mutants demonstrate increased susceptibility to aminoglycoside antibiotics. Determination of bacterial growth (OD_{600}) for the wild-type, Δ*arcA* and Δ*arcB* strains in the presence of increasing concentrations of: (A) Gentamicin, (B) Kanamycin, and (C) Neomycin. Data is derived from three independent experiments, with error bars shown as +/- SEM.

The accumulation of oxaloacetate in *arcA* mutant cells leads to aminoglycoside hyper-susceptibility: Work by others in *E. coli* and *Edwardsiella tarda* has shown that the addition of glutamate results in elevated levels of oxaloacetate, which favors the formation of pyruvate and acetyl-coA that enters the TCA cycle[208]. This has the interesting side-effect of an increased susceptibility to aminoglycoside antibiotics. In the same study, a strain with a mutation in *pckG*, which encodes a phosphoenolpyruvate carboxykinase (converts oxaloacetate to phosphoenolpyruvate) had a null PMF and increased susceptibility to aminoglycosides. This is believed to function via a redistribution of metabolites that are directed into other metabolic pathways as a result of a disrupted TCA cycle, leading to accumulation of TCA intermediates that can act synergistically with aminoglycosides independent of PMF. Given that we observed elevated levels of oxaloacetate in our mutants, we next tested our collection of strains for sensitivity to aminoglycosides, alongside an array of control antimicrobial agents. Intriguingly, both of our mutants showed specific increased susceptibility to

aminoglycosides when treated with ≥3.12µg/mL of gentamicin and neomycin, and ≥25 µg /mL of kanamycin (**Figure 13**). In contrast, the wild-type exhibited a resistant phenotype to all concentrations of aminoglycosides tested. Importantly, no significant changes in resistance profiles between the mutants and parental strain were observed for any of the other antibiotics tested (**Supplemental Figure S5**). Thus, the increased susceptibility to aminoglycosides of our mutant strains appears to result from an overflow of metabolites as a result of the altered metabolism upon disruption of the ArcAB system.

DISCUSSION

In this study we follow up on our previous work exploring the regulatory networks of *A. baumannii*, identifying an uncharacterized TCS with highly structural similarities to that of ArcAB in *E. coli*. A key finding of our study was the response of the *arcAB* promoter to the protonophore CCCP. The protonophore CCCP, has been shown to bypass the ATP synthase-dependent active transport of protons (H^+) into the cytoplasm by increasing membrane permeability to H^+. As a result, a halt in activity of ATP synthase and ATP synthesis takes place, leading to disruption of the electron transport chain. This has the effect of limiting the transfer of electrons to quinones and decreases the PMF; altering the energy status of the cell.[165,209 210]. The effects of CCCP impacting energy generation are similar to those observed during the transition from aerobic to anaerobic growth in *E. coli*. As oxygen becomes limited, a reduction in energy generation via the respiratory chain results in reduced quinone pools. This is sensed by two conserved cysteine residues (aa180, aa241) within ArcB, which are oxidized when quinone pools are plentiful.

Consequently, their depletion as a result of diminished oxygen levels leads to reduction of the cysteine residues, activating the kinase activity of ArcB. It then undergoes autophosphorylation, passing its phosphate group to ArcA, which in turn activates the expression of genes involved in alternative energy generations pathways.

Importantly, during our bioinformatic study of the *A. baumannii* ArcB protein we observed that one of these two cysteine residues was indeed conserved [167]. When looking at other ArcB homologs, we noted that the dual cysteine arrangement was only considered between *E. coli* and the closely related *S. enterica*, whilst *V. cholera* and *A. baumannii* retain only the first Cysteine residue (aa180), and *H. influenzae* and *S. oneidensis* lack both. Notably, the ArcB of *H. influenzae* is incapable of fully complementing an *arcB* mutant of *E. coli*, highlighting the importance of these residues in sensing oxygen gradients via ubiquinone [171]. Furthermore, the genes encoding for ubiquinone production are absent in *H. influenzae*, perhaps eliminating the need for these cysteine residues in its ArcB protein [211,212]. As such, one might speculate that the ArcB of *A. baumannii* also senses ubiquinone pools, and is regulated by oxidation at its lone cysteine residue, which is perhaps sufficient to control its kinase activity in a manner similar to that reported in *E. coli*.

To explore our findings with CCCP a little more fully, we tested the impact of other uncouplers with distinct mechanisms of action towards membrane energetics on the *arcAB* promoter. These included DCCD, valinomycin, and 2-4 Dinitrophenol; none of which altered the expression of this TCS. This is perhaps explained by their specific and

discrete effects on the cell, for example DCCD inhibits ATPase activity without significantly reducing electron flow through the ETC [213-215]. Similarly, the disruption of membrane potential caused by valinomycin has little impact on oxygen consumption [216]. Finally, 2-4 DNP has been shown to accelerate respiration by stimulating complete oxidation of intermediate metabolites such as succinate and fumarate[217,218]. As such, given that none of these agents induce activity of the *arcAB* promoter, the specific response of the *arcAB* system to CCCP could be explained by its targeted effects on quinones pools, as it is the only uncoupler that inhibits hydrogen pumping by cytochrome c and disrupts the electrochemical gradient[192,219] This would be in line with our assertions above proposing a role for ArcB in controlling membrane energetics through the oxidation status of its conserved cysteine residues; akin to that seen in other organisms.

When we examined the effects of disruption of ArcAB on components of the PMF, we observed that our mutants exhibited an absence of proton gradient in the presence of glucose, as well as depolarization of their membranes, suggesting an inability to generate energy from glucose. Of note, *A. baumannii* is unable to assimilate glucose, but instead generates energy from the conversion of glucose to gluconate via the PQQ pathway, which produces electrons that feeds the respiratory chain. PQQ synthesis is dependent on the expression of six genes arranged in an operon *pqqABCDEF*[220]. Previous studies on regulation of PQQ biosynthesis in the soil bacteria *Pseudomonas putida* and *M. extorquens* found that expression of *pqqB* or *ppqF* drives the synthesis of PQQ, and that levels of *pqqA* expression appear to have little effect on the amount of PQQ produced [221] [222]. This suggests that despite the decreased expression of *pqqA* in our *arcA* mutant, the

levels of PQQ produced may be sufficient to convert glucose to gluconate, as we observed accumulation of pyruvate which is a product of glucose processing via glycolysis in our mutants.

Pyruvate is further oxidized via TCA cycle feeding the ETC. However, the absence of changes in intracellular pH in the presence of glucose in our mutants suggest that the loss of *arcA* function could diminished function of any of the components of the ETC, causing an inability to generate a proton gradient. The regulatory function of ArcA on components of the respiratory chain has been documented previously[223]. Consistent with this, we observed that our mutants have decreased expression of genes encoding components of the respiratory chain, which would prevent generation of a proton gradient, irrespective of glucose oxidation. In addition, in aerobically growing cells, NADH is generated via the TCA cycle, with the electrons transferred to the respiratory chain. Disruption of *arcA* in *E. coli* leads to overproduction of NADH that is thought to exert allosteric control on activity of succinate dehydrogenase (complex II), likely interrupting electron flow from the TCA cycle to the respiratory chain[224]. Each of these changes leads to alteration that mirrors those caused by CCCP, disrupting the respiratory chain and decreasing quinone pools that our mutant would be unable to sense and respond to by regulating genes that are required for the restoration of membrane energy.

Further to this, elevated levels of NADH cause a disruption in succinate dehydrogenase activity, resulting in replacement of the TCA cycle with the glyoxylate pathway. Indeed, we observed accumulated succinate in our mutants and altered metabolic gene expression that would suggest a switch to the glyoxylate cycle, an effect seen in other

organisms bearing a disrupted ArcAB module[225]. A primary regulatory role for ArcAB has been attributed to control of the TCA cycle and glyoxylate shunt pathway. Specifically, a study exploring the effects of *arcA* deletion in *E. coli* during aerobic growth demonstrated a high influx of metabolites through the TCA cycle, suggesting an altered metabolic function[226]. Similarly, in *S. enterica* disruption of *arcA* led to the upregulation of genes that are part of the glyoxylate shunt, glycolysis, and fermentation[174]. In line with these findings, a study investigating the transcriptional changes of *E. coli* upon switching from anaerobic to aerobic conditions (which ArcB senses) found upregulation of several genes involved in the TCA cycle, terminal oxidases with high affinity to oxygen, and an abundance of reduced equivalents for the respiratory chain. Thus, the altered expression of genes involved in glycolysis and TCA cycle in our *arcA* mutant further support an altered function in energy generation similar to that reported for other ArcAB systems[223].

Among the genes altered in expression in our *arcA* mutant was the *pta-ackA* operon, which was significantly upregulated. This module is activated in response to increased levels of glucose, oxygen, and high metabolic activity, and converts pyruvate to acetyl-coA under aerobic conditions[120,225]. Conversely, this pathway produces mixed-acid products, lactate, ethanol, and acetate under anaerobic conditions[201]. A hallmark of *Acinetobacter* species is their ability to grow on acetate as a sole carbon source; thus it is possible that our mutant's response to CCCP-dependent decreases in quinone pools is translated into a hyperactive glyoxylate pathway that causes carbon overflow, diverting into the Pta-AckA pathway. Notably, we observed higher levels of pyruvate and acetate

in our mutants that could likely be explained by the increased expression of genes encoding pyruvate dehydrogenases and the Pta-AckA pathway [227] [201].

To date, our data supports a metabolic overflow status in our mutants that result in saturation of the main energy generation pathways of glycolysis and the TCA cycle. These alterations lead to accumulation of NADH, acetate, and metabolites of the TCA cycle. Reducing equivalents generated from the above pathways are oxidized via the ETC during aerobic respiration to generate ATP via oxidative phosphorylation. In *E. coli,* decreased activity of cytochrome oxidase with high affinity to oxygen under microaerobic conditions was found in an *arcA* mutant[228] In line with this observation, and the regulatory role for ArcA in controlling components of the ETC[223], we observed that activity of the terminal cytochrome oxidase was diminished in our mutants . This would tend to suggest that ATP generation via substrate phosphorylation prevails in our mutants to compensate for their inability to generate ATP via oxidative phosphorylation.

In summary, the data presented in this study demonstrates the importance of the ArcAB TCS for controlling membrane energetics in *A. baumannii*. We reveal that loss of of ArcAB function renders this organism unable to sense changes in ubiquinones levels resulting from altered respiratory chain function. This consequently leads to altered metabolic pathway utilization, affecting energy generation - highlighting the importance of ArcAB in maintaining energy homeostasis. As such, herein we provide evidence of a novel regulatory role of the TCS ABUW_2426/ABUW24/27 in *A. baumannii*, extending our knowledge of regulatory networks in this important human pathogen.

CHAPTER IV

CHARACTERIZATION OF A NOVEL *FEC*-OPERON RESPONSIVE TO HEMIN IN *ACINETOBACTER BAUMANNII*

ABSTRACT. Iron acquisition systems are essential for bacteria to overcome the limitation of iron encounter during infection in their host. Although genes encoding for the acinetobactin system with high affinity to ferric iron exists in *A. baumannii*, identification of heme acquisition systems have yet to be described in *A. baumannii*. Previous work published in our lab identified an operon with high similarity to the first Fec-operon genes *fecI*, *fecR* and *fecA* found in *E. coli* , 4 genes with unknown function, and 1 gene encoding a heme oxygenase. Screening of mutant strains with disruption of the *fecI*, *fecR* and *hemO* showed altered growth phenotypes linked to hemin and hemoglobin utilization as a sole source of iron. Further transcriptional studies using a reported gene showed that the outer membrane receptor FecA is induced in the presence of hemin and appears to be dependent on FecI-FecR activity. RNA-seq analysis revealed an altered transcription of several genes in response to hemin limitation including downregulation of the *fec*-operon. Lastly, given the importance of heme degradation in iron utilization, we explored the effects of disruption the *hemO* and found that it alters its ability to survive in serum, accumulates hemin in the cell and displayed a growth defect in the presence of hemin suggesting its important role in hemin utilization. In summary, our data supports the

hypothesis that *fecI* regulates the activity of this operon in the presence of hemin and appears to be mediated via a signaling mechanisms involving the hemin receptor FecA.

INTRODUCTION

The importance of iron for living organisms, including humans and bacteria, is defined by its requirement for the enzymatic activity of redox proteins involved in cellular processes such as respiration and DNA synthesis[229]. Because of its highly reactive nature in the presence of oxygen, resulting in the generation of free iron and hydroxyl radicals that can cause cellular damage, iron exists in the human body mostly bound to host proteins such as albumin, transferrin, lactoferrin, hemoglobin, and hemopexin[230]. As a result of this, free iron within our system is limited to a concentration of around 10^{-24} M, which is clearly lower than the 10^{-7} M needed to support bacterial growth[231,232]. To combat this, bacteria possess transport machineries that use the secretion of siderophores or hemophores alongside dedicated outer membrane receptors, to capture iron from host-iron containing proteins [233,234]. The activity of these systems is subject to hierarchical regulation, to either avoid the potential toxic effects of excess iron accumulation, or to adapt when iron becomes scarce in niches such as those encountered during infection within a host[234].

The major regulator directly linked to iron acquisition in bacteria is the ferric-uptake regulator, Fur. In times of iron abundance, Fur acts as a negative regulator of iron uptake in a manner that is mediated via binding of ferrous iron to the Fur protein. This event acts as a signal that in turn leads to repression of a variety of genes, including those encoding iron regulated proteins and iron transport systems. Conversely, iron scarcity results in

reduced ferrous iron concentrations, leaving Fur unbound, which serves as a signal for Fur to relieve repression of genes required for iron transport[235]. The next tier of iron mediated regulation, at least in Gram-negative bacteria, is exerted by sigma (σ) factors, particularly those from the extracytoplasmic function (ECF) family, where several have been described as controlling the process of iron acquisition[236-239]. This positive mode of regulation often induces iron transport systems, and was first described for the *fec*-operon of *E. coli* [240,241]. In this example, the proposed model of activation of this operon is described as follows: the outermembrane receptor FecA binds ferric citrate, which in turn induces a conformational change of FecA allowing its N-terminal to interact with the C-terminal of FecR. Upon this, FecR binds to the region 4 of the σ factor FecI , resulting in activation of genes dedicated to the active transport of iron[239,240]. The mechanistic understanding of FecI inactivation still unclear. As such, the two following inactivation mechanism for FecI have been proposed. The first one involved degradation via proteolysis upon release of FecI from FecR. The second one argues for an inactive form of FecR bound to FecI that prevents association of this complex to the RNA polymerase. Homologs of the Fec system have also been described in other Gram-negative organisms as being involved in iron acquisition. For example, in environments devoid of iron, *Pseudomonas aeruginosa* secretes the siderophore pyoverdine that upon loading with ferric iron binds the outer membrane receptor FvpA. Following this interaction, the signal is transmitted to the PdvS σ factor, which subsequently activates the pyoverdine chromophore *pvcABCD* operon to synthesize pyoverdine [242]. Similarly, *Bordetella avium, Bordetella pertussis and Serratia marcescens* all have systems homologous to FecI. In these first two organisms a parallel HurI-HurR-BhuR / RuhI-RhuR-BhuR axis exists that

senses heme during iron limited conditions, resulting in activation of the *bhuRSTUV* operon that encodes an ABC transporter dedicated to heme transport [238,243]. In *S. marcescens*, beyond a HasI-HasS-HasR system that is homologous to FecA-FecR-FecI, the activation and function of this system is very different to the canonical mechanism described in *E. coli*[244,245]. Here, under heme limited conditions, the HasA hemophore, a protein that scavenges heme from hemoglobin, binds to HasS, a TonB receptor homolog of FecA. This interaction is required for releasing of the sigma factor HasI from HasS, resulting in transcription of the HasADEB operon, which encodes a hemophore secretion system that allows binding to free heme or heme bound to host proteins. [246,247] [236].

In the context of infection, the complex molecule hemin is a major source of iron for pathogenic bacteria. Upon uptake of this iron source, bacteria can either incorporate it directly into their own hemin-requiring proteins, or further degrade it to generate free iron and other useful byproducts such as bilirubin, which has antioxidant properties. The presence of hemin uptake systems has been reported in several pathogenic bacteria, where they serve to overcome host iron sequestration mechanisms. These hemin acquisition systems are typically comprised of genes encoding a TonB-like outermembrane receptor, and an ABC permease transporter system, all of which are activated by cognate σ factors during iron limiting conditions. In *A. baumannii* the presence of iron acquisition systems that synthesize siderophores with high affinity to ferric iron have been described. Regarding hemin uptake, a previous bioinformatic study from our lab reported the presence of a *fec*-like operon containing genes for a putative hemin acquisition system that is conserved in ~50% of clinical *A. baumannii* isolates.

Interestingly, within the *A. baumannii fec*-like operon, there appears to be a novel hemin oxygenase encoding gene, which further suggests the utilization of this system for hemin assimilation.

In this study, we begin characterization of the *A. baumannii fec*-like operon by measuring the effects of disruption of genes encoding homologs of FecI and FecR, as well as the novel HemO protein, in the presence of a variety of iron sources. Our data indicates that growth of mutants was specifically altered in the presence of both hemin or hemoglobin, but not other iron sources, such as ferric citrate. Individual and global transcriptional studies revealed that the *fec-like* operon of *A. baumannii* is induced in the presence of hemin, and disruption of the *fecI* gene led to altered expression of genes encoding iron regulated proteins involved in energy generation and metabolism. Finally, disruption of *hemO* resulted in growth defects, the accumulation of hemin, and diminished survival in serum. Taken together, the data presented here reveal that the this *fec*-like operon is responsive to hemin and the *fecI* gene plays a major role in transcription control during hemin limited conditions. Furthermore, *fecI-fecR* expression is required for *fecA* induction by hemin, supporting a model of positive regulation for this system.

MATERIAL AND METHODS

Bioinformatic analysis. A BLASTP analysis of the FecI, FecR and FecA proteins against their corresponding homologs in *Escherichia coli, Bordetella pertussis*, *Bordetella avium,* and *Serratia marcescens* was performed using the https://blast.ncbi.nlm.nih.gov/Blast.cgi

server. Protein sequences of TonB-like proteins within the *fec*-operons of *A. baumannii*, *E. coli, B. pertussis*, *B. avium,* and *S. marcescens* were downloaded from the NCBI ftp server (www.ncbi.nlm.nih.gov/genome) and topology maps were generated using the protter tool (http://wlab.ethz.ch/protter/start/).

Strains and growth conditions. The strains and cloning primers used in this study are listed in **Table 4**. All strains were cultured in lysogeny broth (LB), unless otherwise indicated, with shaking at 37°C. Where appropriate, antibiotics were added for selection: tetracycline at a final concentration of 5 µg/mL and hygromycin at a final concentration of 140 µg/mL. Mutants of ABUW_2987 (*fecI*), ABUW_2986 (*fecR*) and ABUW_2981 (*hemO*) were acquired from the AB5075 transposon mutant library[179]. Strains were confirmed using primers OL4383/OL4384 (*fecI*), OL4436/OL4437 (*fecR*), and OL4575/OL4576 *hemO*)

Construction of a *fecA-lacZ* transcriptional fusion strain. A PCR fragment was generated that begins 500 nt 5' of *fecA* and ends 762 nt 3' of it, using primers OL4380/OL4381. This fragment was cloned into the vector pAZ106, which contains a promoter-less *lacZ* cassette, creating plasmid pSLG5. This plasmid was then used to amplify the *fecA-lacZ*

fusion fragment using primers OL4382/OL4232, which was subsequently cloned into the *A. baumannii* shuttle vector pMQ557, resulting in plasmid pSLG6. AB5075 was then transformed with pSLG6, and colonies were selected using LB plates supplemented with hygromycin (plasmid encoded). All strains were then confirmed by PCR.

Construction of *fecR* and *hemO* complementation strains. A 1,362 bp fragment including 500 bp upstream and downstream of the *hemO* gene, and a 2,232 bp fragment including 500 bp upstream and downstream of the *fecI* gene, was amplified using primers OL4575/OL4576 and OL4436/OL4437. These PCR products were cloned into pMQ557, creating plasmids pSLG7 and pSLG8. Clones were confirmed by PCR and Sanger sequencing (MWG Operon), before being transformed into the *A. baumannii hemO* and *fecR* mutant strains, respectively. Strains were again confirmed by PCR and Sanger sequencing (MWG Operon).

Table 1. Bacteria strains, plasmids and cloning primers

Strain	Description	Source
E. coli		
DH5α	Cloning strain	[248]
A. baumannii		
AB5075	Parental strain	[179]
AB5075 176::T26	AB5075 with transposon insertion in ABUW_2987	[179]
AB5075 170::T26	AB5075 with transposon insertion in ABUW_2986	[179]
AB5075 126::T26	AB5075 with transposon insertion in ABUW_2981	[179]
LGC 2610	AB5075 126::T26 complemented with pMQ557::*hemO*	This study
LGC 2611	AB5075 containing pSLG6 (P_{fecA}–*lacZ* fusion)	This study
LGC 2612	AB5075 170::T26 complemented with pMQ557::*fecR*	This study
Plasmids		
pMQ557	Cloning vector for complementation	Gift, Dr. R. Shanks, University of Pittsburgh
pAZ106	Promotorless *lacZ* insertion vector	[249]
pSLG5	pAZ106::P_{fecA}–*lacZ*	This study
pSLG6	pMQ557::P_{fecA}–*lacZ*	This study
pSLG7	pMQ557::*hemO*	This study
pSLG8	pMQ557::*fecR*	This study
Primers		
OL4232	ATGGCGGCCGCGACCCAACGCTGCCCGAGAAA	This study
OL4380	ATGGGATCCGTAGAAGCCACACAGGTTAA	This study
OL4381	ATGGAATTCACTGATTCAGTACGTTAGCA	This study

Table 4. (Continued)

OL4382	ATGCTCGAGGTAGAAGCCACACAGGTTAA	This study
OL4383	ATGCCCGGGGATACCTATTTGGTCGGC	This study
OL4384	ATGCCCGGGTTA GTGGTGGTGGTGGTGGTG AATGTAAGCGTCCATGTC	This study
OL4436	ATGGCGGCCGCGATACCTATTTGGTCGGC	This study
OL4437	ATGCTCGAGTTAGTGGTGGTGGTGGTGGTGTTT TAAAGAAACCATGACCA	This study
OL4575	ATGGCGGCCGCCCTCAATCTACCTTACACAG	This study
OL4576	ATGCTCGAGTTAGTGGTGGTGGTGGTGGTGTTT CAATTCATCAAGCTGATC	This study

*Underscore indicates restriction enzyme site

Growth assays. For iron containing experiments, cultures of the wild-type, *fecI, fecR* and *hemO* mutants, alongside the *hemO*$^+$ and *fecR*$^+$ complemented strains, were grown overnight in RPMI media supplemented with 1% casamino acid and 100μM 2-2 dipyridyl (DIP). Overnight cultures were diluted 1:100 in fresh media and grown for an additional 3 hours. These cultures were then used to inoculate new media to an OD_{600} of 0.05. Test media used in these studies was RPMI supplemented with 0.1μM/mL ferric citrate; 0.1μM/mL hemin (Sigma-Aldrich) and 0.1μg/mL apo-transferrin (Sigma-aldrich); or 0.5μg/mL hemoglobin (Sigma-Aldrich) and 0.1μg/mL apo-transferrin. Growth was monitored over time and OD_{600} values were read every two hours. Data is derived from three independent replicates.

Transcriptional profiling assays using β-galactosidase. For expression over time of the *A. baumannii* P_{fecA}-*lacZ* fusion strain in the WT, *ΔfecI,* and *ΔfecR* backgrounds the overnight cultures grew in iron depleted media were used to standardized and

synchronized cultures at an OD_{600} of 0.05, before the following compounds were added to final concentration of : 1% Casamino acids, 0.1μM/mL ferric citrate, 0.1μM/mL hemin and 0.1μg/mL apo-transferrin, and 0.5μg/mL hemoglobin and 0.1μg/mL apo-transferrin. Cultures were incubated with shaking at 37°C, with 0.1mL samples collected every hour. Levels of β-galactosidase were measured as described previously[181]. Results are presented from three independent experiments.

RNA-seq analsyis. RNA-seq experiments were performed as described previously[182] . Briefly, the *A. baumannii* wild-type and *fecI* mutant strains were grown in RPMI with 1% casamino acid overnight at 37°C with shaking in biological triplicate. Overnight cultures were diluted 1:100 into 100mL of fresh RPMI with 1% casamino acids, grown to exponential phase, and subsequently used to seed new 100mL cultures supplemented with 0.1μM/mL hemin and 0.1μg/mL apo-transferrin at an OD_{600} of 0.05. Cultures were allowed to grow for 3 hours, before 5 mL was harvested from each flask. This was added to 5 mL of ice-cold PBS, pelleted by centrifugation at 4°C, and the supernatant removed. Total RNA was isolated using a RNeasy Kit (Qiagen) and DNA was removed using a TURBO DNA-free kit (Ambion). Sample quality was assessed using an Agilent 2100 Bioanalyzer system with an RNA 6000 Nano kit (Agilent). An RNA integrity value of >9.7 was used as a cutoff. Prior to mRNA enrichment, biological triplicate RNA samples were pooled at equal concentrations followed by rRNA removal using a Ribo-Zero Kit for Gram Negative Bacteria (Illumina) and a MICROBExpress Bacterial mRNA enrichment kit (Agilent). Removal efficiency of rRNA was confirmed using an Agilent 2100 Bioanalyzer system and an RNA 6000 Nano kit (Agilent). Library preparation was performed using the

TruSeq Stranded mRNA Kit (Illumina) omitting mRNA enrichment steps. Quality, concentration, and the average fragment size of each sample was assessed with an Agilent TapeStation and High Sensitivity DNA ScreenTape kit. Library concentration for the pooling of barcoded samples was assessed by qPCR using a KAPA Library Quantification kit (KAPA Biosystems). Samples were run on an Illumina MiSeq with a corresponding 150-cycle MiSeq Reagent kit. Upon completion, data was exported from BaseSpace (Illumina) in fastq format and uploaded to Qiagen Bioinformatics for analysis. Data was aligned to the AB5075 reference genome (NZ_CP008706.1), and experimental comparisons were carried out after quantile normalization using the Qiagen Bioinformatics experimental fold change feature.

qRT-PCR. Quantitative real time PCR (qPCR) analyses were conducted as described previously using primers detailed in **Table 5**.[181] Bacterial cultures were prepared and RNA extracted as described for the RNA-seq experiments. Data is derived from three independent replicates.

Table 2. List of qPCR primers used in this study.

Strain		**qPCR Gene**
OL4498	CCTAGAGATAGTGGACGTTACTCG	*16S* **R**
OL4499	CCAGTATCGAATGCAATTCCCAAG	*16S* **F**
OL4405	CAAAGCTGGCTTCACCAATG	*fecI* **F**
OL4406	GTCTCGGGTTTGTAGCAGTTTA	*fecI* **R**
OL4407	GCCAAAGACAAGACCAGAC	*fecR* **F**

Table 5. (Continued)

OL4408	CGGTTGCCGAAGGATCATAA	*fecR* **R**
OL4409	AGAAAGAGGGTGTAGCTGGA	*hemO* **F**
OL4410	CCCGTTGGGTTGAATACCTAAA	*hemO* **R**
OL4602	TCAGACCCTTAAACTGACTTACC	*fecA* **F**
OL4603	CACCCAAGTCAGGCGTAATA	*feA* **R**
OL4700	AGTTCATACAACCGCCAATAC	*citN* **F**
OL4701	CACAGTCACCGTAGACATAGA	*citN* **R**
OL4612	GTACGCCAATGGTTGATGGA	*paaI2* **F**
OL4613	GGGCGCTTAATTCAGGAAG	*paaI2* **R**
OL4614	GGTGATCAGTATTGGCTGGT	*citN* **F**
OL4615	AGCTCAATCACGCCTAAACG	*citN* **R**

Letters in bold indicate F= Forward ; R= Reverse

Hemin measurements. The wild-type, *hemO* mutant and *hemO*$^{+}$ complemented strains were grown in RPMI supplemented with 1% casamino acid and 100μM DIP as described above and used to generate synchronized cultures in fresh RPMI supplemented with 1μM/mL hemin. These were grown for 6 hours, before cells were pelleted by centrifugation and resuspended in hemin buffer (Sigma-Aldrich), before being lysed using a Mini BeadBeater -16 (Biospec). Hemin quantification was performed using a hemin colorimetric assay kit MAK316 (Sigma-Aldrich) following the manufacturer's protocol. Data is derived from three independent replicates.

Human serum survival assay. The wild-type, *hemO* mutant and its complemented strain were separately seeded into 100µL of human serum at an OD_{600} of 0.05. Samples were incubated for 4 hours at 37 °C, before aliquots were withdrawn and CFU/mL determined by serial dilution and plating onto LB agar. Data is derived from three independent experiments

RESULTS

The FecI operon of *A. baumannii* has a distinct set of genes compared to homologs in other organisms. In previous work by our group we identified the complete proteinaceous regulome of *A. baumannii* strain AB5075 [153]. As part of this, we found an 8-gene operon (**Figure 14)** that begins with an ORF (ABUW_2987) that encodes an ECF-sigma factor bearing homology to FecI from a variety of different organisms (Table 6). Immediately downstream of the putative *fecI* we found genes encoding homologs of two other proteins typically found in other Fec systems, a FecR like transmembrane regulatory protein (ABUW_2986), and the outer membrane receptor FecA/TonB (ABUW_2985) (Table 6) [153].

Upon syntenic comparison with homologous systems in *E. coli*, *B. pertussis, B. avium, and S. marcescens* we found that, despite sharing the *fecI-fecR-fecA* arrangement, the *fec*-operon in *A. baumannii* appears to have a very different collection of genes downstream of this unit (**Figure 14**). For example, in *E. coli*, the 4 genes located downstream of *fecI-fecR-fecA* encode an ABC transporter dedicated for iron citrate uptake [244]. Similarly, in *B. pertussis* and *B. avium,* downstream of the genes encoding for HurI-HurR-BhuR / RuhI-RhuR-BhuR, the heme surface regulatory system

homologous to FecI-FecR-FecA, 4 genes are found that encode an ABC transporter utilized for heme transport [238,243]. In *S. marcescens*, the HasI-HasS-HasR system that is homologous to FecA-FecR-FecI has 4 genes located immediately downstream of it that encode for a hemophore secretion system comprised of the hemophore HasA, inner membrane proteins HasD and HasE, and a TonB dependent heme transport protein HasB [246,247 236].

Table 3. BLAST analysis of ABUW_2987, ABUW_2986 and ABUW_2985 from *A. baumannii* identifies them as homologs of FecI, FecR and FecA, respectively.

Organism	Protein	Identity[1]	Similarity[2]	Reference
Escherichia coli	FecI	36%	60%	
	FecR	31%	48%	
	FecA	25%	40%	232
Bordetella pertussis	HurI	42%	64%	
	HurR	23%	42%	
	BhuR	26%	45%	240
Bordetella avium	HurI	41%	67%	
	HurR	22%	40%	
	BhuR	24%	41%	241
Serratia marcescens	HasI	30%	48%	
	HasS	28%	49%	
	HasR	24%	41%	228

[1]Shown is the percent identity from a BLASTP analysis using ABUW_2987 (FecI), ABUW_2986 (FecR) and ABUW_2985 (FecA).
[2]Shown is the percent similarity from a BLASTP analysis using ABUW_2987 (FecI), ABUW_2986 (FecR) and ABUW_2985 (FecA).

Interestingly, in *A. baumannii* there are five genes immediately downstream of the *fecI-fecR-fecA* cluster in the same transcriptional orientation (and would appear to form an operon based on our previously published RNAseq data[198]), but whose products share no homology to *fec*-operon proteins from our comparator organisms. These are: three hypothetical proteins with no discernable function (ABUW_2984, ABUW_2983 and

ABUW_2980); another TonB-like protein that is predicted to have an N-terminus orienting to the cytoplasm, 1 transmembrane domain and a C-terminus orienting to the periplasm (ABUW_2982), which is quite different to TonB proteins present in *fec-like* operons from other organisms (**Figure 15**); and a putative heme oxygenase (ABUW_2981). As such, despite shared homology to the FecI sigma factor, and its controlling counterparts, the *fec*-operon of *A. baumannii* is structured in a very different manner to that of other organisms, perhaps reflecting a novel function.

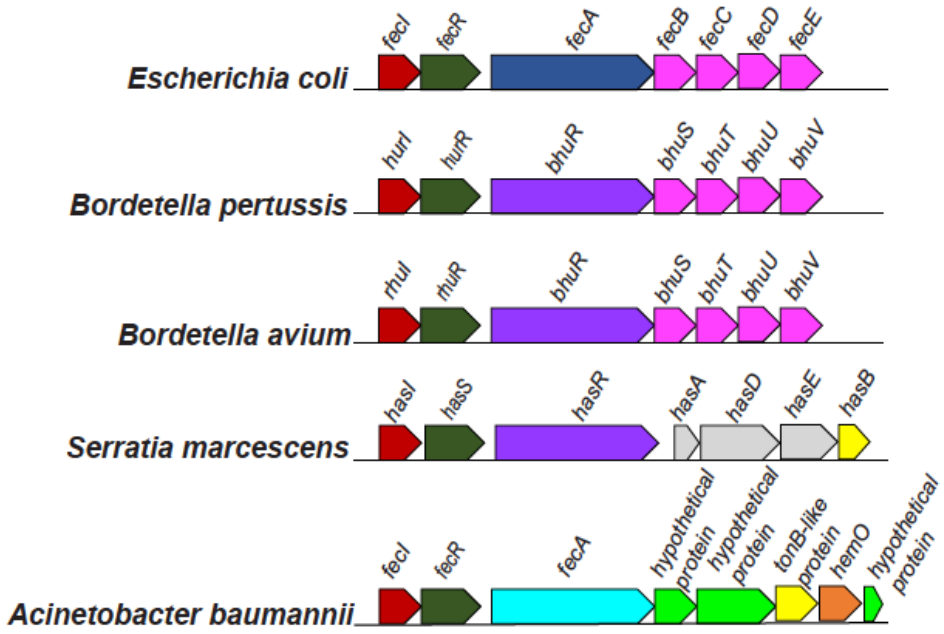

Figure 14. **Genomic organization of the *fecI*-like operon from *A. baumannii* and related Gram-negative organisms**. The genomic arrangement for *Escherichia coli, Bordetella pertussis, Bordetella avium, Serratia marcescens and Acinetobacter baumannii* was generated and adapted from IMG/ MER Integrated Microbial Genomes & Microbiomes. Organized from left to right, shown are genes encoding homologs of the FecI sigma factor (red) and FecR anti-sigma factor (green). Also shown is the FecA outer-membrane receptor that is specific for ferric iron in *E. coli* (dark blue) and its homologs that are specific for hemin in *Bordetella pertussis, Bordetella avium* (both named BhuR) and *Serratia marcescens* (HasR) (all three in purple), alongside the uncharacterized FecA homolog from *A. baumannii* (light blue). Other genes encoding known ABC transporter systems (magenta), a hemophore secretion system (silver), tonB-like proteins (yellow); a putative heme oxygenase (orange), and hypothetical proteins of unknown function (light green) are also shown.

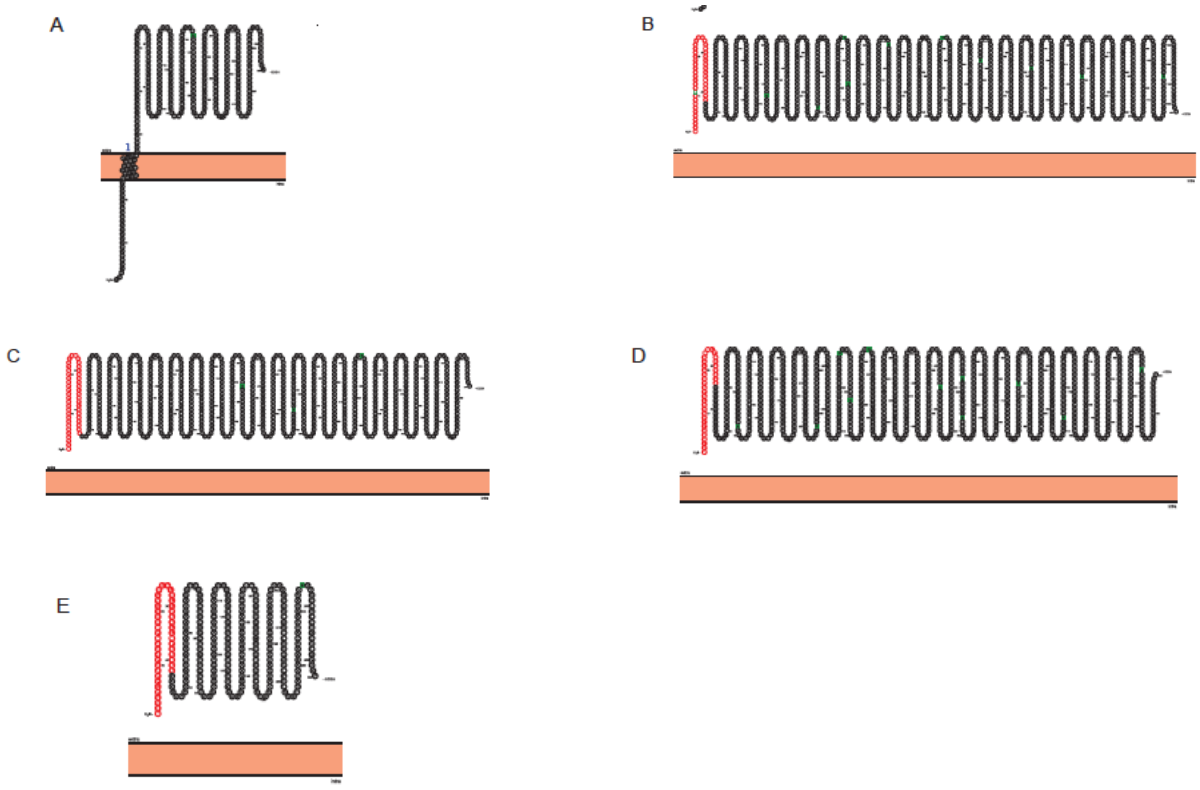

Figure 15. Predicted topology plots of outermembrane receptor proteins within the homologous *fec* operons. The topology of outermembrane receptor proteins present in the *fec* operons of *Acinetobacter baumannii, Escherichia coli,* and *Serratia marcescens* are shown. Predictions were generated using the Protter bioinformatic website. (A) The TonB-dependent protein encoded by ABUW_2982 in *A. baumannii*. (B) The FecA homolog of *A. baumannii* encoded by ABUW_2985. (C) FecA from *E. coli*. (D) The HasR, TonB-dependent protein of *S. marcescens*. (E) The HasB, TonB-dependent protein of *S. marcescens*. Red shading indicates predicted signal peptide sequences.

The presence of hemin or hemoglobin as a sole iron source impacts growth of the *fecI* and *fecR* mutant strains. The *fec*-like operon of *A. baumannii* is of particular interest because it is not present in all strains of this organism, but instead appears to reside in those clinical isolates with enhanced pathogenic potential [153]. Indeed, work by Leseleuc *et. al*. also found the conservation of this operon in more virulent strains of *A. baumannii*, including the clinical strain LAC-4, which displays a more robust growth in the presence of heme iron (hemin) compared to *A. baumannii* strains lacking this operon [250]. As such, we hypothesized that the presence of this operon in AB5075 may be required for heme

acquisition in this strain. To test this, the wild-type along with the *fecI* and *fecR* mutant strains were incubated in RPMI media supplemented with ferric citrate, hemin, or human hemoglobin as sole iron sources, alongside standard LB (rich media) as a control, with growth monitored every two hours. As a note, Apo-transferrin was also added to media containing hemin or human hemoglobin so as to chelate any Fe(III) as a result of hemin oxidation, ensuring hemin or hemoglobin were the sole iron sources. Upon analysis, both the *fecI* and *fecR* mutants displayed similar growth profiles to the wild-type in LB, indicating no role in growth in rich media. (**Figure 16A**). Similarly, growth of our mutants in the presence of ferric citrate as a sole iron source was no different to that of the wild type (**Figure 16B**). Conversely, when these strains were grown in the presence of hemin

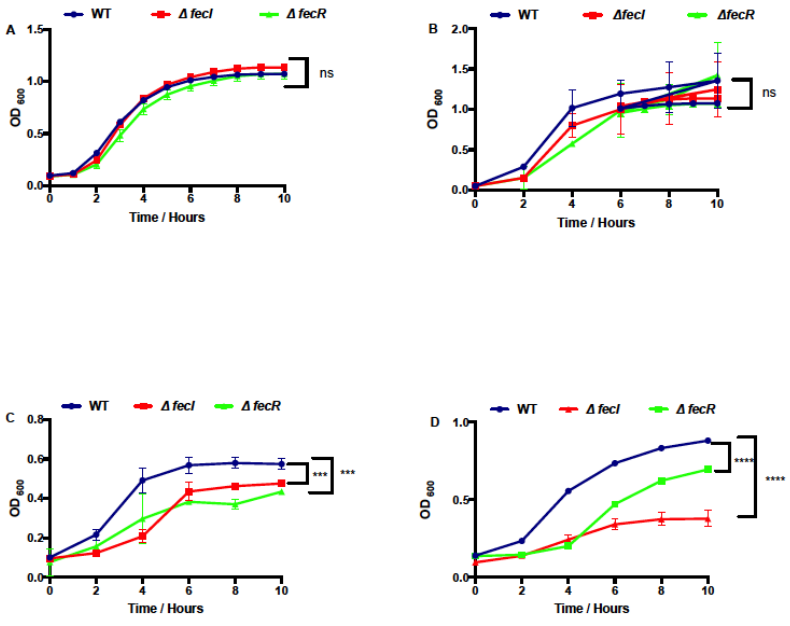

Figure 16. The presence of hemin or hemoglobin as a sole iron source affects growth of the *fecI* and *fecR* mutant strains. Shown is growth of the WT, *ΔfecI*, and *ΔfecR* strains in: **(A)** LB media; **(B)** RPMI supplemented with 0.1μM/mL ferric citrate**;** (**C)** RPMI supplemented with 0.1μM/mL hemin and 0.1μg/mL apo-transferrin; and **(D)** RPMI supplemented with 0.5μg/mL hemoglobin and 0.1μg/mL apo-transferrin. Data is derived from three biological replicates with error bars shown +/- SEM. A 2-way ANOVA analysis was used to define statistical significance, $p<0.001$ = ***, $p<0.0001$ = ****, ns = not significant compared to the wild-type.

or human hemoglobin we noticed that our *fecI* and *fecR* mutant strains displayed less robust growth (**Figure 16 C and D).** From the observed phenotypes, it appears that *fecI* and *fecR* both are required for optimal growth in the presence of either hemin or hemoglobin as the only iron source available. To explore this further, we constructed a *ΔfecR*$^{+}$ complemented strain (generating a *fecI*$^{+}$ complemented strain proved not to be possible), and tested its ability to restore growth of the *ΔfecR* strain in RPMI media supplemented with different iron sources. In so doing, we observed that the *ΔfecR*$^{+}$ construct restored growth to wild-type levels (**Figure 17 A-C**).

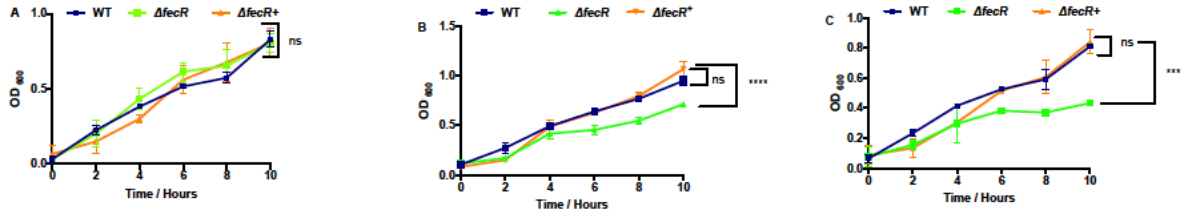

Figure 17. Complementation of *ΔfecR in trans* restores growth to wild-type levels in the presence of hemoglobin or hemin as sole iron sourcse. Growth of the WT, *ΔfecR*, and *ΔfecR*$^{+}$ strains in RPMI media supplemented with either: 0.1μM/mL ferric citrate **(A);** 0.1μM/mL hemin and 0.1μg/mL apo-transferrin (**B);** and 0.5μg/mL hemoglobin and 0.1μg/mL apo-transferrin (**C**). Data is derived from three biological replicates with error bars shown +/- SEM. A 2-way ANOVA analysis was used to define statistical significance p<0.001 = ***, p<0.0001 = ****, ns = not significant compared to the wild-type

Transcriptional analysis reveals that *A. baumannii fecA* is induced in response to hemin and hemoglobin. Previously published RNA-seq data from our group demonstrates that the expression of genes in the *fec*-like operon of *A. baumannii* is very low during growth in rich media[198]. Given that in homologous systems the presence and abundance of specific types of iron is mediated via the outermembrane protein FecA, we sought to assess the transcriptional inducibility of the *A. baumannii fecA* to a variety of

iron sources. As such, we constructed a *lacZ-reporter* gene fusion for the *fecA* promoter in our wildtype strain, and its corresponding *fecI* and *fecR* mutants. We next measured β-Galactosidase activity in RPMI media supplemented with ferric citrate, hemin, hemoglobin, or casamino acids without iron. Upon analysis, we observed that hemin and hemoglobin strongly induce the expression of *fecA* in the wildtype background, in contrast to ferric citrate or casamino acids, which do not (**Figure 18A**). Importantly, when we assessed this same series of conditions in the *fecI* and *fecR* mutants we noted that the presence of hemin or hemoglobin was no longer able to stimulate expression *fecA* (**Figure 18B-C**). This finding suggests that *fecA* is hemin and hemoglobin responsive in *A. baumannii* in a FecI-FecR dependent manner.

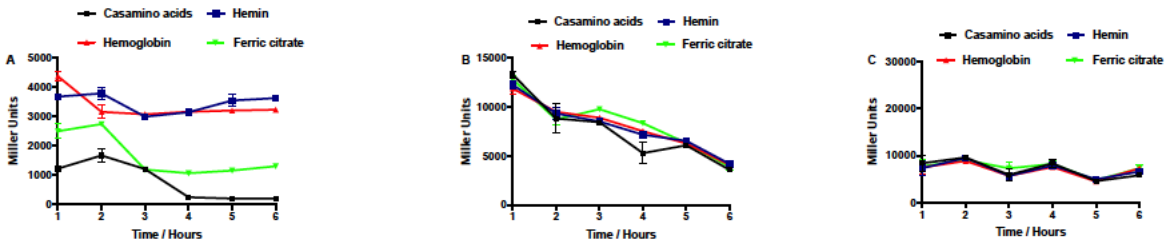

Figure 18. The *fecA* promoter of *A. baumannii* is specifically responsive to either hemin or hemoglobin in a FecI-FecR dependent manner. ß-galactosidase activity of the *fecA-lacZ* fusion in the wild-type **(A)**, *ΔfecI* **(B)**, and *ΔfecR* **(C)** strains was measured hourly in the presence of 1% Casamino acids (black), 0.1μM/mL ferric citrate (green), 0.1μM/mL hemin and 0.1μg/mL apo-transferrin (blue), and 0.5μg/mL hemoglobin and 0.1μg/mL apo-transferrin (red). Transcriptional activity is expressed as Miller Units. Data is derived from three independent experiments, with error bars shown +/- SEM.

Global transcriptomic analysis reveals altered expression of iron metabolic pathways upon disruption of *fecI*. Given that our *fecI* mutant displayed altered growth in the presence of hemin and appears to be required for hemin-induced *fecA* expression, we used RNA-seq technologies to identify the regulome of the *A. baumannii* FecI-sigma

factor. The wild-type and *fecI* mutant strains were thus grown in RPMI in the presence of hemin and apotransferrin (as in **Figure 16C**), with RNA harvested after three hours growth. Following RNAseq analysis, we observed that 293 genes displayed a significant alteration in expression between the two strains at a level ≥ 3-fold. (**Figure 19A**, Supplemental Table S1). This included 128 genes that were downregulated, and 165 that were upregulated, in the *fecI* mutant. When we explored this data ontologically (**Figure 19B**) we observed the altered expression of genes clustered into functions such as aromatic metabolism, energy production, ion transport, general metabolism, efflux pumps, biofilm formation, and motility.

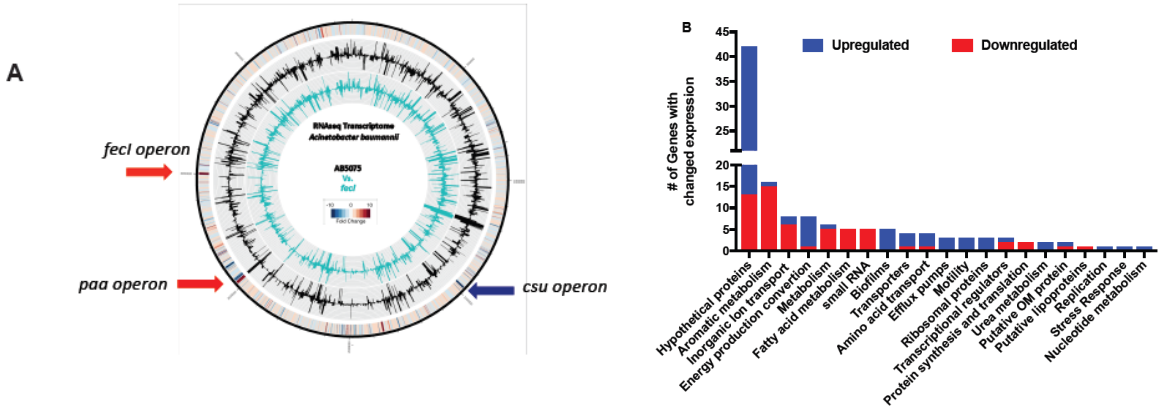

Figure 19. Transcriptomic Profiling of the *fecI* mutant. **(A)** Genomic map showing major transcriptional changes in *ΔfecI* compared to the parental strain after 3h growth in RPMI containing 0.1μM/mL hemin and 0.1μg/mL apo-transferrin. The outermost circle represents a heat map of changes for *ΔfecI* compared to the wild-type. The middle circle (black) depicts RPKM values for the parent, whilst the inner circle (turquoise) depicts RPKM values for *ΔfecI*. Arrows at specific locations within the map highlight operons with significant downregulated (red) or upregulated (blue) changes. **(B)** Categorization of genes differentially expressed in *ΔfecI* compared to the wild-type based on predicted function.

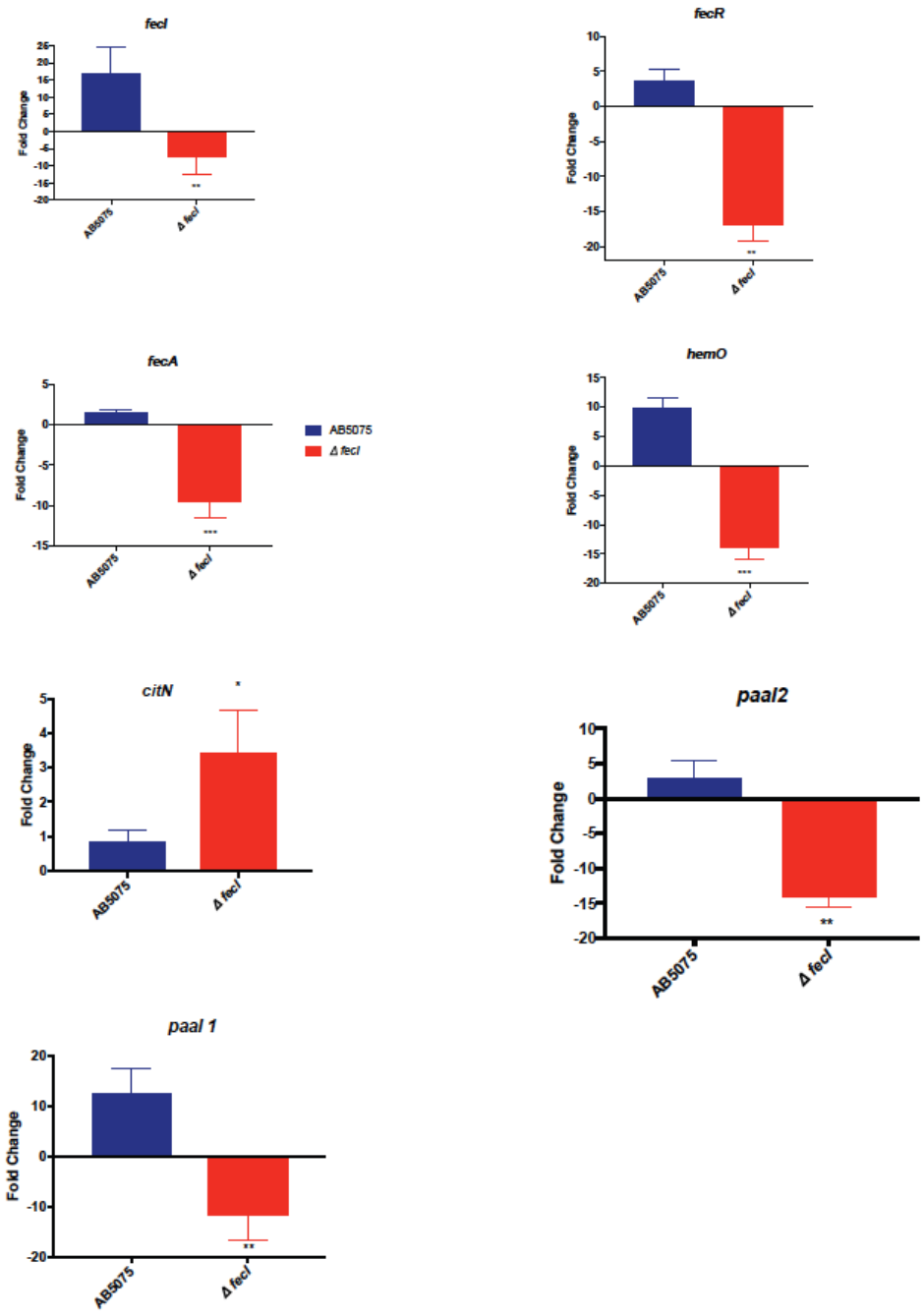

Figure 20. qRT-PCR analysis validates RNA-seq data for genes with altered expression upon *ΔfecI* disruption. The RNA-seq dataset was validated using qRT-PCR to analyze expression of selected genes in the WT and *ΔfecI* strains. Each were grown in a manner identical to that of the RNAseq experiments. Error bars are shown +/- SEM. Student's t-test was used to assess statistical significance, $p<0.05$ = *, $p<0.001$ = **, $p<0.001$ = ***.

When examining the expression of genes involved in iron acquisition, we noted that all genes in the *fec*-operon were downregulated in the *fecI* mutant: *fecR* = -14.74 fold; *fecA* = -45.16 fold; ABUW_2984 = -93.29 fold; ABUW_2983 = -34.12 fold; ABUW_2982 = -25.8 fold; and ABUW_2981 = -17.7 fold. This was an important finding because we hypothesized that this operon may have a role in hemin acquisition, and our transcriptional studies showed that *fecI* appears to be required for hemin -induced activity of the *fecA* promoter from this cluster. Conversely, we observed upregulation of the outermembrane ferric enterobactin (*pfeA* = 3 fold) and an additional putative *tonB* receptor (ABUW_3403 = 3.43 fold). This could be the result of *fecI* disruption mediated iron starvation inducing expression of additional iron acquisition systems in an attempt to acquire iron from the environment.

Another operon found to be upregulated in the mutant was the *csu* operon (*csuA* = 150.9 fold, *csuB* = 74.5 fold, csuC = 89.17 fold, *csuD* = 101.48 fold, and *csuE* = 150.9 fold). This operon encodes a pilus assembly machinery and is required for twitching motility and adherence in *A. baumannii*. Thus, in conditions of iron starvation, one might suggest that the upregulation of these genes is the result of a need to explore new environments to acquire iron. Additionally, genes encoding the *adeABC* efflux pumps (*adeA* = 4.45, *adeB* = 4.45, *adeC* = 4.75) were upregulated in our mutant strain. It has been previously shown that this efflux pump system is upregulated in response to iron limitation in *A. baumannii*, however no further studies have investigated the significance of this response or specificity of this system to any iron source. The PAA pathway generates acetyl and succinyl-coA from the degradation of aromatic compounds to provide intermediates to the

TCA cycle [251]. Interestingly, the genes in this operon were downregulated (*paaG* = -11.95, *paaH* = -11.01, *paaI2* = -9.08, *paaJ* = -7.95, *paaK* = -8.98) in the *fecI* mutant. The function of genes involved in this pathway, including those encoding the PA-coA oxygenase, require iron for enzymatic activity [251]. Thus, it is possible that this operon is downregulation as a result of a need for iron conservation in the mutant strain. From our data, it seems that disruption of the FecI-sigma factor affects the expression of a number of genes that respond to iron limitation or require iron for enzymatic activity, and consequently may affect energy generation in the cell under iron limitation. To confirm this dataset, we performed qRT-PCR on a random selection of genes, all of which displayed similar fold changes to the RNA-seq study (**Figure 20**).

Disruption of the heme oxygenase *hemO* leads to hemin and hemoglobin dependent growth impairment. Approximately 67% of the total iron in the body exists in the form of heme bound to hemoglobin within red blood cells. In serum, heme is bound to albumin or hemopexin, and is consequently transferred to host cells containing heme oxygenases that can degrade heme to non-toxic products. As discussed above, our data suggests that the *fec*-operon in *A. baumannii* appears to be required for heme (hemin) acquisition. In bacteria, the role of heme oxygenases in degrading heme results in the liberation of iron that can be further used to meet nutritional requirements or for the enzymatic activity of certain proteins. Given their important role in iron metabolism, and the presence of a heme oxygenase in the *fec*-operon of *A. baumannii*, we focused our attention on the impact of *hemO* disruption on growth in the presence of hemin or hemoglobin. When using rich media (LB), the *hemO* mutant grew to levels comparable to

the wildtype (**Figure 21A**). Conversely, in the presence of hemin or human hemoglobin our mutant showed a defect in growth compared to the wild-type, a phenotype that was reversed upon complementation (**Figure 21B-C**). This thus suggests that expression of the heme oxygenase gene appears to be needed for growth in conditions when hemin is present either alone or bound to hemoglobin as a sole iron source.

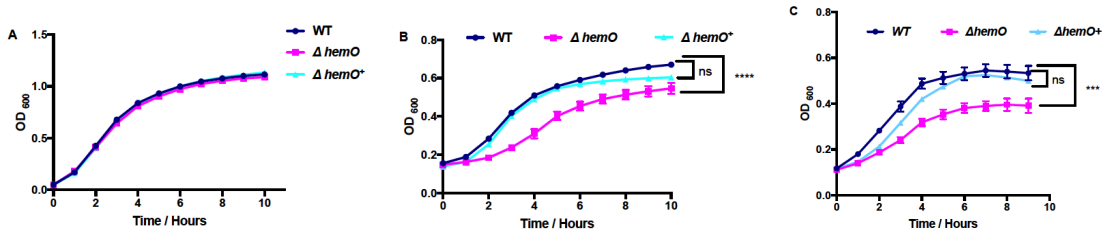

Figure 21. Disruption of *hemO* leads to growth impairment in the presence of hemin or human hemoglobin. The wild-type, ∆*hemO* and ∆*hemO*$^{+}$ strains were grown the presence of: (**A)** LB media; **or** in RPMI media supplemented with **(B)** 0.1μM hemin and 0.1μg/mL apo-transferrin or (C) 0.5μg/mL Human Hemoglobin. Data is derived from three biological replicates with error bars shown +/- SEM. A 2-way ANOVA analysis was used to define statistical significance, p<0.001 = ***, p<0.0001 = ****, ns = not significant compared to the wild-type.

Disruption of *hemO* results in a higher intracellular heme concentration compared to the wild-type. Since we observed a growth defect in the *hemO* mutant strain when hemin is present as a sole source of iron, we hypothesize that the *hemO* mutant strain would have a higher intracellular hemin concentration as a result of its inability to degrade hemin. Accordingly, we used a colorimetric based assay to detects hemin content within cells for our wild-type, mutant and complemented strain. In this experiment, our limited iron conditions (0.1μM hemin) were not detectable by the kit, thus the wild-type, *hemO* mutant, and complemented strains were grown in cultures supplemented with hemin to a final concentration of 1μM. After 6 hours of growth, cells were collected and lysed, before being treated with the hemin detection reagent. Upon analysis, we observed an increased

hemin content of 23% in the *hemO* mutant compared to the wild-type (**Figure 22**). The levels of hemin in the complemented strain was restored to wild-type levels suggesting that the lack of hemin oxygenase in the mutant strain results in less degradation of hemin within the cell.

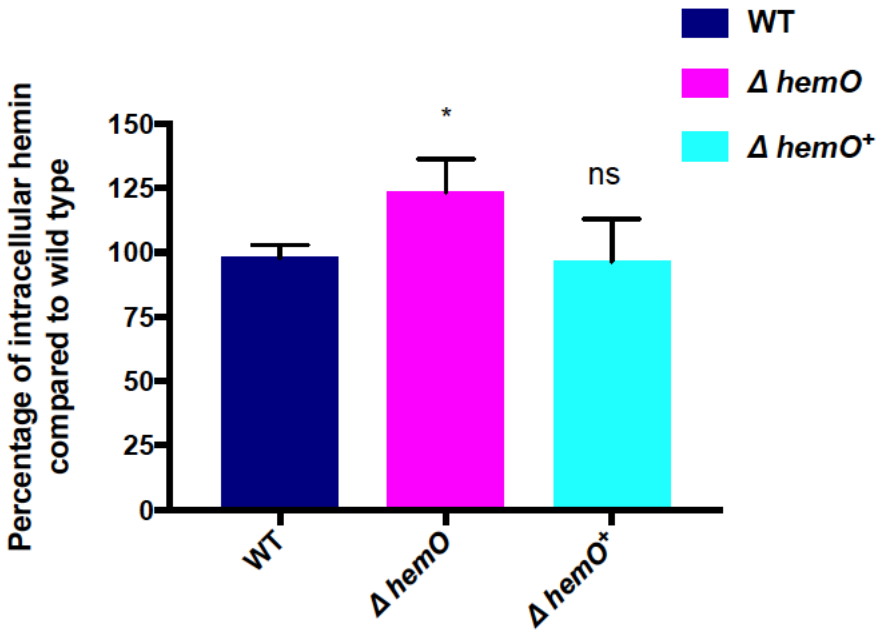

Figure 22. Disruption of *hemO* leads to increased levels of hemin within the *A, baumannii* cell. Intracellular levels of hemin were measured in cultures grown for 6 hours in the presence of 1μM hemin using a heme assay kit (Sigma-Aldrich). Data is derived from three biological replicates with error bars are shown +/- SEM. Student's t-test was used to assess statistical significance, * = $p<0.05$, ns = not significant compared to the wild-type.

Disruption of *hemO* leads to decreased survival of *A. baumannii* in human serum. The addition of Ga (III) protophoryn IX (GaPPIX), which blocks hemin acquisition systems in bacteria, was reported to impair the growth of *A. baumannii* strain LAC-4 in mouse serum. Interestingly LAC-4 growth levels in these conditions were found to be comparable to strain ATCC 17978, which lacks the *fec*-operon, further suggesting a role for this system in hemin acquisition. Given that our data supports a role for this operon in heme (hemin)

acquisition, and serum provides iron sources such as ferric iron bound to transferrin or hemin bound to albumin or hemopexin, we next set out to investigate if disruption of *hemO* could have an impact on survival in serum. Accordingly, we incubated our wild-type, *hemO* mutant and *hemO* complemented strain in Non-Heat Inactivated (NHI) and Heat Inactivated (HI) human serum. Upon analysis we observed that the *hemO* mutant had reduced survival, with a 1 log decrease in viability compared to the wild type and its complemented strain (**Figure 23A**). Additionally, we observe similar results in survival when compared to strains incubated in serum-HI (**Figure 23B**). Therefore, it appears that the reduced survival in the *hemO* mutant could be due to a less efficient assimilation of hemin, rather than an active complement system.

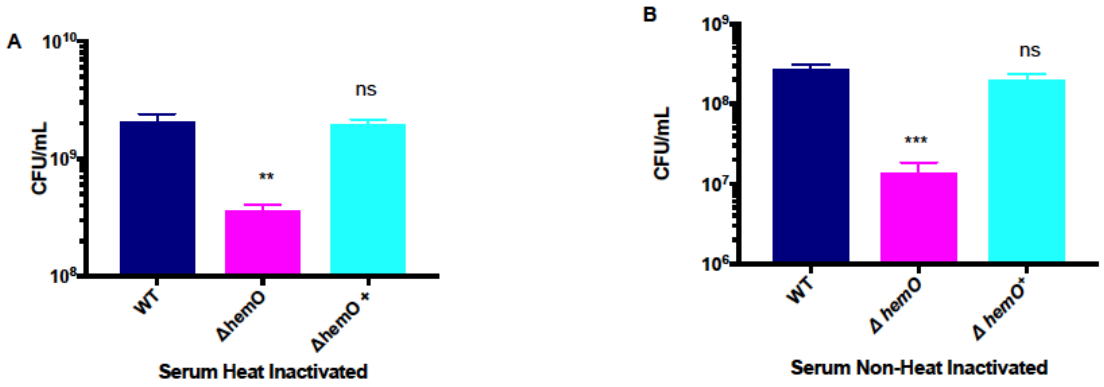

Figure 23. Disruption of *hemO* leads to reduce survival in human serum. Strains were inoculated into 100 µL of heat inactivated or non-heat inactivated human serum and incubated at 37°C for 4 hours, before viability was determined by serial dilution. Data is derived from three biological replicates, with error bars are shown +/- SEM. Student's t-test was used to assess statistical significance, $p<0.001$ = **, $p<0.001$ = ***, ns = not significant compared to the wild-type

DISCUSSION

In this study, we characterize a set of 8 genes organized within an operon, determining that the first three genes, annotated as ABUW_2987, ABUW_2986, and ABUW_2985, are predicted to encode homologs of FecI, FecR and FecA from *E. coli*, respectively. In *E. coli,* this operon is dedicated to regulation of the ferric citrate transport and utilization system. In addition, we found that FecI, FecR, and FecA from *A. baumannii* also shares similarity to FecI, FecR and FecA counterparts in *B. pertussis* and *B. avium* (HurI , HurR and BhuR), and in *S. marcescens* (HasI , HasS, and HasR). An interesting outcome in this study was that, although similarities between the FecI, FecR and FecI proteins exist, the downstream genes, which dictate specificity and function, are quite distinct from each other. Along these lines, the *A. baumannii* clinical isolate Lac-4 was reported to be more proficient at hemin utilization than other isolates due to the presence of the Fec operon in this strain. Indeed, although several iron acquisition systems expressing siderophores specific for ferric iron acquisition have been characterized in *A. baumannii*, a hemin acquisition system have not yet been characterized in this organism.

As such, we sought to investigate the effect of several iron sources in conjunction with mutants of the two predicted regulatory genes for this operon: *fecI* and *fecR.* When examined, growth of our mutants in the presence of either hemin or hemoglobin resulted in a significant growth defect compared to the wild-type. These observations, alongside our transcriptional studies, supports a role for acquisition and utilization of hemin and hemoglobin by this system. During infection, sequestration of iron is a defense host

mechanism to limit bacterial growth. With heme as the major iron source in the body, which is found to be in complex with hemoglobin or bound to host heme binding proteins, the existence of bacterial iron acquisition systems with specificity to these iron sources has previously been described in several pathogenic bacteria. For example, *Neisseria meningitidis* has a system comprised of an outermembrane receptor HpuB and a lipoprotein HpuA that together acquire heme from hemoglobin and the hemoglobin-haptoglobin complex. Interestingly, in several Gram-negative organisms, outermembrane receptors found in heme acquisition systems alongside ABC transporters or hemophore secretion proteins are under the regulatory control of FecI-FecR. Unlike the genomic organization found in these hemin acquisition systems, the *fec*-operon of our strain harbors a unique set of genes, including two predicted periplasmic proteins, a second Ton-B dependent protein and a gene encoding a heme oxygenase. Importantly, mutation of this latter gene also demonstrated growth defects in the presence of hemoglobin and hemin. Therefore, it could be that interaction of FecR with FecA in *A. baumannii* is required for activation of this system to acquire hemin in a similar manner to that described for the fec-operon of *E. coli*. However, with the presence of a *hemO* gene and the absence of an ABC transporter, the possibility exists that this operon and its genes encodes for a system with a distinct mechanism to acquire heme or hemoglobin to that previously described.

Under iron limited conditions in *E. coli*, ferric citrate is perceived by the FecA protein, inducing a signaling cascade via FecR that activates FecI. In *S. marcescens* and *B. pertussis* a similar mechanism has been described in iron starvation condition when

hemin is supplemented as sole iron source. In *B. avium*, a study demonstrated that disruption of *rhuR* (*fecR* homolog) renders the promoter of *bhuR* (*fecA* homolog) unresponsive to hemin, suggesting a positive regulatory function [243,252]. Another study using an *E. coli* strain with a deletion of the entire *fec* operon demonstrated that *fecI* and *fecA* together failed to complement this null strain, and that the function of this operon is only restored when complemented with f*ecI, fecR* and *fecI*[253]. Interestingly, we observed that our *fecI* and *fecR* mutant strains no longer respond to hemin as an inducer of transcription suggesting that induction of the *fecA* promoter in the presence of hemin depends on an active FecI- FecR system, which is necessary for inducing active transport of hemin; mirroring findings from the homologue systems in *B. avium*.

RNA-seq transcriptional analysis with a *fecI* mutant revealed the altered expression of genes involved in energy generation and iron-dependent metabolism in response to hemin. From this set of genes, the *fec*-operon displayed a downregulation in expression, supporting its role in transcription of this operon. As such, we investigated the effects of hemin upon disruption of *hemO*, given that a previous study linked the presence of this gene with hemin utilization in A*. baumannii*[250]. Notably, the *hemO* mutant displayed a growth defect in the presence of hemin as a sole iron source, decreased survival in serum, and increased levels of hemin within its cell. The role of bacterial hemin oxygenase in hemin uptake systems has been described in several organisms. For example, in *Pseudomonas aeruginosa* the hemin oxygenase PhuO has been shown to degrade hemin into biliverdin, carbon monoxide, and iron. In *Staphylococcus aureus* the hemin oxygenases IsdG and IsdI are required for hemin degradation. Therefore, the increased

levels of hemin in our *hemO* mutant is likely explained by its inability to degrade hemin, resulting in less robust growth when hemin is the only iron source. The decreased survival of the *hemO* mutant in serum also highlights the importance of its encoded Heme oxygenase for survival in restrictive iron environments, such as those found in a host during infection.

In summary, our data suggests that *A. baumannii* appears to deploy its *fec*-operon to regulate the acquisition and degradation of hemin. Although the mechanism in which this occurs is far from decoded, our data sheds light onto the possible manner in which this occurs. We propose that FecA senses hemin and transmits this signal, via FecR, to FecI to further enhance transcription of the *fec*-operon (**Figure 24**). This is supported by our transcriptional studies that demonstrate the effect of hemin on transcription of the *fec* operon and activity of the *fecA* promoter. Furthermore, regulation of hemin assimilation appears to be regulated by this system given the presence of HemO ,and deficiency of fec-operon mutant strains to grow in the presence of hemin and hemoglobin. With regards to this latter point, it is possible that the rest of the genes in this operon may be involved in a parallel mechanism to acquire hemin from hemoglobin and further transport it for degradation and utilization. Further work is currently being done to characterize the role of the genes present in this operon in hemin acquisition and utilization.

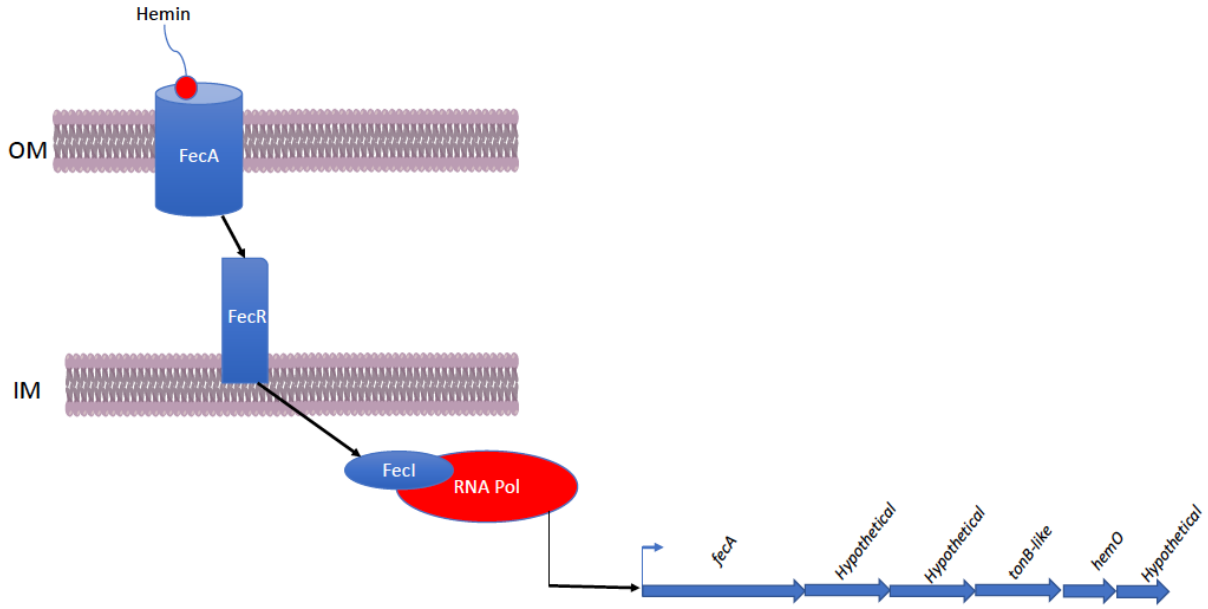

Figure 24. Model for perceiving hemin in the environment via the *fec*-operon of *A. baumannii.* Based on our transcriptional studies and the defined regulatory mechanism for Fec-operon homologs in other Gram-negative organisms, we propose that hemin induces activity of the FecA receptor and transmits this signal to FecI, via FecR, resulting in activation of genes necessary for hemin uptake and utilization.

CHAPTER V

FINAL DISCUSSION

The recognition of *Acinetobacter* species as pathogenic organisms in the last century occurred as a result of its recurrent isolation from clinical samples, presenting a need to define phenotypic characteristics that would allow for its accurate identification. As such, the definition of inherent phenotypic traits belonging to *Acinetobacter* species has revealed the opportunistic nature of the genus, with *A. baumannii* being the most representative human pathogen. While epidemiological studies in the 1980's began to document *A. baumannii* outbreaks in hospitals globally, the existence of effective antibiotic therapies to treat *A. baumannii* infections undermined its pathogenic nature. The underappreciation of its pathogenic potential, however, was soon after replaced by concerns of its rapid evolution towards multi-drug resistance. As a result, the characterization of genes encoding virulence factors in different clinical isolates has driven much of the *Acinetobacter* research over the last several decades.

Another important aspect that we have learned in the context of *A. baumannii*'s pathogenic evolution is its ability to acquire genes that facilitate survival under harsh conditions during the infectious process, for example nutrient scarcity, host immune defensive mechanism, and antibiotic pressures. Like any other bacteria, *A. baumannii* must possess regulatory systems that allow it to sense changes in the environment,

relaying this information as a signal transmitted to an effector protein that consequently elicits a rapid response in the form of orchestrated gene expression that ultimately is required for adaptation. The necessity of bacterial regulatory systems is explained by the energy required for synthesis of nucleotides and amino acids, and the assembly of a translation machinery that together is required for protein production [254]. In the absence of regulatory control, gene expression is a costly process that translates into burden during growth, and an altered energy status within the cell due to uncontrolled energy investment.

Given the importance of regulatory networks, it is of fundamental importance to understand how they enable bacteria to sense and respond to diverse stressful conditions, striving for survival and adaptation to specific niches in the context of pathogenicity. Although several genes encoding proteins with roles in antimicrobial resistance and disease causation have been characterized in *A. baumannii*, our knowledge regarding how these genes are regulated is limited to 6 TFs and 7 TCSs studied in recent years. To put this in perspective, *A. baumannii* has a genome size of 4.0Mbp, whilst *E. coli* with a genome size of 4.6Mbp has 304 annotated TFs. From this set of regulatory proteins, 185 TFs have been characterized in *E. coli* [255]. As such, a complete survey of the regulatory network in *A. baumannii* would provide a starting point to elucidate the systems used by this organism to interact with its environment and their relevance in the context of *A. baumannii* MDR infections. With this in mind, the initial work presented in chapter II of this dissertation was developed with the goal of defining the proteinaceous regulome of *A. baumannii* to provide a foundation that could serve to

investigate individual role of regulatory proteins in assisting this organism during infection. Given that *A. baumannii* AB5075 is a hypervirulent MDR strain when compared to other clinical isolates with different degrees of MDR phenotypes and pathogenicity, it was used as a model for our studies. The use of a combination of bioinformatic tools and available scientific literature allowed us to uncover the presence of 243 TFs, 14TCSs, and 5 σ factors. This is the first such study of its kind, providing a comprehensive collection of regulatory genes with most of them yet to be characterized in *A. baumannii*[153].

After defining the proteinaceous regulome of the hypervirulent strain AB5075, we next sought to understand how conservation or the absence of regulatory proteins could correlate to variations in pathogenicity across representative clinical strains with different degree of pathogenicity and antibiotic resistance. Interestingly, 202 TFs, 14 TCSs and 4 σ factors were found to be conserved among clinically relevant *A. baumannii* strains. This finding perhaps reflects their role in regulating essential biological process such as DNA synthesis and repair, cell division, and metabolic adaptation. In order to establish a link between our set of regulatory proteins and their potential role in virulence, we compared our curated genome of AB5075 to the screening of a recent developed AB5075 Tn library in a *Galleria mellonella* model of infection[110]. In doing so, we were able to find genes with putative regulatory functions that were required for survival during infection, providing a pathogenetic context to our work that can be used as tool for further investigation into specific roles of these uncharacterized regulatory proteins.

As an example, 4 secretion systems, including the type II secretion system (T2SS), the type VI secretion system, the autotransporter Ata, and the outer membrane vesicle (OMV), have been identified in *A. baumannii* with roles in virulence and lipid metabolism. Although mechanism of their regulation have not yet been identified, we found a putative TF (ABUW_2741) that was required for survival in the *G. mellonella* model of infection. Interestingly, in our analysis we found that this TF is a homolog of the Crp protein from *P. aeruginosa* that controls expression of genes encoding type III secretion system components. As such, one could speculate that this TF could have a regulatory role in governing secretion system expression in *A. baumannii*, particularly given its essentiality for survival in the worm infection model.

Another regulatory protein that, although not required for pathogenicity in the *Galleria* model, represents a good candidate for study is the *A. baumannii* homolog of the FecI σ factor from *E. coli*. Iron is an essential metal required for the function of a variety of proteins involved in essential biological functions in all living organisms, including bacteria[230]. Its limitation hinders these processes, resulting in growth inhibition and an impaired infectious capacity in pathogenic bacteria. Indeed, understanding the strategies utilized by such bacteria to acquire and assimilate essential metals such as iron has been an active area of research in the recent years. As such, this σ factor was of interest, particularly because it is only conserved in the highly pathogenic strains of *A. baumannii* used in our analysis, suggesting it may provide an advantage during disease causation. These findings, and insights into the iron regulatory systems extant within AB5075, will be further discussed in the last part of this chapter.

The information provided by our work investigating regulatory circuits in *A. baumannii* offers insights into potential regulatory functions of uncharacterized proteins. With this being said, we expect that our work will provide a foundation to guide further research in deconvoluting regulatory networks in this organism. Indeed, the work presented in chapter II enabled us to further pursue investigations into uncharacterized regulatory proteins in *A. baumannii* , and to demonstrate the usefulness of this resource. Specifically, we utilized our fully curated annotation of TCSs in the genome of AB5075 to explore those that have not been characterized. Interestingly, we found that the TCS ABUW_2426/2427 exhibited high homology to a TCS named ArcAB (Aerobic Respiratory Control) previously characterized in *E. coli*, *S. enterica, S. oneidensis, and H. influenzae*[168-172]. Protein alignments of the ABUW_2426 and ABUW_2427, encoding a response regulator and its sensor kinase, respectively, with the ArcAB systems from other organisms provided unique insights into the potential evolution of this system and its regulatory function in *A. baumannii.* The ArcAB system in *E. coli* serves to sense transition from aerobic to anaerobic conditions via the redox state of two conserved cysteine residues found in the ArcB sensor; which occurs as a result of changes in quinone pools. This in turn triggers a kinase reaction that phosphorylates ArcA and ultimately induces a remodeling of metabolic-energy generation pathways required for survival in the absence of oxygen[167]. In *A. baumannii*, the absence of one of the cysteine residues and a phosphotransfer domain in its ArcB, alongside its classification as strictly aerobic organism, argues for a divergent function and perhaps an alternative kinase mechanism for ArcAB and its response to stimuli that perturb metabolic pathways affecting energy generation.

Because a previously RNA seq analysis performed in our lab showed that the ABUW_2426/2427 is lowly expressed in LB media, we performed transcriptomic profiling on the *arcAB* system using different chemical stressor that would allow us to determine how its transcription could be induced. Our data showed that this TCS responded to the uncoupler CCCP, which perturbs the levels of electron carriers by inhibition of the ETC. These effects mirror those conditions in which decreased oxygen levels lead bacteria to use alternative electron transport chains via alternative electron donors/acceptors, such as nitrogen or fumarate. Thus, this finding suggests that the ArcAB of *A. baumannii* could regulate genes required to maintain sufficient energy levels to support essential cellular functions in response to oxygen tension. Of note, bone infections are characterized by the presence of necrotic tissue and abscesses, restricting blood flow and oxygen, and promoting bacteria attachment and biofilm formation[256]. Given that AB5075 was first isolated from an acute bone infection, one could speculate that the ArcAB system may function to regulate metabolic pathways that would allow it to survive in such harsh conditions encountered in infected bone tissue, including low oxygen levels and nutrients scarcity.

An indicator of the energy state of the cell is the PMF, which is known to be influenced by several external factors, including changes in oxygen availability and pH levels. Because the PMF is originated from a series of oxidation and reduction reactions that involve a functional glycolysis, TCA cycle, and ETC, creating a proton gradient to energize the membrane, its regulation is of importance for metabolic adaptability in bacteria. In this vein, the role of TCSs in regulating genes involved in these metabolic pathways has been

documented by others, including for ArcAB, RegAB and PhoPQ[257]. Indeed, disruption of the RR PhoP, associated with the regulation of metabolic pathways in *E. coli*, resulted in an altered PMF leading to changes in membrane polarity; highlighting the importance of these pathways to maintain energy balance in the cell [258,259].

Given that transcription of ArcAB in *A. baumannii* was induced upon exposure to CCCP, which is also known to disrupt the PMF, we examined the transmembrane proton gradient (△pH) and transmembrane potential (ΔΨ), both component of the PMF. Our findings showed that in the absence of either ArcA or ArcB both components were affected, further supporting a role for this TCS in the regulation of metabolic pathways to generate energy. Because the response of ArcAB to the effects of CCCP was highly specific, we also examined changes in gene expression upon disruption of *arcA* upon exposure to CCCP. After analysis of our dataset, we observed that mainly genes with functions in metabolism and energy generation were altered. Among these genes, significant changes in transcription were observed for genes involved in glycolysis, the TCA cycle, and the electron transport chain. Interestingly, some of these genes have been previously shown to be part of the regulome of ArcAB in *E. coli.* Aerobic organisms can generate energy from glucose oxidation via glycolysis, involving a number of enzymatic reactions that convert glucose to pyruvate. Pyruvate is then further converted to acetyl-coA, and enters the TCA cycle. Additional oxidation steps in the TCA cycle generates intermediate metabolites and reduced equivalents that donate electrons to the ETC, and in turn the ETC generates energy in the form of ATP. This process is relevant to findings in our work of rapid growth of our mutants in the presence of glucose (data no shown), alongside the

accumulation of glucose within the cell, suggesting an overwhelmed and overactive metabolic machinery. A response to high glucose concentrations described in *Saccharomyces cerevisiae*, also known as the Crabtree effect, involves inhibition of the TCA cycle, leading to decreased oxygen consumption. As a consequence, the generation of ATP via substrate phosphorylation is highly favorable under such conditions. These effects have also been observed in *E. coli,* in which excess glucose leads to the release of acetate as a result of active energy generation pathways replacing aerobic respiration. With this information, we measured the abundance of several metabolites produced by glycolysis and the TCA cycle that could provide a better understanding of metabolic alterations as a result of the disruption of the the ArcAB system in *A. baumannii*. Our results showed that our mutants have higher levels of pyruvate, suggesting an altered glycolytic pathway. Given the observed accumulation of glucose in our mutants, one could argue that higher levels of pyruvate could be the result of an overwhelmed glycolytic pathway that slows conversion of pyruvate to acetyl CoA. This is a phenomenon, known as pyruvate overflow, which was previously described in *E. coli* as response to increased glucose levels in the cell. Other side effects of glucose accumulation in the cell would be an allosteric inhibition of succinate dehydrogenase and induction of the glyoxylate shunt, favoring acetate production. One of the roles of the glyoxylate shunt is to accommodate the excess acetyl-coA that is generated from oxidation of carbon sources such as glucose, and to divert metabolic overflow towards the generation of acetate and metabolites such as oxaloacetate that feeds gluconeogenesis. Certainly, when we measured the abundance of succinate, our mutants had higher levels, supporting an allosteric inhibition of this complex as a result of glucose accumulation. In addition, levels

of oxaloacetate and acetate were higher in our mutants compared to our wildtype supporting a hyperactive glyoxylate shunt as a result of ArcAB disruption.

With a hyperactive glyoxylate shunt, we also observed increased NADH levels in our mutants compared to its wild-type, which could again be explained by metabolic overflow, inducing NADH production in the absence of ArcA . Indeed, a study published by Vemuri *et al* investigating overflow metabolism and redox homeostasis in an *arcA* mutant of *E. coli* showed that a hyperactive TCA cycle produces higher levels of NADH as a consequence of ArcA mediated control of this system[225]. In addition to this, our RNA-seq data showed that several genes encoding cytochrome oxidases and the ATP generation machinery, were downregulated, suggesting decreased function of the ETC in our mutants, which relies on oxidative phosphorylation that could contribute to the accumulation of reduced equivalents, such as NADH, that are not oxidized via ETC.

To further gain insight into the function of the ETC in our mutants, we tested their ability to generate ATP via oxidative phosphorylation and substrate phosphorylation. We found that disruption of the ArcAB system favors production of ATP via substrate phosphorylation, suggesting decreased activity of the ETC as a consequence of metabolic imbalances in the cell. We were able to analyze the activity of the cytochrome oxidase and found that its activity was lower in our mutants, supporting a disrupted function of the ETC upon *arcAB* disruption. As such, our data collectively supports a proposed role for ArcAB in *A. baumannii* in controlling metabolic pathways, while maintaining energy balance in the cell.

Lastly, our findings within the proteinaceous regulome of AB5075 presented in chapter II revealed the presence of a putative ECF-FecI-like sigma factor. In *E. coli*, the Fec system is comprised of FecA (a TonB outer-membrane protein) that upon sensing low external iron concentrations transmits a signal to the FecI sigma factor via the periplasmic protein FecR[240,241,244,260]. Interestingly, when we examined the genomic organization of genes next to the putative *fecI* in *A. baumannii*, we found that the *fecA*, *fecR,* and *fecI* gene arrangement of *E. coli* was conserved, suggesting a similar regulatory role in the context of iron acquisition.

The putative ECF-Fec-operon in *A. baumannii* presents a unique collection of genes, specifying two hypothetical periplasmic proteins and a TonB-like protein that perhaps could be part of an auxiliary iron transport system. An iron acquisition system with a secondary TonB-like protein (HasB) involved in heme transport has been described in *S. marcescens*[246]. Interestingly, we also found a *hemO*-like oxygenase gene in the *A. baumannii fec* operon, alongside an additional gene encoding a hypothetical protein. Bacterial heme oxygenases in Gram-negative organisms are required for assimilation of hemin within the cell. Upon the transport of hemin, heme oxygenases degrade it via three major enzymatic reactions, involving the cleavage and reduction of the ferric atom contained within the porphyrin ring to ferrous iron, before further oxidation to ferric iron and biliverdin. The distinct genes contained in the *A. baumannii fec* operon differ from the canonical heme – Fec dependent systems found in other pathogenic bacteria, which rely on an ABC transport system, implying the existence of a unique mechanism for transport and assimilation of hemin in this organism.

When testing strains with disrupted genes for FecI, FecR, FecA and HemO, a trend amongst the mutants became apparent: a growth defect was observed when the iron source provided contained hemin or hemoglobin. This finding is indicative of the potential role of these genes in the acquisition or assimilation of hemin or hemoglobin. Because the canonical surface signaling activation mechanism described for Fec- iron regulatory systems is initiated upon FecA sensing a specific iron source, we examined the transcriptional response of the *fecA* promoter in our collection of strains. Here we showed that this promoter was responsive to hemin, further supporting a potential regulatory function of this operon in hemin acquisition[250]. Next, we evaluated transcriptional changes upon exposure to hemin in the wild-type and *fecI* mutant strains. Upon analysis, we found a significant decrease in expression of the entire Fec-operon, suggesting a role for this system in the acquisition of hemin as an iron source.

Although disruption of the *fec*-operon appears to have no influence on the pathogenicity of AB5075 when tested in a *Galleria model* of infection, its role in virulence should not be dismissed. *G. mellonella* only contains ferric iron as an iron source, which is bound to iron binding proteins such as ferritin, apoferritin and holoferritin. [261] Thus, the absence of hemin as an available iron source in the larval model of infection, and the ability of *A. baumannii* to produce siderophores with high affinity for ferric iron, could explain why the genes present in the *fec*-operon of *A. baumannii* are not required for survival in such model of infection. We did, however, observe that disruption of *fecI, fecR,* and *hemO* resulted in less survival when strains were grown in human blood or serum. As hemin is one of the most abundant iron sources in the body, representing almost 70% of total, the

presence of a fec-operon dedicated to the acquisition and assimilation of hemin would be of great advantage for survival of *A. baumannii* within the host.

Future directions

Collectively, we expect that the work performed herein will contribute towards our understanding of the role of regulatory proteins in *A. baumannii*. In collaboration with computational biologists we were able to defined a complete set of regulatory proteins and create a resource that can be used to guide investigation on the function of uncharacterized regulatory proteins. Using this basis for our own projects, we were able to provide insights into the regulatory function of the ArcAB system of *A. baumannii* in the context of metabolism and energy state of the cell, and aminoglycosides resistance. However, our structural analysis of the ArcB protein of *A. baumannii* revealed distinct features such as the lack of conservation one of the cysteine residues (cys 241 in *E. coli*) that is required for sensing variation in oxygen levels via quinones concentration, a signal that determines the kinase activity of ArcB in *E. coli*. To determine whether the only conserved Cys (490) in *A. baumannii* is required for its kinase activity, the use of site directed mutagenesis in combination with kinase assays could be used to determine its requirement for ArcB autokinase activity in *A. baumannii*. Briefly, the conserved cysteine residue could be mutated to an alanine. ArcB from WT and $ArcB^{C490A}$ could be overexpressed from a plasmid and further purified to test their kinase activity. Purified proteins are incubated with $Y^{32}P$ and upon stopping the reactions samples could be visualized by SDS/PAGE and analyzed using a phosphorimaging. In the case that the

conserved cysteine residue is required for kinase activity of ArcB further phenotypic assays will assess its impact of the ArcB function.

Another finding of our structural analysis of the ArcAB system of *A. baumannii* revealed that this system is comprised of a TCS hybrid and the RR. This system appears to rely on a phophorelay mechanism for its activation based on conserved domains; however, the lack of a phosphotransferase domain in ArcB indicates the possibility of a protein with a Hpt domain that could assist on transfer of the phosphate group from the sensor to the receiver domain of ArcA (**Figure 25**). Thus, an initial computational screening using Hpt domain as a seed to search in the genome of AB5075 could provide with protein candidates that could be part of the ArcAB phosphorelay system. As such, the specificity of the Hpt protein for transferring of the phosphate to ArcA could be tested in an *in vitro* phosphorelay system. As such, purified phosphorylated ArcB and Hpt proteins of interest are incubated to allow phosphorylation of Hpt. Further incubation of these reactions with ArcA would allow transfer of the phosphate group to ArcA. Reactions could be analyzed using SDS /phosphorimaging. Finally, interaction between ArcB and identified Hpt protein would be evaluated using a bacterial hybrid assay. Overall these experiments would shed light into the signaling mechanism of the ArcAB system of *A. baumannii.*

With respect to the *fec*-operon of *A. baumannii*, our bioinformatic findings in combination with the generated RNA-seq data suggest the existence of four promoters induced under hemin limitation in this operon (**Figure 26**). As such we will be using the 5'-3 rapid amplification of cDNA (RACE) and Northern Blot analysis to confirm hemin-dependent

transcripts from each putative promoter. With this information, mapping and examination of this operon could be performed to identify features that will provide insights into the molecular regulation of the *fec*-operon. The activity of identified promoters could be further evaluated using qPCR in the presence of a variety of iron sources to assess their level of response to these iron forms. To further characterize the signaling mechanism of this operon, reconstitution of the signaling cascade using *lacZ* constructs in the best studied *fec*-system *E. coli* could provide further information in regard to the regulation of this system in *A. baumannii.* This approach has been proven to be successful in elucidating a similar heme surface signaling mechanism in *S. marcescens*[236]. As such, a *fecA*-lacZ fusion strain could be integrated into the chromosome of an *E. coli* strain with deletion of the *fur* gene to avoid repression of fur regulated genes and a WT *E. coli*. This newly created strain could be transformed with plasmids containing either: (a) *fecI,* (b) *fecI* and *fecR, or* (c) *fecI, fecR and fecA* to determine the transcriptional effects of each on *fecA*.

Currently, we are in the process of confirming complemented strains of the *fecI* and *fecA* genes to evaluate their ability to restore survival in serum and blood in vitro assay. Additionally, screening of genes with Tn insertions in hypothetical genes of these operon to evaluate their phenotypes under iron limitation are undergoing in our lab to completely characterize the *fec*-operon and its regulatory function in this organism.

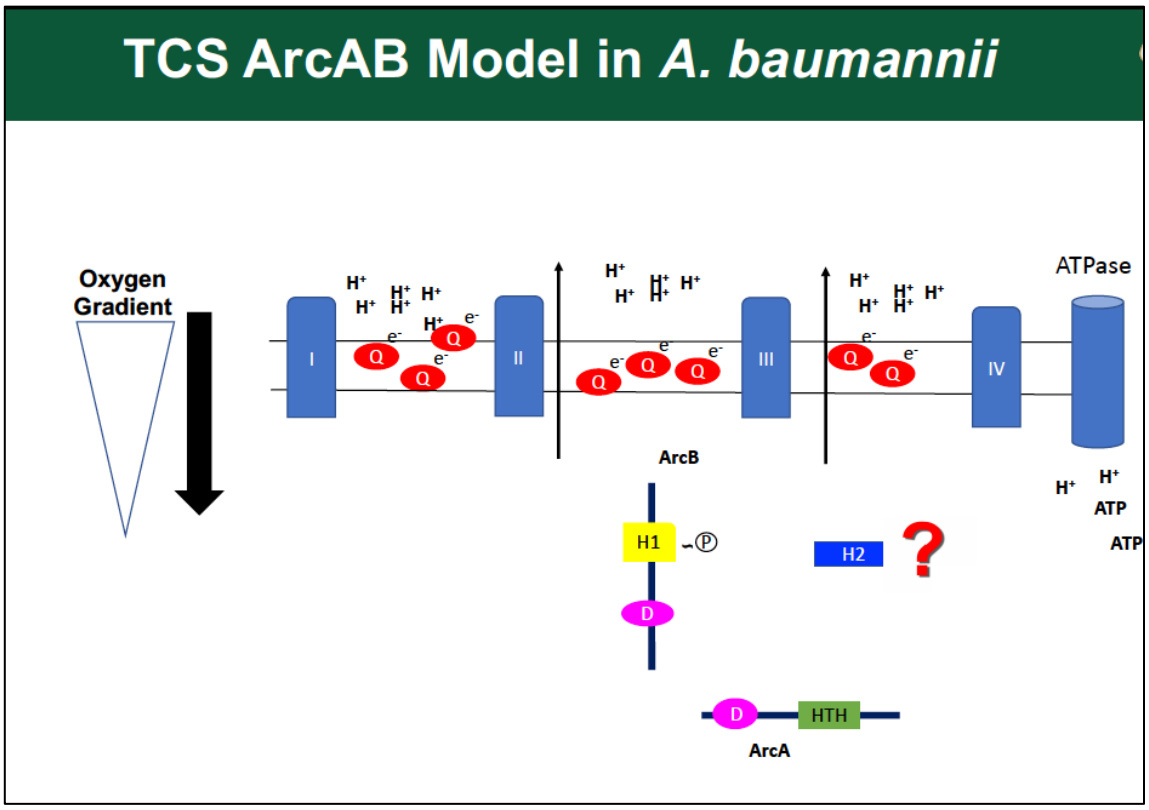

Figure 25. Proposed model of activation of ArcAB in *A. baumannii.*

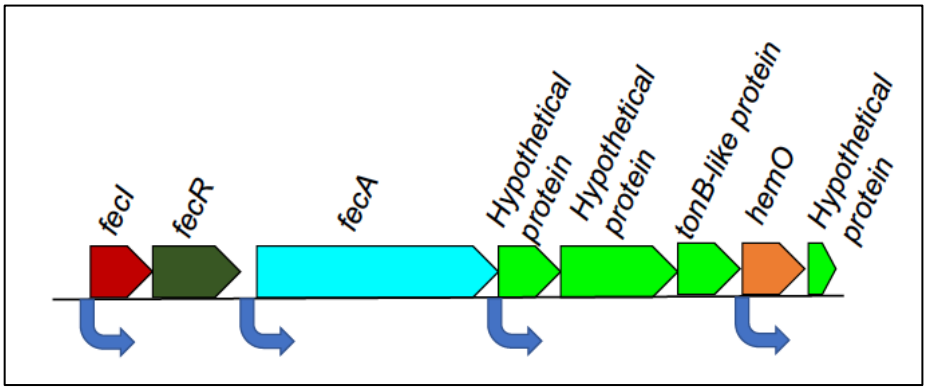

Figure 26. *fec*-like operon present in *A. baumannii* and predicted promoters based on transcripts generated from the RNA-seq data and bioinformatic analysis.

REFERENCES

1 K. J Towner, E. B.-B. a. C. A. F. *The Biology of Acinetobacter* (Springer Sicence 1991).

2 Audureau, U. A. [Not Available]. *Ann Inst Pasteur (Paris)* **73**, 690-693 (1947).

3 Bovre, K. & Henriksen, S. D. An approach to transformation studies in Moraxella. *Acta Pathol Microbiol Scand* **56**, 223-228 (1962).

4 Baumann, P., Doudoroff, M. & Stanier, R. Y. Study of the Moraxella group. I. Genus Moraxella and the Neisseria catarrhalis group. *J Bacteriol* **95**, 58-73 (1968).

5 Baumann, P., Doudoroff, M. & Stanier, R. Y. A study of the Moraxella group. II. Oxidative-negative species (genus Acinetobacter). *J Bacteriol* **95**, 1520-1541 (1968).

6 Joly-Guillou, M. L. [Bacteria of the Acinetobacter genus]. *Pathol Biol (Paris)* **46**, 245-252 (1998).

7 Lessel, E. F. International Committee on Nomenclature of Bacteria Subcommittee on the Taxonomy of Moraxella and Allied Bacteria: Minutes of the Meeting, 11 August 1970. Room Constitution C, Maria-Isabel Hotel, Mexico City, Mexico

. *International Journal of Systematic and Evolutionary* **21**, 213-214, doi:10.1099/00207713-21-2-213 (1971).

8 Daly, A. K., Postic, B. & Kass, E. H. Infections due to organisms of the genus Herellea. B5W and B. anitratum. *Arch Intern Med* **110**, 580-591 (1962).

9 Robinson, R. G., Garrison, R. G. & Brown, R. W. Evaluation of the Clinical Significance of the Genus Herellea. *Ann Intern Med* **60**, 19-27 (1964).

10 Glew, R. H., Moellering, R. C., Jr. & Kunz, L. J. Infections with Acinetobacter calcoaceticus (Herellea vaginicola): clinical and laboratory studies. *Medicine (Baltimore)* **56**, 79-97 (1977).

11 Tokiwa, H., Inoue, Y. & Takeyoshi, H. [Genus Acinetobacter isolated from the blood culture of the patients with septicemia]. *Igaku To Seibutsugaku* **82**, 47-51 (1971).

12 Abrutyn, E., Goodhart, G. L., Roos, K., Anderson, R. & Buxton, A. Acinetobacter calcoaceticus outbreak associated with peritoneal dialysis. *Am J Epidemiol* **107**, 328-335 (1978).

13 Bouvet P, G. P. Taxonomy of the Genus Acinetobacter with the Recognition of Acinetobacter baumannii sp. nov., Acinetobacter haemolyticus sp. nov., Acinetobacter johnsonii sp. nov., and Acinetobacter junii sp. nov. and Emended Descriptions of Acinetobacter calcoaceticus and Acinetobacter lwoffii. *International Journal of Systematic and Evolutionary Microbiology*, 228-240, doi:doi:10.1099/00207713-36-2-228

.

14 Nishimura Y, I. T., Iizuka H. Acinetobacter radioresistens sp. nov. Isolated from Cotton and Soil. *International Journal of Systematic and Evolutionary Microbiology* 38(32):209-211, doi:10.1099/00207713-38-2-209 (01 April 1988).
15 Vaneechoutte, M. *et al.* Identification of Acinetobacter genomic species by amplified ribosomal DNA restriction analysis. *J Clin Microbiol* **33**, 11-15 (1995).
16 Di Nocera, P. P., Rocco, F., Giannouli, M., Triassi, M. & Zarrilli, R. Genome organization of epidemic Acinetobacter baumannii strains. *BMC Microbiol* **11**, 224, doi:10.1186/1471-2180-11-224 (2011).
17 Peleg, A. Y., Seifert, H. & Paterson, D. L. Acinetobacter baumannii: emergence of a successful pathogen. *Clin Microbiol Rev* **21**, 538-582, doi:10.1128/CMR.00058-07 (2008).
18 Forder, A. A. A brief history of infection control - past and present. *S Afr Med J* **97**, 1161-1164 (2007).
19 Brodie, J. & Henderson, A. Mima polymorpha infection. *J Clin Pathol* **16**, 49-52 (1963).
20 Castle, M., Tenney, J. H., Weinstein, M. P. & Eickhoff, T. C. Outbreak of a multiply resistant Acinetobacter in a surgical intensive care unit: epidemiology and control. *Heart Lung* **7**, 641-644 (1978).
21 Villegas, M. V. & Hartstein, A. I. Acinetobacter outbreaks, 1977-2000. *Infect Control Hosp Epidemiol* **24**, 284-295, doi:10.1086/502205 (2003).
22 Siau, H., Yuen, K. Y., Wong, S. S., Ho, P. L. & Luk, W. K. The epidemiology of acinetobacter infections in Hong Kong. *J Med Microbiol* **44**, 340-347, doi:10.1099/00222615-44-5-340 (1996).
23 Retailliau, H. F., Hightower, A. W., Dixon, R. E. & Allen, J. R. Acinetobacter calcoaceticus: a nosocomial pathogen with an unusual seasonal pattern. *J Infect Dis* **139**, 371-375 (1979).
24 Bergogne-Berezin, E. & Towner, K. J. Acinetobacter spp. as nosocomial pathogens: microbiological, clinical, and epidemiological features. *Clin Microbiol Rev* **9**, 148-165 (1996).
25 Houang, E. T. *et al.* Epidemiology and infection control implications of Acinetobacter spp. in Hong Kong. *J Clin Microbiol* **39**, 228-234, doi:10.1128/JCM.39.1.228-234.2001 (2001).
26 Vila, J. *et al.* Spread of amikacin resistance in Acinetobacter baumannii strains isolated in Spain due to an epidemic strain. *J Clin Microbiol* **37**, 758-761 (1999).
27 Lai, S. W. *et al.* Acinetobacter baumannii bloodstream infection: clinical features and antimicrobial susceptibilities of isolates. *Kaohsiung J Med Sci* **15**, 406-413 (1999).
28 Lu, C. H., Chang, W. N. & Chuang, Y. C. Resistance to third-generation cephalosporins in adult gram-negative bacillary meningitis. *Infection* **27**, 208-211 (1999).
29 Rello, J., Sa-Borges, M., Correa, H., Leal, S. R. & Baraibar, J. Variations in etiology of ventilator-associated pneumonia across four treatment sites: implications for antimicrobial prescribing practices. *Am J Respir Crit Care Med* **160**, 608-613, doi:10.1164/ajrccm.160.2.9812034 (1999).
30 Nemec, A., Janda, L., Melter, O. & Dijkshoorn, L. Genotypic and phenotypic similarity of multiresistant Acinetobacter baumannii isolates in the Czech Republic. *J Med Microbiol* **48**, 287-296, doi:10.1099/00222615-48-3-287 (1999).

31 Raad, II *et al.* The prevention of biofilm colonization by multidrug-resistant pathogens that cause ventilator-associated pneumonia with antimicrobial-coated endotracheal tubes. *Biomaterials* **32**, 2689-2694, doi:10.1016/j.biomaterials.2010.12.015 (2011).
32 Wong, D. *et al.* Clinical and Pathophysiological Overview of Acinetobacter Infections: a Century of Challenges. *Clin Microbiol Rev* **30**, 409-447, doi:10.1128/CMR.00058-16 (2017).
33 Centers for Disease, C. & Prevention. Acinetobacter baumannii infections among patients at military medical facilities treating injured U.S. service members, 2002-2004. *MMWR Morb Mortal Wkly Rep* **53**, 1063-1066 (2004).
34 Davis, K. A., Moran, K. A., McAllister, C. K. & Gray, P. J. Multidrug-resistant Acinetobacter extremity infections in soldiers. *Emerg Infect Dis* **11**, 1218-1224, doi:10.3201/eid1108.050103 (2005).
35 Ressner, R. A. *et al.* Outcomes of bacteremia in burn patients involved in combat operations overseas. *J Am Coll Surg* **206**, 439-444, doi:10.1016/j.jamcollsurg.2007.09.017 (2008).
36 Maragakis, L. L. & Perl, T. M. Acinetobacter baumannii: epidemiology, antimicrobial resistance, and treatment options. *Clin Infect Dis* **46**, 1254-1263, doi:10.1086/529198 (2008).
37 Shorr, A. F., Zilberberg, M. D., Micek, S. T. & Kollef, M. H. Predictors of hospital mortality among septic ICU patients with Acinetobacter spp. bacteremia: a cohort study. *BMC Infect Dis* **14**, 572, doi:10.1186/s12879-014-0572-6 (2014).
38 Mittal, J., Szymczak, W. A., Robbins, N., Harris, C. & Nori, P. An unusual cause of community-acquired pneumonia. *IDCases* **11**, 41-43, doi:10.1016/j.idcr.2017.12.010 (2018).
39 Howard, A., O'Donoghue, M., Feeney, A. & Sleator, R. D. Acinetobacter baumannii: an emerging opportunistic pathogen. *Virulence* **3**, 243-250, doi:10.4161/viru.19700 (2012).
40 Dexter, C., Murray, G. L., Paulsen, I. T. & Peleg, A. Y. Community-acquired Acinetobacter baumannii: clinical characteristics, epidemiology and pathogenesis. *Expert Rev Anti Infect Ther* **13**, 567-573, doi:10.1586/14787210.2015.1025055 (2015).
41 Magnet, S., Courvalin, P. & Lambert, T. Resistance-nodulation-cell division-type efflux pump involved in aminoglycoside resistance in Acinetobacter baumannii strain BM4454. *Antimicrob Agents Chemother* **45**, 3375-3380, doi:10.1128/AAC.45.12.3375-3380.2001 (2001).
42 Vila, J. *et al.* In vitro antimicrobial production of beta-lactamases, aminoglycoside-modifying enzymes, and chloramphenicol acetyltransferase by and susceptibility of clinical isolates of Acinetobacter baumannii. *Antimicrob Agents Chemother* **37**, 138-141 (1993).
43 Seward, R. J., Lambert, T. & Towner, K. J. Molecular epidemiology of aminoglycoside resistance in Acinetobacter spp. *J Med Microbiol* **47**, 455-462, doi:10.1099/00222615-47-5-455 (1998).
44 Alvarez, M. & Mendoza, M. C. Molecular epidemiology of two genes encoding 3-N-aminoglycoside acetyltransferases AAC(3)I and AAC(3)II among gram-negative bacteria from a Spanish hospital. *Eur J Epidemiol* **9**, 650-657 (1993).

45 Obara, M. & Nakae, T. Mechanisms of resistance to beta-lactam antibiotics in Acinetobacter calcoaceticus. *J Antimicrob Chemother* **28**, 791-800 (1991).
46 Bou, G. & Martinez-Beltran, J. Cloning, nucleotide sequencing, and analysis of the gene encoding an AmpC beta-lactamase in Acinetobacter baumannii. *Antimicrob Agents Chemother* **44**, 428-432 (2000).
47 Okpara, A. U. & Maswoswe, J. J. Emergence of multidrug-resistant isolates of Acinetobacter baumannii. *Am J Hosp Pharm* **51**, 2671-2675 (1994).
48 Hoban, D. J. *et al.* Comparative in vitro activity of gemifloxacin, ciprofloxacin, levofloxacin and ofloxacin in a North American surveillance study. *Diagn Microbiol Infect Dis* **40**, 51-57 (2001).
49 Karlowsky, J. A., Hoban, D. J., Hackel, M. A., Lob, S. H. & Sahm, D. F. Antimicrobial susceptibility of Gram-negative ESKAPE pathogens isolated from hospitalized patients with intra-abdominal and urinary tract infections in Asia-Pacific countries: SMART 2013-2015. *J Med Microbiol* **66**, 61-69, doi:10.1099/jmm.0.000421 (2017).
50 Choi, H. K., Kim, Y. K., Kim, H. Y. & Uh, Y. Inhaled colistin for treatment of pneumonia due to colistin-only-susceptible Acinetobacter baumannii. *Yonsei Med J* **55**, 118-125, doi:10.3349/ymj.2014.55.1.118 (2014).
51 Jang, J. Y. *et al.* Efficacy and toxicity of high-dose nebulized colistin for critically ill surgical patients with ventilator-associated pneumonia caused by multidrug-resistant Acinetobacter baumannii. *J Crit Care* **40**, 251-256, doi:10.1016/j.jcrc.2017.04.004 (2017).
52 Qureshi, Z. A. *et al.* Colistin-resistant Acinetobacter baumannii: beyond carbapenem resistance. *Clin Infect Dis* **60**, 1295-1303, doi:10.1093/cid/civ048 (2015).
53 Agodi, A. *et al.* Spread of a carbapenem- and colistin-resistant Acinetobacter baumannii ST2 clonal strain causing outbreaks in two Sicilian hospitals. *J Hosp Infect* **86**, 260-266, doi:10.1016/j.jhin.2014.02.001 (2014).
54 Pogue, J. M., Cohen, D. A. & Marchaim, D. Editorial commentary: Polymyxin-resistant Acinetobacter baumannii: urgent action needed. *Clin Infect Dis* **60**, 1304-1307, doi:10.1093/cid/civ044 (2015).
55 Al-Sweih, N. A., Al-Hubail, M. A. & Rotimi, V. O. Emergence of tigecycline and colistin resistance in Acinetobacter species isolated from patients in Kuwait hospitals. *J Chemother* **23**, 13-16, doi:10.1179/joc.2011.23.1.13 (2011).
56 Marchand, I., Damier-Piolle, L., Courvalin, P. & Lambert, T. Expression of the RND-type efflux pump AdeABC in Acinetobacter baumannii is regulated by the AdeRS two-component system. *Antimicrob Agents Chemother* **48**, 3298-3304, doi:10.1128/AAC.48.9.3298-3304.2004 (2004).
57 Fournier, P. E. *et al.* Comparative genomics of multidrug resistance in Acinetobacter baumannii. *PLoS Genet* **2**, e7, doi:10.1371/journal.pgen.0020007 (2006).
58 Wachino, J. & Arakawa, Y. Exogenously acquired 16S rRNA methyltransferases found in aminoglycoside-resistant pathogenic Gram-negative bacteria: an update. *Drug Resist Updat* **15**, 133-148, doi:10.1016/j.drup.2012.05.001 (2012).
59 Shakil, S., Khan, R., Zarrilli, R. & Khan, A. U. Aminoglycosides versus bacteria--a description of the action, resistance mechanism, and nosocomial battleground. *J Biomed Sci* **15**, 5-14, doi:10.1007/s11373-007-9194-y (2008).

60 Pelletier, M. R. *et al.* Unique structural modifications are present in the lipopolysaccharide from colistin-resistant strains of Acinetobacter baumannii. *Antimicrob Agents Chemother* **57**, 4831-4840, doi:10.1128/AAC.00865-13 (2013).
61 Moffatt, J. H. *et al.* Colistin resistance in Acinetobacter baumannii is mediated by complete loss of lipopolysaccharide production. *Antimicrob Agents Chemother* **54**, 4971-4977, doi:10.1128/AAC.00834-10 (2010).
62 Cunha, B. A., Klimek, J. J., Gracewski, J., McLaughlin, J. C. & Quintiliani, R. A common source outbreak of Acinetobacter pulmonary infections traced to Wright respirometers. *Postgrad Med J* **56**, 169-172 (1980).
63 French, G. L. & Casewell, M. W. Controlling the spread of acinetobacter infection. *Br Med J* **281**, 388 (1980).
64 Smego, R. A., Jr. Endemic nosocomial Acinetobacter calcoaceticus bacteremia. Clinical significance, treatment, and prognosis. *Arch Intern Med* **145**, 2174-2179 (1985).
65 Spellberg, B. & Rex, J. H. The value of single-pathogen antibacterial agents. *Nat Rev Drug Discov* **12**, 963, doi:10.1038/nrd3957-c1 (2013).
66 Centers for Disease, C. Antibiotic Resistance Threat in the United States. (2013).
67 Visca, P., Seifert, H. & Towner, K. J. Acinetobacter infection--an emerging threat to human health. *IUBMB Life* **63**, 1048-1054, doi:10.1002/iub.534 (2011).
68 Chapartegui-Gonzalez, I. *et al.* Acinetobacter baumannii maintains its virulence after long-time starvation. *PLoS One* **13**, e0201961, doi:10.1371/journal.pone.0201961 (2018).
69 Jawad, A., Seifert, H., Snelling, A. M., Heritage, J. & Hawkey, P. M. Survival of Acinetobacter baumannii on dry surfaces: comparison of outbreak and sporadic isolates. *J Clin Microbiol* **36**, 1938-1941 (1998).
70 Strassle, P. *et al.* The effect of terminal cleaning on environmental contamination rates of multidrug-resistant Acinetobacter baumannii. *Am J Infect Control* **40**, 1005-1007, doi:10.1016/j.ajic.2012.05.027 (2012).
71 Espinal, P., Marti, S. & Vila, J. Effect of biofilm formation on the survival of Acinetobacter baumannii on dry surfaces. *J Hosp Infect* **80**, 56-60, doi:10.1016/j.jhin.2011.08.013 (2012).
72 Wagenvoort, J. H. & Joosten, E. J. An outbreak Acinetobacter baumannii that mimics MRSA in its environmental longevity. *J Hosp Infect* **52**, 226-227 (2002).
73 Spellberg, B. & Bonomo, R. A. "Airborne assault": a new dimension in Acinetobacter baumannii transmission*. *Crit Care Med* **41**, 2042-2044, doi:10.1097/CCM.0b013e31829136c3 (2013).
74 Adams, M. D. *et al.* Resistance to colistin in Acinetobacter baumannii associated with mutations in the PmrAB two-component system. *Antimicrob Agents Chemother* **53**, 3628-3634, doi:10.1128/AAC.00284-09 (2009).
75 Greene, C., Wu, J., Rickard, A. H. & Xi, C. Evaluation of the ability of Acinetobacter baumannii to form biofilms on six different biomedical relevant surfaces. *Lett Appl Microbiol* **63**, 233-239, doi:10.1111/lam.12627 (2016).
76 Gaddy, J. A. & Actis, L. A. Regulation of Acinetobacter baumannii biofilm formation. *Future Microbiol* **4**, 273-278, doi:10.2217/fmb.09.5 (2009).

77 Brossard, K. A. & Campagnari, A. A. The Acinetobacter baumannii biofilm-associated protein plays a role in adherence to human epithelial cells. *Infect Immun* **80**, 228-233, doi:10.1128/IAI.05913-11 (2012).
78 Sugawara, E. & Nikaido, H. OmpA is the principal nonspecific slow porin of Acinetobacter baumannii. *J Bacteriol* **194**, 4089-4096, doi:10.1128/JB.00435-12 (2012).
79 Iyer, R., Moussa, S. H., Durand-Reville, T. F., Tommasi, R. & Miller, A. Acinetobacter baumannii OmpA Is a Selective Antibiotic Permeant Porin. *ACS Infect Dis* **4**, 373-381, doi:10.1021/acsinfecdis.7b00168 (2018).
80 Perez, A. *et al.* The FhaB/FhaC two-partner secretion system is involved in adhesion of Acinetobacter baumannii AbH12O-A2 strain. *Virulence* **8**, 959-974, doi:10.1080/21505594.2016.1262313 (2017).
81 Harding, C. M. *et al.* Pathogenic Acinetobacter species have a functional type I secretion system and contact-dependent inhibition systems. *J Biol Chem* **292**, 9075-9087, doi:10.1074/jbc.M117.781575 (2017).
82 Russo, T. A. *et al.* The K1 capsular polysaccharide of Acinetobacter baumannii strain 307-0294 is a major virulence factor. *Infect Immun* **78**, 3993-4000, doi:10.1128/IAI.00366-10 (2010).
83 Moffatt, J. H. *et al.* Lipopolysaccharide-deficient Acinetobacter baumannii shows altered signaling through host Toll-like receptors and increased susceptibility to the host antimicrobial peptide LL-37. *Infect Immun* **81**, 684-689, doi:10.1128/IAI.01362-12 (2013).
84 Erridge, C., Moncayo-Nieto, O. L., Morgan, R., Young, M. & Poxton, I. R. Acinetobacter baumannii lipopolysaccharides are potent stimulators of human monocyte activation via Toll-like receptor 4 signalling. *J Med Microbiol* **56**, 165-171, doi:10.1099/jmm.0.46823-0 (2007).
85 Stahl, J., Bergmann, H., Gottig, S., Ebersberger, I. & Averhoff, B. Acinetobacter baumannii Virulence Is Mediated by the Concerted Action of Three Phospholipases D. *PLoS One* **10**, e0138360, doi:10.1371/journal.pone.0138360 (2015).
86 Antunes, L. C., Imperi, F., Carattoli, A. & Visca, P. Deciphering the multifactorial nature of Acinetobacter baumannii pathogenicity. *PLoS One* **6**, e22674, doi:10.1371/journal.pone.0022674 (2011).
87 Mussi, M. A. *et al.* The opportunistic human pathogen Acinetobacter baumannii senses and responds to light. *J Bacteriol* **192**, 6336-6345, doi:10.1128/JB.00917-10 (2010).
88 McQueary, C. N. *et al.* Extracellular stress and lipopolysaccharide modulate Acinetobacter baumannii surface-associated motility. *J Microbiol* **50**, 434-443, doi:10.1007/s12275-012-1555-1 (2012).
89 King, L. B., Pangburn, M. K. & McDaniel, L. S. Serine protease PKF of Acinetobacter baumannii results in serum resistance and suppression of biofilm formation. *J Infect Dis* **207**, 1128-1134, doi:10.1093/infdis/jis939 (2013).
90 Tilley, D., Law, R., Warren, S., Samis, J. A. & Kumar, A. CpaA a novel protease from Acinetobacter baumannii clinical isolates deregulates blood coagulation. *FEMS Microbiol Lett* **356**, 53-61, doi:10.1111/1574-6968.12496 (2014).

91 van Dessel, H. *et al.* Identification of a new geographically widespread multiresistant Acinetobacter baumannii clone from European hospitals. *Res Microbiol* **155**, 105-112, doi:10.1016/j.resmic.2003.10.003 (2004).
92 Diancourt, L., Passet, V., Nemec, A., Dijkshoorn, L. & Brisse, S. The population structure of Acinetobacter baumannii: expanding multiresistant clones from an ancestral susceptible genetic pool. *PLoS One* **5**, e10034, doi:10.1371/journal.pone.0010034 (2010).
93 Imperi, F. *et al.* The genomics of Acinetobacter baumannii: insights into genome plasticity, antimicrobial resistance and pathogenicity. *IUBMB Life* **63**, 1068-1074, doi:10.1002/iub.531 (2011).
94 Adams, M. D. *et al.* Comparative genome sequence analysis of multidrug-resistant Acinetobacter baumannii. *J Bacteriol* **190**, 8053-8064, doi:10.1128/JB.00834-08 (2008).
95 Iacono, M. *et al.* Whole-genome pyrosequencing of an epidemic multidrug-resistant Acinetobacter baumannii strain belonging to the European clone II group. *Antimicrob Agents Chemother* **52**, 2616-2625, doi:10.1128/AAC.01643-07 (2008).
96 Nemec, A., Dolzani, L., Brisse, S., van den Broek, P. & Dijkshoorn, L. Diversity of aminoglycoside-resistance genes and their association with class 1 integrons among strains of pan-European Acinetobacter baumannii clones. *J Med Microbiol* **53**, 1233-1240, doi:10.1099/jmm.0.45716-0 (2004).
97 Huys, G. *et al.* Repetitive-DNA-element PCR fingerprinting and antibiotic resistance of pan-European multi-resistant Acinetobacter baumannii clone III strains. *J Med Microbiol* **54**, 851-856, doi:10.1099/jmm.0.45986-0 (2005).
98 Snitkin, E. S. *et al.* Genome-wide recombination drives diversification of epidemic strains of Acinetobacter baumannii. *Proc Natl Acad Sci U S A* **108**, 13758-13763, doi:10.1073/pnas.1104404108 (2011).
99 Lin, M. F., Lin, Y. Y., Yeh, H. W. & Lan, C. Y. Role of the BaeSR two-component system in the regulation of Acinetobacter baumannii adeAB genes and its correlation with tigecycline susceptibility. *BMC Microbiol* **14**, 119, doi:10.1186/1471-2180-14-119 (2014).
100 Richmond, G. E. *et al.* The Acinetobacter baumannii Two-Component System AdeRS Regulates Genes Required for Multidrug Efflux, Biofilm Formation, and Virulence in a Strain-Specific Manner. *MBio* **7**, e00430-00416, doi:10.1128/mBio.00430-16 (2016).
101 Lin, M. F., Lin, Y. Y. & Lan, C. Y. The Role of the Two-Component System BaeSR in Disposing Chemicals through Regulating Transporter Systems in Acinetobacter baumannii. *PLoS One* **10**, e0132843, doi:10.1371/journal.pone.0132843 (2015).
102 Cerqueira, G. M. *et al.* A global virulence regulator in Acinetobacter baumannii and its control of the phenylacetic acid catabolic pathway. *J Infect Dis* **210**, 46-55, doi:10.1093/infdis/jiu024 (2014).
103 Tomaras, A. P., Flagler, M. J., Dorsey, C. W., Gaddy, J. A. & Actis, L. A. Characterization of a two-component regulatory system from Acinetobacter baumannii that controls biofilm formation and cellular morphology. *Microbiology* **154**, 3398-3409, doi:10.1099/mic.0.2008/019471-0 (2008).
104 Geisinger, E., Mortman, N. J., Vargas-Cuebas, G., Tai, A. K. & Isberg, R. R. A global regulatory system links virulence and antibiotic resistance to envelope homeostasis

in Acinetobacter baumannii. *PLoS Pathog* **14**, e1007030, doi:10.1371/journal.ppat.1007030 (2018).
105 Peleg, A. Y. *et al.* Prokaryote-eukaryote interactions identified by using Caenorhabditis elegans. *Proc Natl Acad Sci U S A* **105**, 14585-14590, doi:10.1073/pnas.0805048105 (2008).
106 Bhuiyan, M. S. *et al.* Acinetobacter baumannii phenylacetic acid metabolism influences infection outcome through a direct effect on neutrophil chemotaxis. *Proc Natl Acad Sci U S A* **113**, 9599-9604, doi:10.1073/pnas.1523116113 (2016).
107 Daniel, C., Haentjens, S., Bissinger, M. C. & Courcol, R. J. Characterization of the Acinetobacter baumannii Fur regulator: cloning and sequencing of the fur homolog gene. *FEMS Microbiol Lett* **170**, 199-209 (1999).
108 Mortensen, B. L. & Skaar, E. P. The contribution of nutrient metal acquisition and metabolism to Acinetobacter baumannii survival within the host. *Front Cell Infect Microbiol* **3**, 95, doi:10.3389/fcimb.2013.00095 (2013).
109 Hood, M. I. *et al.* Identification of an Acinetobacter baumannii zinc acquisition system that facilitates resistance to calprotectin-mediated zinc sequestration. *PLoS Pathog* **8**, e1003068, doi:10.1371/journal.ppat.1003068 (2012).
110 Gebhardt, M. J. *et al.* Joint Transcriptional Control of Virulence and Resistance to Antibiotic and Environmental Stress in Acinetobacter baumannii. *MBio* **6**, e01660-01615, doi:10.1128/mBio.01660-15 (2015).
111 Chin, C. Y. *et al.* A high-frequency phenotypic switch links bacterial virulence and environmental survival in Acinetobacter baumannii. *Nat Microbiol* **3**, 563-569, doi:10.1038/s41564-018-0151-5 (2018).
112 Gebhardt, M. J. & Shuman, H. A. GigA and GigB are Master Regulators of Antibiotic Resistance, Stress Responses, and Virulence in Acinetobacter baumannii. *J Bacteriol* **199**, doi:10.1128/JB.00066-17 (2017).
113 Wylie, J. L. & Worobec, E. A. The OprB porin plays a central role in carbohydrate uptake in Pseudomonas aeruginosa. *J Bacteriol* **177**, 3021-3026 (1995).
114 Soares, N. C. *et al.* 2-DE analysis indicates that Acinetobacter baumannii displays a robust and versatile metabolism. *Proteome Sci* **7**, 37, doi:10.1186/1477-5956-7-37 (2009).
115 Farrugia, D. N. *et al.* The complete genome and phenome of a community-acquired Acinetobacter baumannii. *PLoS One* **8**, e58628, doi:10.1371/journal.pone.0058628 (2013).
116 Nairn, B. L. *et al.* The Response of Acinetobacter baumannii to Zinc Starvation. *Cell Host Microbe* **19**, 826-836, doi:10.1016/j.chom.2016.05.007 (2016).
117 Mussi, M. A., Relling, V. M., Limansky, A. S. & Viale, A. M. CarO, an Acinetobacter baumannii outer membrane protein involved in carbapenem resistance, is essential for L-ornithine uptake. *FEBS Lett* **581**, 5573-5578, doi:10.1016/j.febslet.2007.10.063 (2007).
118 Wang, N., Ozer, E. A., Mandel, M. J. & Hauser, A. R. Genome-wide identification of Acinetobacter baumannii genes necessary for persistence in the lung. *MBio* **5**, e01163-01114, doi:10.1128/mBio.01163-14 (2014).
119 Abbott, B. J., Laskin, A. I. & McCoy, C. J. Growth of Acinetobacter calcoaceticus on ethanol. *Appl Microbiol* **25**, 787-792 (1973).

120 Wolfe, A. J. The acetate switch. *Microbiol Mol Biol Rev* **69**, 12-50, doi:10.1128/MMBR.69.1.12-50.2005 (2005).
121 Camarena, L., Bruno, V., Euskirchen, G., Poggio, S. & Snyder, M. Molecular mechanisms of ethanol-induced pathogenesis revealed by RNA-sequencing. *PLoS Pathog* **6**, e1000834, doi:10.1371/journal.ppat.1000834 (2010).
122 Palmer, L. D. & Skaar, E. P. Transition Metals and Virulence in Bacteria. *Annu Rev Genet* **50**, 67-91, doi:10.1146/annurev-genet-120215-035146 (2016).
123 Harding, C. M., Hennon, S. W. & Feldman, M. F. Uncovering the mechanisms of Acinetobacter baumannii virulence. *Nat Rev Microbiol* **16**, 91-102, doi:10.1038/nrmicro.2017.148 (2018).
124 Dorsey, C. W., Beglin, M. S. & Actis, L. A. Detection and analysis of iron uptake components expressed by Acinetobacter baumannii clinical isolates. *J Clin Microbiol* **41**, 4188-4193 (2003).
125 Antunes, L. C., Imperi, F., Towner, K. J. & Visca, P. Genome-assisted identification of putative iron-utilization genes in Acinetobacter baumannii and their distribution among a genotypically diverse collection of clinical isolates. *Res Microbiol* **162**, 279-284, doi:10.1016/j.resmic.2010.10.010 (2011).
126 Mihara, K. *et al.* Identification and transcriptional organization of a gene cluster involved in biosynthesis and transport of acinetobactin, a siderophore produced by Acinetobacter baumannii ATCC 19606T. *Microbiology* **150**, 2587-2597, doi:10.1099/mic.0.27141-0 (2004).
127 Gaddy, J. A. *et al.* Role of acinetobactin-mediated iron acquisition functions in the interaction of Acinetobacter baumannii strain ATCC 19606T with human lung epithelial cells, Galleria mellonella caterpillars, and mice. *Infect Immun* **80**, 1015-1024, doi:10.1128/IAI.06279-11 (2012).
128 Subashchandrabose, S. *et al.* Acinetobacter baumannii Genes Required for Bacterial Survival during Bloodstream Infection. *mSphere* **1**, doi:10.1128/mSphere.00013-15 (2016).
129 Mortensen, B. L., Rathi, S., Chazin, W. J. & Skaar, E. P. Acinetobacter baumannii response to host-mediated zinc limitation requires the transcriptional regulator Zur. *J Bacteriol* **196**, 2616-2626, doi:10.1128/JB.01650-14 (2014).
130 Juttukonda, L. J., Chazin, W. J. & Skaar, E. P. Acinetobacter baumannii Coordinates Urea Metabolism with Metal Import To Resist Host-Mediated Metal Limitation. *MBio* **7**, doi:10.1128/mBio.01475-16 (2016).
131 Tsakiridou, E. *et al.* Acinetobacter baumannii infection in prior ICU bed occupants is an independent risk factor for subsequent cases of ventilator-associated pneumonia. *Biomed Res Int* **2014**, 193516, doi:10.1155/2014/193516 (2014).
132 Guerrero, D. M. *et al.* Acinetobacter baumannii-associated skin and soft tissue infections: recognizing a broadening spectrum of disease. *Surg Infect (Larchmt)* **11**, 49-57, doi:10.1089/sur.2009.022 (2010).
133 Doyle, J. S., Buising, K. L., Thursky, K. A., Worth, L. J. & Richards, M. J. Epidemiology of infections acquired in intensive care units. *Semin Respir Crit Care Med* **32**, 115-138, doi:10.1055/s-0031-1275525 (2011).
134 Bou, G. *et al.* Fast assessment of resistance to carbapenems and ciprofloxacin of clinical strains of Acinetobacter baumannii. *J Clin Microbiol* **50**, 3609-3613, doi:10.1128/JCM.01675-12 (2012).

135 Morfin-Otero, R. *et al.* Acinetobacter baumannii infections in a tertiary care hospital in Mexico over the past 13 years. *Chemotherapy* **59**, 57-65, doi:10.1159/000351098 (2013).
136 Mera, R. M., Miller, L. A., Amrine-Madsen, H. & Sahm, D. F. Acinetobacter baumannii 2002-2008: increase of carbapenem-associated multiclass resistance in the United States. *Microb Drug Resist* **16**, 209-215, doi:10.1089/mdr.2010.0052 (2010).
137 Zarrilli, R. *et al.* Molecular epidemiology of sequential outbreaks of Acinetobacter baumannii in an intensive care unit shows the emergence of carbapenem resistance. *J Clin Microbiol* **42**, 946-953 (2004).
138 Hujer, K. M. *et al.* Analysis of antibiotic resistance genes in multidrug-resistant Acinetobacter sp. isolates from military and civilian patients treated at the Walter Reed Army Medical Center. *Antimicrob Agents Chemother* **50**, 4114-4123, doi:10.1128/AAC.00778-06 (2006).
139 Carvalho, K. R. *et al.* Dissemination of multidrug-resistant Acinetobacter baumannii genotypes carrying bla(OXA-23) collected from hospitals in Rio de Janeiro, Brazil. *Int J Antimicrob Agents* **34**, 25-28, doi:10.1016/j.ijantimicag.2008.12.009 (2009).
140 Clark, N. M., Zhanel, G. G. & Lynch, J. P., 3rd. Emergence of antimicrobial resistance among Acinetobacter species: a global threat. *Curr Opin Crit Care* **22**, 491-499, doi:10.1097/MCC.0000000000000337 (2016).
141 Willyard, C. The drug-resistant bacteria that pose the greatest health threats. *Nature* **543**, 15, doi:doi:10.1038/nature.2017.21550 (2017).
142 Fang, F. C., Frawley, E. R., Tapscott, T. & Vazquez-Torres, A. Bacterial Stress Responses during Host Infection. *Cell Host Microbe* **20**, 133-143, doi:10.1016/j.chom.2016.07.009 (2016).
143 Fiester, S. E. & Actis, L. A. Stress responses in the opportunistic pathogen Acinetobacter baumannii. *Future Microbiol* **8**, 353-365, doi:10.2217/fmb.12.150 (2013).
144 Boor, K. J. Bacterial stress responses: what doesn't kill them can make then stronger. *PLoS Biol* **4**, e23 (2006).
145 Laub, M. T. & Goulian, M. Specificity in two-component signal transduction pathways. *Annu Rev Genet* **41**, 121-145, doi:10.1146/annurev.genet.41.042007.170548 (2007).
146 Vicente, M., Chater, K. F. & De Lorenzo, V. Bacterial transcription factors involved in global regulation. *Mol Microbiol* **33**, 8-17 (1999).
147 Alm, E., Huang, K. & Arkin, A. The evolution of two-component systems in bacteria reveals different strategies for niche adaptation. *PLoS Comput Biol* **2**, e143, doi:10.1371/journal.pcbi.0020143 (2006).
148 Bhate, M. P., Molnar, K. S., Goulian, M. & DeGrado, W. F. Signal transduction in histidine kinases: insights from new structures. *Structure* **23**, 981-994, doi:10.1016/j.str.2015.04.002 (2015).
149 Cheung, J. & Hendrickson, W. A. Sensor domains of two-component regulatory systems. *Curr Opin Microbiol* **13**, 116-123, doi:10.1016/j.mib.2010.01.016 (2010).
150 Mascher, T. Intramembrane-sensing histidine kinases: a new family of cell envelope stress sensors in Firmicutes bacteria. *FEMS Microbiol Lett* **264**, 133-144, doi:10.1111/j.1574-6968.2006.00444.x (2006).

151 Mascher, T., Helmann, J. D. & Unden, G. Stimulus perception in bacterial signal-transducing histidine kinases. *Microbiol Mol Biol Rev* **70**, 910-938, doi:10.1128/MMBR.00020-06 (2006).
152 Mitrophanov, A. Y. & Groisman, E. A. Signal integration in bacterial two-component regulatory systems. *Genes Dev* **22**, 2601-2611, doi:10.1101/gad.1700308 (2008).
153 Casella, L. G., Weiss, A., Perez-Rueda, E., Antonio Ibarra, J. & Shaw, L. N. Towards the complete proteinaceous regulome of Acinetobacter baumannii. *Microb Genom* **3**, mgen000107, doi:10.1099/mgen.0.000107 (2017).
154 Arroyo, L. A. *et al.* The pmrCAB operon mediates polymyxin resistance in Acinetobacter baumannii ATCC 17978 and clinical isolates through phosphoethanolamine modification of lipid A. *Antimicrob Agents Chemother* **55**, 3743-3751, doi:10.1128/AAC.00256-11 (2011).
155 Liou, M. L. *et al.* The sensor kinase BfmS mediates virulence in Acinetobacter baumannii. *J Microbiol Immunol Infect* **47**, 275-281, doi:10.1016/j.jmii.2012.12.004 (2014).
156 Tipton, K. A. & Rather, P. N. An ompR/envZ Two-Component System Ortholog Regulates Phase Variation, Osmotic Tolerance, Motility, and Virulence in Acinetobacter baumannii strain AB5075. *J Bacteriol*, doi:10.1128/JB.00705-16 (2016).
157 Nowak, J., Schneiders, T., Seifert, H. & Higgins, P. G. The Asp20-to-Asn Substitution in the Response Regulator AdeR Leads to Enhanced Efflux Activity of AdeB in Acinetobacter baumannii. *Antimicrob Agents Chemother* **60**, 1085-1090, doi:10.1128/AAC.02413-15 (2016).
158 Iuchi, S. & Lin, E. C. arcA (dye), a global regulatory gene in Escherichia coli mediating repression of enzymes in aerobic pathways. *Proc Natl Acad Sci U S A* **85**, 1888-1892 (1988).
159 Iuchi, S., Cameron, D. C. & Lin, E. C. A second global regulator gene (arcB) mediating repression of enzymes in aerobic pathways of Escherichia coli. *J Bacteriol* **171**, 868-873 (1989).
160 Iuchi, S., Matsuda, Z., Fujiwara, T. & Lin, E. C. The arcB gene of Escherichia coli encodes a sensor-regulator protein for anaerobic repression of the arc modulon. *Mol Microbiol* **4**, 715-727 (1990).
161 Georgellis, D., Lynch, A. S. & Lin, E. C. In vitro phosphorylation study of the arc two-component signal transduction system of Escherichia coli. *J Bacteriol* **179**, 5429-5435 (1997).
162 Kwon, O., Georgellis, D. & Lin, E. C. Phosphorelay as the sole physiological route of signal transmission by the arc two-component system of Escherichia coli. *J Bacteriol* **182**, 3858-3862 (2000).
163 Bauer, C. E., Elsen, S. & Bird, T. H. Mechanisms for redox control of gene expression. *Annu Rev Microbiol* **53**, 495-523, doi:10.1146/annurev.micro.53.1.495 (1999).
164 Alvarez, A. F., Rodriguez, C. & Georgellis, D. Ubiquinone and menaquinone electron carriers represent the yin and yang in the redox regulation of the ArcB sensor kinase. *J Bacteriol* **195**, 3054-3061, doi:10.1128/JB.00406-13 (2013).
165 Bekker, M. *et al.* Changes in the redox state and composition of the quinone pool of Escherichia coli during aerobic batch-culture growth. *Microbiology* **153**, 1974-1980, doi:10.1099/mic.0.2007/006098-0 (2007).

166 Bekker, M. *et al.* The ArcBA two-component system of Escherichia coli is regulated by the redox state of both the ubiquinone and the menaquinone pool. *J Bacteriol* **192**, 746-754, doi:10.1128/JB.01156-09 (2010).
167 Malpica, R., Franco, B., Rodriguez, C., Kwon, O. & Georgellis, D. Identification of a quinone-sensitive redox switch in the ArcB sensor kinase. *Proc Natl Acad Sci U S A* **101**, 13318-13323, doi:10.1073/pnas.0403064101 (2004).
168 Sengupta, N., Paul, K. & Chowdhury, R. The global regulator ArcA modulates expression of virulence factors in Vibrio cholerae. *Infect Immun* **71**, 5583-5589 (2003).
169 Yuan, J., Wei, B., Lipton, M. S. & Gao, H. Impact of ArcA loss in Shewanella oneidensis revealed by comparative proteomics under aerobic and anaerobic conditions. *Proteomics* **12**, 1957-1969, doi:10.1002/pmic.201100651 (2012).
170 Ding, L. *et al.* The arcA gene contributes to the serum resistance and virulence of Haemophilus parasuis serovar 13 clinical strain EP3. *Vet Microbiol* **196**, 67-71, doi:10.1016/j.vetmic.2016.10.011 (2016).
171 Georgellis, D., Kwon, O., Lin, E. C., Wong, S. M. & Akerley, B. J. Redox signal transduction by the ArcB sensor kinase of Haemophilus influenzae lacking the PAS domain. *J Bacteriol* **183**, 7206-7212, doi:10.1128/JB.183.24.7206-7212.2001 (2001).
172 Wan, F. *et al.* Impaired cell envelope resulting from arcA mutation largely accounts for enhanced sensitivity to hydrogen peroxide in Shewanella oneidensis. *Sci Rep* **5**, 10228, doi:10.1038/srep10228 (2015).
173 Wong, S. M., Alugupalli, K. R., Ram, S. & Akerley, B. J. The ArcA regulon and oxidative stress resistance in Haemophilus influenzae. *Mol Microbiol* **64**, 1375-1390, doi:10.1111/j.1365-2958.2007.05747.x (2007).
174 Morales, E. H. *et al.* Probing the ArcA regulon under aerobic/ROS conditions in Salmonella enterica serovar Typhimurium. *BMC Genomics* **14**, 626, doi:10.1186/1471-2164-14-626 (2013).
175 Evans, M. R. *et al.* Analysis of the ArcA regulon in anaerobically grown Salmonella enterica sv. Typhimurium. *BMC Microbiol* **11**, 58, doi:10.1186/1471-2180-11-58 (2011).
176 Loui, C., Chang, A. C. & Lu, S. Role of the ArcAB two-component system in the resistance of Escherichia coli to reactive oxygen stress. *BMC Microbiol* **9**, 183, doi:10.1186/1471-2180-9-183 (2009).
177 Jones, S. A. *et al.* Respiration of Escherichia coli in the mouse intestine. *Infect Immun* **75**, 4891-4899, doi:10.1128/IAI.00484-07 (2007).
178 Pardo-Este, C. *et al.* The ArcAB two-component regulatory system promotes resistance to reactive oxygen species and systemic infection by Salmonella Typhimurium. *PLoS One* **13**, e0203497, doi:10.1371/journal.pone.0203497 (2018).
179 Gallagher, L. A. *et al.* Resources for Genetic and Genomic Analysis of Emerging Pathogen Acinetobacter baumannii. *J Bacteriol* **197**, 2027-2035, doi:10.1128/JB.00131-15 (2015).
180 Shaw, L. N. *et al.* Identification and characterization of sigma, a novel component of the Staphylococcus aureus stress and virulence responses. *PLoS One* **3**, e3844, doi:10.1371/journal.pone.0003844 (2008).

181 Miller, H. K. *et al.* The extracytoplasmic function sigma factor sigmaS protects against both intracellular and extracytoplasmic stresses in Staphylococcus aureus. *J Bacteriol* **194**, 4342-4354, doi:10.1128/JB.00484-12 (2012).
182 Carroll, R. K., Weiss, A. & Shaw, L. N. RNA-Sequencing of Staphylococcus aureus Messenger RNA. *Methods Mol Biol* **1373**, 131-141, doi:10.1007/7651_2014_192 (2016).
183 West, A. H. & Stock, A. M. Histidine kinases and response regulator proteins in two-component signaling systems. *Trends Biochem Sci* **26**, 369-376 (2001).
184 Appleby, J. L., Parkinson, J. S. & Bourret, R. B. Signal transduction via the multi-step phosphorelay: not necessarily a road less traveled. *Cell* **86**, 845-848 (1996).
185 Imamura, A., Yoshino, Y. & Mizuno, T. Cellular localization of the signaling components of Arabidopsis His-to-Asp phosphorelay. *Biosci Biotechnol Biochem* **65**, 2113-2117, doi:10.1271/bbb.65.2113 (2001).
186 Chen, M. H. *et al.* Characterization of the RcsC-->YojN-->RcsB phosphorelay signaling pathway involved in capsular synthesis in Escherichia coli. *Biosci Biotechnol Biochem* **65**, 2364-2367 (2001).
187 Lassak, J., Bubendorfer, S. & Thormann, K. M. Domain analysis of ArcS, the hybrid sensor kinase of the Shewanella oneidensis MR-1 Arc two-component system, reveals functional differentiation of its two receiver domains. *J Bacteriol* **195**, 482-492, doi:10.1128/JB.01715-12 (2013).
188 Toro-Roman, A., Mack, T. R. & Stock, A. M. Structural analysis and solution studies of the activated regulatory domain of the response regulator ArcA: a symmetric dimer mediated by the alpha4-beta5-alpha5 face. *J Mol Biol* **349**, 11-26, doi:10.1016/j.jmb.2005.03.059 (2005).
189 Aravind, L., Anantharaman, V., Balaji, S., Babu, M. M. & Iyer, L. M. The many faces of the helix-turn-helix domain: transcription regulation and beyond. *FEMS Microbiol Rev* **29**, 231-262, doi:10.1016/j.femsre.2004.12.008 (2005).
190 Kolar, S. L. *et al.* NsaRS is a cell-envelope-stress-sensing two-component system of Staphylococcus aureus. *Microbiology* **157**, 2206-2219, doi:10.1099/mic.0.049692-0 (2011).
191 Goldsby, R. A. & Heytler, P. G. Uncoupling of Oxidative Phosphorylation by Carbonyl Cyanide Phenylhydrazones. Ii. Effects of Carbonyl Cyanide M-Chlorophenylhydrazone on Mitochondrial Respiration. *Biochemistry* **2**, 1142-1147 (1963).
192 Otten, M. F. *et al.* The reduction state of the Q-pool regulates the electron flux through the branched respiratory network of Paracoccus denitrificans. *Eur J Biochem* **261**, 767-774 (1999).
193 Cao, X., Qi, Y., Xu, C., Yang, Y. & Wang, J. Transcriptome and metabolome responses of Shewanella oneidensis MR-1 to methyl orange under microaerophilic and aerobic conditions. *Appl Microbiol Biotechnol* **101**, 3463-3472, doi:10.1007/s00253-016-8087-2 (2017).
194 Calderon, I. L. *et al.* Response regulator ArcA of Salmonella enterica serovar Typhimurium downregulates expression of OmpD, a porin facilitating uptake of hydrogen peroxide. *Res Microbiol* **162**, 214-222, doi:10.1016/j.resmic.2010.11.001 (2011).

195 Taylor, B. L. Role of proton motive force in sensory transduction in bacteria. *Annu Rev Microbiol* **37**, 551-573, doi:10.1146/annurev.mi.37.100183.003003 (1983).
196 Mitchell, P. Chemiosmotic coupling in oxidative and photosynthetic phosphorylation. 1966. *Biochim Biophys Acta* **1807**, 1507-1538, doi:10.1016/j.bbabio.2011.09.018 (2011).
197 Perrenoud, A. & Sauer, U. Impact of global transcriptional regulation by ArcA, ArcB, Cra, Crp, Cya, Fnr, and Mlc on glucose catabolism in Escherichia coli. *J Bacteriol* **187**, 3171-3179, doi:10.1128/JB.187.9.3171-3179.2005 (2005).
198 Weiss, A., Broach, W. H., Lee, M. C. & Shaw, L. N. Towards the complete small RNome of Acinetobacter baumannii. *Microb Genom* **2**, e000045, doi:10.1099/mgen.0.000045 (2016).
199 Goosen, N., Horsman, H. P., Huinen, R. G. & van de Putte, P. Acinetobacter calcoaceticus genes involved in biosynthesis of the coenzyme pyrrolo-quinoline-quinone: nucleotide sequence and expression in Escherichia coli K-12. *J Bacteriol* **171**, 447-455 (1989).
200 Beardmore-Gray, M. & Anthony, C. The oxidation of glucose by Acinetobacter calcoaceticus: interaction of the quinoprotein glucose dehydrogenase with the electron transport chain. *J Gen Microbiol* **132**, 1257-1268, doi:10.1099/00221287-132-5-1257 (1986).
201 Enjalbert, B., Millard, P., Dinclaux, M., Portais, J. C. & Letisse, F. Acetate fluxes in Escherichia coli are determined by the thermodynamic control of the Pta-AckA pathway. *Sci Rep* **7**, 42135, doi:10.1038/srep42135 (2017).
202 Singh, R., Mailloux, R. J., Puiseux-Dao, S. & Appanna, V. D. Oxidative stress evokes a metabolic adaptation that favors increased NADPH synthesis and decreased NADH production in Pseudomonas fluorescens. *J Bacteriol* **189**, 6665-6675, doi:10.1128/JB.00555-07 (2007).
203 Park, S. J., Tseng, C. P. & Gunsalus, R. P. Regulation of succinate dehydrogenase (sdhCDAB) operon expression in Escherichia coli in response to carbon supply and anaerobiosis: role of ArcA and Fnr. *Mol Microbiol* **15**, 473-482 (1995).
204 Deckers-Hebestreit, G. & Altendorf, K. The F0F1-type ATP synthases of bacteria: structure and function of the F0 complex. *Annu Rev Microbiol* **50**, 791-824, doi:10.1146/annurev.micro.50.1.791 (1996).
205 Richardson, D. J. Bacterial respiration: a flexible process for a changing environment. *Microbiology* **146 (Pt 3)**, 551-571, doi:10.1099/00221287-146-3-551 (2000).
206 Amarasingham, C. R. & Davis, B. D. Regulation of alpha-ketoglutarate dehydrogenase formation in Escherichia coli. *J Biol Chem* **240**, 3664-3668 (1965).
207 Rose, I. A., Grunberg-Manago, M., Korey, S. R. & Ochoa, S. Enzymatic phosphorylation of acetate. *J Biol Chem* **211**, 737-756 (1954).
208 Su, Y. B. *et al.* Pyruvate cycle increases aminoglycoside efficacy and provides respiratory energy in bacteria. *Proc Natl Acad Sci U S A* **115**, E1578-E1587, doi:10.1073/pnas.1714645115 (2018).
209 Burstein, C., Tiankova, L. & Kepes, A. Respiratory control in Escherichia coli K 12. *Eur J Biochem* **94**, 387-392 (1979).
210 Ghoul, M., Pommepuy, M., Moillo-Batt, A. & Cormier, M. Effect of carbonyl cyanide m-chlorophenylhydrazone on Escherichia coli halotolerance. *Appl Environ Microbiol* **55**, 1040-1043 (1989).

211 Tatusov, R. L. *et al.* Metabolism and evolution of Haemophilus influenzae deduced from a whole-genome comparison with Escherichia coli. *Curr Biol* **6**, 279-291 (1996).
212 Fleischmann, R. D. *et al.* Whole-genome random sequencing and assembly of Haemophilus influenzae Rd. *Science* **269**, 496-512 (1995).
213 Shinkarev, V. P., Ugulava, N. B., Takahashi, E., Crofts, A. R. & Wraight, C. A. Aspartate-187 of cytochrome b is not needed for DCCD inhibition of ubiquinol: cytochrome c oxidoreductase in Rhodobacter sphaeroides chromatophores. *Biochemistry* **39**, 14232-14237 (2000).
214 Clejan, L., Bosch, C. G. & Beattie, D. S. Inhibition by dicyclohexylcarbodiimide of proton ejection but not electron transfer in rat liver mitochondria. *J Biol Chem* **259**, 13017-13020 (1984).
215 Degli Esposti, M. & Lenaz, G. A clarification of the effects of DCCD on the electron transfer and antimycin binding of the mitochondrial bc1 complex. *J Bioenerg Biomembr* **17**, 109-121 (1985).
216 Azarkina, N. & Konstantinov, A. A. Stimulation of menaquinone-dependent electron transfer in the respiratory chain of Bacillus subtilis by membrane energization. *J Bacteriol* **184**, 5339-5347 (2002).
217 Clifton, C. E. Microbiology--past, present, and future. *Annu Rev Microbiol* **20**, 1-12, doi:10.1146/annurev.mi.20.100166.000245 (1966).
218 Clifton, C. E. & Logan, W. A. On the Relation between Assimilation and Respiration in Suspensions and in Cultures of Escherichia coli. *J Bacteriol* **37**, 523-540 (1939).
219 Bogachev, A. V., Murtazine, R. A., Shestopalov, A. I. & Skulachev, V. P. Induction of the Escherichia coli cytochrome d by low delta mu H+ and by sodium ions. *Eur J Biochem* **232**, 304-308 (1995).
220 Puehringer, S., Metlitzky, M. & Schwarzenbacher, R. The pyrroloquinoline quinone biosynthesis pathway revisited: a structural approach. *BMC Biochem* **9**, 8, doi:10.1186/1471-2091-9-8 (2008).
221 Toyama, H. & Lidstrom, M. E. pqqA is not required for biosynthesis of pyrroloquinoline quinone in Methylobacterium extorquens AM1. *Microbiology* **144 (Pt 1)**, 183-191, doi:10.1099/00221287-144-1-183 (1998).
222 An, R. & Moe, L. A. Regulation of Pyrroloquinoline Quinone-Dependent Glucose Dehydrogenase Activity in the Model Rhizosphere-Dwelling Bacterium Pseudomonas putida KT2440. *Appl Environ Microbiol* **82**, 4955-4964, doi:10.1128/AEM.00813-16 (2016).
223 Park, D. M., Akhtar, M. S., Ansari, A. Z., Landick, R. & Kiley, P. J. The bacterial response regulator ArcA uses a diverse binding site architecture to regulate carbon oxidation globally. *PLoS Genet* **9**, e1003839, doi:10.1371/journal.pgen.1003839 (2013).
224 Levanon, S. S., San, K. Y. & Bennett, G. N. Effect of oxygen on the Escherichia coli ArcA and FNR regulation systems and metabolic responses. *Biotechnol Bioeng* **89**, 556-564, doi:10.1002/bit.20381 (2005).
225 Vemuri, G. N., Altman, E., Sangurdekar, D. P., Khodursky, A. B. & Eiteman, M. A. Overflow metabolism in Escherichia coli during steady-state growth: transcriptional regulation and effect of the redox ratio. *Appl Environ Microbiol* **72**, 3653-3661, doi:10.1128/AEM.72.5.3653-3661.2006 (2006).

226 Partridge, J. D., Scott, C., Tang, Y., Poole, R. K. & Green, J. Escherichia coli transcriptome dynamics during the transition from anaerobic to aerobic conditions. *J Biol Chem* **281**, 27806-27815, doi:10.1074/jbc.M603450200 (2006).
227 Akhova, A. V. & Tkachenko, A. G. ATP/ADP alteration as a sign of the oxidative stress development in Escherichia coli cells under antibiotic treatment. *FEMS Microbiol Lett* **353**, 69-76, doi:10.1111/1574-6968.12405 (2014).
228 Alexeeva, S., de Kort, B., Sawers, G., Hellingwerf, K. J. & de Mattos, M. J. Effects of limited aeration and of the ArcAB system on intermediary pyruvate catabolism in Escherichia coli. *J Bacteriol* **182**, 4934-4940 (2000).
229 Krewulak, K. D. & Vogel, H. J. Structural biology of bacterial iron uptake. *Biochim Biophys Acta* **1778**, 1781-1804, doi:10.1016/j.bbamem.2007.07.026 (2008).
230 Cassat, J. E. & Skaar, E. P. Iron in infection and immunity. *Cell Host Microbe* **13**, 509-519, doi:10.1016/j.chom.2013.04.010 (2013).
231 Bullen, J. J., Rogers, H. J. & Griffiths, E. Role of iron in bacterial infection. *Curr Top Microbiol Immunol* **80**, 1-35 (1978).
232 Lewis, J. P. Metal uptake in host-pathogen interactions: role of iron in Porphyromonas gingivalis interactions with host organisms. *Periodontol 2000* **52**, 94-116, doi:10.1111/j.1600-0757.2009.00329.x (2010).
233 Choby, J. E. & Skaar, E. P. Heme Synthesis and Acquisition in Bacterial Pathogens. *J Mol Biol* **428**, 3408-3428, doi:10.1016/j.jmb.2016.03.018 (2016).
234 Skaar, E. P. The battle for iron between bacterial pathogens and their vertebrate hosts. *PLoS Pathog* **6**, e1000949, doi:10.1371/journal.ppat.1000949 (2010).
235 Troxell, B. & Hassan, H. M. Transcriptional regulation by Ferric Uptake Regulator (Fur) in pathogenic bacteria. *Front Cell Infect Microbiol* **3**, 59, doi:10.3389/fcimb.2013.00059 (2013).
236 Biville, F. *et al.* Haemophore-mediated signalling in Serratia marcescens: a new mode of regulation for an extra cytoplasmic function (ECF) sigma factor involved in haem acquisition. *Mol Microbiol* **53**, 1267-1277, doi:10.1111/j.1365-2958.2004.04207.x (2004).
237 Vanderpool, C. K. & Armstrong, S. K. Integration of environmental signals controls expression of Bordetella heme utilization genes. *J Bacteriol* **186**, 938-948 (2004).
238 Vanderpool, C. K. & Armstrong, S. K. The Bordetella bhu locus is required for heme iron utilization. *J Bacteriol* **183**, 4278-4287, doi:10.1128/JB.183.14.4278-4287.2001 (2001).
239 Stiefel, A. *et al.* Control of the ferric citrate transport system of Escherichia coli: mutations in region 2.1 of the FecI extracytoplasmic-function sigma factor suppress mutations in the FecR transmembrane regulatory protein. *J Bacteriol* **183**, 162-170, doi:10.1128/JB.183.1.162-170.2001 (2001).
240 Ochs, M., Angerer, A., Enz, S. & Braun, V. Surface signaling in transcriptional regulation of the ferric citrate transport system of Escherichia coli: mutational analysis of the alternative sigma factor FecI supports its essential role in fec transport gene transcription. *Mol Gen Genet* **250**, 455-465 (1996).
241 Van Hove, B., Staudenmaier, H. & Braun, V. Novel two-component transmembrane transcription control: regulation of iron dicitrate transport in Escherichia coli K-12. *J Bacteriol* **172**, 6749-6758 (1990).

242 Miyazaki, H., Kato, H., Nakazawa, T. & Tsuda, M. A positive regulatory gene, pvdS, for expression of pyoverdin biosynthetic genes in Pseudomonas aeruginosa PAO. *Mol Gen Genet* **248**, 17-24 (1995).
243 King, N. D., Kirby, A. E. & Connell, T. D. Transcriptional control of the rhuIR-bhuRSTUV heme acquisition locus in Bordetella avium. *Infect Immun* **73**, 1613-1624, doi:10.1128/IAI.73.3.1613-1624.2005 (2005).
244 Angerer, A. & Braun, V. Iron regulates transcription of the Escherichia coli ferric citrate transport genes directly and through the transcription initiation proteins. *Arch Microbiol* **169**, 483-490 (1998).
245 Mahren, S., Enz, S. & Braun, V. Functional interaction of region 4 of the extracytoplasmic function sigma factor FecI with the cytoplasmic portion of the FecR transmembrane protein of the Escherichia coli ferric citrate transport system. *J Bacteriol* **184**, 3704-3711 (2002).
246 Paquelin, A., Ghigo, J. M., Bertin, S. & Wandersman, C. Characterization of HasB, a Serratia marcescens TonB-like protein specifically involved in the haemophore-dependent haem acquisition system. *Mol Microbiol* **42**, 995-1005 (2001).
247 Ghigo, J. M., Letoffe, S. & Wandersman, C. A new type of hemophore-dependent heme acquisition system of Serratia marcescens reconstituted in Escherichia coli. *J Bacteriol* **179**, 3572-3579 (1997).
248 Salisbury, V., Hedges, R. W. & Datta, N. Two modes of "curing" transmissible bacterial plasmids. *J Gen Microbiol* **70**, 443-452, doi:10.1099/00221287-70-3-443 (1972).
249 Kemp, E. H., Sammons, R. L., Moir, A., Sun, D. & Setlow, P. Analysis of transcriptional control of the gerD spore germination gene of Bacillus subtilis 168. *J Bacteriol* **173**, 4646-4652 (1991).
250 de Leseleuc, L., Harris, G., KuoLee, R., Xu, H. H. & Chen, W. Serum resistance, gallium nitrate tolerance and extrapulmonary dissemination are linked to heme consumption in a bacteremic strain of Acinetobacter baumannii. *Int J Med Microbiol* **304**, 360-369, doi:10.1016/j.ijmm.2013.12.002 (2014).
251 Teufel, R. *et al.* Bacterial phenylalanine and phenylacetate catabolic pathway revealed. *Proc Natl Acad Sci U S A* **107**, 14390-14395, doi:10.1073/pnas.1005399107 (2010).
252 Kirby, A. E., King, N. D. & Connell, T. D. RhuR, an extracytoplasmic function sigma factor activator, is essential for heme-dependent expression of the outer membrane heme and hemoprotein receptor of Bordetella avium. *Infect Immun* **72**, 896-907 (2004).
253 Ochs, M. *et al.* Regulation of citrate-dependent iron transport of Escherichia coli: fecR is required for transcription activation by FecI. *Mol Microbiol* **15**, 119-132 (1995).
254 Frumkin, I. *et al.* Gene Architectures that Minimize Cost of Gene Expression. *Mol Cell* **65**, 142-153, doi:10.1016/j.molcel.2016.11.007 (2017).
255 Gao, Y. *et al.* Systematic discovery of uncharacterized transcription factors in Escherichia coli K-12 MG1655. *Nucleic Acids Res* **46**, 10682-10696, doi:10.1093/nar/gky752 (2018).
256 Mader, J. T. & Calhoun, J. in *Medical Microbiology* (eds th & S. Baron) (1996).

257 Elsen, S., Swem, L. R., Swem, D. L. & Bauer, C. E. RegB/RegA, a highly conserved redox-responding global two-component regulatory system. *Microbiol Mol Biol Rev* **68**, 263-279, doi:10.1128/MMBR.68.2.263-279.2004 (2004).
258 Alteri, C. J., Lindner, J. R., Reiss, D. J., Smith, S. N. & Mobley, H. L. The broadly conserved regulator PhoP links pathogen virulence and membrane potential in Escherichia coli. *Mol Microbiol* **82**, 145-163, doi:10.1111/j.1365-2958.2011.07804.x (2011).
259 Montero, M. *et al.* Escherichia coli glycogen metabolism is controlled by the PhoP-PhoQ regulatory system at submillimolar environmental Mg2+ concentrations, and is highly interconnected with a wide variety of cellular processes. *Biochem J* **424**, 129-141, doi:10.1042/BJ20090980 (2009).
260 Angerer, A., Enz, S., Ochs, M. & Braun, V. Transcriptional regulation of ferric citrate transport in Escherichia coli K-12. FecI belongs to a new subfamily of sigma 70-type factors that respond to extracytoplasmic stimuli. *Mol Microbiol* **18**, 163-174 (1995).
261 Kim, B. S. *et al.* Characterization and immunological analysis of ferritin from the hemolymph of Galleria mellonella. *Comp Biochem Physiol A Mol Integr Physiol* **129**, 501-509 (2001).

APENDIX 1

PERMISSION AND PUBLISHED MANUSCRIPT FOR CHAPTER 2

MICROBIAL GENOMICS
Bases to Biology

Microb Genom. 2017 Mar; 3(3): mgen000107.
Published online 2017 Mar 23. doi: [10.1099/mgen.0.000107]
PMCID: PMC5382811
PMID: 28663824

Towards the complete proteinaceous regulome of *Acinetobacter baumannii*

Leila G Casella,[#1,†] Andy Weiss,[✉#1†] Ernesto Pérez-Rueda,[2,3] J Antonio Ibarra,[4] and Lindsey N Shaw[✉1]

Author information ► Article notes ► Copyright and License information ▼ Disclaimer

MICROBIAL GENOMICS

RESEARCH ARTICLE

Casella *et al.*, *Microbial Genomics* 2017;3

DOI 10.1099/mgen.0.000107

Towards the complete proteinaceous regulome of *Acinetobacter baumannii*

Leila G. Casella,[1]† Andy Weiss,[1,*]† Ernesto Pérez-Rueda,[2,3] J. Antonio Ibarra[4] and Lindsey N. Shaw[1,*]

Abstract

The emergence of *Acinetobacter baumannii* strains, with broad multidrug-resistance phenotypes and novel virulence factors unique to hypervirulent strains, presents a major threat to human health worldwide. Although a number of studies have described virulence-affecting entities for this organism, very few have identified regulatory elements controlling their expression. Previously, our group has documented the global identification and curation of regulatory RNAs in *A. baumannii*. As such, in the present study, we detail an extension of this work, the performance of an extensive bioinformatic analysis to identify regulatory proteins in the recently annotated genome of the highly virulent AB5075 strain. In so doing, 243 transcription factors, 14 two-component systems (TCSs), 2 orphan response regulators, 1 hybrid TCS and 5 σ factors were found. A comparison of these elements between AB5075 and other clinical isolates, as well as a laboratory strain, led to the identification of several conserved regulatory elements, whilst at the same time uncovering regulators unique to hypervirulent strains. Lastly, by comparing regulatory elements compiled in this study to genes shown to be essential for AB5075 infection, we were able to highlight elements with a specific importance for pathogenic behaviour. Collectively, our work offers a unique insight into the regulatory network of *A. baumannii* strains, and provides insight into the evolution of hypervirulent lineages.

DATA SUMMARY

The updated GenBank files for AB5075 and ATCC 17978, containing the revised transcription factor descriptions and annotations, have been deposited in Figshare: https://figshare.com/s/690a28e453bbe85eb683. Overviews and comparisons of TFs and two-component systems in various *Acinetobacter baumannii* genomes are shown in Tables S1 and S2 (available in the online Supplementary Material).

INTRODUCTION

Acinetobacter baumannii is a Gram-negative pathogen that is becoming increasingly problematic due to its ability to survive on fomite surfaces, resist the action of common disinfectants and evade treatment with antimicrobial agents [1, 2]. Consequently, this organism causes severe infections in both hospital and community settings, including pneumonia, skin and soft-tissue infections, urinary-tract infections, endocarditis, and meningitis [1, 3–6].

Most studies exploring the mechanisms of disease causation by this important pathogen have been performed using two *A. baumannii* strains, ATCC 19606 and ATCC 17978, both isolated in the 1950s. However, several genomic differences between these strains and more recent clinical isolates make both suboptimal for the study of pathogenesis. For example, each of these strains lacks the 86 kb pathogenicity island AbaR1 that harbours genes important for resistance to metal ions and an array of antibiotics [7]. This renders both strains susceptible to common therapeutics that are ineffective against the antibiotic-resistant and highly virulent strains currently found in most hospital settings [8–10]. Furthermore, recent clinical isolates display extensive genomic variation, as well as hypervirulent phenotypes, when

Received 27 October 2016; Accepted 27 January 2017

Author affiliations: [1]Department of Cell Biology, Microbiology and Molecular Biology, University of South Florida, 4202 East Fowler Avenue, ISA 2015, Tampa, FL 33620-5150, USA; [2]Instituto de Investigaciones en Matemáticas Aplicadas y en Sistemas, UNAM, Mérida, Yucatán, Mexico; [3]Instituto de Biotecnología, UNAM, Cuernavaca, Morelos, Mexico; [4]Laboratorio de Genética Microbiana, Departamento de Microbiología, Escuela Nacional de Ciencias Biológicas, Instituto Politécnico Nacional, Prolongación de Carpio y Plan de Ayala S/N, Colonia Santo Tomás, Delegación Miguel Hidalgo, CP, 11340 Mexico, DF, Mexico.

***Correspondence:** Andy Weiss, andyweiss@mail.usf.edu; Lindsey N. Shaw, shaw@usf.edu

Keywords: transcription factors; two-component systems; sigma factors; genome comparison; *Acinetobacter baumannii* AB5075.

Abbreviations: HMM, hidden Markov model; MDR, multidrug resistant; NCBI, National Center for Biotechnology Information; RR, response regulator; TCS, two-component system; TF, transcription factor.

†These authors contributed equally to this work.

Two supplementary tables are available with the online Supplementary Material.

compared to their historic counterparts, highlighting the rapid evolution of contemporary isolates [11].

In line with this, a recent study sought to characterize modern clinical strains of *A. baumannii* using genetic approaches, alongside a murine model of pneumonia and a *Galleria mellonella* model of infection [12]. This study identified strain AB5075, a multidrug-resistant (MDR) wound isolate recovered from a patient at the Walter Reed Army Medical Center, USA [13], as being highly virulent, suggesting the potential for novel genes and regulatory mechanisms that enable this strain to colonize, disseminate and persist in different infection sites [14].

Amongst the genes found to be important for pathogenicity in *A. baumannii*, several transcriptional regulators have been identified. This is perhaps unsurprising, as the production of virulence determinants in *A. baumannii*, much like in other bacteria, is a finely tuned process that allows for adaptation to changing environmental conditions and survival in specific niches. This tight regulation of gene expression is, amongst others things, controlled by transcription factors (TFs, also known as one-component systems), which are classified into several families, commonly generally based on two key features: (i) a DNA-binding domain that interacts with enhancer, silencer or promoter regions; and (ii) a trans-acting domain that often serves as a sensor, receiving signals such as protein–protein interaction or the binding of small molecules [15]. Similarly to TFs, two-component systems (TCSs), which typically consist of a membrane-embedded sensor kinase and a cytoplasmically located response regulator (RR), can react to environmental stimuli and trigger a cellular response by influencing the transcriptional process [16]. Finally, alternative σ factors can also influence regulatory networks by facilitating DNA-dependent RNA polymerase (RNAP) recognition of unique promoters [17]. Each of these different regulatory elements (TFs, TCSs, σ factors) interacts with RNAP in specific and discrete ways, modulating promoter recognition and transcriptional initiation of target genes [15].

To date, only a handful of TFs have been characterized in *A. baumannii*, including AdeL, a LysR-type regulator, and AdeN, a TetR-like regulator, controlling expression of the AdeFGH and AdeIJK efflux pumps, respectively [18–20]. Additionally, the ferric-uptake regulator (Fur) has been described as controlling expression of genes involved in siderophore production [21, 22]. A fourth TF, SoxR, is a MerR-like regulator governing transcription of the AbuO outer-membrane protein, which is important for resistance to osmotic and oxidative stress [23]. Finally, Zur is a Fur-like regulator identified as being critical for zinc homeostasis in a mouse model of *A. baumannii* infection [24]. With respect to TCSs, only five have thus far been characterized in *A. baumannii*. The first, BfmSR, controls production of capsular exopolysaccharides as well as pilus assembly, and consequently, cell attachment and biofilm formation [25, 26]. Additionally, the PmrAB TCS has been described as sensing low Mg^{2+} concentrations, as well as cationic antibiotics such as polymyxin B [27]. Another two TCSs, AdeRS and BaeRS, were shown to be connected with antibiotic exposure, both controlling the expression of AdeABC, a major efflux pump conferring resistance to tigecycline [28–30]. Finally, GacS, a hybrid TCS, which interacts with GacA, an orphan RR, controls the phenylacetic acid catabolic pathway, as well as genes involved in biofilm formation, pilus synthesis and motility [31]. To date, there are no studies describing the role of alternative σ factors in *A. baumannii*.

Previously, we have documented the global identification and curation of regulatory RNAs in *A. baumannii* strain AB5075 [32]. In the context of proteinaceous regulators, however, their essential role in cellular physiology and pathogenesis is still largely unexplored. As such, our goal was to perform a comprehensive evaluation of the AB5075 genome to identify and classify every TF, TCS and σ factor. Following this, we compared the distribution of these elements among susceptible and MDR strains. This comparison provides a unique insight into *A. baumannii*-specific regulators, and sheds light onto the influence of TFs in the evolution of pathogenesis in this organism.

IMPACT STATEMENT

In the last two decades, the rise of *Acinetobacter baumannii* infections has presented an immense burden for patients and the public-health sector. Despite the increased number of reports describing clinical *A. baumannii* isolates expressing a wealth of virulence factors, and displaying resistance to most commonly used antimicrobials, little is known about the regulatory networks governing cellular behaviour. Indeed, very few regulatory elements, including transcription factors and two-component systems, have been described in *A. baumannii*. In this work, we identified all regulatory elements in the genome of the highly pathogenic AB5075 strain, and assessed their conservation across several clinical isolates and a laboratory isolate. Given the importance of regulatory elements, and their potential as therapeutic targets, this comprehensive analysis provides unique insight into conserved, yet uncharacterized, regulators, and those present only in pathogenic strains. These findings represent a foundation for further investigation towards the importance of these novel regulatory elements, and their contribution to *A. baumannii* pathogenicity.

METHODS

Identification of TFs

To identify TFs in *A. baumannii* AB5075, we used a combination of information sources and bioinformatics tools. The complete set of TFs identified in *Escherichia coli* [33], *Bacillus subtilis* [34] and *Staphylococcus aureus* [35] were used as

seeds to search for homologues in the complete genome of *A. baumannii* strains using BLASTP searches (with an *E* value $\leq 10^{-3}$ and a coverage of $\geq$60 %). In addition, we used a battery of hidden Markov model (HMM) profiles associated with the three bacterial reference datasets to identify potential TFs not resolved by BLASTP searches. Finally, PFAM, Superfamily and CD-search were used to assign evolutionary families, and to exclude proteins with no regulatory activity (i.e. false positives). In all cases, an *E* value $\leq 10^{-3}$ was used as a cut-off. For each TF identified in *A. baumannii* AB5075, a BLASTN AND BLASTP search against other *A. baumannii* genomes was performed. For a protein to be considered a homologue, a BLASTP *E* value $\leq 10^{-20}$ and coverage of $\geq$60 % relative to the seed sequence was required. Further classification of TF families was performed using PFAM database annotations and the database of Clusters of Orthologous Groups of proteins (COGs); all of which were verified using BLAST searches against annotated protein families. Assignments of putative function to uncharacterized regulatory elements in AB5075 were performed using a combination of BLASTP and literature searches of hits corresponding to well-characterized proteins. An *E* value $\leq 10^{-10}$ and coverage $\geq$30 % of aligned proteins was used as a cut-off for this analysis. Updated genome annotations files for AB5075 and ATCC 17978, containing the results of our bioinformatics analyses, have been deposited in Figshare (https://figshare.com/s/690a28e453bbe85eb683).

Proteomes analysed

In order to determine conservation of TFs in the genome of AB5075, we analysed six *Acinetobacter* genomes. These were: *A. baumannii* AB5075 (https://dx.doi.org/10.6084/m9.figshare.1592959.v1); *A. baumannii* AB0057 (GenBank accession no. CP001182); *A. baumannii* AB307 0294 (GenBank accession no. NC_011595); *A. baumannii* ACICU (GenBank accession no. NC_010611); *A. baumannii* ATCC 17978 (GenBank accession no. CP000521.1); and *A. baumannii* AYE (GenBank accession no. NC_010410). Unless noted otherwise, sequences were downloaded from the National Center for Biotechnology Information (NCBI) ftp server (www.ncbi.nlm.nih.gov/genome).

Identification of σ factors

In order to identify σ factors present in AB5075, we used the genome sequences of *E. coli* K-12 MG1655 (GenBank accession no. NC_000913) and *Pseudomonas aeruginosa* PAO1 (GenBank accession no. NC_002516.2). Sequences were downloaded from the NCBI ftp server (www.ncbi.nlm.nih.gov/genome). A search for homologues in the genome of AB5075, and subsequent conservation analysis in the six other *A. baumannii* strains, was performed using BLASTP searches (with an *E* value $\leq 10^{-20}$ and coverage of $\geq$60 %). Further alignments were generated using CLC Genomics Workbench (version 7.6.1; CLC bio).

RESULTS AND DISCUSSION

Identification of TFs in the *A. baumannii* 5075 genome

In order to enhance our understanding of regulatory networks within *A. baumannii*, we performed a genome-wide analysis of TFs present in strain AB5075. This strain was chosen because it has a fully annotated genome, is hypervirulent in animal models of infection, is resistant to many commonly used antibiotics, and belongs to one of the three main clonal lineages most prevalent in hospital outbreaks worldwide [14, 36–38]. Accordingly, we surveyed the entire genome of AB5075 using HMM profiling to predict the presence of TFs. These findings were manually curated by validation of protein sequences against PFAM libraries and by BLAST searches against the NCBI database. This resulted in the identification of 243 TFs (Table S1, available in the online Supplementary Material). These TFs were classified into 42 different families (Fig. 1, Table S1), with the majority corresponding to the LysR (59) and TetR families (42).

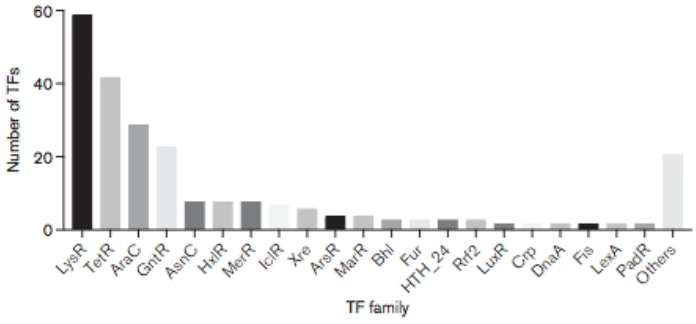

Fig. 1. Classification of TFs identified in *A. baumannii* AB5075. The grouping of TFs into families was performed by BLASTP analysis. Groups that contained only one protein were combined under 'others'.

One of the regulatory proteins identified was DnaA (ABUW_0001). In *E. coli*, DnaA has a dual role, functioning both as an initiator of replication and also acting as a transcriptional regulator [39, 40]. This latter function includes the repression and activation of several genes, including *guaA, dam, rpoH, ftsA and mioC*, which are involved in metabolic functions, chromosomal replication, cell division and stress response [39]. Therefore, the corresponding DnaA protein of *A. baumannii* was included as a TF in our study.

Notably, and as suggested above, of all the TFs identified in AB5075, only a limited number have been characterized thus far in any *A. baumannii* isolate (Table S1). These include: (i) the TetR and LysR proteins AdeN (ABUW_1731) and AdeL (ABUW_1338) [19]; (ii) two members of the Fur family, Fur (ABUW_3033) and Zur (ABUW_3741) [21, 22, 24]; and (iii) the MerR-like protein SoxR (ABUW_2555) [23].

As functions for the majority of regulators identified in our screen have not been reported in *A. baumannii*, we performed a BLASTP analysis and literature search for similar proteins to query sequences, thereby allowing us to propose theoretical functions (Table 1). In so doing, we were able to assign putative functions to 29 TFs, corresponding to AraC, ArsR, Bhl, Crp, DnaA, Fis, GntR, IclR, LysR, LytR, MarR, MerR, NrdR, Rrf2 and TetR family proteins, based on characterized factors with strong sequence similarity in the NCBI database. This included TFs that function in: the response to iron starvation, the production of exotoxins and utilization of aromatic compounds as carbon sources, as well as more general metabolic processes (Table 1). Notably, despite the large amount of LysR and TetR proteins identified, very few were found to have homologues in other organisms. One such element, ABUW_2970 (TetR family), displayed a sequence identity of 81 % to the TF BetI, which acts as a

Table 1. Putative functions of TFs in *A. baumannii* AB5075

Shaded rows indicate genes required for *A. baumannii* infection of *G. mellonella* [12]. T3SS, Type III secretion system.

Protein ID	Family	Comment	Identity (*E* value)	Reference
ABUW_3565	AraC	Regulator of methylation damage in *E. coli*	32 % (2*e*−49)	[93]
ABUW_2370	ArsR	Involved in arsenic detoxification in *E.coli*	52 % (3*e*−30)	[94]
ABUW_3668	ArsR	Regulator of the *ars* operon in *E. coli*	59 % (4*e*−35)	[95]
ABUW_2198	Bhl	Nucleoid organization and regulation in *E. coli*	71 % (8*e*−46)	[96]
ABUW_2241	Bhl	Required for site-specific recombination system expression in *E. coli*	56 % (6*e*−40)	[42]
ABUW_3279	Bhl	Integration host factor (IhfA) in *E. coli* controlling type 1-fimbrial expression *(fimA)*	68 % (5*e*−47)	[43]
ABUW_2741	Crp	Regulator of genes involved in the production of exotoxin and secretion systems (T3SS) in *P. aeruginosa*	55 % (9*e*−83)	[44, 97]
ABUW_0001	DnaA	Regulates initiation of bacterial replication in *E. coli*	48 % (2*e*−159)	[98]
ABUW_1533	Fis	Homeostatic regulator of DNA topology in *E. coli*	59 % (8*e*−33)	[45, 46]
ABUW_3813	GntR	Regulator of genes involved in transport and catabolism of L-lactate in *E. coli*	48 % (4*e*−78)	[99, 100]
ABUW_2775	GntR	Repressor for utilization of vanillate in *A. baylyi* ADP1	84 % (6*e*−141)	[101]
ABUW_0075	GntR	Regulator of histidine utilization genes in *Brucella abortus*	31 % (7*e*−42)	[102]
ABUW_1848	IclR	Controls protocatechuate degradation in *A. baylyi* ADP1	82 % (3*e*−172)	[47, 48]
ABUW_2488	IclR	Regulation of *pobA* in response to *B*-hydroxybenzoate in *A. baylyi* ADP1	82 % (2*e*−170)	[103]
ABUW_0067	IclR	Repressor of an aromatic catabolic pathway in *Pseudomonas putida*	31 % (7*e*−32)	[104]
ABUW_1599	LysR	Involved in regulation of genes responsible for swarming in *P. aeruginosa*.	47 % (1*e*−77)	[105]
ABUW_1878	LysR	Repressor of benzoate catabolism in *P. putida*	39 % (6*e*−65)	[106]
ABUW_2709	LysR	Regulation of benzoate degradation in *A. baylyi* ADP1	65 % (2*e*−149)	[107, 108]
ABUW_2849	LysR	Inhibitor of DNA replication in *E. coli*	36 % (3*e*−34)	[109]
ABUW_3471	LysR	Regulation of 3-phenylpropionic acid catabolism in *E. coli*	43 % (1*e*−75)	[110]
ABUW_1016	LysR	Positive regulation of sulfate starvation inducible genes	52 % (2*e*−12)	[111–113]
ABUW_3615	LytTR	Regulator of alginate biosynthesis in *P. aeruginosa*	47 % (2*e*−78)	[53]
ABUW_3790	MarR	Leucine-responsive regulatory protein (Lrp) in *E. coli*	57 % (1*e*−59)	[114]
ABUW_2706	MerR	Regulator of copper export in *E. coli*	41 % (2*e*−42)	[115]
ABUW_3015	MerR	Positive regulation of *slpA*, resulting in excision of cryptic prophage (CP4–57) in *E. coli*	40 % (8*e*−04)	[116, 61]
ABUW_3665	MerR	Cadmium-induced regulator in *P. aeruginosa*	49 % (3*e*−36)	[117, 118]
ABUW_3653	NrdR	Regulator of ribonucleotide reductases operons in *E. coli*.	55 % (3*e*−64)	[54]
ABUW_2201	Rrf2	Regulator of iron–sulfur clusters in *E. coli*	54 % (2*e*−49)	[49]
ABUW_2970	TetR	Choline-responsive repressor in *A. baylyi*	81 % (9*e*−130)	[41]

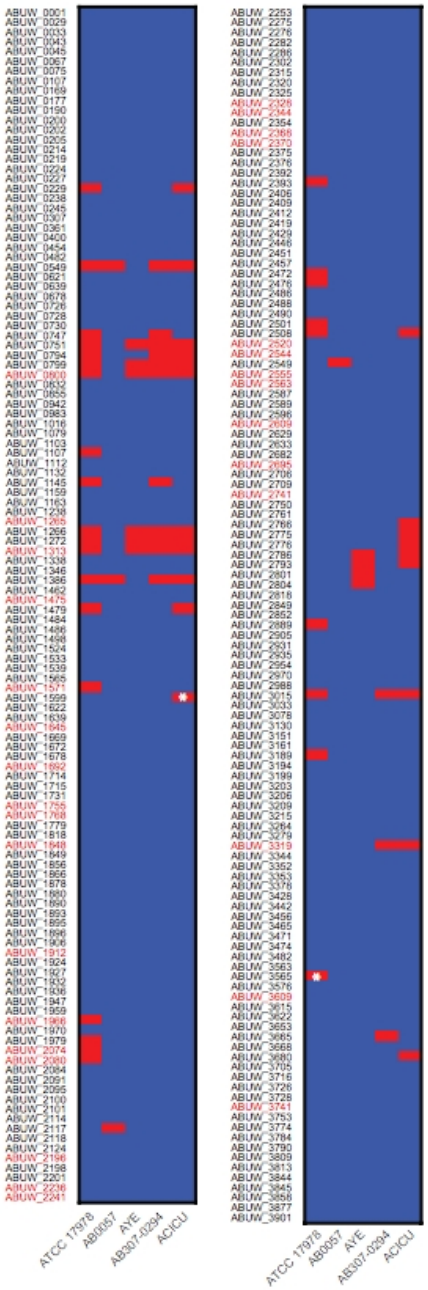

Fig. 2. Conservation of TFs across *A. baumannii* strains. Homologues to AB5075 regulatory proteins were identified as outlined in Methods. A blue box denotes the presence of an homologue, while red boxes mark the absence of a given regulator. An asterisk highlights frame-shift mutation(s) in the homologous ORF. Gene names that are in red font highlight factors that have been shown to be essential for AB5075 infection in a worm model [12].

repressor of two choline transporters, and the *betIBA* operon, which regulates the choline oxidation pathway, in *Acinetobacter baylyi* (Table 1) [41].

In an attempt to provide some pathogenic context to this curation of TFs, we compared our findings to recent work by Gebhardt and colleagues, who screened a transposon insertion sequence library (TnSeq) of AB5075 in a *G. mellonella* infection model [12]. This resulted in 31 TFs reported as being essential for growth in their worm model (Table S1, highlighted in Fig. 2). Interestingly, among the TFs with putative functions listed in Table 1, four were reported to be essential for survival of AB5075 in *G. mellonella* (shaded in grey in Table 1). This group includes ABUW_2241, a member of the Bhl family required for regulation of genes controlling several cellular processes, including lambda site-specific recombination, in *E. coli* [42, 43]. Additionally, a member of the Crp family (ABUW_2741) was found to be important for infection in the worm model. Of interest, a homologue to this protein serves to regulate the type III secretion system in *P. aeruginosa* [44]. Finally, two proteins, ABUW_1848 and ABUW_2370, members of the IclR and ArsR families of transcriptional regulators, respectively, were also required for *A. baumannii* virulence. A homologue of ABUW_2370 has been reported to control expression of genes involved in regulating arsenic detoxification in *E. coli*, whilst an ABUW_1848 homologue controls aromatic catabolism in *A. baylyi* ADP1. [45–49].

TF distribution in AB5075

Core regulatory elements

Next, we sought to investigate the conservation of AB5075 TFs in other *A. baumannii* strains. We hypothesized that the absence of certain TFs in less pathogenic strains, when compared to their hypervirulent counterparts, may aid in explaining their decreased ability to infect mammalian hosts. As such, we analysed the laboratory strain ATCC 17978, which is susceptible to the majority of antibiotics used for *A. baumannii* infections, as well as four clinical isolates, including the drug susceptible AB307-0294 strain, and three MDR isolates: AB0057, AYE and ACICU [10, 50–52]. In so doing, we found a set of 202 TFs to be conserved in each genome; thus, presenting the core regulatory elements of these species (Fig. 2, Table S1). Within this set, only 22 TFs had putatively assigned functions. For these TFs, homologues in other organisms are involved in the regulation of metabolism, detoxification and virulence, suggesting that they may fine tune the expression of essential genes important for basal and conserved physiological processes [49, 53–60].

Next, we investigated the number of conserved TFs in relation to the genome size for each *A. baumannii* strain. Despite the fact that ATCC 17978 and AB5075 both have a genome size of approximately 4.0 Mbp, the conservation of TFs between these two strains is only 88.5 %, reflecting significant potential genomic alterations due to horizontal gene transfer, insertions or deletions. Conversely, AB0057, AYE, AB307-0294 and ACICU showed TF conservation of 98.4, 95.9, 94.2 and 91.4 %, respectively (Table 2), indicating a closer evolutionary proximity to AB5075. An important note is that, for these conservation analyses, we used an AB5075 centric view, in that we did not assess TFs present in other strains but not in AB5075 itself. As such, there remains the possibility that the loss of certain elements, which might be common to strains other than AB5075, could help to explain the hypervirulence of the latter. Nevertheless, as we were primarily interested in understanding the physiology of AB5075, we placed an emphasis on the specific regulatory elements in this strain.

Table 2. Comparison of genome size and the presence of homologues to AB5075 regulators in various *A. baumannii* strains

Strain	Genome size (nt)	No. of conserved TFs	Conservation relative to AB5075 (%)
AB0057	4 050 513	239	98.4
AYE	3 936 291	233	95.9
AB307-0294	3 760 981	229	94.2
ACICU	3 904 116	222	91.4
ATCC 17978	3 857 743	215	88.5

Non-conserved elements

In contrast to the TFs conserved across each of the different isolates, we found several proteins to be absent in one or more of the investigated strains (Fig. 2, Table S1). For example, ABUW_3015, a putative member of the MerR family of regulators, is only conserved in AB0057 and AB307-0294. Of note, ABUW_3015 showed 40 % sequence identity to a TF in *E. coli*, AlpA, previously characterized as a positive regulator of *slpA*, a gene that is part of a cryptic prophage suggested to be involved in biofilm formation (Table 1) [61]. Importantly, the presence of phage-like regions in the chromosome of several *A. baumannii* clinical strains has been previously reported, including for AB0057 and AB5075; however, their significance has yet to be elucidated [37, 50]. Likewise, ABUW_1599, a LysR-type regulator, was absent in the ACICU strain. According to the putative function assigned in this work (Table 1), ABUW_1599 may be involved in the regulation of swarming motility. Interestingly, this phenotype has been reported to be absent in ACICU, although the genes encoding a type IV pilus are present in ACICU [62].

Non-conserved elements that are important for virulence

The recent *in vivo* screening of an AB5075 transposon library using a *G. mellonella* infection model [12] identified several TFs that were found not to be conserved across *A. baumannii* strains (Table S1) [12, 63]. Among these are ABUW_2074, a member of the Fur family, which is absent in the non-pathogenic strain ATCC 17978. Interestingly, this strain also lacks a heme uptake system and heme oxygenase, which have both been shown as necessary for virulence [64]. Given that Fur family proteins are known to be involved in the regulation of iron uptake, and that ABUW_2074 is conserved in all four clinical *A. baumannii* strains studied herein, this may suggest a central role for ABUW_2074 in controlling nutrient acquisition in the host [64, 65]. Additionally, ABUW_1966, a member of the LysR family, is absent in ATCC 17978. Interestingly, ABUW_1966 has been shown to be necessary for resistance to antibiotics targeting cell-wall synthesis, and is required for growth in *G. mellonella* [12]. In this context, ATCC 17978 is a drug-sensitive strain, possibly suggesting ABUW_1966 may have a role in regulating genes required for antimicrobial resistance.

TCSs in AB5075

In addition to TFs, another layer of regulation found in bacteria is mediated by TCSs. These systems typically combine a sensor kinase protein that receives a signal following a specific stimulus, and transduces this to a RR protein via phosphorylation, resulting in altered gene expression [66]. Given that a TF might interact with a sensory protein and serve as a RR, we combined HMM profiling with BLASTP analysis using a list of TCSs corresponding to the *P. aeruginosa* PAO1 genome to detect these elements in AB5075. We identified 14 RR proteins encoded together with a sensor kinase protein. This set of 14 TCSs includes: (i) 11 members of the OmpR family; (ii) 2 members of the HTH_8 family; and (iii) 1 member of the LuxR family (Table S2). This latter TCS corresponds to a sensor protein (ABUW_2427) that possesses both histidine kinase and RR domains, and is encoded adjacent to the RR protein ABUW_2426. Given that the hybrid sensor kinase ABUW_2427 and RR ABUW_2426 are localized within the same operon it has been included in the set of 14 TCSs. Of note, from the 14 RR/sensor pairs identified, only 4 have previously been studied in *A. baumannii* (Table S2). ABUW_0608/ABUW_0609 and ABUW1972/ABUW1973 have previously been named BaeSR and AdeRS, respectively, and described as having regulatory roles in the expression of efflux pumps [30, 67]. Likewise, ABUW_0828/ABUW_0829 corresponds to the PmrAB TCS that was found to confer resistance to the cationic antimicrobial colistin [27]. Finally, ABUW_3180/ABUW_3181 was characterized as TCS BfmSR, which controls biofilm formation, motility and exopolysaccharide production, and is required for pathogenicity in a *G. mellonella* infection model [12, 25–27, 30, 67].

As with our analysis of TFs, we next searched for homologues to the remaining 10 TCSs to identify those that may have been characterized in other species. In so doing, we

assigned putative functions to seven additional elements (Table 3). Of these, two members of the HTH_8 family, ABUW_1732 and ABUW_3641, showed sequence similarity to hitherto characterized proteins. ABUW_1732 shows 64 % identity to NtcR, a RR that controls the *nifLA* operon, which is required for nitrogen assimilation in *Klebsiella pneumoniae*; while ABUW_3641 displays 51 % identity to a type IV fimbriae RR in *P. aeruginosa* [55, 68]. The five remaining factors were all OmpR RRs, and had similarity to systems controlling the response to phosphate, heavy metals, osmotic stress or the expression of flagella (Table 3). Of note, although not yet characterized, ABUW_1514/1515 was found to be required for growth in *G. mellonella*, which implies its importance for AB5075 pathogenicity (Table S2) [12].

In addition to TCSs, we also identified two orphan RRs that were not associated with a histidine kinase, ABUW_0180 and ABUW_3639, which are members of the LuxR and GerE families, respectively. Interestingly, ABUW_3639 has been previously characterized as GacA, an orphan RR of the phenylacetic acid catabolic pathway, which interacts with a hybrid sensor kinase GacS [31]. In concert both elements control expression of the *csu* operon, which is involved in pilus synthesis, required for virulence in *A. baumannii* ATCC 17978, as well as genes involved in biofilm formation. [31]. Lastly, ABUW_3306 was identified as a hybrid TCS, harbouring sensory and regulatory domains. Upon analysis, it was determined that the protein showed 100 % identity to GacS in ATCC 17978 [31].

TCS distribution in AB5075

Of the 14 TCS RRs identified in this study, only 1 was found not to be conserved in all the five strains used in this analysis. This was ABUW_ 3641, a member of the HTH_8 family, which was marked as absent (Table S2) in the laboratory strain ATCC 17978 based on a combination of protein and nucleotide BLAST analysis (discussed further below). The conservation of ABUW_3641 may reflect its role in regulating genes required for twitching motility, which is a common phenotype reported in *A. baumannii* strains, with the exception of ATCC 17978 [62, 69, 70]. In contrast, the remaining 13 TCS RRs, 2 orphan RRs and the hybrid TCS identified were common to all *A. baumannii* strains. Of note, seven of the conserved TCS RRs had predicted functions, including the response to osmotic stress, heavy metal efflux and the regulation of motility [71].

σ factors in AB5075

Along with TFs, σ factors provide another, and perhaps more basal, level of regulation, guiding RNAP to unique promoters to initiate transcription of specific genes in response to external stimuli [17]. Given their vital regulatory role, we next explored the genome of AB5075 to identify potential σ factors genes. To do this, we generated a list of known σ factors present in the genomes of the *P. aeruginosa* strain PAO1 and *E. coli* strain K-12, both of which contain multiple σ factors that have been well described [72–79]. The amino acid sequence for each of these elements was then used in BLASTP searches against the AB5075 genome. Resulting hits were subsequently analysed using the PFAM database to determine conservation of domains inherent to σ factor activity. Alignments of each putative AB5075 σ factor were then generated for *E. coli* K-12 and *P. aeruginosa* PAO1 homologues to identify specific active site residues required for σ factor function.

Consequently, we identified five putative σ factors in AB5075, including ABUW_0862, which is the *A. baumannii* RpoD (σ^A) homologue. Specifically, ABUW_0862 showed sequence identity of 62 and 63 % to RpoD of *E. coli* and *P. aeruginosa*, respectively. As shown in Fig. 3(a), alignment of amino acid sequences revealed the conservation of regions 2.4 and 4.2, which is in agreement with the function of these domains in recognizing the −10 and −35 sequences of housekeeping genes. The inhibitory domain, region 1, and the RNAP binding domain, region 3, were also present [80]. Other than σ^A, we identified ABUW_1375 as having 64 % identity to RpoH of *P. aeruginosa* and 59 % to RpoH from *E. coli*. Comparative alignments for RpoH proteins revealed the conservation of two motifs (QRKLFFNLR and LRNWRIVK) located in region 2.4, both reported binding sites for DnaK, a protein chaperone that controls RpoH stability (Fig. 3b) [81]. A third putative σ factor, ABUW_3253, was found to have conserved regions characteristic of RpoN, a member of the σ^{54} family, involved in regulating nitrogen metabolism and bacterial virulence [76]. Two distinct regions in ABUW_3253 were found to be similar to the RpoN

Table 3. List of TCSs found in AB5075 with putatively assigned functions

Protein ID	Family	Comment	Identity (*E* value)	Reference
ABUW_1732	HTH_8	Regulator of nitrogenase synthesis in *K. pneumoniae*	64 % (0)	[55, 119]
ABUW_3641	HTH_8	Regulator of type IV fimbriae in *P. aeruginosa*	51 % (2e−165)	[68]
ABUW_0106	OmpR	Regulator of the PhoB regulon during phosphate starvation in *E.coli*	62 % (6e−104)	[120]
ABUW_0257	OmpR	Two-component OmpR–EnvZ regulator that senses osmotic stress in *E. coli*	69 % (2e−117)	[121], [122]
ABUW_1506	OmpR	Regulator of genes involved in resistance to cadmium and zinc in *Burkholderia pseudomallei*	53 % (6e−89)	[71]
ABUW_1585	OmpR	Involved in K^+ ion transport regulation in *E. coli*	42 % (4e−67)	[123]
ABUW_3323	OmpR	RR involved in copper resistance in *E. coli*	62 % (2e−109)	[124, 125]

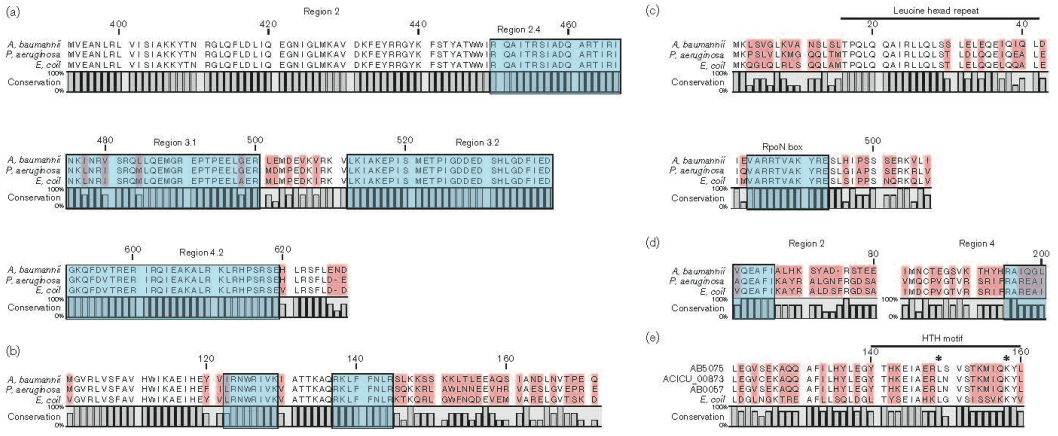

Fig. 3. Alignment of σ factors from *E. coli*, *P. aeruginosa* and *A. baumannii*. Multiple alignments were performed for σ factors found in *A. baumannii* AB5075, *E. coli* and *P. aeruginosa*. (a) Conservation in regions 2.4 and 4.2, which are essential for promoter recognition, as well as region 3 (all indicated by blue boxes), were observed. (b) Two conserved amino acid sequences critical for binding to DnaK (blue boxes) were noted for all three RpoH proteins. (c) Several leucine residues, within a conserved heptad motif, and a conserved amino acid sequence only found in σ54 family proteins (blue box), were identified in RpoN homologues. (d) Blue boxes indicate a conserved amino acid sequence within regions 2 and 4 of RpoE, important for transcription of *rpoE* and promoter recognition in general. (e) Asterisks indicate conservation of a leucine residue essential for FecI–FecR interaction, and a lysine residue critical for binding to the β subunit of RNAP. Throughout this figure, pink boxes represent amino acids that display divergence between the compared sequences.

protein of *E. coli* (Fig. 3c): region 1 of ABUW_3253 contains several leucine residues within a heptad motif previously reported to be important for recognition of −12 promoter elements; whilst a signature σ^{54} amino acid sequence (ARRTVAKYRE), also known as the RpoN box, required for DNA binding, was also found [76, 82, 83]. Lastly, ABUW_0988 and ABUW_2987 were found to have conserved regions in domains σ_2 and σ_4 found in the extracytoplasmic σ factors RpoE and FecI, which have been reported to function in cell envelope stress and iron acquisition, respectively [84, 85]. Alignments of ABUW_0988 with RpoE of *E. coli* and AlgU from *P. aeruginosa*, a homologue of RpoE (Fig. 3d), showed conservation of the VQEAFI sequence in region 2, which is thought to be critical for transcription of *rpoE*. Further to this, several amino acid residues, such as arginine, lysine, leucine and isoleucine, were found in region 4, which are believed to be important for recognition of −35 promoter regions and binding of anti-σ factor proteins [75, 86, 87]. With regards to ABUW_2987, it is noteworthy that it is located in an apparent operon that has similar organization to the *fecABCDE* operon required for ferric citrate transport in *E. coli* [88]. Interestingly, alignment of ABUW_2987 with FecI of *E. coli* identified two conserved residues (L146 and K155), both within a helix-turn-helix motif in region 4.2, that have been reported as being essential for FecI–FecR interaction and binding to the β' subunit of RNAP, respectively (Fig. 3e) [84].

We next explored conservation of AB5075 σ factor proteins in the genomes of other *A. baumannii* strains. We found that four of the five σ factors were ubiquitously conserved, but, quite surprisingly, the FecI-like protein ABUW_2987 was absent in all *A. baumannii* strains with the exception of two MDR clinical isolates, AB0057 and ACICU [52]. Of note, FecI is found in AB5075 within a cluster of eight genes, encoding protein homologues of FecR, TonB and HemO, which encode a cytoplasmic protein sensor of ferric citrate, a TonB-dependent outer membrane transport protein and a heme oxygenase, respectively. Similarly, this cluster is also absent in ATCC 17978, AB307-0294 and AYE strains. Interestingly, this locus is conserved in ACICU and AB0057, as well as in *A. baumannii* LAC-4, a virulent isolate with tolerance to chelators of ferric iron [64]. It is possible that the lack of conservation of this cluster in some *A. baumannii* strains is due to recent acquisition via lateral transfer. This notion is supported by the idea that possession of this operon might represent a mechanism for acquisition of heme as an alternative iron source, providing an advantage for survival in iron-limited environments, such as during infection, for virulent clinical strains [89–91].

8. **Post V, White PA, Hall RM.** Evolution of AbaR-type genomic resistance islands in multiply antibiotic-resistant *Acinetobacter baumannii*. *J Antimicrob Chemother* 2010;65:1162–1170.
9. **Adams MD, Chan ER, Molyneaux ND, Bonomo RA.** Genomewide analysis of divergence of antibiotic resistance determinants in closely related isolates of *Acinetobacter baumannii*. *Antimicrob Agents Chemother* 2010;54:3569–3577.
10. **Smith MG, Gianoulis TA, Pukatzki S, Mekalanos JJ, Ornston LN *et al.*** New insights into *Acinetobacter baumannii* pathogenesis revealed by high-density pyrosequencing and transposon mutagenesis. *Genes Dev* 2007;21:601–614.
11. **Sahl JW, Johnson JK, Harris AD, Phillippy AM, Hsiao WW *et al.*** Genomic comparison of multi-drug resistant invasive and colonizing *Acinetobacter baumannii* isolated from diverse human body sites reveals genomic plasticity. *BMC Genomics* 2011;12:291.
12. **Gebhardt MJ, Gallagher LA, Jacobson RK, Usacheva EA, Peterson LR *et al.*** Joint transcriptional control of virulence and resistance to antibiotic and environmental stress in *Acinetobacter baumannii*. *MBio* 2015;6:e01660-15.
13. **Zurawski DV, Thompson MG, Mcqueary CN, Matalka MN, Sahl JW *et al.*** Genome sequences of four divergent multidrug-resistant *Acinetobacter baumannii* strains isolated from patients with sepsis or osteomyelitis. *J Bacteriol* 2012;194:1619–1620.
14. **Jacobs AC, Thompson MG, Black CC, Kessler JL, Clark LP *et al.*** AB5075, a highly virulent isolate of *Acinetobacter baumannii*, as a model strain for the evaluation of pathogenesis and antimicrobial treatments. *MBio* 2014;5:e01076-14.
15. **Balleza E, López-Bojorquez LN, Martínez-Antonio A, Resendis-Antonio O, Lozada-Chávez I *et al.*** Regulation by transcription factors in bacteria: beyond description. *FEMS Microbiol Rev* 2009;33:133–151.
16. **Mitrophanov AY, Groisman EA.** Signal integration in bacterial two-component regulatory systems. *Genes Dev* 2008;22:2601–2611.
17. **Feklístov A, Sharon BD, Darst SA, Gross CA.** Bacterial sigma factors: a historical, structural, and genomic perspective. *Annu Rev Microbiol* 2014;68:357–376.
18. **Yoon EJ, Courvalin P, Grillot-Courvalin C.** RND-type efflux pumps in multidrug-resistant clinical isolates of *Acinetobacter baumannii*: major role for AdeABC overexpression and AdeRS mutations. *Antimicrob Agents Chemother* 2013;57:2989–2995.
19. **Coyne S, Rosenfeld N, Lambert T, Courvalin P, Périchon B.** Overexpression of resistance-nodulation-cell division pump AdeFGH confers multidrug resistance in *Acinetobacter baumannii*. *Antimicrob Agents Chemother* 2010;54:4389–4393.
20. **Rosenfeld N, Bouchier C, Courvalin P, Périchon B.** Expression of the resistance-nodulation-cell division pump AdeIJK in *Acinetobacter baumannii* is regulated by AdeN, a TetR-type regulator. *Antimicrob Agents Chemother* 2012;56:2504–2510.
21. **Daniel C, Haentjens S, Bissinger MC, Courcol RJ.** Characterization of the *Acinetobacter baumannii* Fur regulator: cloning and sequencing of the *fur* homolog gene. *FEMS Microbiol Lett* 1999;170:199–209.
22. **Mihara K, Tanabe T, Yamakawa Y, Funahashi T, Nakao H *et al.*** Identification and transcriptional organization of a gene cluster involved in biosynthesis and transport of acinetobactin, a siderophore produced by *Acinetobacter baumannii* ATCC 19606T. *Microbiology* 2004;150:2587–2597.
23. **Srinivasan VB, Vaidyanathan V, Rajamohan G.** AbuO, a TolC-like outer membrane protein of *Acinetobacter baumannii*, is involved in antimicrobial and oxidative stress resistance. *Antimicrob Agents Chemother* 2015;59:1236–1245.
24. **Mortensen BL, Rathi S, Chazin WJ, Skaar EP.** *Acinetobacter baumannii* response to host-mediated zinc limitation requires the transcriptional regulator Zur. *J Bacteriol* 2014;196:2616–2626.
25. **Tomaras AP, Flagler MJ, Dorsey CW, Gaddy JA, Actis LA.** Characterization of a two-component regulatory system from *Acinetobacter baumannii* that controls biofilm formation and cellular morphology. *Microbiology* 2008;154:3398–3409.
26. **Geisinger E, Isberg RR.** Antibiotic modulation of capsular exopolysaccharide and virulence in *Acinetobacter baumannii*. *PLoS Pathog* 2015;11:e1004691.
27. **Arroyo LA, Herrera CM, Fernandez L, Hankins JV, Trent MS *et al.*** The pmrCAB operon mediates polymyxin resistance in *Acinetobacter baumannii* ATCC 17978 and clinical isolates through phosphoethanolamine modification of lipid A. *Antimicrob Agents Chemother* 2011;55:3743–3751.
28. **Peleg AY, Adams J, Paterson DL.** Tigecycline efflux as a mechanism for nonsusceptibility in *Acinetobacter baumannii*. *Antimicrob Agents Chemother* 2007;51:2065–2069.
29. **Lopes BS, Amyes SG.** Insertion sequence disruption of adeR and ciprofloxacin resistance caused by efflux pumps and gyrA and parC mutations in *Acinetobacter baumannii*. *Int J Antimicrob Agents* 2013;41:117–121.
30. **Lin MF, Lin YY, Yeh HW, Lan CY.** Role of the BaeSR two-component system in the regulation of *Acinetobacter baumannii* adeAB genes and its correlation with tigecycline susceptibility. *BMC Microbiol* 2014;14:119.
31. **Cerqueira GM, Kostoulias X, Khoo C, Aibinu I, Qu Y *et al.*** A global virulence regulator in *Acinetobacter baumannii* and its control of the phenylacetic acid catabolic pathway. *J Infect Dis* 2014;210:46–55.
32. **Weiss A, Broach WH, Lee MC, Shaw LN.** Towards the complete small RNome of *Acinetobacter baumannii*. *Microb Genom* 2016;2: doi: 10.1099/mgen.0.000045
33. **Pérez-Rueda E, Tenorio-Salgado S, Huerta-Saquero A, Balderas-Martínez YI, Moreno-Hagelsieb G.** The functional landscape bound to the transcription factors of *Escherichia coli* K-12. *Comput Biol Chem* 2015;58:93–103.
34. **Moreno-Campuzano S, Janga SC, Pérez-Rueda E.** Identification and analysis of DNA-binding transcription factors in *Bacillus subtilis* and other firmicutes - a genomic approach. *BMC Genomics* 2006;7:147.
35. **Ibarra JA, Pérez-Rueda E, Carroll RK, Shaw LN.** Global analysis of transcriptional regulators in *Staphylococcus aureus*. *BMC Genomics* 2013;14:126.
36. **Diancourt L, Passet V, Nemec A, Dijkshoorn L, Brisse S.** The population structure of *Acinetobacter baumannii*: expanding multiresistant clones from an ancestral susceptible genetic pool. *PLoS One* 2010;5:e10034.
37. **Gallagher LA, Ramage E, Weiss EJ, Radey M, Hayden HS *et al.*** Resources for genetic and genomic analysis of emerging pathogen *Acinetobacter baumannii*. *J Bacteriol* 2015;197:2027–2035.
38. **Jones CL, Clancy M, Honnold C, Singh S, Snesrud E *et al.*** Fatal outbreak of an emerging clone of extensively drug-resistant *Acinetobacter baumannii* with enhanced virulence. *Clin Infect Dis* 2015;61:145–154.
39. **Messer W, Weigel C.** DnaA as a transcription regulator. *Methods Enzymol* 2003;370:338–349.
40. **Bogan JA, Helmstetter CE.** mioC transcription, initiation of replication, and the eclipse in *Escherichia coli*. *J Bacteriol* 1996;178:3201–3206.
41. **Scholz A, Stahl J, de Berardinis V, Müller V, Averhoff B.** Osmotic stress response in *Acinetobacter baylyi* : identification of a glycine-betaine biosynthesis pathway and regulation of osmoadaptive choline uptake and glycine-betaine synthesis through a choline-responsive BetI repressor. *Environ Microbiol Rep* 2016;8:316–322.
42. **Lee EC, Hales LM, Gumport RI, Gardner JF.** The isolation and characterization of mutants of the integration host factor (IHF) of *Escherichia coli* with altered, expanded DNA-binding specificities. *EMBO J* 1992;11:305–313.
43. **Eisenstein BI, Sweet DS, Vaughn V, Friedman DI.** Integration host factor is required for the DNA inversion that controls phase

variation in *Escherichia coli*. *Proc Natl Acad Sci USA* 1987;84:6506–6510.

44. **West SE, Sample AK, Runyen-Janecky LJ.** The vfr gene product, required for *Pseudomonas aeruginosa* exotoxin A and protease production, belongs to the cyclic AMP receptor protein family. *J Bacteriol* 1994;176:7532–7542.
45. **González-Gil G, Bringmann P, Kahmann R.** FIS is a regulator of metabolism in *Escherichia coli*. *Mol Microbiol* 1996;22:21–29.
46. **Schneider R, Travers A, Muskhelishvili G.** The expression of the *Escherichia coli* fis gene is strongly dependent on the superhelical density of DNA. *Mol Microbiol* 2000;38:167–175.
47. **Popp R, Kohl T, Patz P, Trautwein G, Gerischer U.** Differential DNA binding of transcriptional regulator PcaU from *Acinetobacter* sp. strain ADP1. *J Bacteriol* 2002;184:1988–1997.
48. **Trautwein G, Gerischer U.** Effects exerted by transcriptional regulator PcaU from *Acinetobacter* sp. strain ADP1. *J Bacteriol* 2001;183:873–881.
49. **Haines S, Arnaud-Barbe N, Poncet D, Reverchon S, Wawrzyniak J *et al.*** IscR regulates synthesis of colonization factor antigen I fimbriae in response to iron starvation in enterotoxigenic *Escherichia coli*. *J Bacteriol* 2015;197:2896–2907.
50. **Adams MD, Goglin K, Molyneaux N, Hujer KM, Lavender H *et al.*** Comparative genome sequence analysis of multidrug-resistant *Acinetobacter baumannii*. *J Bacteriol* 2008;190:8053–8064.
51. **Poirel L, Menuteau O, Agoli N, Cattoen C, Nordmann P.** Outbreak of extended-spectrum beta-lactamase VEB-1-producing isolates of *Acinetobacter baumannii* in a French hospital. *J Clin Microbiol* 2003;41:3542–3547.
52. **Iacono M, Villa L, Fortini D, Bordoni R, Imperi F *et al.*** Whole-genome pyrosequencing of an epidemic multidrug-resistant *Acinetobacter baumannii* strain belonging to the European clone II group. *Antimicrob Agents Chemother* 2008;52:2616–2625.
53. **Whitchurch CB, Alm RA, Mattick JS.** The alginate regulator AlgR and an associated sensor FimS are required for twitching motility in *Pseudomonas aeruginosa*. *Proc Natl Acad Sci USA* 1996;93:9839–9843.
54. **Torrents E, Grinberg I, Gorovitz-Harris B, Lundström H, Borovok I *et al.*** NrdR controls differential expression of the *Escherichia coli* ribonucleotide reductase genes. *J Bacteriol* 2007;189:5012–5021.
55. **Espin G, Alvarez-Morales A, Cannon F, Dixon R, Merrick M.** Cloning of the glnA, ntrB and ntrC genes of *Klebsiella pneumoniae* and studies of their role in regulation of the nitrogen fixation (nif) gene cluster. *Mol Gen Genet* 1982;186:518–524.
56. **Huillet E, Velge P, Vallaeys T, Pardon P.** LadR, a new PadR-related transcriptional regulator from *Listeria monocytogenes*, negatively regulates the expression of the multidrug efflux pump MdrL. *FEMS Microbiol Lett* 2006;254:87–94.
57. **Fibriansah G, Kovács ÁT, Pool TJ, Boonstra M, Kuipers OP *et al.*** Crystal structures of two transcriptional regulators from *Bacillus cereus* define the conserved structural features of a PadR subfamily. *PLoS One* 2012;7:e48015.
58. **Ueguchi C, Kakeda M, Mizuno T.** Autoregulatory expression of the *Escherichia coli* hns gene encoding a nucleoid protein: H-Ns functions as a repressor of its own transcription. *Mol Gen Genet* 1993;236:171–178.
59. **Robbe-Saule V, Schaeffer F, Kowarz L, Norel F.** Relationships between H-NS, sigma S, SpvR and growth phase in the control of spvR, the regulatory gene of the *Salmonella* plasmid virulence operon. *Mol Gen Genet* 1997;256:333–347.
60. **Yurimoto H, Hirai R, Matsuno N, Yasueda H, Kato N *et al.*** HxlR, a member of the DUF24 protein family, is a DNA-binding protein that acts as a positive regulator of the formaldehyde-inducible hxlAB operon in *Bacillus subtilis*. *Mol Microbiol* 2005;57:511–519.
61. **Wang X, Kim Y, Wood TK.** Control and benefits of CP4-57 prophage excision in *Escherichia coli* biofilms. *ISME J* 2009;3:1164–1179.
62. **Antunes LC, Imperi F, Carattoli A, Visca P.** Deciphering the multifactorial nature of *Acinetobacter baumannii* pathogenicity. *PLoS One* 2011;6:e22674.
63. **Peleg AY, Jara S, Monga D, Eliopoulos GM, Moellering RC *et al.*** *Galleria mellonella* as a model system to study *Acinetobacter baumannii* pathogenesis and therapeutics. *Antimicrob Agents Chemother* 2009;53:2605–2609.
64. **De Léséleuc L, Harris G, Kuolee R, Xu HH, Chen W.** Serum resistance, gallium nitrate tolerance and extrapulmonary dissemination are linked to heme consumption in a bacteremic strain of *Acinetobacter baumannii*. *Int J Med Microbiol* 2014;304:360–369.
65. **Mcconnell MJ, Actis L, Pachón J.** *Acinetobacter baumannii*: human infections, factors contributing to pathogenesis and animal models. *FEMS Microbiol Rev* 2013;37:130–155.
66. **Krell T, Lacal J, Busch A, Silva-Jiménez H, Guazzaroni ME *et al.*** Bacterial sensor kinases: diversity in the recognition of environmental signals. *Annu Rev Microbiol* 2010;64:539–559.
67. **Marchand I, Damier-Piolle L, Courvalin P, Lambert T.** Expression of the RND-type efflux pump AdeABC in *Acinetobacter baumannii* is regulated by the AdeRS two-component system. *Antimicrob Agents Chemother* 2004;48:3298–3304.
68. **Jin S, Ishimoto KS, Lory S.** PilR, a transcriptional regulator of piliation in *Pseudomonas aeruginosa*, binds to a cis-acting sequence upstream of the pilin gene promoter. *Mol Microbiol* 1994;14:1049–1057.
69. **Eijkelkamp BA, Stroeher UH, Hassan KA, Papadimitrious MS, Paulsen IT *et al.*** Adherence and motility characteristics of clinical *Acinetobacter baumannii* isolates. *FEMS Microbiol Lett* 2011;323:44–51.
70. **Clemmer KM, Bonomo RA, Rather PN.** Genetic analysis of surface motility in *Acinetobacter baumannii*. *Microbiology* 2011;157:2534–2544.
71. **Jones AL, Deshazer D, Woods DE.** Identification and characterization of a two-component regulatory system involved in invasion of eukaryotic cells and heavy-metal resistance in *Burkholderia pseudomallei*. *Infect Immun* 1997;65:4972–4977.
72. **Gross CA, Grossman AD, Liebke H, Walter W, Burgess RR.** Effects of the mutant sigma allele rpoD800 on the synthesis of specific macromolecular components of the *Escherichia coli* K12 cell. *J Mol Biol* 1984;172:283–300.
73. **Grossman AD, Zhou YN, Gross C, Heilig J, Christie GE *et al.*** Mutations in the rpoH (htpR) gene of *Escherichia coli* K-12 phenotypically suppress a temperature-sensitive mutant defective in the sigma 70 subunit of RNA polymerase. *J Bacteriol* 1985;161:939–943.
74. **Siegele DA, Hu JC, Walter WA, Gross CA.** Altered promoter recognition by mutant forms of the sigma 70 subunit of *Escherichia coli* RNA polymerase. *J Mol Biol* 1989;206:591–603.
75. **Rouvière PE, de Las Peñas A, Mecsas J, Lu CZ, Rudd KE *et al.*** rpoE, the gene encoding the second heat-shock sigma factor, sigma E, in *Escherichia coli*. *EMBO J* 1995;14:1032–1042.
76. **Taylor M, Butler R, Chambers S, Casimiro M, Badii F *et al.*** The RpoN-box motif of the RNA polymerase sigma factor sigma N plays a role in promoter recognition. *Mol Microbiol* 1996;22:1045–1054.
77. **Mahren S, Braun V.** The FecI extracytoplasmic-function sigma factor of *Escherichia coli* interacts with the β' subunit of RNA polymerase. *J Bacteriol* 2003;185:1796–1802.
78. **Potvin E, Sanschagrin F, Levesque RC.** Sigma factors in *Pseudomonas aeruginosa*. *FEMS Microbiol Rev* 2008;32:38–55.
79. **Hirschman J, Wong PK, Sei K, Keener J, Kustu S.** Products of nitrogen regulatory genes ntrA and ntrC of enteric bacteria activate glnA transcription in vitro: evidence that the ntrA product is a sigma factor. *Proc Natl Acad Sci USA* 1985;82:7525–7529.
80. **Arnold HM, Sawyer AM, Kollef MH.** Use of adjunctive aerosolized antimicrobial therapy in the treatment of *Pseudomonas*

aeruginosa and *Acinetobacter baumannii* ventilator-associated pneumonia. *Respir Care* 2012;57:1226–1233.

81. **Mccarty JS, Rüdiger S, Schönfeld HJ, Schneider-Mergener J, Nakahigashi K *et al.*** Regulatory region C of the *E. coli* heat shock transcription factor, sigma32, constitutes a DnaK binding site and is conserved among eubacteria. *J Mol Biol* 1996;256:829–837.
82. **Hsieh M, Gralla JD.** Analysis of the N-terminal leucine heptad and hexad repeats of sigma 54. *J Mol Biol* 1994;239:15–24.
83. **Doucleff M, Malak LT, Pelton JG, Wemmer DE.** The C-terminal RpoN domain of sigma54 forms an unpredicted helix-turn-helix motif similar to domains of sigma70. *J Biol Chem* 2005;280:41530–41536.
84. **Mahren S, Enz S, Braun V.** Functional interaction of region 4 of the extracytoplasmic function sigma factor FecI with the cytoplasmic portion of the FecR transmembrane protein of the *Escherichia coli* ferric citrate transport system. *J Bacteriol* 2002;184:3704–3711.
85. **Campbell EA, Tupy JL, Gruber TM, Wang S, Sharp MM *et al.*** Crystal structure of *Escherichia coli* sigmaE with the cytoplasmic domain of its anti-sigma RseA. *Mol Cell* 2003;11:1067–1078.
86. **Tam C, Collinet B, Lau G, Raina S, Missiakas D.** Interaction of the conserved region 4.2 of sigma(E) with the RseA anti-sigma factor. *J Biol Chem* 2002;277:27282–27287.
87. **Lane WJ, Darst SA.** The structural basis for promoter -35 element recognition by the group IV sigma factors. *PLoS Biol* 2006;4:e269.
88. **Braun V, Mahren S, Ogierman M.** Regulation of the FecI-type ECF sigma factor by transmembrane signalling. *Curr Opin Microbiol* 2003;6:173–180.
89. **Schmitt MP.** Transcription of the *Corynebacterium diphtheriae* hmuO gene is regulated by iron and heme. *Infect Immun* 1997;65:4634–4641.
90. **Zhu W, Hunt DJ, Richardson AR, Stojiljkovic I.** Use of heme compounds as iron sources by pathogenic neisseriae requires the product of the hemO gene. *J Bacteriol* 2000;182:439–447.
91. **Ratliff M, Zhu W, Deshmukh R, Wilks A, Stojiljkovic I.** Homologues of neisserial heme oxygenase in gram-negative bacteria: degradation of heme by the product of the pigA gene of *Pseudomonas aeruginosa*. *J Bacteriol* 2001;183:6394–6403.
92. **Carroll RK, Weiss A, Broach WH, Wiemels RE, Mogen AB *et al.*** Genome-wide annotation, identification, and global transcriptomic analysis of regulatory or small RNA gene expression in *Staphylococcus aureus*. *MBio* 2016;7:e01990-15.
93. **Takinowaki H, Matsuda Y, Yoshida T, Kobayashi Y, Ohkubo T.** The solution structure of the methylated form of the N-terminal 16-kDa domain of *Escherichia coli* Ada protein. *Protein Sci* 2006;15:487–497.
94. **Carlin A, Shi W, Dey S, Rosen BP.** The ars operon of *Escherichia coli* confers arsenical and antimonial resistance. *J Bacteriol* 1995;177:981–986.
95. **Xu C, Shi W, Rosen BP.** The chromosomal *arsR* gene of *Escherichia coli* encodes a *trans*-acting metalloregulatory protein. *J Biol Chem* 1996;271:2427–2432.
96. **Giangrossi M, Giuliodori AM, Gualerzi CO, Pon CL.** Selective expression of the beta-subunit of nucleoid-associated protein HU during cold shock in *Escherichia coli*. *Mol Microbiol* 2002;44:205–216.
97. **Fuchs EL, Brutinel ED, Jones AK, Fulcher NB, Urbanowski ML *et al.*** The *Pseudomonas aeruginosa* vfr regulator controls global virulence factor expression through cyclic AMP-dependent and -independent mechanisms. *J Bacteriol* 2010;192:3553–3564.
98. **Kücherer C, Lother H, Kölling R, Schauzu MA, Messer W.** Regulation of transcription of the chromosomal *dnaA* gene of *Escherichia coli*. *Mol Gen Genet* 1986;205:115–121.
99. **Gao YG, Suzuki H, Itou H, Zhou Y, Tanaka Y *et al.*** Structural and functional characterization of the LldR from *Corynebacterium glutamicum*: a transcriptional repressor involved in L-lactate and sugar utilization. *Nucleic Acids Res* 2008;36:7110–7123.
100. **Aguilera L, Campos E, Giménez R, Badía J, Aguilar J *et al.*** Dual role of LldR in regulation of the *lldPRD* operon, involved in L-lactate metabolism in *Escherichia coli*. *J Bacteriol* 2008;190:2997–3005.
101. **Morawski B, Segura A, Ornston LN.** Repression of *Acinetobacter* vanillate demethylase synthesis by VanR, a member of the GntR family of transcriptional regulators. *FEMS Microbiol Lett* 2000;187:65–68.
102. **Sieira R, Arocena GM, Bukata L, Comerci DJ, Ugalde RA.** Metabolic control of virulence genes in *Brucella abortus*: hutc coordinates *virB* expression and the histidine utilization pathway by direct binding to both promoters. *J Bacteriol* 2010;192:217–224.
103. **Kok RG, D'Argenio DA, Ornston LN.** Mutation analysis of PobR and PcaU, closely related transcriptional activators in Acinetobacter. *J Bacteriol* 1998;180:5058–5069.
104. **Arias-Barrau E, Olivera ER, Luengo JM, Fernández C, Galán B *et al.*** The homogentisate pathway: a central catabolic pathway involved in the degradation of L-phenylalanine, L-tyrosine, and 3-hydroxyphenylacetate in *Pseudomonas putida*. *J Bacteriol* 2004;186:5062–5077.
105. **Yeung AT, Torfs EC, Jamshidi F, Bains M, Wiegand I *et al.*** Swarming of *Pseudomonas aeruginosa* is controlled by a broad spectrum of transcriptional regulators, including MetR. *J Bacteriol* 2009;191:5592–5602.
106. **Chugani SA, Parsek MR, Chakrabarty AM.** Transcriptional repression mediated by LysR-type regulator CatR bound at multiple binding sites.. *J Bacteriol* 1998;180:2367–2372.
107. **Craven SH, Ezezika OC, Haddad S, Hall RA, Momany C *et al.*** Inducer responses of BenM, a LysR-type transcriptional regulator from *Acinetobacter baylyi* ADP1. *Mol Microbiol* 2009;72:881–894.
108. **Collier LS, Gaines GL, Neidle EL.** Regulation of benzoate degradation in *Acinetobacter* sp. strain ADP1 by BenM, a LysR-type transcriptional activator.. *J Bacteriol* 1998;180:2493–2501.
109. **Marbaniang CN, Gowrishankar J.** Role of ArgP (lciA) in lysine-mediated repression in *Escherichia coli*. *J Bacteriol* 2011;193:5985–5996.
110. **Díaz E, Ferrández A, García JL.** Characterization of the *hca* cluster encoding the dioxygenolytic pathway for initial catabolism of 3-phenylpropionic acid in *Escherichia coli* K-12. *J Bacteriol* 1998;180:2915–2923.
111. **van der Ploeg JR, Eichhorn E, Leisinger T.** Sulfonate-sulfur metabolism and its regulation in *Escherichia coli*. *Arch Microbiol* 2001;176:1–8.
112. **Kertesz MA.** Riding the sulfur cycle – metabolism of sulfonates and sulfate esters in gram-negative Bacteria.. *FEMS Microbiol Rev* 2000;24:135–175.
113. **Stec E, Witkowska-Zimny M, Hryniewicz MM, Neumann P, Wilkinson AJ *et al.*** Structural basis of the sulphate starvation response in *E. coli*: crystal structure and mutational analysis of the cofactor-binding domain of the cbl transcriptional regulator. *J Mol Biol* 2006;364:309–322.
114. **Graveline R, Garneau P, Martin C, Mourez M, Hancock MA *et al.*** Leucine-responsive regulatory protein lrp and PapI homologues influence phase variation of CS31A fimbriae. *J Bacteriol* 2014;196:2944–2953.
115. **Stoyanov JV, Hobman JL, Brown NL.** CueR (YbbI) of *Escherichia coli* is a MerR family regulator controlling expression of the copper exporter CopA. *Mol Microbiol* 2001;39:502–512.
116. **Kirby JE, Trempy JE, Gottesman S.** Excision of a P4-like cryptic prophage leads to alp protease expression in *Escherichia coli*. *J Bacteriol* 1994;176:2068–2081.

Appendix 2 Supplemental figures

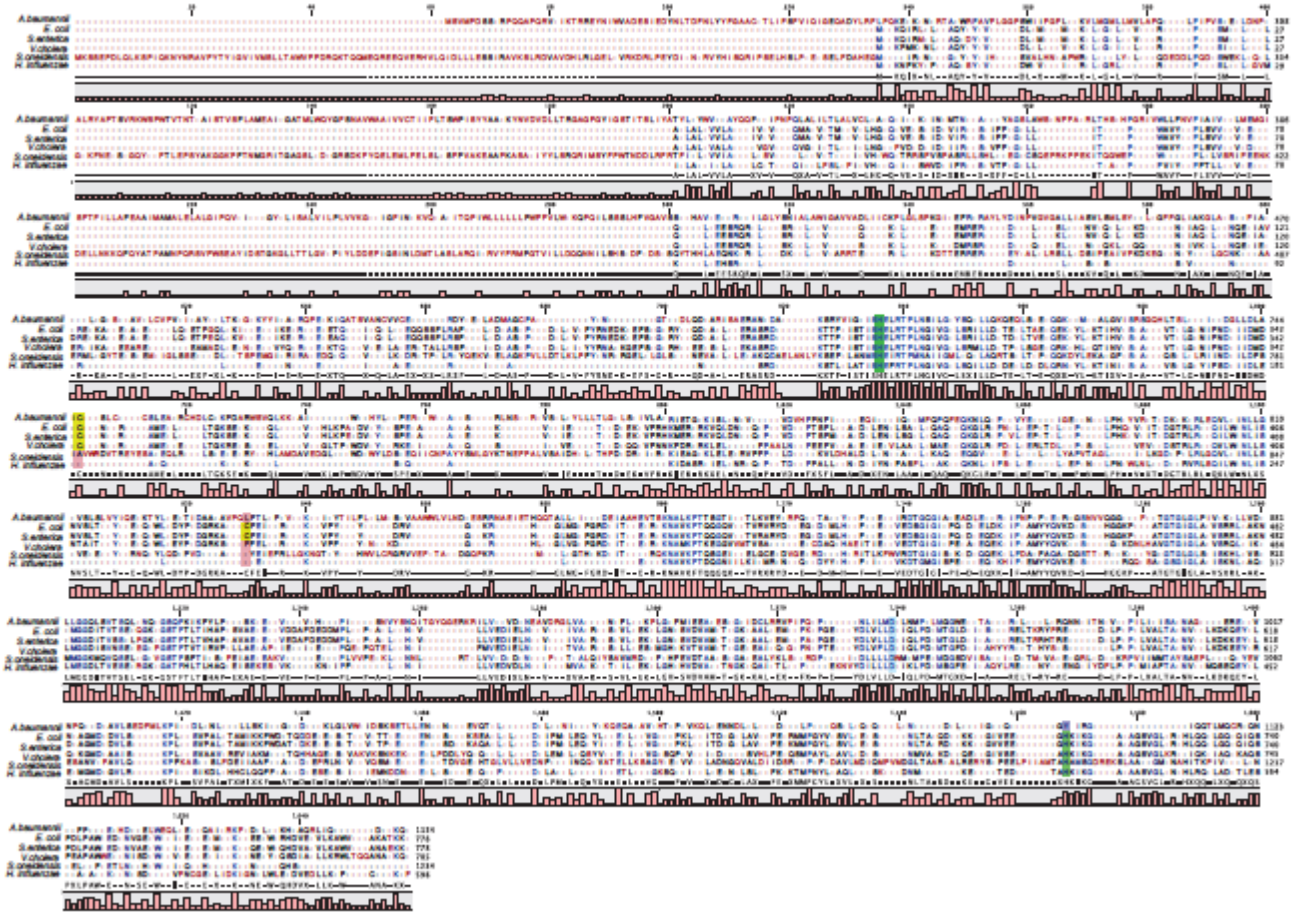

Supplemental Figure S1. Protein alignments of ABUW_2427 from A. baumannii alongside ArcB proteins from a variety of organisms. Protein alignments from *Acinetobacter baumannii*, *Escherichia coli*, *Salmonella enterica*, *Vibrio cholera*, *Shewanella oneidensis*, and *Haemophilus influenzae* showing conservation and divergence of amino acids found among ArcB homologs. Yellow shading indicates conservation of the Cys 180 and Cys 241 amino acids that are required for ArcB kinase regulation in *E. coli*, whilst pink shading shows divergence of these residues. Blue shading shows conservation of the aspartic acid residue. Green shading shows conservation of histidine residues, with violet indicating the absence of the second of these in *A. baumannii*

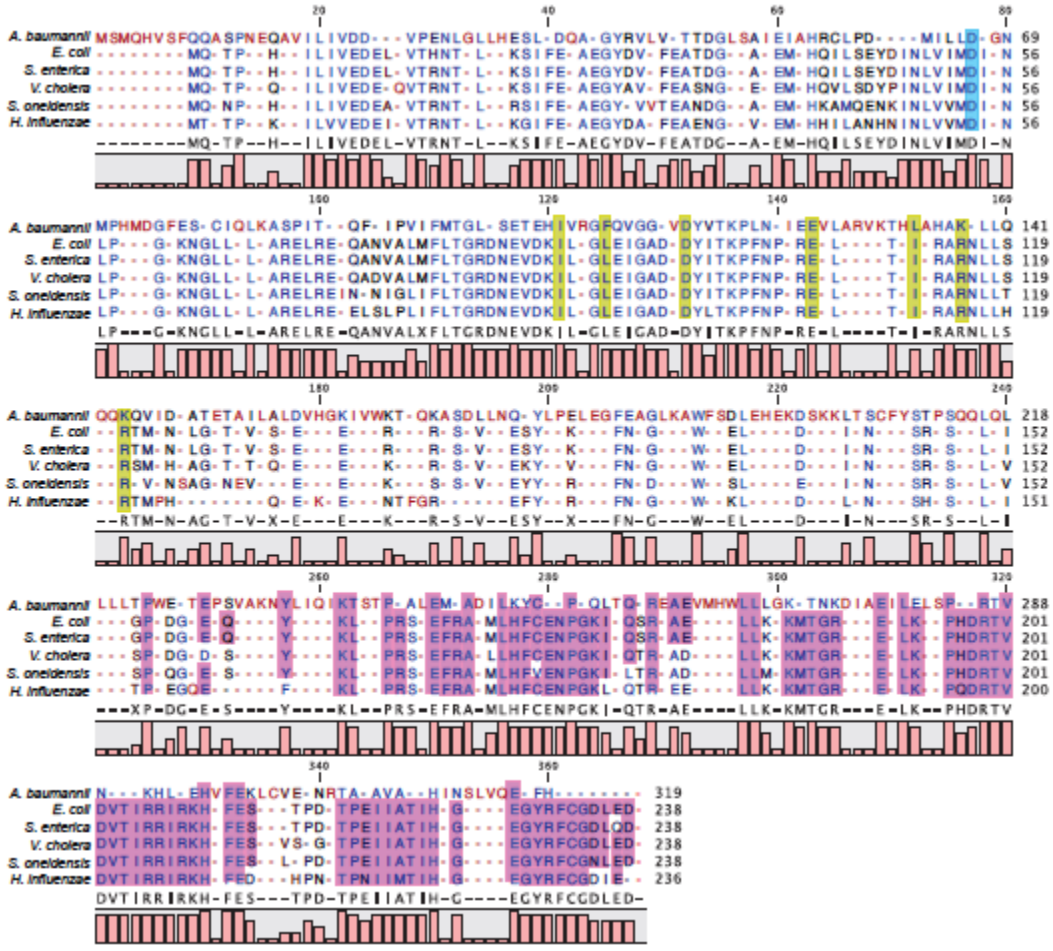

Supplemental Figure S2. Protein alignments of ABUW_2426 from A. baumannii alongside ArcA proteins from a variety of organisms. Protein alignments from *Acinetobacter baumannii*, *Escherichia coli*, *Salmonella enterica*, *Vibrio cholera*, *Shewanella oneidensis*, and *Haemophilus influenzae* showing conservation and divergence of amino acids found among ArcA homologs. Blue shading highlights conservation of the aspartic acid residue required for phosphorylation of ArcA. Yellow shading highlights conservation of amino acids found in the regulatory domain that are important for dimerization, allowing an active conformational state of ArcA. Pink shading shows conservation of amino acids found within the helix turn helix domain of the *E. coli* ArcA protein.

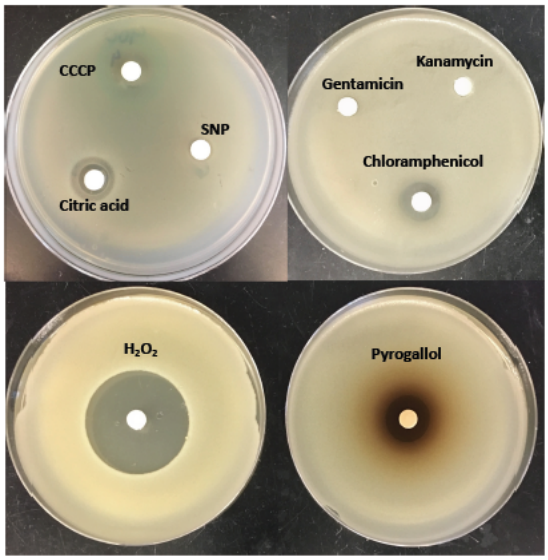

Supplemental Figure S3. The arcAB promoter is induced upon exposure to CCCP. LB plates supplemented with X-Gal were inoculated with the wild-type bearing an *arcAB-lacZ* reporter-gene fusion strain. Sterile filter disks were placed onto plates, and inoculated with the compounds noted. The induction of expression is visualized as a blue ring around the zone of inhibition. Shown are four representative plates

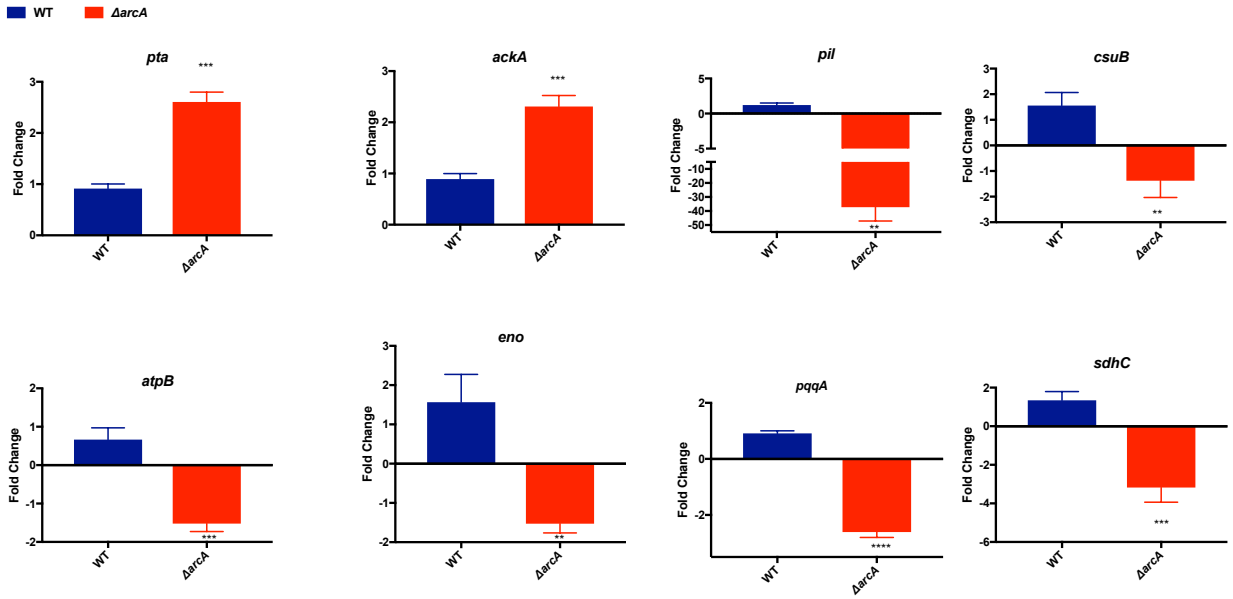

Supplemental Figure S4. qPCR validation of RNA-seq data arcA expression in the wild-type and arcA mutant. Changes from the RNA-seq dataset were confirmed using qRT-PCR analysis for a random selection of genes and comparing fold changes in expression of the arcA mutant relative to the wild-type. Measurements are derived from three independent replicates with error bars shown as +/- SEM. Student's t-test was used to assess statistical significance ** = p<0.001, *** = p<0.001.

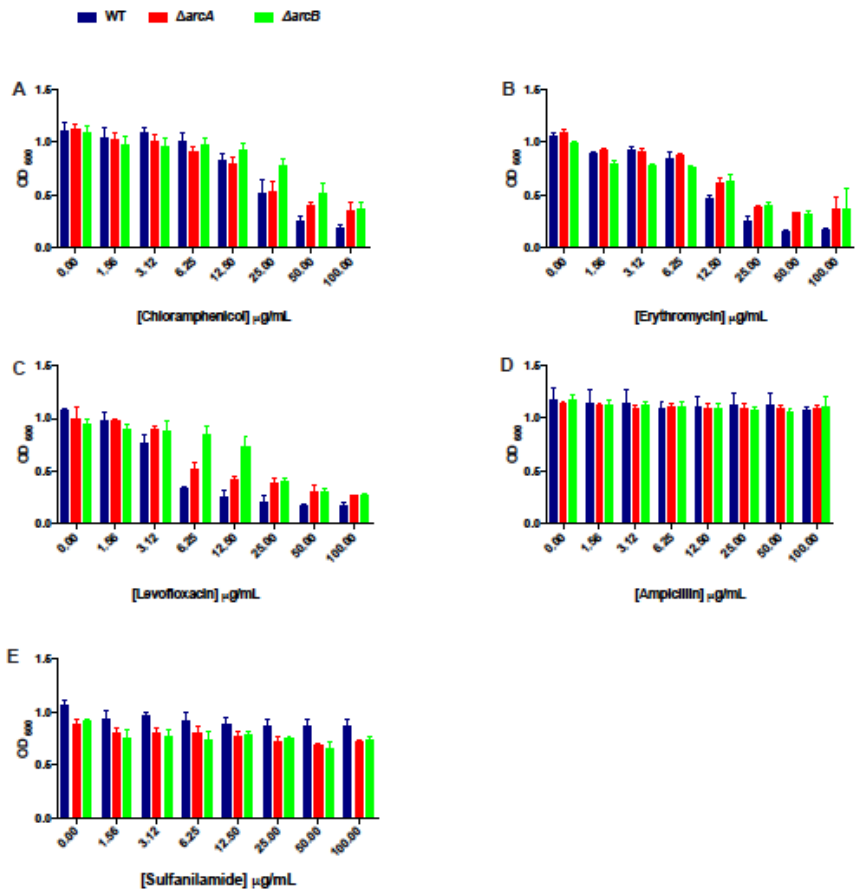

.

Supplemental Figure S5. Disruption of ArcAB does not affect susceptibility to non-aminoglycoside antibiotics. Determination of minimal inhibitory concentration (MIC) for the wild-type, Δ*arcA* and Δ*arcB* strains was determined for: (A) Chloramphenicol, (B) Erythromycin, (C) Levofloxacin, (D) Ampicillin, and (E) Sulfanilamide. Data is derived from three independent experiments, with error bars shown as +/- SEM.

APENDIX 3 Supplemental Tables

Table 1S Genes differentially expressed in the *arcA* mutant strain

Locus Tag	Gene	Protein / Function	Fold Change
Hypothetical protein			
ABUW_1004	-	hypothetical protein	14.66
ABUW_2433	-	KGG domain-containing protein	12.31
ABUW_0157	-	hypothetical protein	10.03
ABUW_3587	-	hypothetical protein	6.68
ABUW_3695	-	hypothetical protein	6.52
ABUW_2984	-	hypothetical protein	5.64
ABUW_1005	-	NIF3 (NGG1p interacting factor 3)	5.32
ABUW_3322	-	exonuclease V beta chain	5.11
ABUW_3516	-	hypothetical protein	5.09
ABUW_1659	-	hypothetical protein	5.03
ABUW_1536	-	hypothetical protein	3.67
ABUW_2065	-	hypothetical protein	3.61
ABUW_2693	-	hypothetical protein	3.57
ABUW_2965	-	hypothetical protein	3.56
ABUW_1649	-	hypothetical protein	3.51
ABUW_0111	-	hypothetical protein	3.42
ABUW_0233	-	hypothetical protein	3.41
ABUW_3278	-	hypothetical protein	3.4
ABUW_0931	-	SnoaL-like polyketide cyclase domain-containing protein	3.36
ABUW_2448	-	beta-barrel domain-containing outer membrane protein	3.3
ABUW_2606	-	glycoside hydrolase/deacetylase family protein	3.3
ABUW_2297	-	hypothetical protein	3.22
ABUW_0710	-	hypothetical protein	3.17

Table 1S (Continued)

ABUW_3147	-	hypothetical protein	3.15
ABUW_2442	-	hypothetical protein	3.12
ABUW_1379	-	hypothetical protein	3.1
ABUW_2058	-	hypothetical protein	3.1
ABUW_0646	-	glycosylase/bleomycin resistance/fosfomycin resistance/dioxygenase domain-containing protein	2.98
ABUW_1987	-	hypothetical protein	2.9
ABUW_1165	-	pirin domain protein	2.89
ABUW_2922	-	hypothetical protein	2.87
ABUW_2156	-	hypothetical protein	2.83
ABUW_1792	-	hypothetical protein	2.83
ABUW_1143	-	hypothetical protein	2.82
ABUW_3433	-	hypothetical protein	2.82
ABUW_2721	-	Putative O-methyl transferase	2.82
ABUW_1629	-	hypothetical protein	2.81
ABUW_0336	-	hypothetical protein	2.77
ABUW_3158	-	hypothetical protein	2.77
ABUW_1594	-	hypothetical protein	2.75
ABUW_1564	-	hypothetical protein	2.72
ABUW_0207	-	pirin family protein	2.68
ABUW_2692	-	hypothetical protein (pseudogene: nonfunctional due to frameshift)	2.65
ABUW_1264	-	hypothetical protein	2.62
ABUW_1471	-	hypothetical protein	2.61
ABUW_0301	-	LemA Family protein	2.6
ABUW_1761	-	hypothetical protein	2.55
ABUW_0220	-	hypothetical protein	2.52
ABUW_0768	-	hypothetical protein	2.51
ABUW_3441	-	hypothetical protein	2.51
ABUW_3524	-	hypothetical protein	2.5
ABUW_0521	-	rhodanese domain protein	2.5
ABUW_2143	-	hypothetical protein	2.5
ABUW_2449	-	putative SAM-dependent methyltransferase	2.45
ABUW_0449	-	hypothetical protein	2.44
ABUW_0302	-	TPM domain-containing protein	2.43

Table 1S (Continued)

ABUW_1256	-	hypothetical protein	2.42
ABUW_2803	-	hypothetical protein	2.41
ABUW_0104	-	secretory lipase	2.41
ABUW_2703	-	hypothetical protein	2.38
ABUW_3149	-	hypothetical protein	2.37
ABUW_0928	-	lytic transglycosylase, catalytic	2.37
ABUW_0217	-	hypothetical protein	2.36
ABUW_0793	-	hypothetical protein	2.36
ABUW_1786	-	tetratricopeptide-like helical domain-containing protein	2.36
ABUW_2860	-	hypothetical protein	2.3
ABUW_3574	-	hypothetical protein	2.29
ABUW_0254	-	acetyltransferase	2.29
ABUW_3113	-	Sua5/YciO/YrdC/YwlC family protein	2.28
ABUW_0053	-	UPF0391 membrane protein	2.27
ABUW_1657	-	hypothetical protein	2.26
ABUW_3058	-	putative metal-dependent hydrolase	2.26
ABUW_1059	-	hypothetical protein	2.23
ABUW_2720	-	hypothetical protein	2.22
ABUW_2554	-	HYpothetical protein	2.15
ABUW_2391	-	hypothetical protein	2.15
ABUW_0673	-	hypothetical protein	2.14
ABUW_3045	-	OmpA/MotB domain protein	2.11
ABUW_3793	-	SnoaL-like polyketide cyclase domain-containing protein	2.07
ABUW_3759	-	hypothetical protein	2.06
ABUW_3101	-	GDYXXLXY domain-containing protein	2.05
ABUW_1283	-	hypothetical protein	2.05
ABUW_2621	-	hypothetical protein	2.05
ABUW_0181	-	hypothetical protein	2
ABUW_3458	-	hypothetical protein	2
ABUW_0206	-	isochorismate hydrolase	2
ABUW_1603	-	putative acetyltransferase	2
ABUW_1988	-	hypothetical protein	-2
ABUW_0593	-	hypothetical protein	-2.01
ABUW_3375	-	hypothetical protein	-2.04
ABUW_3827	-	hypothetical protein	-2.06

Table 1S (Continued)

ABUW_2610	-	hypothetical protein	-2.07
ABUW_2886	-	hypothetical protein	-2.07
ABUW_0703	-	hypothetical protein	-2.07
ABUW_0058	-	hypothetical protein	-2.09
ABUW_0117	-	hypothetical protein	-2.09
ABUW_3702	-	hypothetical protein	-2.09
ABUW_3282	-	hypothetical protein	-2.1
ABUW_0382	-	hypothetical protein	-2.1
ABUW_2612	-	hypothetical protein	-2.13
ABUW_2962	-	YaeQ domain-containing protein	-2.13
ABUW_2677	-	hypothetical protein	-2.15
ABUW_1451	-	GatB/Yqey domain protein	-2.17
ABUW_1971	-	hypothetical protein	-2.18
ABUW_0902	-	hypothetical protein	-2.18
ABUW_1051	-	hypothetical protein	-2.18
ABUW_3001	-	hypothetical protein	-2.2
ABUW_3582	-	hypothetical protein	-2.21
ABUW_1752	-	hypothetical protein	-2.22
ABUW_2660	-	hypothetical protein	-2.23
ABUW_3882	-	hypothetical protein	-2.24
ABUW_0813	-	hypothetical protein	-2.25
ABUW_3698	-	putative lysozyme	-2.25
ABUW_3825	-	hypothetical protein	-2.27
ABUW_2599	-	hypothetical protein	-2.28
ABUW_0524	-	YCII-related protein	-2.28
ABUW_3337	-	Hypothetical protein	-2.29
ABUW_1443	-	Hypothetical protein	-2.3
ABUW_1045	-	GGDEF family protein	-2.3
ABUW_3687	-	hypothetical protein	-2.32
ABUW_1237	-	hypothetical protein	-2.32
ABUW_0088	-	hypothetical protein	-2.33
ABUW_1455	-	AAA ATPase superfamily protein	-2.33
ABUW_3866	-	hypothetical protein	-2.34
ABUW_1331	-	exodeoxyribonuclease X, putative	-2.34
ABUW_2181	-	Hypothetical protein	-2.35
ABUW_3555	-	hypothetical protein	-2.37
ABUW_2626	-	Hypothetical protein	-2.38

Table 1S (Continued)

ABUW_2665	-	Hypothetical protein	-2.38
ABUW_1534	-	hypothetical protein	-2.4
ABUW_1644	-	hypothetical protein	-2.41
ABUW_2317	-	hypothetical protein	-2.42
ABUW_1797	-	hypothetical protein	-2.43
ABUW_1746	-	hypothetical protein	-2.43
ABUW_1083	-	Hypothetical protein	-2.46
ABUW_1245	-	Hypothetical protein	-2.46
ABUW_0506	-	GGDEF domain protein	-2.46
ABUW_1990	-	Hypothetical protein	-2.48
ABUW_0865	-	rhodanese domain protein	-2.49
ABUW_0346	-	hypothetical protein	-2.53
ABUW_1719	-	Hypothetical protein	-2.57
ABUW_2868	-	Hypothetical protein	-2.58
ABUW_1554	-	RDD family protein	-2.58
ABUW_2862	-	Hypothetical protein	-2.59
ABUW_1587	-	Hypothetical protein	-2.59
ABUW_2932	-	Hypothetical protein	-2.61
ABUW_0864	-	hypothetical protein	-2.62
ABUW_0554	-	hypothetical protein	-2.63
ABUW_1241	-	hypothetical protein	-2.63
ABUW_0636	-	hypothetical protein	-2.64
ABUW_0087	-	histidine kinase domain-containing ATPase-like protein	-2.65
ABUW_0365	-	hypothetical protein	-2.71
ABUW_0514	-	Hypothetical protein	-2.72
ABUW_0937	-	Hypothetical protein	-2.73
ABUW_1727	-	Hypothetical protein	-2.74
ABUW_1995	-	Hypothetical protein	-2.76
ABUW_0435	-	Hypothetical protein	-2.76
ABUW_3112	-	hypothetical protein	-2.8
ABUW_2932	-	Hypothetical protein	-2.61
ABUW_0864	-	hypothetical protein	-2.62
ABUW_0554	-	hypothetical protein	-2.63
ABUW_1241	-	hypothetical protein	-2.63
ABUW_0636	-	hypothetical protein	-2.64

Table 1S (Continued)

ABUW_0087	-	histidine kinase domain-containing ATPase-like protein	-2.65
ABUW_0365	-	hypothetical protein	-2.71
ABUW_0514	-	Hypothetical protein	-2.72
ABUW_0937	-	Hypothetical protein	-2.73
ABUW_1727	-	Hypothetical protein	-2.74
ABUW_1995	-	Hypothetical protein	-2.76
ABUW_0435	-	Hypothetical protein	-2.76
ABUW_3112	-	hypothetical protein	-2.8
ABUW_2932	-	Hypothetical protein	-2.61
ABUW_0864	-	hypothetical protein	-2.62
ABUW_0554	-	hypothetical protein	-2.63
ABUW_1241	-	hypothetical protein	-2.63
ABUW_0636	-	hypothetical protein	-2.64
ABUW_0087	-	histidine kinase domain-containing ATPase-like protein	-2.65
ABUW_0365	-	hypothetical protein	-2.71
ABUW_0514	-	Hypothetical protein	-2.72
ABUW_0937	-	Hypothetical protein	-2.73
ABUW_1727	-	Hypothetical protein	-2.74
ABUW_1995	-	Hypothetical protein	-2.76
ABUW_0435	-	Hypothetical protein	-2.76
ABUW_3112	-	hypothetical protein	-2.8
ABUW_1126	-	putative transferase	-2.82
ABUW_3453	-	Hypothetical protein	-2.84
ABUW_2061	-	Hypothetical protein	-2.85
ABUW_3271	-	Hypothetical protein	-2.91
ABUW_3452	-	Hypothetical protein	-2.92
ABUW_0697	-	Hypothetical protein	-2.92
ABUW_1918	-	Hypothetical protein	-2.93
ABUW_0596	-	Hypothetical protein	-2.96
ABUW_2655	-	hypothetical protein	-3.02
ABUW_2200	-	hypothetical protein	-3.03
ABUW_1317	-	hypothetical protein	-3.05
ABUW_0683	-	hypothetical protein	-3.06
ABUW_2672	-	hypothetical protein	-3.13

Table 1S (Continued)

ABUW_2445	-	hypothetical protein	-3.14
ABUW_1541	-	hypothetical protein	-3.15
ABUW_1920	-	hypothetical protein	-3.15
ABUW_0225	-	hypothetical protein	-3.16
ABUW_3016	-	hypothetical protein	-3.16
ABUW_2439	-	hypothetical protein	-3.18
ABUW_2833	-	hypothetical protein	-3.18
ABUW_1769	-	hypothetical protein	-3.19
ABUW_2103	-	hypothetical protein	-3.2
ABUW_2346	-	hypothetical protein	-3.3
ABUW_0187	-	hypothetical protein	-3.31
ABUW_2145	-	hypothetical protein	-3.31
ABUW_2374	-	isochorismatase hydrolase	-3.34
ABUW_1919	-	hypothetical protein	-3.38
ABUW_1318	-	hypothetical protein	-3.43
ABUW_1641	-	hypothetical protein	-3.45
ABUW_2673	-	hypothetical protein	-3.48
ABUW_0886	-	hypothetical protein	-3.55
ABUW_2595	-	hypothetical protein	-3.58
ABUW_2672	-	hypothetical protein	-3.13
ABUW_2445	-	hypothetical protein	-3.14
ABUW_1541	-	hypothetical protein	-3.15
ABUW_1920	-	hypothetical protein	-3.15
ABUW_0225	-	hypothetical protein	-3.16
ABUW_3016	-	hypothetical protein	-3.16
ABUW_2439	-	hypothetical protein	-3.18
ABUW_2833	-	hypothetical protein	-3.18
ABUW_1769	-	hypothetical protein	-3.19
ABUW_2103	-	hypothetical protein	-3.2
ABUW_2346	-	hypothetical protein	-3.3
ABUW_0187	-	hypothetical protein	-3.31
ABUW_2145	-	hypothetical protein	-3.31
ABUW_2374	-	isochorismatase hydrolase	-3.34
ABUW_1919	-	hypothetical protein	-3.38
ABUW_1318	-	hypothetical protein	-3.43
ABUW_1641	-	hypothetical protein	-3.45
ABUW_2673	-	hypothetical protein	-3.48

Table 1S (Continued)

ABUW_0886	-	hypothetical protein	-3.55
ABUW_2595	-	hypothetical protein	-3.58
ABUW_0786	-	hypothetical protein	-3.69
ABUW_2811	-	hypothetical protein	-3.7
ABUW_2616	-	hypothetical protein	-3.72
ABUW_2103	-	hypothetical protein	-3.2
ABUW_2346	-	hypothetical protein	-3.3
ABUW_0187	-	hypothetical protein	-3.31
ABUW_2145	-	hypothetical protein	-3.31
ABUW_2374	-	isochorismatase hydrolase	-3.34
ABUW_1919	-	hypothetical protein	-3.38
ABUW_1318	-	hypothetical protein	-3.43
ABUW_1641	-	hypothetical protein	-3.45
ABUW_2673	-	hypothetical protein	-3.48
ABUW_0886	-	hypothetical protein	-3.55
ABUW_2595	-	hypothetical protein	-3.58
ABUW_0786	-	hypothetical protein	-3.69
ABUW_2811	-	hypothetical protein	-3.7
ABUW_2616	-	hypothetical protein	-3.72
ABUW_3710	-	putative acetyltransferase	-3.78
ABUW_1162	-	hypothetical protein	-3.93
ABUW_3025	-	hypothetical protein	-3.97
ABUW_0236	-	hypothetical protein	-3.98
ABUW_3656	-	hypothetical protein	-4.02
ABUW_1376	-	hypothetical protein	-4.2
ABUW_1598	-	hypothetical protein	-4.21
ABUW_2598	-	hypothetical protein	-4.43
ABUW_2756	-	hypothetical protein	-4.47
ABUW_3526	-	hypothetical protein	-4.47
ABUW_3718	-	hypothetical protein	-4.52
ABUW_0364	-	hypothetical protein	-4.54
ABUW_3805	-	hypothetical protein	-4.69
ABUW_0507	-	hypothetical protein	-4.77
ABUW_0688	-	hypothetical protein	-4.98
ABUW_3006	-	hypothetical protein	-5.02
ABUW_3283	-	hypothetical protein	-5.15
ABUW_1780	-	hypothetical protein	-5.18

Table 1S (Continued)

ABUW_0462	-	hypothetical protein	-5.26
ABUW_2211	-	hypothetical protein	-5.26
ABUW_0901	-	hypothetical protein	-5.27
ABUW_0812	-	hypothetical protein	-5.35
ABUW_0796	-	hypothetical protein	-5.49
ABUW_3232	-	hypothetical protein	-5.6
ABUW_0520	-	hypothetical protein	-5.61
ABUW_1052	-	hypothetical protein	-5.65
ABUW_1725	-	hypothetical protein	-5.9
ABUW_1961	-	hypothetical protein	-6.22
ABUW_2191	-	hypothetical protein	-6.41
ABUW_1592	-	hypothetical protein	-8.11
ABUW_0835	-	hypothetical protein	-12.29
ABUW_2600	-	hypothetical protein	-13.82
ABUW_3156	-	hypothetical protein	-25.92
ABUW_3184	-	hypothetical protein	-32.06
ABUW_2832	-	hypothetical protein	-33
ABUW_2700	-	hypothetical protein	-45.63
ABUW_2666	-	Hypothetical protein	-68.58
Small RNA			
ABUWs050	-	small RNA	6.56
ABUWs008	-	small RNA	6.28
ABUWs056	-	small RNA	5.84
ABUWs011	-	small RNA	5.74
ABUWs001	-	small RNA	4.74
ABUWs047	-	small RNA	4.52
ABUWs043	-	small RNA	4.46
ABUWs033	-	small RNA	4.34
ABUWs044	-	small RNA	4.05
ABUWs046	-	small RNA	3.98
ABUWs052	-	small RNA	3.8
ABUWs009	-	small RNA	3.56
ABUWs069	-	small RNA	3.55
ABUWs017	-	small RNA	3.41
ABUWs030	-	small RNA	3.4
ABUWs048	-	small RNA	3.15
ABUWs042	-	small RNA	3.09

ABUWs071	-	small RNA	2.93
ABUWs035	-	small RNA	2.89
ABUWs010	-	small RNA	2.81
ABUWs019	-	small RNA	2.8
ABUWs073	-	small RNA	2.77
ABUWs068	-	small RNA	2.53
ABUWs003	-	small RNA	2.47
ABUWs062	-	small RNA	2.46
ABUWs064	-	small RNA	2.44
ABUWs018	-	small RNA	2.43
ABUWs024	-	small RNA	2.41
ABUWs026	-	small RNA	2.38
ABUWs029	-	small RNA	2.25
ABUWs036	-	small RNA	2.22
ABUWs049	-	small RNA	2.09
ABUWs014	-	small RNA	2.07
ABUWs080	-	small RNA	-2.96
ABUWs004	-	small RNA	-5.51
ABUWs054	-	Small RNA	-14.32
Amino acid metabolism			
ABUW_3214	*gcdH*	glutaryl-CoA dehydrogenase	6.88
ABUW_3217	*add2*	adenosine deaminase	5.89
ABUW_1464	*mmsA2*	methylmalonate-semialdehyde dehydrogenase	5.09
ABUW_3018	*ggt*	gamma-glutamyltransferase	4.27
ABUW_1726	-	D-amino acid dehydrogenase 3 small subunit	4.25
ABUW_2452	-	isovaleryl-CoA dehydrogenase	3.19
ABUW_0077	*hutU*	urocanate hydratase	3.08
ABUW_3463	*leuC*	3-isopropylmalate dehydratase, large subunit	2.46
ABUW_1638	-	chorismate mutase	2.56
ABUW_1200	*trpC*	indole-3-glycerol phosphate synthase	-2.01
ABUW_2823	*argG*	argininosuccinate synthase	-2.04
ABUW_0894	*carA*	carbamoyl-phosphate synthase, small subunit	-2.49
ABUW_0704	*agcS*	amino acid transport protein	-2.6
ABUW_3150	-	lysine exporter protein	-2.8
ABUW_2976	*arcD*	arginine/ornithine antiporter	-2.85
ABUW_1777	*brnQ*	branched-chain amino acid transport system II carrier protein	-2.86
Regulators			

Table 1S (Continued)

ABUW_1266	-	regulator protein, putative	4.99
ABUW_3665	*cadR*	Transcriptional regulator	3.33
ABUW_2284	*npdA*	NAD-dependent deacetylase regulatory protein	2.92
ABUW_3741	*zur*	transcriptional regulator, Fur family	2.73
ABUW_3653	*nrdR*	transcriptional regulator NrdR	2.59
ABUW_2775	*vanR*	transcriptional regulator, GntR family	2.53
ABUW_0190	-	transcriptional regulator, TetR family	2.44
ABUW_2354	-	transcriptional regulator, AraC family	2.44
ABUW_0219	-	transcriptional regulator, AraC family	2.43
ABUW_3209	-	LysR-family transcriptional regulator	2.4
ABUW_3639	*gacA*	response regulator	2.32
ABUW_1732	*ntrC*	nitrogen metabolism transcriptional regulator, NtrC, Fis Family	2.31
ABUW_0942	-	transcriptional regulator, TetR family	2.27
ABUW_0257	*ompR*	two-component system response regulator protein	2.24
ABUW_0855	-	transcriptional regulator, HxlR family	2.2
ABUW_1338	-	transcriptional regulator, LysR family	2.05
ABUW_3615	*algR*	alginate biosynthesis regulatory protein	2.01
ABUW_1533	*fis*	transcriptional regulator, Fis-type	-2.01
ABUW_0169	-	transcriptional regulator, ArsR family	-2.04
ABUW_1856	-	transcriptional regulator, MarR-family	-2.05
ABUW_3595	*nusG*	transcription termination/antitermination factor NusG	-2.07
ABUW_1145	-	transcriptional regulator, LysR family	-2.09
ABUW_2472	*dcaR*	transcriptional regulator, IclR family	-2.1
ABUW_3627	*dksA*	DnaK suppressor protein	-2.1
ABUW_2376	-	transcriptional regulator, GntR family	-2.11
ABUW_1016	*cbl*	transcriptional regulator, LysR family	-2.13
ABUW_1585	*kdpE*	two-component system regulatory protein KdpE	-2.14
ABUW_3203	-	transcriptional regulator, AraC family	-2.17
ABUW_3206	-	transcriptional regulator, LysR family	-2.18
ABUW_2074	-	transcriptional regulator, fur family	-2.2
ABUW_2236	-	transcriptional regulator, AraC family	-2.22
ABUW_0892	*greA*	transcription elongation factor GreA	-2.23
ABUW_1715	-	transcriptional regulator, GntR family	-2.24

Table 1S (Continued)

ABUW_0431	*rpoA*	RNA polymerase alpha subunit	-2.25
ABUW_2276	-	Transcription Factor	-2.33
ABUW_2101	-	Transcription Factor	-2.33
ABUW_2852	-	Transcription Factor	-2.4
ABUW_1103	-	Transcription Factor	-2.4
ABUW_1896	-	Transcription Factor	-2.46
ABUW_0832	-	Transcription Factor	-2.48
ABUW_2446	-	Transcription Factor	-2.53
ABUW_3033	*fur*	Transcription Factor	-2.53
ABUW_2801	-	Transcription Factor	-2.59
ABUW_3877	-	transcriptional regulator, LysRfamily	-2.65
ABUW_3640	*pilS*	sensor protein histidine kinase	-2.68
ABUW_3261	-	Anti-Anti sigma factor	-2.72
ABUW_2328	-	transcriptional regulator, TetR family	-3.26
ABUW_3845	-	transcriptional regulator, TetR family	-3.28
ABUW_2084	-	transcriptional regulator, AraC family	-3.98
ABUW_1692	-	transcriptional regulator, TetR family	-4.14
ABUW_0678	*pilG*	type IV pilus response regulator receiver protein PilG	-4.38
ABUW_1731	-	transcriptional regulator, TetR family	-4.56
ABUW_3264	-	transcriptional regulator OhrR	-4.63
ABUW_0400	-	transcriptional regulator, BadM/Rrf2 family	-4.87
ABUW_2275	-	transcriptional regulator, TetR family	-4.87
ABUW_1848	*pcaU*	pca operon regulatory protein	-4.97
ABUW_3352	-	putative transcriptional regulator	-7.62
ABUW_2344	-	transcriptional regulator, Crp/Fnr family	-8.41
ABUW_1103	-	Transcription Factor	-2.4
ABUW_1896	-	Transcription Factor	-2.46
ABUW_0832	-	Transcription Factor	-2.48
ABUW_2446	-	Transcription Factor	-2.53
ABUW_3033	*fur*	Transcription Factor	-2.53
ABUW_2801	-	Transcription Factor	-2.59
ABUW_3877	-	transcriptional regulator, LysRfamily	-2.65
ABUW_3640	*pilS*	sensor protein histidine kinase	-2.68
ABUW_3261	-	Anti-Anti sigma factor	-2.72
ABUW_2328	-	transcriptional regulator, TetR family	-3.26
ABUW_3845	-	transcriptional regulator, TetR family	-3.28

Table 1S (Continued)

ABUW_2084	-	transcriptional regulator, AraC family	-3.98
ABUW_1692	-	transcriptional regulator, TetR family	-4.14
ABUW_0678	*pilG*	type IV pilus response regulator receiver protein PilG	-4.38
ABUW_1731	-	transcriptional regulator, TetR family	-4.56
ABUW_3264	-	transcriptional regulator OhrR	-4.63
ABUW_0400	-	transcriptional regulator, BadM/Rrf2 family	-4.87
ABUW_2275	-	transcriptional regulator, TetR family	-4.87
ABUW_1848	*pcaU*	pca operon regulatory protein	-4.97
ABUW_3352	-	putative transcriptional regulator	-7.62
ABUW_2344	-	transcriptional regulator, Crp/Fnr family	-8.41
Energy production and conversion			
ABUW_2458	-	oxidoreductase	8.16
ABUW_2411	-	glutathione S-transferase family protein	5.63
ABUW_1227	-	acyl-CoA dehydrogenase	5.43
ABUW_2099	-	acetyl-CoA acetyltransferase	5.24
ABUW_3849	-	short chain dehydrogenase	4.77
ABUW_2390	*cioB*	cytochrome D ubiquinol oxidase, subunit II	4.72
ABUW_1467	-	acyl-CoA dehydrogenase	4.54
ABUW_2503	-	cytochrome B561	4.3
ABUW_2389	*cioA*	cytochrome bd ubiquinol oxidase, subunit I	4.27
ABUW_2122	-	oxidoreductase	3.85
ABUW_0944	-	oxidoreductase alpha (molybdopterin) subunit	3.84
ABUW_3806	*acnD*	2-methylisocitrate dehydratase, Fe/S-dependent	3.82
ABUW_0175	*acsA*	acetate--CoA ligase	3.69
ABUW_0662	-	NADPH dehydrogenase	3.52
ABUW_2770	-	GMC oxidoreductase	3.51
ABUW_1887	-	oxidoreductase FMN-binding	3.49
ABUW_0218	-	aldo-keto reductase	3.22
ABUW_2435	-	oxidoreductase	3.17
ABUW_1196	*xdhA*	xanthine dehydrogenase, small subunit	2.88
ABUW_1588	-	ubiquinone biosynthesis protein COQ7	2.77
ABUW_1888	-	saccharopine dehydrogenase	2.74
ABUW_1573	-	acyl-CoA dehydrogenase	2.67
ABUW_2594	-	glutathione-dependent formaldehyde dehydrogenase	2.52

Table 1S (Continued)

ABUW_1572	-	short-chain dehydrogenase/reductase	2.42
ABUW_1794	*cydB*	cytochrome D ubiquinol oxidase, subunit II	2.42
ABUW_1843	*quiA*	quinate/shikimate dehydrogenase	2.41
ABUW_2835	-	oxidoreductase, FAD/FMN-binding	2.38
ABUW_0912	*glpD*	glycerol-3-phosphate dehydrogenase	2.32
ABUW_2410	-	glutathione S-transferase family protein	2.29
ABUW_2779	*hcaB*	aldehyde dehydrogenase	2.27
ABUW_3443	-	alcohol dehydrogenase, zinc-binding	2.26
ABUW_3865	-	putative flavoprotein	2.17
ABUW_2437	-	Iron-containing redox enzyme family protein	2.16
ABUW_0011	-	iron-sulfur cluster assembly accessory protein	2.15
ABUW_3429	*calB*	aldehyde dehydrogenase	2.15
ABUW_1978	-	flavin binding monooxygenase	2.11
ABUW_0433	-	flavin-containing monooxygenase FMO	2.09
hppD	*hppD*	4-hydroxyphenylpyruvate dioxygenase	2.08
ABUW_3390	*gapN*	aldehyde dehydrogenase	2.03
ABUW_0702	-	nitroreductase	2.01
ABUW_2902	*rubA*	rubredoxin	2
ABUW_1980	-	oxidoreductase	2
ABUW_2076	-	2,3-dihydro-2,3-dihydroxybenzoate dehydrogenase	-2.04
ABUW_0350	*gdh*	glutamate dehydrogenase	-2.08
ABUW_1449	*tkrA*	2-ketogluconate reductase	-2.1
ABUW_3798	-	short-chain dehydrogenase/reductase SDR	-2.21
ABUW_2913	-	carbonate dehydratase	-2.21
ABUW_3830	-	UDP-glucose/GDP-mannose dehydrogenase	-2.22
ABUW_0376	*aroE*	shikimate 5-dehydrogenase	-2.26
ABUW_0874	*lpdA1*	dihydrolipoamide dehydrogenase	-2.47
ABUW_1549	*cyoE*	protoheme IX farnesyltransferase (transferase)	-2.64
ABUW_0160	-	metallo-beta-lactamase family protein	-2.65
ABUW_3135	-	cytochrome c assembly protein	-2.81
ABUW_2753	-	cytochrome B561	-4.14
ABUW_1344	-	iron-sulfur cluster-binding protein	-4.73
ABUW_2071	*pqqA*	Energy metabolism	-30.47
TCA Cycle			
ABUW_3346	*acnA*	aconitate hydratase 1	5.42

Table 1S (Continued)

ABUW_2097	*atoA*	3-oxoacid CoA-transferase, subunit B	5.18
ABUW_3396	*pta*	phosphate acetyltransferase	3.54
ABUW_3395	*ackA*	acetate kinase	3.37
ABUW_3807	*prpC*	2-methylcitrate synthase	2.18
ABUW_2888	*aceA*	isocitrate lyase	2.05
ABUW_0871	*sdhB*	succinate dehydrogenase iron-sulfur subunit	-2.04
ABUW_2113	*sucC*	succinate dehydrogenase	-2.05
ABUW_0869	*sdhD*	succinate dehydrogenase, hydrophobic membrane anchor protein	-2.43
ABUW_0868	*sdhC*	succinate dehydrogenase, cytochrome b556 subunit	-3.72
General metabolism			
ABUW_2454	*mgh*	3-methylglutaconyl-CoA hydratase	8.05
ABUW_1020	-	alpha/beta hydrolase fold protein	7.96
ABUW_1468	-	LmbE-like protein	7.78
ABUW_2453	-	methylcrotonoyl-CoA carboxylase beta chain	7.22
ABUW_3123	*otsA*	trehalose-6-phosphate synthase	6.43
ABUW_2425	-	acetyltransferase, gnat family	6.34
ABUW_0055	-	glucose sorbosone dehydrogenase	6.32
ABUW_1470	-	glycosyl transferase, family 2	6.17
ABUW_2398	*mdcE*	malonate decarboxylase, gamma subunit	6.12
ABUW_1064	-	glycosyltransferase	5.8
ABUW_1111	-	aldehyde dehydrogenase	5.74
ABUW_2455	-	methylcrotonoyl-CoA carboxylase subunit alpha	5.65
ABUW_2129	*acoC*	dihydrolipoamide acetyltransferase	5.04
ABUW_2881	*ureE*	urease accessory protein E	4.4
ABUW_2456	-	hydroxymethylglutaryl-CoA lyase	4.29
ABUW_2092	*bdhA*	3-hydroxybutyrate dehydrogenase	4.2
ABUW_1113	-	indole-3-pyruvate decarboxylase	3.97
ABUW_1521	*sndH1*	L-sorbosone dehydrogenase	3.92
ABUW_2603	*bccA*	carbamoyl-phosphate synthase	3.9
ABUW_2126	-	zinc-binding alcohol dehydrogenase	3.79
ABUW_1621	*ald1*	aldehyde dehydrogenase	3.47
ABUW_0191	-	alcohol dehydrogenase, zinc-binding	3.23
ABUW_1469	-	methyltransferase type 12	3.22
ABUW_2128	*lpdA2*	dihydrolipoamide dehydrogenase	3.2
ABUW_2506	-	3-hydroxy-3-methylglutaryl-CoA lyase	3.02

Table 1S (Continued)

ABUW_2933	-	aldose 1-epimerase	2.67
ABUW_2373	-	amidohydrolase	2.62
ABUW_3204	-	amidohydrolase	2.55
ABUW_1712	*moaCB*	molybdenum cofactor biosynthesis protein C	2.53
ABUW_2780	*hcaC*	feruloyl-CoA synthetase	2.51
ABUW_1671	*tal*	transaldolase	2.44
ABUW_2787	-	NADP-dependent fatty aldehyde dehydrogenase	2.41
ABUW_1905	-	isochorismatase hydrolase	2.41
ABUW_0156	*aceF*	pyruvate dehydrogenase complex dihydrolipoamide acetyltransferase	2.21
ABUW_3309	*hyi*	hydroxypyruvate isomerase	2.2
ABUW_1871	*pcaD2*	3-oxoadipate enol-lactonase	2.04
actP2	*actP2*	copper-translocating P-type ATPase	2.65
ABUW_0184	-	Na+/solute symporter	2.65
ABUW_2332	*gltJ*	glutamate/aspartate transport system permease protein GltJ	2.63
ABUW_3321	*copA*	copper resistance protein A	2.57
ABUW_1015	*carO*	outer membrane protein CarO	2.38
ABUW_3019	*emrB*	multidrug resistance protein B	2.34
ABUW_1003	-	MFS family drug transporter	2.33
ABUW_2093	-	GntP family transporter	2.24
ABUW_2330	*gltL*	glutamate/aspartate transport ATP-binding protein GltL	2.21
ABUW_3446	-	RhtB family transporter	2.2
ABUW_0328	-	hemerythrin	2.15
ABUW_0182	-	Solute carrier 5 family, sodium/glucose transporters a	2.11
ABUW_3320	*copB*	copper resistance protein B	2.07
ABUW_2747	*epd*	glyceraldehyde 3-phosphate dehydrogenase	-2.03
ABUW_3246	*pabB*	P-aminobenzoate synthetase PabB	-2.03
ABUW_3231	*rpe*	ribulose-phosphate 3-epimerase	-2.06
ABUW_2296	*metK*	methionine adenosyltransferase	-2.06
ABUW_1097	*thiE*	thiamine-phosphate pyrophosphorylase	-2.07
ABUW_2218	*cysQ*	3'(2'),5'-bisphosphate nucleotidase	-2.12
ABUW_0685	-	alpha/beta hydrolase fold protein	-2.19
ABUW_1050	*gap*	glyceraldehyde-3-phosphate dehydrogenase	-2.34
ABUW_3133	*coaX*	pantothenate kinase, type III	-2.35

Table 1S (Continued)

ABUW_0591	-	glycosyltransferase	-2.4
ABUW_0615	-	vitamin B12 receptor	-2.4
ABUW_0913	*pckG*	phosphoenolpyruvate carboxykinase	-2.4
ABUW_3686	*ppa*	inorganic diphosphatase	-2.44
ABUW_3092	*ispE*	4-(cytidine 5'-diphospho)-2-C-methyl-D-erythritol kinase	-2.54
ABUW_1827	*eno*	phosphopyruvate hydratase (enolase)	-2.55
ABUW_2863	-	5-formyltetrahydrofolate cyclo-ligase	-2.75
ABUW_3826	-	family 1 glycosyl transferase	-3.09
ABUW_1364	-	alpha/beta hydrolase fold protein	-3.44
ABUW_1750	-	HAD-superfamily hydrolase	-3.59
Fatty acid metabolism			
ABUW_2098	*atoE*	short-chain fatty acid transporter	3.4
lpxL	-	lipid A biosynthesis lauroyl acyltransferase	2.83
ABUW_2096	*atoD*	3-oxoacid CoA-transferase, subunit A	2.83
ABUW_3573	*fadA*	acetyl-CoA C-acyltransferase FadA	2.4
ABUW_3808	*prpB*	methylisocitrate lyase	2.09
ABUW_3065	*fabB*	3-oxoacyl-[acyl-carrier-protein] synthase 1	-2.02
ABUW_1745	*lpxA*	acyl-(acyl-carrier-protein)--UDP-N-acetylglucosamine O-acyltransferase	-2.12
ABUW_1744	*fabZ*	beta-hydroxyacyl-(acyl-carrier-protein) dehydratase	-2.17
ABUW_1696	*accC*	acetyl-CoA carboxylase, biotin carboxylase	-2.18
ABUW_2307	*bioB*	biotin synthase	-2.29
ABUW_0997	*ybgC*	tol-pal system-associated acyl-CoA thioesterase	-2.45
ABUW_3108	*fabG*	3-oxoacyl-(acyl-carrier-protein) reductase	-2.49
ABUW_3107	*acpP*	acyl carrier protein	-3.47
DNA repair/metabolism			
ABUW_2210	*mfd*	transcription-repair coupling factor	2.48
ABUW_2431	*umuD*	DNA polymerase V component	2.45
ABUW_0189	*uvrA*	excinuclease ABC, A subunit	2.12
ABUW_0660	-	DNA-3-methyladenine glycosylase	2.05
ABUW_2736	*cinA2*	competence/damage-inducible protein CinA	-2.11
ABUW_2198	*hup*	DNA-binding protein HU	-2.18
ABUW_3723	*dprA*	DNA protecting protein DprA	-2.19
ABUW_2247	*ung*	uracil-DNA glycosylase	-2.38
ABUW_0319	*comF*	pilin like competence factor	-2.82

Table 1S (Continued)

ABUW_3647	*holC*	DNA polymerase III, chi subunit	-3.39
ABUW_3299	-	putative DNA uptake protein ComEA	-3.42
ABUW_0538	-	putative integrase/recombinase	-3.73
ABUW_2279	-	nucleoprotein/polynucleotide-associated enzyme	-4.21
Transporters			
ABUW_2381	*tauB*	taurine import ATP-binding protein	6.88
ABUW_1886	*cpo*	alpha/beta hydrolase	6.35
ABUW_2380	*tauC*	taurine transport system permease protein	5.01
ABUW_0057	-	formate/nitrite transporter family	4.22
ABUW_2430	-	transporter, LysE family	3.95
ABUW_3124	-	major facilitator superfamily MFS_1	3.92
ABUW_1021	*cysP*	thiosulfate-binding protein	3.58
ABUW_2708	-	Heavy metal Transport detoxification	3.35
ABUW_2333	*gltI*	glutamate/aspartate ABC transporter, periplasmic glutamate/aspartate-binding protein	3.24
ABUW_1583	*kdpC*	K+-transporting ATPase, C subunit	3.03
actP2	*actP2*	copper-translocating P-type ATPase	2.65
ABUW_0184	-	Na+/solute symporter	2.65
ABUW_2332	*gltJ*	glutamate/aspartate transport system permease protein GltJ	2.63
ABUW_3321	*copA*	copper resistance protein A	2.57
ABUW_1015	*carO*	outer membrane protein CarO	2.38
ABUW_3019	*emrB*	multidrug resistance protein B	2.34
ABUW_1003	-	MFS family drug transporter	2.33
ABUW_2093	-	GntP family transporter	2.24
ABUW_2330	*gltL*	glutamate/aspartate transport ATP-binding protein GltL	2.21
ABUW_3446	-	RhtB family transporter	2.2
ABUW_0328	-	hemerythrin	2.15
ABUW_0182	-	Solute carrier 5 family, sodium/glucose transporters a	2.11
ABUW_3320	*copB*	copper resistance protein B	2.07
ABUW_1805	-	K+ uptake system component	-2.01
ABUW_2925	*pit*	phosphate transporter	-2.02
ABUW_3632	*feoB*	ferrous iron transport protein B	-2.02
ABUW_0159	-	TonB-dependent receptor protein	-2.04

Table 1S (Continued)

ABUW_2792	-	EamA-like transporter family protein	-2.07
ABUW_3424	-	biopolymer transport protein ExbD/TolR	-2.13
ABUW_3831	*wza*	polysaccharide export protein	-2.18
ABUW_3425	-	MotA/TolQ/ExbB proton channel	-2.2
ABUW_2182	-	TonB-dependent receptor	-2.22
ABUW_1800	-	ferrichrome-iron receptor	-2.25
ABUW_1798	-	iron-sulfur cluster-binding protein, Rieske family	-2.26
ABUW_0426	*secY*	preprotein translocase, SecY subunit	-2.32
ABUW_2277	*sstT*	inner membrane symporter YgjU	-2.36
ABUW_0707	-	microcin B17 transport protein	-2.4
ABUW_1509	-	ABC transporter, ATP-binding protein	-2.56
ABUW_2916	*pfeA*	TonB dependent outer membrane siderophore receptor protein	-2.59
ABUW_3596	*secE*	Protein translocase subunit SecE	-2.62
ABUW_3403	-	TonB-dependent receptor	-2.65
ABUW_2316	-	EamA-like transporter family protein	-2.66
ABUW_3426	-	TonB protein	-2.96
ABUW_3449	*dctA*	C4-dicarboxylate transport protein	-3.16
ABUW_2154	-	tolA_full family protein	-3.17
ABUW_2403	-	MFS permease	-3.33
ABUW_1845	-	sulfur transport domain-containing protein	-3.37
ABUW_0857	-	putrescine importer	-3.58
ABUW_1520	-	EamA-like transporter family protein	-5.96
ABUW_3037	-	hemerythrin/HHE cation-binding motif-containing protein	-42.1
			Stress response
ABUW_2737	*clpB*	ATP-dependent chaperone ClpB	4.55
ABUW_3252	*raiA*	ribosomal subunit interface protein	3.39
ABUW_3515	*cbpA*	curved DNA-binding protein	3.34
ABUW_3473	-	glutathione S-transferase	3.18
ABUW_0687	*ecnB*	entericidin EcnAB	3.13
ABUW_0133	-	ribosomal protein S30EA/sigma 54 modulation protein	3.1
ABUW_1661	-	universal stress protein family	2.87
ABUW_2639	-	universal stress protein family	2.64
ABUW_0372	-	phage shock protein C	2.32
ABUW_1749	*hslR*	heat shock protein 15	2.04

Table 1S (Continued)

ABUW_2513	*csp2*	cold-shock DNA-binding domain protein	-2.01
ABUW_2197	*ppiD*	peptidyl-prolyl cis-trans isomerase	-2.02
ABUW_0492	*sspA*	stringent starvation protein A	-2.23
ABUW_2690	*csp1*	cold-shock DNA-binding domain protein	-5.77
ABUW_2901	-	activator of HSP90 ATPase	-19.87
			tRNA / tRNA processing
ABUW_0906	-	tRNA	7.76
ABUW_3219	-	tRNA	5.49
ABUW_3546	-	tRNA	5.43
ABUW_0537	-	tRNA	4.65
ABUW_3467	*nudH*	(di)nucleoside polyphosphate hydrolase	2.8
ABUW_0231	-	tRNA	2.31
ABUW_0326	*truB*	tRNA pseudouridine synthase B	-2.54
ABUW_2146	*rnd*	ribonuclease D	-2.69
ABUW_3905	*rnpA*	ribonuclease P protein componen	-2.99
ABUW_2289	*trmA*	tRNA (uracil-5-)-methyltransferase	-4.41
Oxidative stress			
ABUW_2436	*katE*	catalase	4.63
ABUW_2504	-	catalase	3.18
ABUW_2356	*msrB*	methionine-R-sulfoxide reductase	2.1
ABUW_1501	*pqiA2*	paraquat-inducible protein A	2.09
ABUW_3469	*katG*	catalase/peroxidase HPI	2.03
ABUW_2342	*ychF*	GTP-binding protein YchF	-2.1
ABUW_1371	-	protein YaaA	-2.44
ABUW_3027	-	OsmC-like peroxiredoxin	-4
Iron acqusition			
ABUW_3125	*bfr2*	bacterioferritin	3.05
ABUW_1188	*basJ*	putative acinetobactin biosynthesis protein	-2.41
ABUW_2189	-	IucA/IucC-family aerobactin siderophore biosynthesis component	-3.22
ABUW_0307	-	BFD-like [2Fe-2S]-binding domain-containing protein	-4.49
ABUW_0143	-	TonB-dependent receptor protein	-4.52
ABUW_2184	-	ferric iron reductase FhuF	-5.37
Virulence			
ABUW_1631	-	spore coat protein U	9.94
ABUW_0885	-	biofilm-associated protein	4.31

Table 1S (Continued)

ABUW_2440	-	surface antigen	3.88
ABUW_1634	-	spore coat protein U	2.53
ABUW_2578	-	type VI secretion system effector, Hcp1 family	2.27
ABUW_1904	-	antibiotic biosynthesis monooxygenase	2.19
ABUW_1633	-	fimbrial biogenesis outer membrane usher protein	2.04
ABUW_2566	-	type IV / VI secretion system protein, DotU family	-2.1
ABUW_2887	-	lipoprotein	-2.18
ABUW_2576	-	type VI secretion protein, family	-2.26
ABUW_0563	-	beta-lactamase OXA-23	-2.28
ABUW_0632	-	hemolysin-3	-2.47
ABUW_0305	-	O-antigen polymerase family	-2.64
ABUW_2572	-	type IV secretion-associated protein, family	-3.03
ABUW_0680	*pilI*	type IV pilus signal transduction protein PilI	-3.12
ABUW_1992	-	zonular occludens toxin (ZOT) protein	-3.19
ABUW_1604	-	RelB/DinJ antitoxin	-5.45
ABUW_1355	-	complement control module protein	-5.48
Translation			
ABUW_0172	-	ribosomal RNA small subunit methyltransferase E	2.91
ABUW_3284	*rplT*	ribosomal protein L20	2.62
ABUW_2937	*def2*	peptide deformylase	2.19
ABUW_1546	*rplI*	ribosomal protein L9	2.08
ABUW_2216	*rpsT*	ribosomal protein S20	-2
ABUW_0494	*rplM*	ribosomal protein L13	-2
ABUW_0322	*trmD*	tRNA (guanine-N1)-methyltransferase	-2.01
ABUW_0418	*rplE*	ribosomal protein L5	-2.04
ABUW_0430	*rpsD*	ribosomal protein S4	-2.13
ABUW_0427	*rpmJ*	ribosomal protein L36	-2.25
ABUW_0714	*gatC*	glutamyl-tRNA(Gln) amidotransferase, C subunit	-2.27
ABUW_2264	*gidB*	methyltransferase GidB	-2.35
ABUW_1141	*efp*	translation elongation factor P	-2.49
ABUW_0424	*rpmD*	ribosomal protein L30	-2.49
ABUW_1609	*hfq*	Host Factor	-2.56
ABUW_0989	-	tRNA/rRNA methyltransferase	-2.71
ABUW_0420	*rpsH*	ribosomal protein S8	-2.73

Table 1S (Continued)

ABUW_3431	*rpmG*	ribosomal protein L33	-2.81
ABUW_0408	*rplW*	ribosomal protein L23	-2.87
ABUW_2847	-	rRNA small subunit methyltransferase 1	-3.12
Post translational modification			
ABUW_0860	*lipB*	lipoate-protein ligase B	-2.14
ABUW_1535	*prmA1*	ribosomal protein L11 methyltransferase	-2.36
ABUW_0745	-	N6 adenine-specific DNA methyltransferase	-2.41
ABUW_0086	-	DNA cytosine methyltransferase	-2.47
ABUW_2961	-	peptidyl-prolyl cis-trans isomerase	-2.85
ABUW_0020	-	glutathione S-transferase	-2.88
Lipoprotein			
ABUW_3874	-	lipoprotein, putative	6.39
ABUW_3875	-	lipoprotein, putative	3.62
ABUW_3588	-	lipoprotein, putative	3.42
ABUW_1048	-	outer membrane lipoprotein Blc	2.13
ABUW_0850	*lolA*	outer membrane lipoprotein carrier protein LolA	2.08
Protease			
ABUW_0072	-	peptidase M15 family	2.72
ABUW_1146	-	proline dipeptidase	2.47
ABUW_3575	-	serine hydrolase domain-containing protein	2.16
ABUW_0711	-	intracellular protease, PfpI family	2.08
ABUW_1630	*pepN*	peptidase M1, alanyl aminopeptidase	2.02
ABUW_2738	-	peptidase M23/M37 family	-3.03
ABUW_1345	-	peptidase U32	-2.08
ABUW_3863	*lspA2*	Signal peptidase II	-2.81
ABUW_3880	-	matrixin superfamily	-5.88
Detoxification			
ABUW_3664	*cadA*	heavy metal detoxification protein	8.11
ABUW_3026	-	glyoxalase	6.13
ABUW_1135	*gloA*	glyoxalase I	2
Lipid transport / metabolism			
ABUW_3383	-	putative phosphatidylglycerophosphatase B	10.43
ABUW_1939	-	2-hydroxy-3-oxopropionate reductase	2.71
ABUW_1683	-	thioesterase family protein	2.14
Nucleotide biosynthesis			
ABUW_1944	-	ADP-ribose pyrophosphatase	2.22

Table 1S (Continued)

ABUW_1943	-	nicotinamide phosphoribosyltransferase	2.77
ABUW_2754	*add1*	adenosine deaminase	-2.01
ABUW_3300	-	nucleoside triphosphate pyrophosphohydrolase	-2.06
ABUW_2239	*pyrF*	orotidine 5'-phosphate decarboxylase	-2.1
ABUW_3381	*ndk*	nucleoside diphosphate kinase	-2.17
ABUW_3142	*dcd*	deoxycytidine triphosphate deaminase	-2.79
Purine metabolism			
ABUW_1197	*xdhB*	xanthine dehydrogenase, molybdopterin binding subunit	3.87
ABUW_0059	*purC*	phosphoribosylaminoimidazole-succinocarboxamide synthase	-2.07
ABUW_3427	*purU*	formyltetrahydrofolate deformylase	-2.09
ABUW_0980	*purN*	phosphoribosylglycinamide formyltransferase	-2.09
ABUW_1122	*purB*	adenylosuccinate lyase	-2.15
ABUW_3897	*hpt*	hypoxanthine phosphoribosyltransferase	-3.32
Proton ion translocation / ATP synthesis			
ABUW_3737	*atpE*	ATP synthase F0, C subunit	-2.02
ABUW_0388	*corA*	magnesium and cobalt transport protein	-2.25
ABUW_3738	*atpB*	ATP synthase F0, A subunit	-2.28
ABUW_3735	*atpH*	ATP synthase F1, delta subunit	-2.65
ABUW_3538	*phaF*	pH adaptation potassium efflux system protein F	-2.92
ABUW_3737	*atpE*	ATP synthase F0, C subunit	-2.02
Cell division			
ABUW_3402	*tig*	trigger factor	-2.06
ABUW_2235	-	cell division protein ZapE	-2.33
ABUW_0525	*ispZ*	intracellular septation protein A	-2.96
Cell wall synthesis			
ABUW_1687	*murB*	UDP-N-acetylenolpyruvoylglucosamine reductase	-2.09
ABUW_1070	-	D-ala-D-ala-carboxypeptidase penicillin-binding protein	-2.11
ABUW_1127	*dacC*	penicillin-binding protein 6 (D-alanyl-D-alanine carboxypeptidase)	-2.14
ABUW_1737	*uppS*	undecaprenyl diphosphate synthase	-2.14
ABUW_1544	*alr*	alanine racemase	-2.16
ABUW_0404	-	glutamine amidotransferase, class I	-5.46

Table 1S (Continued)

ABUW_0074	-	acyltransferase 3	-5.33
Cell adhesion / motility			
ABUW_0294	*comQ*	fimbrial assembly protein PilQ	-2.09
ABUW_2313	-	fimbrial protein	-2.17
ABUW_2310	-	fimbrial protein	-2.46
ABUW_2312	*fimD*	fimbrial biogenesis outer membrane usher protein	-2.89
ABUW_2311	-	pili assembly chaperone	-3.32
ABUW_0648	-	type 4 fimbrial biogenesis protein FimT	-3.37
ABUW_1489	-	CsuB	-8.84
ABUW_0304	-	type IV pilin structural subunit	-11
Protein synthesis			
ABUW_0014	*tyrS*	tyrosyl-tRNA synthetase	-2.06
ABUW_0432	*rplQ*	ribosomal protein L17	-2.14
ABUW_3099	*pth*	peptidyl-tRNA hydrolase	-2.21
ABUW_0411	*rplV*	ribosomal protein L22	-3.34
ABUW_3490	*rpmE2*	ribosomal protein L31	-10.27
Phage			
ABUW_2322	-	phage integrase	-5.99
ABUW_1312	-	phage protein	-5.26
ABUW_3569	-	bacteriophage SFi21 - peptidoglycan hydrolase	-3.37
Outer membrane protiens			
ABUW_0021	-	outer membrane protein	-2.8
ABUW_3833	*ptk*	tyrosine-protein kinase ptk	-2.11
ABUW_3583	-	putative phosphatidylglycerophosphatase B	-7.55
Membrane proteins			
ABUW_3829	-	UDP-N-acetylglucosamine 2-epimerase	-2.25
ABUW_3890	-	undecaprenyl-diphosphatase	-2.52
ABUW_0505	-	tRNA/rRNA methyltransferase	-2.67
ABUW_2473	-	major facilitator superfamily MFS_1	-3.97
ABUW_1610	-	integral membrane protein	-8.52

Table 2S. Genes differentially expressed in the *fecI* mutant strain

Locus Tag	Gene	Protein / Function	Fold Change
Hypothetical proteins			
ABUW_1914	-	hypothetical protein	41.94
ABUW_2607	-	hypothetical protein	36.48
ABUW_2605	-	hypothetical protein	25.89
ABUW_2445	-	hypothetical protein	14.4
ABUW_1792	-	hypothetical protein	10.7
ABUW_2626	-	hypothetical protein	9.91
ABUW_1158	-	hypothetical protein	9.12
ABUW_3186	-	hypothetical protein	7.9
ABUW_2812	-	hypothetical protein	7.04
ABUW_1416	-	hypothetical protein	6.66
ABUW_2060	-	hypothetical protein	6.46
ABUW_2655	-	hypothetical protein	5.92
ABUW_0044	-	hypothetical protein	5.46
ABUW_2796	-	hypothetical protein	5.38
ABUW_0748	-	hypothetical protein	5.35
ABUW_2550	-	hypothetical protein	5.2
ABUW_2309	-	hypothetical protein	5.05
ABUW_0187	-	hypothetical protein	4.76
ABUW_1988	-	hypothetical protein	4.63
ABUW_2179	-	hypothetical protein	4.54
ABUW_1282	-	hypothetical protein	4.44
ABUW_2797	-	hypothetical protein	4.3
ABUW_1268	-	hypothetical protein	4.12
ABUW_0746	-	hypothetical protein	3.5
ABUW_2611	-	hypothetical protein	3.48
ABUW_2433	-	KGG domain-containing protein	3.43
ABUW_0933	-	hypothetical Protein	3.12
ABUW_1796	-	hypothetical Protein	3.09
ABUW_3193	-	hypothetical Protein	3.09
ABUW_2676	-	Hypothetical Protein	3.07
ABUW_3702	-	Hypothetical Protein	-3.06
ABUW_2290	-	Hypothetical Protein	-3.18

Table 2S (Continued)

ABUW_0720	-	Hypothetical Protein	-3.53
ABUW_2686	-	Hypothetical Protein	-3.84
ABUW_0220	-	Hypothetical Protein	-3.86
ABUW_0814	-	Hypothetical Protein	-4.4
ABUW_3198	-	Hypothetical Protein	-4.55
ABUW_2671	-	Hypothetical Protein	-5.42
ABUW_1485	-	Hypothetical Protein	-5.53
ABUW_3851	-	Hypothetical Protein	-8.12
ABUW_1860	-	Hypothetical Protein	-11.23
ABUW_2980	-	Hypothetical Protein	-17.48
ABUW_2983	-	Hypothetical Protein	-34.12
Small RNA			
ABUWs081	-		-10.83
ABUWs083	-		-3.83
ABUWs002	-		-3.3
ABUWs072	-		-3.15
ABUWs005	-		-3.14
Amino Acid Transport and Metabolism			
ABUW_2548	-	proline racemase	29.52
ABUW_2543	-	shikimate transporter	8.63
ABUW_2541	-	amino acid transporter	8.04
ABUW_1114	*aroP3*		-4.36
ABUW_2548	-	proline racemase	29.52
Aromatic Metabolism			
ABUW_2092	*bdhA*	3-hydroxybutyrate dehydrogenase	3.26
ABUW_2359	*aspQ*	L-asparaginase 2	5.04
ABUW_1862	-	aromatic-ring-hydroxylating dioxygenase beta subunit	-21.81
ABUW_2535	paaG	phenylacetate-CoA oxygenase, PaaG subunit	-11.95
ABUW_2534	*paaH*	phenylacetate-CoA oxygenase, PaaH subunit	-11.01
ABUW_2533	*paaI2*	phenylacetate-CoA oxygenase, PaaI subunit	-9.08

Table 2S (Continued)

ABUW_2531	*paaK*	phenylacetate-CoA oxygenase/reductase, PaaK subunit	-8.98
ABUW_2536	*paaN*	phenylacetic acid degradation protein PaaN	-8.51
ABUW_2527	*paaE*	beta-ketoadipyl CoA thiolase	-8.39
ABUW_2529	*paaB*	enoyl-CoA hydratase	-8.33
ABUW_1863	-	short-chain dehydrogenase/reductase	-8.22
ABUW_2532	*paaJ*	phenylacetate-CoA oxygenase, PaaJ subunit	-7.95
ABUW_2528	*paaC*	3-hydroxyacyl-CoA dehydrogenase	-7.8
ABUW_2526	*paaF*	phenylacetate-CoA ligase	-7.69
ABUW_2525	*paaX*	phenylacetic acid degradation operon negative regulatory protein PaaX	-3.93
ABUW_2524	*paaY*	phenylacetic acide degradation protein PaaY	-3.35
ABUW_1834	*pcaB*	3-carboxy-cis,cis-muconate cycloisomerase	-3.09
Metabolism			
ABUW_3782	*mmsB*	3-hydroxyisobutyrate dehydrogenase	-7.78
ABUW_1861	-	ring hydroxylating dioxygenase, Rieske	-6.51
Fatty Acid Metabolism			
ABUW_2530	caiD	enoyl-coA hydratase	-6.38
ABUW_3780	-	acyl-CoA dehydrogenase	-5.72
ABUW_3779	-	short-chain enoyl-CoA hydratase	-4.88
ABUW_2630	-	lipid A biosynthesis lauroyl acyltransferase	-3.56
Biofilm			
ABUW_1487	*CsuA/B*		255.69
ABUW_1488	*CsuA*		150.91
ABUW_1491	*CsuD*		101.48
ABUW_1490	*CsuC*		89.17

Table 2S (Continued)

ABUW_1492	*CsuE*		76.91
ABUW_1489	*CsuB*		74.5
Carbohydrate Metabolism			
ABUW_2606	-	glycoside hydrolase/deacetylase family protein	22.63
Efflux Pumps			
ABUW_1976	*adeC*	multidrug efflux protein AdeC	4.75
ABUW_1974	*adeA*	multidrug efflux protein AdeA	4.45
ABUW_1975	*adeB*	multidrug efflux protein AdeB	4.45
Energy Conversion			
ABUW_2546	-	2Fe-2S ferredoxin-type domain-containing protein	79
ABUW_2547	-	FAD dependent oxidoreductase	54.22
ABUW_2542	*aldH*	aldehyde dehydrogenase	42.61
ABUW_2545	-	pyridine nucleotide-disulfide oxidoreductase	26.91
ABUW_1795	*cydA*	cytochrome D ubiquinol oxidase subunit I	7.05
ABUW_2385	-	monooxygenase, NtaA/SnaA/SoxA family	4.9
ABUW_1794	*cydB*	cytochrome D ubiquinol oxidase, subunit II	4.85
ABUW_1864	-	2Fe-2S iron-sulfur cluster binding domain protein	-4.86
ABUW_3403	ABUW_3403	TonB-dependent receptor	3.43
ABUW_1115	ABUW_1115	phosphate ABC transporter, substrate-binding protein	3.33
Metabolism			
ABUW_2551	ABUW_2551	dihydrodipicolinate synthetase	4.35
ABUW_3781	-	acetyl-coenzyme A synthetase	-4.77

Table 2S (Continued)

ABUW_3783	*mmsA1*	methylmalonate-semialdehyde dehydrogenase	-4.58
ABUW_1113	-	indole-3-pyruvate decarboxylase	-3.93
Motility			
ABUW_2310	-	fimbrial protein	12.84
ABUW_2053	-	pili assembly chaperone	4.74
ABUW_2052	-	fimbrial subunit	4.33
Nucleotide metabolism			
ABUW_3042	*dut*	deoxyuridine 5'-triphosphate nucleotidohydrolase	3.22
Outermebrane			
ABUW_3583	-	putative outer membrane protein W	35.02
Replication			
ABUW_3007	-	single-strand binding protein	3.61
Ribosomal Protein			
ABUW_0408	*rplW*	ribosomal protein L23	5.68
ABUW_0406	*rplC*	ribosomal protein L3	3.24
Transcriptional Regulators			
ABUW_1159	-	transcriptional regulator, TetR family	15.7
ABUW_2986	-	Anti-sigma factor fecR	-14.74
ABUW_0224	-	transcriptional regulator, HxlR family	-3.13
Transport			
ABUW_3201	-	transporter	6.7
ABUW_2892	*citN*	citrate transporter	3.72
ABUW_2602	-	voltage-gated chloride channel	3.19
Urea Metabolism			
ABUW_2604	-	allophanate hydrolase	28.98
ABUW_2603	*bccA*	carbamoyl-phosphate synthase	17.54
Inorganic Ion Transport and Metabolism			

Table 2S (Continued)

ABUW_2985	-	TonB Outermembrane receptor	-45.16
ABUW_2982	-	TonB C binds Fe+3 siderophore complex	-25.8
ABUW_2981	-	Hemeoxygenase	-17.7
ABUW_2707	*actP2*	copper-translocating P-type ATPase	-5.36
ABUW_2708		heavy metal transport / detoxification protein	-4.37
ABUW_0280	*sbp*	thiosulfate-binding protein	-3.13
Lipid Metabolism			
ABUW_1858	-	acyl-CoA dehydrogenase	-16.96
Posttranslational modification, protein turnover, chaperones			
ABUW_2901	-	activator of HSP90 ATPase	-3.59
Protein synthesis			
ABUW_1857	-	Glu-tRNA amidotransferase	-11.73
Putative Lipoprotein			
ABUW_3874	-	lipoprotein, putative	-3.35
Putative Outermebrane protein			
ABUW_1656		OmpW family protein	-5.73
transporter, LysE family			
ABUW_2430	-		-5.95